frontiers
RESEARCH TOPICS

MAGNETIC RESONANCE IMAGING OF DISTURBED BRAIN CONNECTIVITY IN PSYCHIATRIC ILLNESS

Hosted by
Alex Fornito and Ben Harrison

frontiers in
PSYCHIATRY

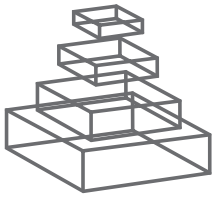

frontiers

Cover image provided by Ibbl sarl, Lausanne CH

ISSN 1664-8714
ISBN 978-2-88919-051-5
DOI 10.3389/978-2-88919-051-5

ABOUT FRONTIERS

Frontiers is more than just an open-access publisher of scholarly articles: it is a pioneering approach to the world of academia, radically improving the way scholarly research is managed. The grand vision of Frontiers is a world where all people have an equal opportunity to seek, share and generate knowledge. Frontiers provides immediate and permanent online open access to all its publications, but this alone is not enough to realize our grand goals.

FRONTIERS JOURNAL SERIES

The Frontiers Journal Series is a multi-tier and interdisciplinary set of open-access, online journals, promising a paradigm shift from the current review, selection and dissemination processes in academic publishing.
All Frontiers journals are driven by researchers for researchers; therefore, they constitute a service to the scholarly community. At the same time, the Frontiers Journal Series operates on a revolutionary invention, the tiered publishing system, initially addressing specific communities of scholars, and gradually climbing up to broader public understanding, thus serving the interests of the lay society, too.

DEDICATION TO QUALITY

Each Frontiers article is a landmark of the highest quality, thanks to genuinely collaborative interactions between authors and review editors, who include some of the world's best academicians. Research must be certified by peers before entering a stream of knowledge that may eventually reach the public - and shape society; therefore, Frontiers only applies the most rigorous and unbiased reviews.
Frontiers revolutionizes research publishing by freely delivering the most outstanding research, evaluated with no bias from both the academic and social point of view.
By applying the most advanced information technologies, Frontiers is catapulting scholarly publishing into a new generation.

WHAT ARE FRONTIERS RESEARCH TOPICS?

Frontiers Research Topics are very popular trademarks of the Frontiers Journals Series: they are collections of at least ten articles, all centered on a particular subject. With their unique mix of varied contributions from Original Research to Review Articles, Frontiers Research Topics unify the most influential researchers, the latest key findings and historical advances in a hot research area!
Find out more on how to host your own Frontiers Research Topic or contribute to one as an author by contacting the Frontiers Editorial Office: researchtopics@frontiersin.org

MAGNETIC RESONANCE IMAGING OF DISTURBED BRAIN CONNECTIVITY IN PSYCHIATRIC ILLNESS

Hosted By:
Alex Fornito, University of Melbourne, Australia
Ben Harrison, University of Melbourne, Australia

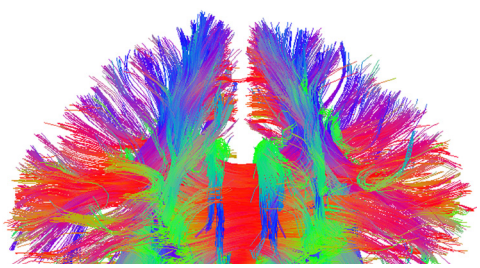

The widespread application of brain imaging to the study of psychiatric disorders has led to a revolution in our understanding of the neural basis of psychiatric illness. In particular, the advent of magnetic resonance imaging (MRI) has provided an unprecedented capacity for quantifying diverse aspects of brain structure and function in vivo, and has been used to identify brain changes associated with the full spectrum of psychopathology. With respect to major psychiatric disorders, it is now abundantly clear from this literature that focal brain dysfunction is rare. Rather, most disorders are associated with abnormalities in large-scale networks of spatially distributed and interconnected brain regions; i.e., they are disorders of brain connectivity. Such considerations highlight the need to understand brain dysfunction in psychiatric illness from a network-based perspective. This goal is starting to be realized through recent advances in the use of MRI to map the brain's complex connectivity architecture. In this special edition, we invite contributions that address brain network dysfunction in psychiatric illnesses. Specifically, the work must be concerned with understanding interactions between brain regions, and how their alterations are affected by psychiatric disease. These interactions can be studied at the level of anatomy using diffusion-MRI or function using functional MRI (fMRI), with the full range of methods available (e.g., tractography, seed-based correlations, independent component analysis, graph analysis, dynamic causal modeling, etc.). Contributions can be either reviews of recent, relevant literature addressing brain network dysfunction in psychiatric disease, or experimental papers describing novel insights into brain network disturbances in such illnesses. Contributions will be invited covering a broad spectrum of psychiatric disease, including mood and anxiety disorders, schizophrenia, autism, attention-deficit hyperactivity disorder and neurodegenerative conditions. It is intended that this volume will provide important insights into how brain networks are perturbed by psychiatric disease, and allow identification of commonalities and differences across diagnostic categories.

Table of Contents

frontiers in PSYCHIATRY

EDITORIAL
published: 27 July 2012
doi: 10.3389/fpsyt.2012.00072

Brain connectivity and mental illness

Alex Fornito[1,2,3]* and Ben J. Harrison[3]

[1] Centre for Neural Engineering, The University of Melbourne, Parkville, VIC, Australia
[2] NICTA Victorian Research Laboratory, The University of Melbourne, Parkville, VIC, Australia
[3] Department of Psychiatry, Melbourne Neuropsychiatry Centre, The University of Melbourne and Melbourne Health, Parkville, VIC, Australia
*Correspondence: fornitoa@unimelb.edu.au

Edited by:
K. Luan Phan, University of Illinois at Chicago, USA

Despite nearly three decades of neuroimaging research in psychiatry, no imaging study to date has identified a single site of pathology in the brain that represents a causal factor in the emergence of any of the major mental illnesses described in current nosological systems. Rather, the available evidence indicates that these disorders are associated with subtle abnormalities distributed throughout the brain (e.g., Fornito et al., 2009, 2012; Bora et al., 2010, 2012), implying that they arise from disordered interactions between connected neural systems rather than damage to any individual brain region. Accordingly, current hopes for the development of more targeted interventions in psychiatry are being placed on research attempting to map the molecular determinants and clinical correlates of neural circuit abnormalities in mental disorders (Insel and Scolnick, 2006; Meyer-Lindenberg, 2010). The impact of this thinking on the field is evident in the emergence of new scientific journals devoted to the study of brain connectivity[1]; increasingly popular workshops devoted to the topic[2]; recent large-scale collaborative initiatives such as the Human Connectome Project[3,4]; freely available software packages dedicated to connectivity analyses[5,6]; and the establishment data-sharing initiatives such as the 1000 connectomes project[7]. These developments offer the potential to greatly enhance our understanding of brain connectivity abnormalities in psychiatric disorders.

This Special Topic of *Frontiers in Psychiatry* presents work illustrating the application of connectomic techniques to study brain network changes in mental disorders. It brings together researchers working to understand brain network abnormalities in disorders as diverse as schizophrenia, attention-deficit hyperactivity disorder (ADHD), major depression, bipolar disorder, post-traumatic stress disorder (PTSD), and Alzheimer's disease, and showcases the diverse range of methods used to interrogate these brain changes.

The article by Fornito and Bullmore (2012) overviews these techniques and reviews their application to the study of genetic influences on brain networks. They conclude that the available literature, albeit preliminary, indicates that risk genes show greater penetrance at the level of distributed brain networks rather than individual regions, and connectomic measures may thus provide more sensitive intermediate phenotypes for psychiatric disorders.

The remaining articles illustrate the application of specific techniques to study different disorders. Independent component analysis (ICA), a popular data-driven technique for decomposing fMRI data into distinct components with characteristic anatomy and temporal dynamics (Calhoun et al., 2004), is applied by Calhoun et al. (2011) to demonstrate phenotypic continuities and discontinuities in the brain functional networks of patients with schizophrenia and bipolar disorder performing an auditory oddball task.

Seed-based techniques are featured in the work of Mills et al. (2012), Mennes et al. (2011), Rabinak et al. (2011), and Davey et al. (2012). The first two articles use multiple seeds to characterize how individual differences in functional connectivity relate to cognitive performance on tests of executive function in children with ADHD and typically developing controls. This work offers welcome new evidence supporting the behavioral relevance of resting-state measures for psychiatric disorders, which is critical for validating any case-control differences observed under such experimental conditions (Fornito and Bullmore, 2010). In war veterans with combat-related PTSD, Rabinak et al. (2011) report a prominent alteration of resting-state functional connectivity between an amygdala seed region and posterior insular cortex, extending prior evidence from task-based activation studies in this patient group. Finally, Davey et al. (2012) provide evidence that adaptive changes in the functional connectivity of the subgenual cingulate cortex may be necessary to support intact executive function early in the course of major depressive disorder (MDD), prior to the emergence of characteristic cognitive deficits.

In a second study of MDD, Almeida et al. (2011) use dynamic causal modeling (DCM) to characterize changes in the effective connectivity (i.e., causal functional interactions) of a circuit linking ventral frontal cortical regions and the amygdala during emotional processing. Their findings shed light on how sex differences in the dynamics of this network may relate to the clinical phenomenology of female compared to male MDD.

Graph analytic techniques are featured in the work of Xie and He (2011) and Collin et al. (2011). Xie and He provide a primer on the basic principles of graph theoretic analysis of neuroimaging data, and comprehensively review the application of these techniques to study disturbances of structural and functional brain network connectivity and topology in Alzheimer's disease. In a resting-state fMRI study, Collin and colleagues use graph analytic techniques to provide some of the first evidence that functional connectivity between cerebellar and cortical and subcortical regions is associated with genetic risk for schizophrenia.

[1] http://www.liebertpub.com/brain
[2] http://www.brain-connectivity-workshop.org/
[3] http://www.humanconnectomeproject.org/
[4] http://www.humanconnectome.org/
[5] https://sites.google.com/a/brain-connectivity-toolbox.net/bct/
[6] https://sites.google.com/site/functionalconnectivitytoolbox/
[7] http://fcon_1000.projects.nitrc.org/

Finally, Lungu and Stip (2012) present an interesting case study of a schizophrenia patient with partial agenesis of the corpus callosum. They report intact activation to perception of visual stimuli but abnormal neural activation during emotional processing in this patient. They interpret this finding as implicating callosal connectivity in patients' emotional and psychotic disturbances, a conclusion consistent with morphometric studies of callosal abnormalities in schizophrenia (Walterfang et al., 2008).

Collectively, the research presented in this Special Topic provides the novice reader with exposure to the diverse array of methods available for interrogating brain network structure and function in health and disease, and offers the expert reader prime examples of cutting-edge applications of these methods to understand psychiatric disorders. The continued development of novel connectivity mapping techniques (Bassett et al., 2011; Fornito et al., 2011a; Friston et al., 2011; Sui et al., 2012; Zalesky et al., 2012a), improvements in available algorithms and network models (Friston et al., 2011; Rubinov and Sporns, 2011; Zalesky et al., 2012b), and the elucidation of genetic influences on brain connectivity (Esslinger et al., 2009; Fornito et al., 2011b), will be critical for advancing work in this field. These advances, coupled with the valuable data to emerge from initiatives such as the Human Connectome Project, will enable researchers to move beyond localized, segregationist pathophysiological models of mental illness to characterize the full complexity of distributed neural circuit disruptions that underlie these conditions.

ACKNOWLEDGMENTS

We would like to thank all authors who contributed to this Special Topic. Alex Fornito and Ben J. Harrison were by National Health and Medical Research Council Fellowships 454797 and 628509, respectively.

REFERENCES

Almeida, J. R., Kronhaus, D. M., Sibille, E. L., Langenecker, S. A., Versace, A., Labarbara, E. J., and Phillips, M. L. (2011). Abnormal left-sided orbitomedial prefrontal cortical-amygdala connectivity during happy and fear face processing: a potential neural mechanism of female MDD. *Front. Psychiatry* 2:69. doi: 10.3389/fpsyt.2011.00069

Bassett, D. S., Wymbs, N. F., Porter, M. A., Mucha, P. J., Carlson, J. M., and Grafton, S. T. (2011). Dynamic reconfiguration of human brain networks during learning. *Proc. Natl. Acad. Sci. U.S.A.* 108, 7641–7646.

Bora, E., Fornito, A., Pantelis, C., and Yücel, M. (2012). Gray matter abnormalities in major depressive disorder: a meta-analysis of voxel based morphometry studies. *J. Affect. Disord.* 138, 9–18.

Bora, E., Fornito, A., Yucel, M., and Pantelis, C. (2010). Voxelwise meta-analysis of gray matter abnormalities in bipolar disorder. *Biol. Psychiatry* 67, 1097–1105.

Calhoun, V. D., Adali, T., and Pekar, J. J. (2004). A method for comparing group fMRI data using independent component analysis: application to visual, motor and visuomotor tasks. *Magn. Reson. Imaging* 22, 1181–1191.

Calhoun, V. D., Sui, J., Kiehl, K., Turner, J., Allen, E., and Pearlson, G. (2011). Exploring the psychosis functional connectome: aberrant intrinsic networks in schizophrenia and bipolar disorder. *Front. Psychiatry* 2:75. doi: 10.3389/fpsyt.2011.00075

Collin, G., Hulshoff Pol, H. E., Haijma, S. V., Cahn, W., Kahn, R. S., and van den Heuvel, M. P. (2011). Impaired cerebellar functional connectivity in schizophrenia patients and their healthy siblings. *Front. Psychiatry* 2:73. doi: 10.3389/fpsyt.2011.00073

Davey, C. G., Yucel, M., Allen, N. B., and Harrison, B. J. (2012). Task-related deactivation and functional connectivity of the subgenual cingulate cortex in major depressive disorder. *Front. Psychiatry* 3:14. doi: 10.3389/fpsyt.2012.00014

Esslinger, C., Walter, H., Kirsch, P., Erk, S., Schnell, K., Arnold, C., Haddad, L., Mier, D., Opitz von Boberfeld, C., Raab, K., Witt, S. H., Rietschel, M., Cichon, S., and Meyer-Lindenberg, A. (2009). Neural mechanisms of a genome-wide supported psychosis variant. *Science* 324, 605.

Fornito, A., and Bullmore, E. T. (2010). What can spontaneous fluctuations of the blood oxygenation-level-dependent signal tell us about psychiatric disorders? *Curr. Opin. Psychiatry* 23, 239–249.

Fornito, A., and Bullmore, E. T. (2012). Connectomic intermediate phenotypes for psychiatric disorders. *Front. Psychiatry* 3:32. doi: 10.3389/fpsyt.2012.00032

Fornito, A., Yoon, J., Zalesky, A., Bullmore, E. T., and Carter, C. S. (2011a). General and specific functional connectivity disturbances in first-episode schizophrenia during cognitive control performance. *Biol. Psychiatry* 70, 64–72.

Fornito, A., Zalesky, A., Bassett, D. S., Meunier, D., Ellison-Wright, I., Yucel, M., Wood, S. J., Shaw, K., O'Connor, J., Nertney, D., Mowry, B. J., Pantelis, C., and Bullmore, E. T. (2011b). Genetic influences on cost-efficient organization of human cortical functional networks. *J. Neurosci.* 31, 3261–3270.

Fornito, A., Yucel, M., Patti, J., Wood, S. J., and Pantelis, C. (2009). Mapping grey matter reductions in schizophrenia: an anatomical likelihood estimation analysis of voxel-based morphometry studies. *Schizophr. Res.* 108, 104–113.

Fornito, A., Zalesky, A., Pantelis, C., and Bullmore, E. T. (2012). Schizophrenia, neuroimaging and connectomics. *NeuroImage*. doi: 10.1016/j.neuroimage/2011/12/090

Friston, K. J., Li, B., Daunizeau, J., and Stephan, K. E. (2011). Network discovery with DCM. *Neuroimage* 56, 1202–1221.

Insel, T. R., and Scolnick, E. M. (2006). Cure therapeutics and strategic prevention: raising the bar for mental health research. *Mol. Psychiatry* 11, 11–17.

Lungu, O., and Stip, E. (2012). Agenesis of corpus callosum and emotional information processing in schizophrenia. *Front. Psychiatry* 3:1. doi: 10.3389/fpsyt.2012.00001

Mennes, M., Vega Potler, N., Kelly, C., Di Martino, A., Castellanos, F. X., and Milham, M. P. (2011). Resting state functional connectivity correlates of inhibitory control in children with attention-deficit/hyperactivity disorder. *Front. Psychiatry* 2:83. doi: 10.3389/fpsyt.2011.00083

Meyer-Lindenberg, A. (2010). From maps to mechanisms through neuroimaging of schizophrenia. *Nature* 468, 194–202.

Mills, K. L., Bathula, D., Dias, T. G., Iyer, S. P., Fenesy, M. C., Musser, E. D., Stevens, C. A., Thurlow, B. L., Carpenter, S. D., Nagel, B. J., Nigg, J. T., and Fair, D. A. (2012). Altered cortico-striatal-thalamic connectivity in relation to spatial working memory capacity in children with ADHD. *Front. Psychiatry* 3:2. doi: 10.3389/fpsyt.2012.00002

Rabinak, C. A., Angstadt, M., Welsh, R. C., Kenndy, A. E., Lyubkin, M., Martis, B., and Phan, K. L. (2011). Altered amygdala resting-state functional connectivity in post-traumatic stress disorder. *Front. Psychiatry* 2:62. doi: 10.3389/fpsyt.2011.00062

Rubinov, M., and Sporns, O. (2011). Weight-conserving characterization of complex functional brain networks. *Neuroimage* 56, 2068–2079.

Sui, J., Adali, T., Yu, Q., Chen, J., and Calhoun, V. D. (2012). A review of multivariate methods for multimodal fusion of brain imaging data. *J. Neurosci. Methods* 204, 68–81.

Walterfang, M., Wood, A. G., Reutens, D. C., Wood, S. J., Chen, J., Velakoulis, D., McGorry, P. D., and Pantelis, C. (2008). Morphology of the corpus callosum at different stages of schizophrenia: cross-sectional study in first-episode and chronic illness. *Br. J. Psychiatry* 192, 429–434.

Xie, T., and He, Y. (2011). Mapping the Alzheimer's brain with connectomics. *Front. Psychiatry* 2:77. doi: 10.3389/fpsyt.2011.00077

Zalesky, A., Cocchi, L., Fornito, A., Murray, M. M., and Bullmore, E. (2012a). Connectivity differences in brain networks. *NeuroImage* 60, 1055–1062.

Zalesky, A., Fornito, A., and Bullmore, E. (2012b). On the use of correlation as a measure of network connectivity. *NeuroImage* 60, 2096–2106.

Received: 30 May 2012; accepted: 11 July 2012; published online: 27 July 2012.
*Citation: Fornito A and Harrison BJ (2012). Brain connectivity and mental illness. Front. Psychiatry **3**:72. doi: 10.3389/fpsyt.2012.00072*
This article was submitted to Frontiers in Neuropsychiatric Imaging and Stimulation, a specialty of Frontiers in Psychiatry.

frontiers in
PSYCHIATRY

REVIEW ARTICLE
published: 19 April 2012
doi: 10.3389/fpsyt.2012.00032

Connectomic intermediate phenotypes for psychiatric disorders

Alex Fornito[1]* and Edward T. Bullmore[2,3]

[1] *Department of Psychiatry, Melbourne Neuropsychiatry Centre, University of Melbourne and Melbourne Health, Carlton South, VIC, Australia*
[2] *Brain Mapping Unit, Behavioural and Clinical Neurosciences Institute, University of Cambridge, Cambridge, UK*
[3] *GlaxoSmithKline Clinical Unit Cambridge, Addenbrooke's Hospital, Cambridge, UK*

Edited by:
Ben Harrison, The University of Melbourne, Australia

Reviewed by:
Lukas Pezawas, Medical University of Vienna, Austria
Jingyu Liu, University of New Mexico, Mexico

****Correspondence:***
Alex Fornito, Department of Psychiatry, Melbourne Neuropsychiatry Centre, University of Melbourne and Melbourne Health, Levels 2 and 3, 161 Barry Street, Carlton South 3053, VIC, Australia.
e-mail: fornitoa@unimelb.edu.au

Psychiatric disorders are phenotypically heterogeneous entities with a complex genetic basis. To mitigate this complexity, many investigators study so-called intermediate phenotypes (IPs) that putatively provide a more direct index of the physiological effects of candidate genetic risk variants than overt psychiatric syndromes. Magnetic resonance imaging (MRI) is a particularly popular technique for measuring such phenotypes because it allows interrogation of diverse aspects of brain structure and function *in vivo*. Much of this work however, has focused on relatively simple measures that quantify variations in the physiology or tissue integrity of specific brain regions in isolation, contradicting an emerging consensus that most major psychiatric disorders do not arise from isolated dysfunction in one or a few brain regions, but rather from disturbed interactions within and between distributed neural circuits; i.e., they are disorders of brain connectivity. The recent proliferation of new MRI techniques for comprehensively mapping the entire connectivity architecture of the brain, termed the human connectome, has provided a rich repertoire of tools for understanding how genetic variants implicated in mental disorder impact distinct neural circuits. In this article, we review research using these connectomic techniques to understand how genetic variation influences the connectivity and topology of human brain networks. We highlight recent evidence from twin and imaging genetics studies suggesting that the penetrance of candidate risk variants for mental illness, such as those in *SLC6A4*, *MAOA*, *ZNF804A*, and *APOE*, may be higher for IPs characterized at the level of distributed neural systems than at the level of spatially localized brain regions. The findings indicate that imaging connectomics provides a powerful framework for understanding how genetic risk for psychiatric disease is expressed through altered structure and function of the human connectome.

Keywords: endophenotype, schizophrenia, depression, Alzheimer's disease, anxiety, complex, graph analysis, default mode

Genetic factors play a major role in liability for mental illness. Most psychiatric disorders are familial (Gottesman, 1991; Sullivan et al., 2000; Hettema et al., 2001), and twin studies of disease heritability – the proportion of illness susceptibility attributable to genes – indicate that genetic contributions are as high as 80–90% for schizophrenia and bipolar disorder (Cannon et al., 1998; Cardno et al., 1999; McGuffin et al., 2003); 40–70% for major depression (Kendler et al., 1993, 2006; Sullivan et al., 2000); 37 to >90% for autism and autistic traits (Hallmayer et al., 2011; Robinson et al., 2012); 30–70% for substance addiction (Agrawal and Lynskey, 2008); and ∼30–50% for anxiety disorders and obsessive–compulsive disorder (Hettema et al., 2001; van Grootheest et al., 2005). This liability has a complex genetic basis, arising from the combined effect of multiple (hundreds or thousands) genetic variants of small-effect, rather than one or a few genes of large effect (e.g., Purcell et al., 2009). This complexity is compounded by the substantial phenotypic heterogeneity that characterizes most of these disorders. Some of this heterogeneity may be intrinsic to the disease process itself, but a large proportion likely reflects our current lack of biologically informed diagnostic criteria. In practice, this failure to appropriately "carve nature at its joints" (Kendler, 2006) introduces considerable noise into any attempts to map illness phenotypes to genetic risk mechanisms and positions psychiatric disorders, as currently diagnosed, far downstream of the pathophysiological effects of genetic variants influencing disease susceptibility.

One strategy proposed to mitigate the phenotypic heterogeneity of psychiatric disorders involves studying intermediate phenotypes (IPs; Meyer-Lindenberg and Weinberger, 2006). IPs are quantitative, biological traits that are interposed between gene and clinical phenotype on the causal pathway leading from inherited vulnerability to disease. They putatively provide a more direct index of the physiological effects of genetic risk variants and can be used to parse a phenotypically heterogeneous disorder with complex genetic basis into more homogeneous phenotypes with a presumably simpler genetic architecture (see Gottesman and Gould, 2003; Cannon and Keller, 2006; though, see Flint and Munafo, 2007; Walters and Owen, 2007; Kendler and Neale, 2010

for critiques)[1]. Various criteria for viable IPs have been proposed (Gottesman and Gould, 2003; Cannon and Keller, 2006; Walters and Owen, 2007), generally stating that such a phenotype should (1) be quantitative and heritable; (2) differentiate patients from controls; (3) be associated with disease causes rather than effects; (4) co-segregate with illness within families; (5) be more frequent in unaffected individuals at increased genetic risk; and (6) be stable over time (although this last criterion has been challenged; see Pantelis et al., 2009; Gogtay et al., 2011).

Psychiatric disorders are disturbances of mental processes mediated by the brain. Neural measures therefore represent a major class of candidate IPs for mental illness, and *in vivo* neuroimaging has provided a powerful means for identifying and characterizing such IPs for a broad spectrum of psychiatric disease, particularly when related to variation in specific candidate risk genes (Meyer-Lindenberg and Weinberger, 2006). This "imaging genetics" approach has been used to elucidate the mechanisms through which genetically mediated variations in brain structure and function might give risk to psychiatric illness, and provide biological validation of candidate variants (Esslinger et al., 2009; Erk et al., 2010). In some cases, neuroimaging has also been used to augment the search for risk genes (Potkin et al., 2009).

Most imaging genetics work has studied relatively simple IPs, defined using measures of task-related activation or anatomical structure (e.g., gray matter volume or cortical thickness) in specific brain regions. Though the simplicity of these measures is attractive, they likely over-simplify relevant (patho)physiological processes in most cases. Over two decades of neuroimaging research has found that most major psychiatric disorders do not arise from isolated damage to one or a few brain regions, but rather from multiple abnormalities distributed throughout the cerebrum (Phillips et al., 2003b; Belmonte et al., 2004; Menzies et al., 2008; Fornito et al., 2009, 2012; Minzenberg et al., 2009). These abnormalities likely have their origin in disturbed interactions between discrete and distributed neural circuits; i.e., disordered brain connectivity. Moreover, many risk genes for psychiatric disorders are expressed diffusely throughout the brain, acting on physiological pathways involved in synaptic function/regulation, neurotransmitter release, degradation or re-uptake, and the development and maintenance of axonal pathways (Harrison and Weinberger, 2005; Bennett, 2011; Lips et al., 2011; Gai et al., 2012). These considerations indicate that a systems-level approach should prove useful for characterizing the neurophysiological impact of candidate risk variants, and in defining novel IPs.

Attempts to understand genetic influences on distributed brain networks have been greatly facilitated by recent attempts to map the structural and functional properties of the human connectome – the complete set of neural elements and inter-connections comprising the brain (Sporns et al., 2005; Sporns, 2011). The use of neuroimaging to achieve this goal, termed imaging connectomics, has led to the development and proliferation of a rich repertoire of tools for characterizing diverse aspects of human brain connectivity (Bullmore and Sporns, 2009; Bullmore et al., 2009; Fornito and Bullmore, 2010; Margulies et al., 2010). These tools are now increasingly being deployed within genetically informative designs to uncover new connectomic IPs (cIPs) that show promise as sensitive measures of genetic variation in brain structure and physiology (Meyer-Lindenberg, 2009). In this article we overview recent work attempting to understand genetic influences on brain connectivity, focusing principally on studies using magnetic resonance imaging (MRI) that provide illustrative examples of the potential utility of cIPs for characterizing genetic risk mechanisms in mental illness. Our intention is not to identify specific cIPs that fulfill all of the above criteria and which may thus be considered to be comprehensively validated, as this is difficult to achieve in practice. Rather, our aim is to draw attention to emerging evidence suggesting the connectomic measures provide particularly sensitive probes of the functional effects of disease risk genes. As an orientation to relevant concepts, we begin with a brief primer on some basic concepts central to the imaging connectomics approach.

A PRIMER ON IMAGING CONNECTOMICS

Magnetic resonance imaging studies have used a wide range of techniques to explore different properties of the human connectome. A simplified conceptual overview of how some of the most commonly used imaging techniques relate to these properties is presented in **Figure 1**.

Broadly, the connectome can be studied in terms of structure or function. Connectome structure refers to the anatomical connections between different brain regions, and is measured in MRI studies using either T1- or diffusion-weighted imaging (DWI). The former indirectly infers connectivity between regions either through voxel-wise mapping of variations in white matter density, or covariance in regional morphometric parameters, such as gray matter volume or cortical thickness. These morphometric covariance analyses (MCA) can be performed either between a single seed region and all other brain voxels (Pezawas et al., 2005; Meyer-Lindenberg et al., 2007), between (many) pairs of *a priori* defined regions (He et al., 2007; Bassett et al., 2008), or following multivariate decomposition of the data using techniques such as independent component analysis (ICA; Xu et al., 2009a,b). DWI provides a more direct measure of the integrity and trajectory of anatomical connections, subject to certain caveats (Mori and Zhang, 2006; Zalesky and Fornito, 2009; Jbabdi and Johansen-Berg, 2011). Voxel-based analysis (VBA) techniques applied to estimates of white matter density/volume or DWI-derived measures (e.g., axial/radial diffusivity and/or fractional anisotropy) allow whole-brain mapping of differences in white matter integrity or morphometry. This includes methods such as tract-based spatial statistics (TBSS; Smith et al., 2006). Alternatively, connectivity may be indexed with DWI by deterministic or probabilistic tractography of fiber trajectories linking different brain regions, either at the level of specific pairs of brain regions, or between every possible pair of regions defined using some comprehensive cerebral parcelation (Hagmann et al., 2008; Zalesky et al., 2010). With

[1] The term intermediate phenotype is often used synonymously with the related term endophenotype, though there are distinctions between the two (Meyer-Lindenberg and Weinberger, 2006; Walters and Owen, 2007; Kendler and Neale, 2010). We use the term intermediate phenotype here to retain consistency with the wider imaging genetics literature, though we acknowledge that it is unclear whether any of the IPs discussed here may truly act as intermediaries between disease gene and phenotype (see Conclusion).

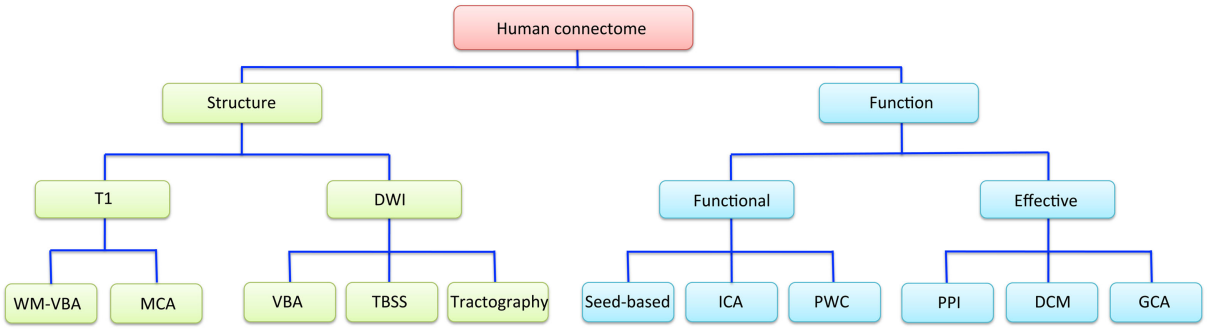

FIGURE 1 | A schematic overview of the different neuroimaging techniques available for measuring structural and functional properties of the human connectome. DCM, dynamic causal modeling; DWI, diffusion-weighted imaging; GCA, Granger causality analysis; ICA, independent component analysis; MCA, morphometric covariance analysis; PPI, psychophysiological interactions; PWC, pair-wise correlations; TBSS, tract-based spatial statistics; T1, T1-weighted imaging; VBA, voxel-based analysis; WM, white matter.

this approach, connectivity is estimated either as the number of tracts intersecting each regional pair (Zalesky et al., 2011), or some index of tissue integrity averaged across the extent of the reconstructed trajectory (van den Heuvel et al., 2010). Note that all of these anatomical measures only provide undirected estimates of inter-regional connectivity; i.e., they may imply that two regions are connected, but they cannot resolve whether the connection runs from region A to B or vice-versa.

Magnetic resonance imaging studies of connectome function generally use blood-oxygenation-level dependent (BOLD) imaging. Functional interactions between regions can be categorized into one of two broad classes: functional and effective connectivity (Friston, 1994). Effective connectivity refers to the influence that one neuronal system exerts over another and allows inferences concerning causal (directed) interactions between regions. The most rudimentary model of effective connectivity is provided by psychophysiological interaction (PPI) analysis (Friston et al., 1997), which involves analyzing task-related changes in connectivity between a seed region and all other brain voxels. Dynamic causal modeling (DCM; Friston et al., 2003) and Granger causality analysis (GCA; Bressler and Seth, 2011) provide more elaborate means for inferring causal interactions between brain regions but have seldom been studied in the context of genetically informative designs (though, see Curcic-Blake et al., 2012 for an exception).

Functional connectivity refers to a statistical dependence between regionally distinct neurophysiological recordings and is undirected in nature. Most frequently, this is measured through simple Pearson correlation of regional activity time courses. This covariance is typically studied between a specific seed region and all other brain voxels (termed a seed-based correlation analysis), or in a pair-wise correlation (PWC) analysis where associations between either a single pair of *a priori* defined regions, or multiple pairs of regions, are computed. Another popular technique for studying functional connectivity involves multivariate spatio-temporal decomposition using techniques such as spatial ICA (Beckmann and Smith, 2004; Calhoun et al., 2004), which offers a data-driven method for identifying spatially independent networks of voxels with temporally coherent activity.

A final important distinction that applies to studies of both connectome function and structure concerns whether inter-regional interactions are studied at the level of connectivity or topology. Studies of connectivity are concerned with measuring variations in the strength and nature (e.g., structural or functional, positive or negative) of connectivity between regions. Studies of topology are concerned with how connections between different brain regions are *configured* with respect to each other. These analyses require relatively comprehensive mapping of inter-regional connectivity using a PWC approach combined with graph analysis to characterize such topological variations (Bullmore and Sporns, 2009; Bullmore and Bassett, 2011). Briefly, graph analysis involves modeling the brain as a graph of nodes, representing brain regions, connected by edges, representing some measure of inter-regional structural or functional interaction. The method allows a wide range of topological properties representing diverse aspects of connectome organization to be computed (Bullmore and Sporns, 2009; Rubinov and Sporns, 2010). Though topology and connectivity are not necessarily independent (Barrat et al., 2004; Alexander-Bloch et al., 2010; Lynall et al., 2010), the distinction between them provides a useful heuristic for evaluating findings in imaging connectomics. In the following, we first consider studies examining genetic influences on brain network connectivity before discussing studies of network topology.

THE GENETICS OF HUMAN BRAIN NETWORK CONNECTIVITY

Most of the connectomic phenotypes studied in imaging genetics studies to date have been relatively specific, focusing on particular neural circuits of theoretical interest. These have typically been investigated by analyzing connectivity between specific pairs of brain regions, or between one seed region and all other brain voxels. Most of this work has used fMRI and therefore focuses on understanding how specific genetic variants influence functional connectivity between regions. Here, we focus on studies of three neural circuits that have been widely studied in imaging genetic research – fronto-limbic, fronto-temporal, and the default mode network. Examples of how genetic variants impact other neural systems can be found elsewhere (e.g., Meyer-Lindenberg et al.,

2007; Tan et al., 2007; Kempf et al., 2008; Krugel et al., 2009; Rasetti et al., 2011).

SLC6A4, MAOA, AND FRONTO-LIMBIC CONNECTIVITY

The first MRI study to examine genetic influences on a connectomic phenotype examined how variation in the human serotonin (5-HT) transporter gene *SLC6A4* impacted functional connectivity between the amygdala and medial prefrontal cortex (mPFC; Heinz et al., 2005). A variable number of tandem repeats (VNTR) in the 5′ promoter region (5-HTTPLR) of *SLC6A4* influences mRNA and protein expression such that a short (*s*) compared to long (*l*) allele is associated with reduced transcriptional efficiency (Heils et al., 1996) and reduced 5-HT transporter binding in the brain (Heinz et al., 2000). Accordingly, the *s* allele has been variably associated with personality traits associated with negative emotionality (Lesch et al., 1996; Munafo et al., 2009), alcohol dependence (McHugh et al., 2010), mood disorders (Clarke et al., 2010), and suicidality (Li and He, 2007). In some cases, these associations may be moderated by environmental factors (Caspi et al., 2010).

Consistent with an association between the *s* allele and negative emotions, an early fMRI study found that human carriers of this allele showed increased amygdala activation during perception of aversive emotional stimuli (Hariri et al., 2002). In a separate study using a similar task, an association was reported between the *s* allele and greater functional connectivity between the amygdala and anterior mPFC (Heinz et al., 2005). This finding was noteworthy given the abundant evidence pointing to the amygdala and mPFC as critical nodes within a broader neural network subserving emotional regulation (Phillips et al., 2003a). These findings were subsequently replicated by an independent group, who also reported an association between the *s* allele and *reduced* functional connectivity between the amygdala and more posterior medial prefrontal regions located in pre- and sub-genual anterior cingulate cortex (ACC; Pezawas et al., 2005). An anatomical basis for these functional effects was suggested by a corresponding reduction in gray matter volume covariance between the amygdala and pre-genual ACC in *s* allele carriers compared to *l*/*l* homozygotes, a finding replicated in an independent study using DTI-derived measures of anatomical connectivity (Pacheco et al., 2009). The functional connectivity measures predicted approximately 30% of the variance in temperamental measures of anxiety-related traits such as harm avoidance. No such association was found with regional indices of activation or volume, indicating that the connectomic measures provided a more direct physiological marker of clinically relevant behavioral phenotypes. Collectively, these results suggest that variation in *SLC6A4* regulates fronto-limbic dynamics in highly specific ways, such that the *s* allele up-regulates functional connectivity between amygdala and anterior mPFC and down-regulates connectivity between amygdala and perigenual ACC (**Figure 2**).

Another genetic variant shown to impact fronto-limbic connectivity is a VNTR in the upstream promoter region of the X-linked Monoamine Oxidase A (*MAOA*) gene (Buckholtz et al., 2008).

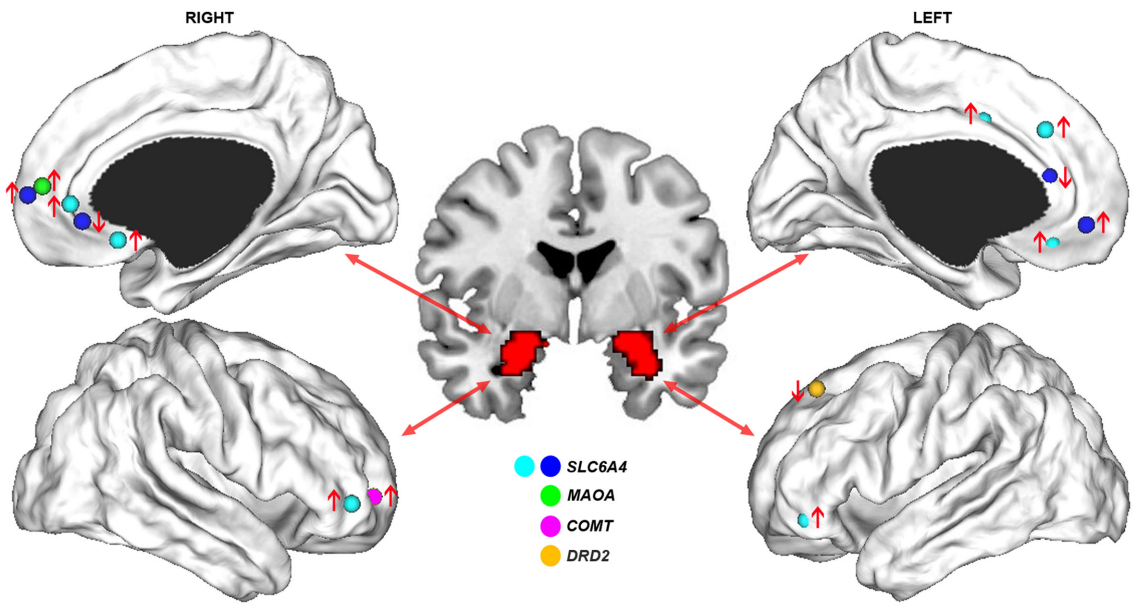

FIGURE 2 | Genetic influences on functional connectivity of fronto-limbic circuits. Cortical surface renderings display the stereotactic peaks of regions in prefrontal cortex where functional connectivity with the amygdala is impacted by common genetic variants. Different colors denote the different genes studied in relation to fronto-limbic functional connectivity; namely, *SLC6A4* (Heinz et al., 2005; Pezawas et al., 2005; Schardt et al., 2010), *MAOA* (Buckholtz et al., 2008), *COMT* (Rasch et al., 2010), and *DRD2* (Blasi et al., 2009). Arrows indicate whether functional connectivity was increased (↑) or decreased (↓) in carriers of the putative risk allele for each gene. The distinction between cyan and blue foci for *SLC6A4* studies differentiates a single study examining functional connectivity during cognitive regulation of emotion (Schardt et al., 2010) from others involving passive perception of emotional stimuli. This distinction illustrates how the risk allele of 5-HTTPLR polymorphism of this gene can be associated with either increased or decreased functional connectivity with the amygdala in adjacent regions of right pre-genual ACC, depending on task context.

MAOA is the main enzyme responsible for catabolizing synaptic 5-HT and norepinephrine, and *MAOA* expression is higher when the VNTR comprises 3.5–4 repeats (*MAOA-H*) than when 2, 3, or 5 repeats are present (*MAOA-L*; Sabol et al., 1998). The low activity allele has been shown to interact with childhood stressors to increase risk for adverse mental health outcomes such as aggressive behavior and mood disturbances (Caspi et al., 2002; Kim-Cohen et al., 2006; Nikulina et al., 2012). Accordingly, functional connectivity between the amygdala and anterior mPFC is higher in *MAOA-L* individuals compared to *MAOA-H* participants performing an emotional perception task (Buckholtz et al., 2008), a finding that parallels the functional connectivity increases between these two regions found in carriers of the *5-HTTPLR-s* allele (Heinz et al., 2005; Pezawas et al., 2005; **Figure 2**).

The common effect of the MAOA-L and 5-HTTPLR-s alleles on amygdala–mPFC circuitry may result from a shared influence on synaptic serotonin levels, as both are thought to be associated with increased brain 5-HT. Greater functional connectivity between the amygdala and anterior mPFC may therefore represent a final common pathway for genetically mediated increases in synaptic 5-HT concentrations. Contrary to this view however, recent imaging evidence suggests that *5-HTPPLR* genotype has little effect on basal synaptic serotonin levels (Jedema et al., 2010; Murthy et al., 2010). As such, the precise mechanism through which the polymorphism influences mPFC–amygdala connectivity remains unclear, but may be related to its emerging role in neurodevelopment (Ansorge et al., 2004). Regardless of the precise mechanism, it is noteworthy that the effects seem specific to variants impacting on *5-HT* function, as functional polymorphisms in genes that do not directly impact this neurotransmitter show no effect on amygdala–mPFC connectivity. For example, two genetic variants that influence synaptic dopamine levels, the $Val^{108/158}$ Met polymorphism of the catechol-*o*-methyl transferase (*COMT*) gene, and the rs1076560 polymorphism of the D_2 receptor gene *DRD2*, influence functional connectivity between the amygdala and lateral, but not medial, PFC (Buckholtz et al., 2008; Blasi et al., 2009; Rasch et al., 2010; **Figure 2**). These findings point to highly specific genetic influences on different components of fronto-limbic circuitry.

Some of these genetic effects can be expressed in different ways depending on psychological context. For example, during conditions requiring cognitive regulation of emotion, *s* allele carriers actually show *increased* functional connectivity between the amygdala and perigenual ACC (Schardt et al., 2010). This result indicates that the previously reported reduction in functional coupling between these regions does not reflect a hard-wired deficit, despite evidence for anatomical connectivity reductions between these regions (Pezawas et al., 2005). Rather, the connectivity reduction may reflect a bias to process aversive stimuli in maladaptive ways, which may be ameliorated given appropriate environmental circumstances. In this regard, the connectivity increase in *s* allele carriers during cognitive regulation of emotion may reflect the deployment of greater processing resources to overcome this processing bias. These context-specific effects on connectomic phenotypes are consistent with evidence for environmental factors such as life stress moderating the influence of *SLC6A4* genotype on functional connectivity of the amygdala (Canli et al., 2006).

To summarize, studies of the *SLC6A4* and *MAOA* genes provide examples of how genetic influences on brain connectivity can be expressed in circuit specific ways, and in a manner contingent on environmental context. The circuit- and context-specificity of these effects is underscored by work on other genes, such as *CA1CNAC* (Erk et al., 2010), α5 acetylcholine receptor subunit (*CHRNA5*; Hong et al., 2010), brain-derived neurotrophic factor (*BDNF*; Mukherjee et al., 2011), and α2b-adrenergic receptor (*ADRA2B*; Rasch et al., 2009). Variants in each of these genes have been shown to impact fronto-limbic circuitry in a task-dependent manner, and in regions outside the amygdala–mPFC loop influenced by *SLC6A4* and *MAOA*. Understanding how each of these variants impact different components of fronto-limbic circuits, and under what conditions, will no doubt prove to be a challenging task.

FRONTO-TEMPORAL CONNECTIVITY AND ZNF804A

Fronto-temporal connectivity is of particular interest to schizophrenia researchers, as diverse lines of evidence point to altered structural and functional interactions between frontal and temporal brain regions as a core feature of the disease phenotype (Weinberger et al., 1992; Meyer-Lindenberg et al., 2005; Ellison-Wright and Bullmore, 2009; van den Heuvel et al., 2010; Fornito et al., 2011a, 2012; Pettersson-Yeo et al., 2011). Accordingly, variation in several candidate risk genes for schizophrenia has been shown to impact fronto-temporal connectivity, including loci in *COMT* (Bertolino et al., 2006; Dennis et al., 2010b), *RGS4* (Buckholtz et al., 2007), *PPP1R1B* encoding DAARP-32 (Curcic-Blake et al., 2012), and *ErbB4* (Konrad et al., 2009).

One genetic variant receiving increasing attention for its effects on fronto-temporal circuitry is the rs1344706 polymorphism of *ZNF804A*. The gene encodes a zinc finger domain protein with unknown function, although preliminary evidence suggests a role in oligodendrocyte regulation (Riley et al., 2010) and neurodevelopment (Chung et al., 2010). The rs1344706 polymorphism has now been implicated as a genome-wide significant risk variant for both schizophrenia and bipolar disorder in several independent samples (O'Donovan et al., 2008; Stefansson et al., 2009; Riley et al., 2010; Steinberg et al., 2011), with fine-mapping of nearly all common variants in the gene confirming that rs1344706 is the most strongly associated marker (Williams et al., 2011). The polymorphism is functional, affecting *ZNF804A* expression (Williams et al., 2011) and DNA–protein binding (Hill and Bray, 2011).

The first study to investigate the effects of the rs1344706 polymorphism on the brain used fMRI to examine activation and functional connectivity during performance of a working memory and emotion perception task (Esslinger et al., 2009). The variant was not found to impact measures of regional activation, but did influence inter-regional functional connectivity, suggesting its effects show higher penetrance at the level of distributed neural systems. Specifically, carriers of the risk associated *A* allele demonstrated reduced functional connectivity of the dorsolateral PFC with other ipsi- and contra-lateral prefrontal regions, as well as increased functional connectivity between dorsolateral PFC and the hippocampal formation, during working memory performance. Increased fronto-hippocampal functional connectivity had previously been reported in a positron emission tomography

study of patients with schizophrenia (Meyer-Lindenberg et al., 2005) and was thus interpreted as a possible cIP mediating the role of *ZNF804A* in risk for the disorder. The *A* allele was also associated with enhanced functional connectivity within fronto-limbic circuits during the emotional perception task, which was interpreted as a possible cIP for bipolar disorder. Thus, this study pointed to context-specific and pleiotropic effects of the rs1344706 polymorphism with relevance for understanding its role in risk for both schizophrenia and bipolar disorder.

A subsequent study in an independent sample using the same working memory task replicated the association between the *A* allele and both increased fronto-hippocampal functional coupling and decreased fronto-frontal connectivity (Rasetti et al., 2011). The lack of a significant effect on regional activation was also replicated. Similar connectivity changes were apparent in schizophrenia patients and their unaffected relatives suggesting that these changes may indeed represent a candidate cIP for the disorder (**Figure 3**). However, the *A* allele carriers in this study showed stronger *negative* fronto-hippocampal functional connectivity, contrasting the original report of higher *positive* functional connectivity between these two regions (Esslinger et al., 2011). These results suggest distinct interpretations: stronger positive connectivity implies greater functional integration or cooperation between regions; stronger negative connectivity points to antagonistic or competitive dynamics (Clare Kelly et al., 2008). The reasons for this discrepancy are unclear, although the fact that stronger negative functional connectivity has been found in patients and their unaffected relatives (Meyer-Lindenberg et al., 2005; Rasetti et al., 2011) suggests that it may provide a more faithful representation of genetically influenced pathophysiological processes in schizophrenia.

The effect of the rs1344706 variant on fronto-hippocampal connectivity may be less robust than its effect on fronto-frontal coupling, and may only be expressed in certain contexts. In one recent study, the variant was found to influence fronto-hippocampal functional connectivity only during working memory performance, whereas it impacted fronto-frontal coupling during working memory, emotion perception, and resting-state paradigms (Esslinger et al., 2011). Thus, the effect on fronto-frontal connectivity may be generalized, possibly resulting from an influence on anatomical connectivity between these regions (Wei et al., 2010), whereas the association with fronto-hippocampal coupling may be context-specific. This result is consistent with research into the effects of *SLC6A4* variation on fronto-limbic circuitry (e.g., Schardt et al., 2010) demonstrating the highly context-specific influences of genetic variants of brain functional dynamics. Precisely mapping the circumstances under which these genetic effects are expressed will be an important step in characterizing the functional significance of any putative cIPs related to *ZNF804A* variation, particularly given recent evidence that schizophrenia may also be characterized by a profile of both generalized and context-specific functional connectivity deficits which affect prefrontal regions in particular (Fornito et al., 2011a).

APOE AND THE DEFAULT MODE NETWORK

The DMN comprises regions of posterior cingulate cortex (PCC), precuneus, medial PFC and lateral parietal cortices, and functionally couples with the hippocampus under certain task contexts (Buckner et al., 2008). The DMN characteristically shows elevated activity during passive rest conditions or tasks requiring introspective processing and deactivates during cognitively demanding tasks (Shulman et al., 1997; Buckner et al., 2008; Harrison et al., 2008, 2011). Alterations of DMN connectivity have been found in patients suffering a range of neuropsychiatric disorders including schizophrenia (Bluhm et al., 2007), autism (Kennedy and Courchesne, 2008), attention-deficit hyperactivity disorder (Castellanos et al., 2008), major depression (Greicius et al., 2007), and Alzheimer's disease (Greicius et al., 2004; see Sonuga-Barke and Castellanos, 2007; Zhang and Raichle, 2010 for reviews). In the case of schizophrenia, similar alterations have been found in patients' unaffected relatives, suggesting an association between DMN connectivity changes and genetic risk for the disorder (Whitfield-Gabrieli et al., 2009). Accordingly, specific variants in genes linked to risk for psychosis, such as the D-Amino Acid Oxidase (*DAAO*; Papagni et al., 2011; Prata et al., 2012) and neuregulin-1 (*NRG1*; Winterer et al., 2008), have been shown to impact structural and functional connectivity of DMN regions.

Confirmation that functional connectivity of the DMN is under genetic control came from a recent resting-state fMRI study of a sample of extended pedigrees comprising 333 individuals selected from 29 families (Glahn et al., 2010). Spontaneous neural dynamics measured during the so-called resting-state, when people lie

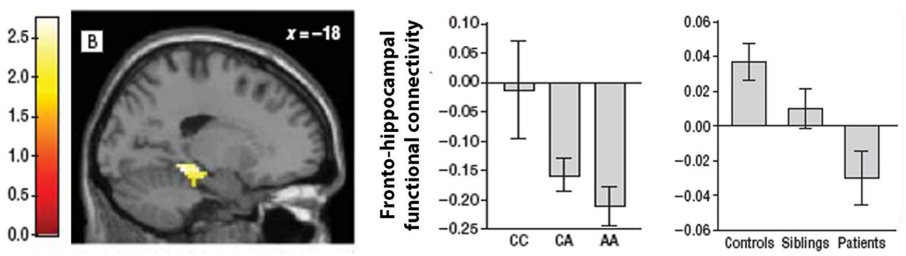

FIGURE 3 | Illustration of the hippocampal region where functional connectivity with a seed in right dorsolateral PFC was influenced by *ZNF804A* variation and was found to differ between schizophrenia patients, their unaffected relatives and healthy controls. The two bar charts plot parameter estimates for fronto-hippocampal functional connectivity as a function of *ZNF804A* in healthy controls (middle), and in controls, patients, and siblings (right). Carriers of the *A* risk allele showed an increasing trend toward greater negative functional connectivity, as did patients with schizophrenia. Image adapted from Rasetti et al. (2011).

quietly in the scanner without performing any specific task, are highly organized and correlate in a manner that recapitulates well-known functional networks (Biswal et al., 1995; Smith et al., 2009). The topography of these networks is robust over time and individuals (Damoiseaux et al., 2006; Shehzad et al., 2009) and has been linked to neurophysiological measures (He et al., 2008; Shmuel and Leopold, 2008). In addition, spontaneous BOLD signal fluctuations influence task-evoked activity (Fox et al., 2006; Mennes et al., 2011), perception (Hesselmann et al., 2008), and behavior (Fox et al., 2007), suggesting that they represent an intrinsic and functionally important component of neural dynamics (Fox and Raichle, 2007; though, see Morcom and Fletcher, 2007; Fornito and Bullmore, 2010 for caveats). The extended pedigree design exploited the varying degree of genetic relatedness between participants to estimate genetic and environmental influences on functional connectivity of the DMN, as characterized using ICA. Genetic influences on an averaged estimate of functional connectivity of the entire DMN were significant, with heritability (h^2) estimated to be 0.42. The degree to which each constituent region of the DMN was functionally connected with the entire network was also heritable, ranging from 0.33 to 0.42 for key nodes such as posterior cingulate/precuneus, mPFC, and lateral parietal cortex.

Despite the DMN's involvement in a wide range of diseases, the most frequently studied genetic locus in relation to DMN connectivity has been the Apolipoprotein E (*APOE*) gene. The gene encodes a lipoprotein that in the central nervous system, plays a role in coordinating mobilization of cholesterol, phospholipids, and fatty acids, and has been implicated in neuronal development, plasticity, and repair (Mahley and Rall, 2000). The gene has three allelic variants – ε2, ε3, and ε4. Homozygosity for the last is the most established genetic risk factor for late-onset Alzheimer's disease, being associated with a >10-fold increase in risk (Farrer et al., 1997; Bertram et al., 2007). In contrast, average allelic summary odds ratios for non-*APOE*-related variants are ∼1.25 (Bertram and Tanzi, 2008). *APOE* has also been implicated in the pathophysiology of schizophrenia and mood disorders (Gibbons et al., 2011).

Several studies have demonstrated an association between the ε4 allele and both increased and decreased functional connectivity of the DMN and medial temporal regions, though reports of increases have been more common in younger samples (Filippini et al., 2009; Dennis et al., 2010a; Sheline et al., 2010a,b; Machulda et al., 2011; Westlye et al., 2011). One hypothesis proposed to explain this age effect is that ε4 carriers inherit a cIP characterized by enhanced DMN connectivity early in life. This enhanced connectivity facilitates the spread of amyloid-β plaques, the primary pathological characteristic of Alzheimer's disease, throughout the network and exacerbates risk of disease onset and progression (Machulda et al., 2011; Seeley, 2011). With advancing age, these plaques accumulate and result in a deterioration of DMN function and concomitant reduction of network connectivity relative to non-risk allele carriers. Though this postulate requires experimental verification, it is supported by reports that DMN regions are among the first to show aggregation of amyloid-β plaques in Alzheimer's disease and that these plaques disperse throughout the network with disease progression (Buckner et al., 2005, 2009). It also accords with reports that gray matter volume loss in neurodegenerative disease occurs within functionally connected networks (Seeley et al., 2009).

The effects of *APOE* genotype on functional connectivity are often apparent in the absence of any differences in gray matter volume, cognitive impairment, or β-amyloid deposition (Dennis et al., 2010a; Sheline et al., 2010a; Machulda et al., 2011). In addition, one recent study found that resting-state connectivity measures of the DMN were able to differentiate between cognitively unimpaired ε4 carriers with a family history of Alzheimer's disease and individuals without any apparent genetic risk with an effect size approximately three times greater than was possible using measures of task-related activation during a memory encoding paradigm (Fleisher et al., 2009). Such findings provide a powerful demonstration of the enhanced sensitivity provided by connectomic measures for indexing the physiological effects of disease risk variants, and support the contention that these variants often show higher penetrance at the level of distributed neural systems.

THE GENETICS OF HUMAN BRAIN NETWORK TOPOLOGY

The preceding discussion illustrates how genetic variation can influence the nature and strength of connectivity between different brain regions. We now consider studies of genetic influences on how connections are arranged in the brain; i.e., how genes influence the topology of the connectome. Such an investigation is motivated by the sparse character of brain connectivity. The human cerebral cortex comprises an estimated 10^{11} neurons connected by 10^{13} fibers (Braitenberg and Schüz, 1991). Though numerous, these connections represent only a small fraction of the total 5×10^{21} connections that are possible. Similarly, neuronal connectivity in the nematode worm *Caenorhabditis elegans*, which has been comprehensively mapped at the level of each and every synapse, comprises <3% of the total number of connections possible while estimates of the degree of inter-regional connectivity (i.e., connectivity between distinct cytoarchitectonic regions) in the macaque monkey *Macaca mulatta* and the feline brain range from 18 to 38% (Latora and Marchiori, 2003; Kaiser and Hilgetag, 2006). This sparsity suggests that connections between brain regions develop according to specific constraints and/or design principles that are likely to be under genetic control.

Ramón y Cajal (1995) proposed over a century ago that one critical organizational principle for brain networks involves the minimization of wiring costs. The adaptive benefit of this principle is clear, as less wiring reduces the total energy required to support neuronal communication (Laughlin and Sejnowski, 2003). Accordingly, a substantial body of evidence has accumulated to suggest that pressure to minimize wiring costs can explain numerous aspects of cortical organization, including axonal branching and cortical folding patterns (Van Essen, 1997; Cherniak et al., 1999), neuronal morphology (Buzsaki et al., 2004; Chklovskii, 2004), the spatial location of neurons and cytoarchitectonic fields (Klyachko and Stevens, 2003; Cherniak et al., 2004), and even the fraction of cortical volume occupied by axons and dendrites (Chklovskii et al., 2002). However, wiring cost minimization alone cannot account for all design features of nervous system networks (Chen et al., 2006; Kaiser and Hilgetag, 2006), and recent evidence points to a trade-off between cost minimization and the

emergence of topological properties such as communication efficiency, which may be behaviorally advantageous but entail a wiring cost premium (Kaiser and Hilgetag, 2006; Bassett et al., 2010).

The topological efficiency of a network can be readily quantified using graph theoretic techniques. In complex networks, communication is more efficient when fewer connections must be traversed to transfer information between any two nodes; the fewer the connections, the faster the rate of information transmission, and the lower the probability of signal degradation or transmission errors (Latora and Marchiori, 2003). In an economically wired network, long-range projections act as topological short-cuts that reduce the mean path length between regions and dramatically increase communication efficiency (Buzsaki et al., 2004; Kaiser and Hilgetag, 2006). However, these short-cuts come at the cost of increased wiring. In principle it would be possible to maximize network efficiency simply by adding more connections (Latora and Marchiori, 2003; Achard and Bullmore, 2007), though the metabolic costs associated with forming and maintaining each connection limit the total volume of wiring that can be supported (Laughlin and Sejnowski, 2003). This balance, between efficiency maximization and connection cost minimization, may be construed as one concerned with the optimization of connection cost-efficiency. The importance of this balance for the connectome was recently underscored by a study showing that the physical embedding of the brain's connectivity architecture in the three-dimensional space of the skull is optimally cost-efficient, subject to certain higher-dimensional constraints (Bassett et al., 2010).

We examined the heritability of cost-efficient properties of functional brain network topology using resting-state fMRI in healthy twins (Fornito et al., 2011b). Network efficiency was measured using established graph theoretic methods (Latora and Marchiori, 2001), whereas connection costs were estimated indirectly using a measure of physical distance between regions. We found that the balance between these two measures, taken as an index of network cost-efficiency, was highly heritable at a global level, with genetic factors accounting for approximately 60% of the phenotypic variance. These influences were not uniformly distributed throughout the cortex, with regional estimates of significant genetic influences ranging from 0.30 to 0.80 (**Figure 4**). Some of the largest effects were seen in regions of lateral PFC and core components of the DMN, such as posterior cingulate and medial prefrontal cortices (**Figure 4**). Heritability estimates in these regions are comparable to those reported for whole-brain and regional gray matter volume ($0.66 < h^2 < 0.97$; Thompson et al., 2001; Peper et al., 2007), cognitive abilities ($0.30 < h^2 < 0.80$; McClearn et al., 1997; Bouchard, 1998; Boomsma et al., 2002), and various measures of personality and psychopathology ($0.50 < h^2 < 0.60$; Boomsma et al., 2002). They also compare favorably with heritability estimates for simple measures of functional connectivity within the DMN ($0.33 < h^2 < 0.42$; Glahn et al., 2010), as well as regional task-related activation ($0.40 < h^2 < 0.80$; Koten et al., 2009; Blokland et al., 2011) and DTI-derived measures of anatomical connectivity ($0.55 < h^2 < 0.85$; Chiang et al., 2009).

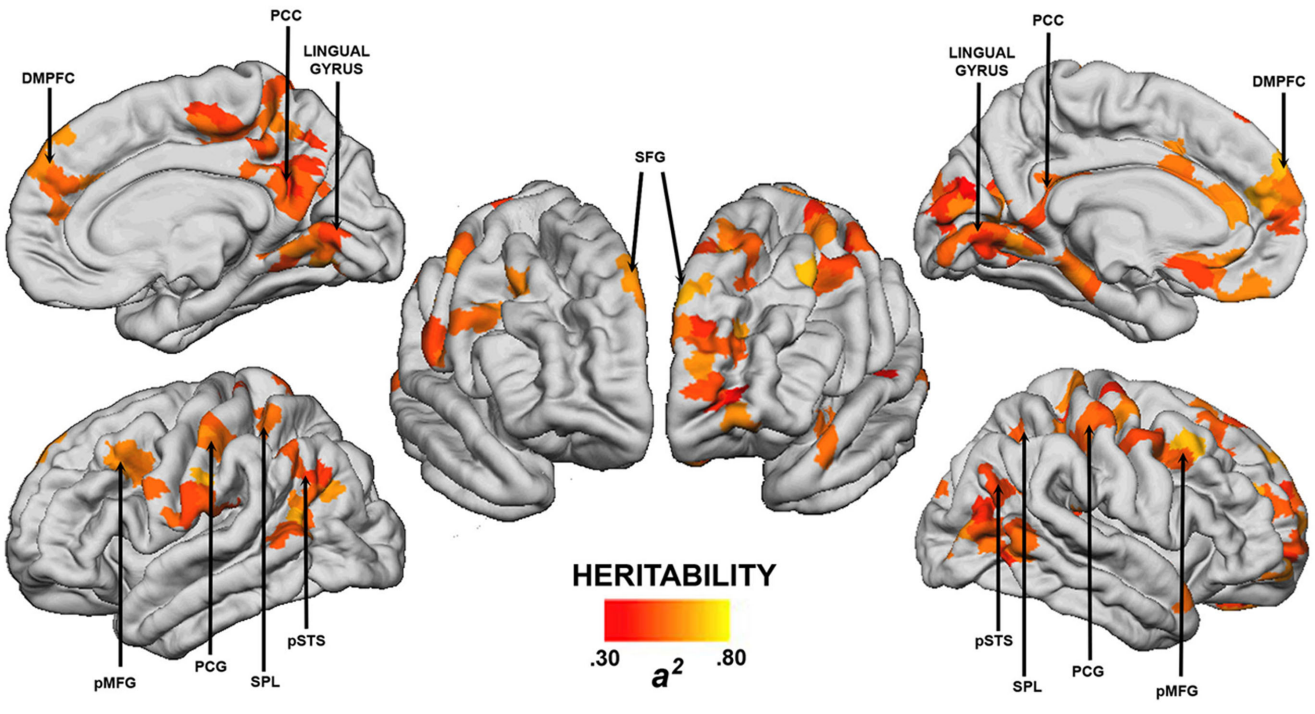

FIGURE 4 | Cortical regions showing statistically significant ($p < 0.05$, corrected) heritability for regional cost-efficiency of network functional connectivity. Arrows highlight regions showing significant genetic effects in both cerebral hemispheres. DMPFC, dorso-medial prefrontal cortex; PCC, posterior cingulate cortex; SFG, superior frontal gyrus; pMFG, posterior middle frontal gyrus; PCG, post-central gyrus; SPL, superior parietal lobule; pSTS, posterior superior temporal sulcus. Left hemisphere is presented on the right. Image reproduced from Fornito et al. (2011b).

The adaptive benefit of a cost-efficient neural architecture is intuitive, and it is plausible that evolution would favor connections that can provide high communication efficiency for low metabolic cost. Evidence that greater topological efficiency and/or greater cost-efficiency predicts better performance on tests of intelligence and working memory (Bassett et al., 2009; Li et al., 2009; van den Heuvel et al., 2009; Zalesky et al., 2011), and that alterations of network efficiency and cost-efficiency are apparent in a range of patient groups, including schizophrenia (Bassett et al., 2009; Lynall et al., 2010; Zalesky et al., 2011), ADHD (Wang et al., 2009), and Alzheimer's disease (Lo et al., 2010), indicates that these findings have clear implications for psychiatric disorders. To our knowledge however, no study to date has examined how variations in specific candidate genes influence brain network cost-efficiency, or any other topological properties of the connectome.

Cost-efficiency optimization is but one of many potential organizational principles for the connectome. Indeed, graph analytic studies of neuroimaging data have pointed to several other candidate topological properties that may be under genetic control. For example, both structural and functional human brain networks are characterized by a small-world topology (Achard et al., 2006; Hagmann et al., 2007), which concurrently supports locally segregated and globally integrated connectivity to provide high dynamical complexity, a property that may have been favored by evolutionary processes (Sporns et al., 2000). The human connectome also possesses a hierarchical, modular architecture; i.e., it can be decomposed into subsets of regions, termed modules, that show relatively high connectivity with each other than with other areas at multiple scales of resolution, allowing the formation of modules within modules and so on (Meunier et al., 2009; Bassett et al., 2010). This property has been associated with enhanced functional stability and diversity (Kaiser et al., 2007), the emergence of self-organized, critical dynamics (Rubinov et al., 2011), and may be intimately linked to optimization of connection cost-efficiency (Bassett et al., 2010).

These considerations raise questions as to whether genetic influences are specific to network cost-efficiency, or are related to other topological variations. In our analysis, we found no evidence for genetic influences on a range of other topological properties frequently studied in the graph theoretic literature, including clustering, path length, small-worldness, and global and local efficiency, although we did not examine modularity (Fornito et al., 2011b). Other studies have however reported heritability values as high as 0.80 for some of these measures, computed for functional networks derived from electroencephalographic (EEG) recordings (Smit et al., 2008). The reasons for these inconsistencies are unclear, but may be related to the imaging techniques employed or the enhanced power provided by the much larger sample analyzed in the EEG study. In general, the high degree of inter-correlation between different topological measures of brain network organization (Alexander-Bloch et al., 2010; Lynall et al., 2010), means that multivariate genetic analyses allowing categorization of different topological measures into distinct groupings defined by common genetic influences will be critical for identifying the primary genetic constraints on connectome development and organization.

CONCLUSION

This brief overview illustrates the potential power of imaging connectomics in the search for IPs for neuropsychiatric disorders. Specifically, the available data indicate that connectomic measures are able to index the physiological effects of disease risk genes when simpler regional measures of activation or volume, or cognition, cannot (Esslinger et al., 2009; Dennis et al., 2010a; Sheline et al., 2010a; Machulda et al., 2011; Rasetti et al., 2011). They also indicate that variations in cIPs correlate with relevant behavioral indices when regional measures do not (Pezawas et al., 2005; Buckholtz et al., 2008), and that certain connectomic phenotypes are highly heritable (Chiang et al., 2009; Glahn et al., 2010; Fornito et al., 2011b). Collectively, these data support the idea that the penetrance of many disease risk genes is higher at the level of distributed brain systems than at the level of isolated brain regions, a conclusion consistent with an emerging consensus that many psychiatric disorders arise from genetically mediated vulnerabilities in discrete neural circuits (Meyer-Lindenberg and Weinberger, 2006; Meyer-Lindenberg, 2009, 2010; Insel, 2011). As such, cIPs may offer greater sensitivity for characterizing genetic effects in imaging genetic designs than more traditional, regionally focused neuroimaging measures.

One potential criticism of cIPs is that, by design, they are more complicated, requiring additional processing steps and assumptions for their derivation. Characterizing activation or volume in a single region is intrinsically univariate, requiring measurement of one property describing the behavior of that region, whereas connectivity measures are intrinsically bi or multivariate as they involve two or more regions by definition. The problem is worse for graph analytic studies, which often incorporate multiple measures and processing steps when computing topological properties. Each additional measure and step can introduce noise into the analysis, making the resulting phenotypic characterizations less reliable (Habeck and Moeller, 2011), and placing an upper limit on power for detecting genetic effects (Kendler and Neale, 2010; Blokland et al., 2011). Moreover, more complex measures presumably have a more complex genetic basis. This emphasis on simplicity and reliability must however be balanced with a need to define valid and pathophysiologically relevant IPs. Most major psychiatric diseases are disorders of brain connectivity, and the physiological effects of putative disease risk variants are likely to be expressed throughout multiple, interconnected neural circuits. Connectomic measures will provide a more sensitive index of these effects. The findings discussed here support these conclusions, and demonstrate that even highly derived topological properties, such as network cost-efficiency, can show high heritability (Fornito et al., 2011b). Moreover, recent studies have shown that connectomic measures, despite their increased complexity, represent more robust biomarkers of schizophrenia (Calhoun et al., 2008; Erhardt et al., 2011; Bassett et al., 2012) and risk for Alzheimer's disease (Fleisher et al., 2009), than simpler, regional measures. Thus, while parsimony and reliability are always important, candidate IPs should be selected for their reliability and their hypothesized role in relevant pathophysiological processes; not purely for their simplicity.

A more general criticism often leveled at the IP approach concerns whether any candidate IPs studied thus far are truly "intermediate" in the sense that they mediate the effects of candidate genetic variants on disease risk or expression (Walters and Owen, 2007; Kendler and Neale, 2010). Under such a mediation model, the risk gene is assumed to influence the IP, which in turn influences illness susceptibility (i.e., gene > IP > disorder); thus, the IP is truly interposed between gene and disorder. In this case the IP is likely to represent a physiological mechanism through which genetic risk is expressed. An alternative possibility however, is that the gene exerts pleiotropic and possibly independent effects on both the IP and disease risk (i.e., IP < gene > disorder). Under this liability model, the IP is not involved in disease pathophysiology but may represent a biomarker of illness susceptibility. Distinguishing between these two possibilities experimentally is challenging (Walters and Owen, 2007; Kendler and Neale, 2010) and it is thus unclear which category the cIPs discussed here fall into. Our use of the term "IP" in reference to the measures discussed here is therefore subject to this caveat. In practice however, the distinction may be overly simplistic as it assumes near-complete genetic overlap between the IP and psychiatric disorder. A more likely scenario is that IPs and psychiatric disorders posses both common and independent genetic influences which require multivariate analyses in genetically informative samples for complete characterization (Kendler and Neale, 2010). To our knowledge, no such studies of cIPs have yet been conducted.

Though it is as yet unclear whether any of the candidate IPs identified to date should be best conceptualized using mediation, liability, or multivariate models, they can certainly provide important clues as to how genetic risk factors influence variation in key phenotypic properties of psychiatric disease. Mapping differences and commonalities in these properties across disorders may prove useful in developing new, biologically informed diagnostic criteria. In addition, preliminary evidence suggests that IPs can augment the search for novel risk genes (Potkin et al., 2009). The research reviewed here indicates that this kind work will benefit from a greater focus on identifying novel IPs that describe systems-level properties of the brain, and that imaging connectomics provides a powerful methodological and conceptual framework for doing so.

ACKNOWLEDGMENTS

Alex Fornito was supported by a National Health and Medical Research Council CJ Martin Fellowship (ID: 454797).

REFERENCES

Achard, S., and Bullmore, E. (2007). Efficiency and cost of economical brain functional networks. *PLoS Comput. Biol.* 3, e17. doi:10.1371/journal.pcbi.0030017

Achard, S., Salvador, R., Whitcher, B., Suckling, J., and Bullmore, E. (2006). A resilient, low-frequency, small-world human brain functional network with highly connected association cortical hubs. *J. Neurosci.* 26, 63–72.

Agrawal, A., and Lynskey, M. T. (2008). Are there genetic influences on addiction: evidence from family, adoption and twin studies. *Addiction* 103, 1069–1081.

Alexander-Bloch, A. F., Gogtay, N., Meunier, D., Birn, R., Clasen, L., Lalonde, F., Lenroot, R., Giedd, J., and Bullmore, E. T. (2010). Disrupted modularity and local connectivity of brain functional networks in childhood-onset schizophrenia. *Front. Syst. Neurosci.* 4:147. doi:10.3389/fnsys.2010.00147

Ansorge, M. S., Zhou, M., Lira, A., Hen, R., and Gingrich, J. A. (2004). Early-life blockade of the 5-HT transporter alters emotional behavior in adult mice. *Science* 306, 879–881.

Barrat, A., Barthelemy, M., Pastor-Satorras, R., and Vespignani, A. (2004). The architecture of complex weighted networks. *Proc. Natl. Acad. Sci. U.S.A.* 101, 3747–3752.

Bassett, D. S., Bullmore, E., Verchinski, B. A., Mattay, V. S., Weinberger, D. R., and Meyer-Lindenberg, A. (2008). Hierarchical organization of human cortical networks in health and schizophrenia. *J. Neurosci.* 28, 9239–9248.

Bassett, D. S., Bullmore, E. T., Meyer-Lindenberg, A., Apud, J. A., Weinberger, D. R., and Coppola, R. (2009). Cognitive fitness of cost-efficient brain functional networks. *Proc. Natl. Acad. Sci. U.S.A.* 106, 11747–11752.

Bassett, D. S., Greenfield, D. L., Meyer-Lindenberg, A., Weinberger, D. R., Moore, S. W., and Bullmore, E. T. (2010). Efficient physical embedding of topologically complex information processing networks in brains and computer circuits. *PLoS Comput. Biol.* 6, e1000748. doi:10.1371/journal.pcbi.1000748

Bassett, D. S., Nelson, B. G., Mueller, B. A., Camchong, J., and Lim, K. O. (2012). Altered resting state complexity in schizophrenia. *Neuroimage* 59, 2196–2207.

Beckmann, C. F., and Smith, S. M. (2004). Probabilistic independent component analysis for functional magnetic resonance imaging. *IEEE Trans. Med. Imaging* 23, 137–152.

Belmonte, M. K., Allen, G., Beckel-Mitchener, A., Boulanger, L. M., Carper, R. A., and Webb, S. J. (2004). Autism and abnormal development of brain connectivity. *J. Neurosci.* 24, 9228–9231.

Bennett, M. R. (2011). Schizophrenia: susceptibility genes, dendritic-spine pathology and gray matter loss. *Prog. Neurobiol.* 95, 275–300.

Bertolino, A., Rubino, V., Sambataro, F., Blasi, G., Latorre, V., Fazio, L., Caforio, G., Petruzzella, V., Kolachana, B., Hariri, A., Meyer-Lindenberg, A., Nardini, M., Weinberger, D. R., and Scarabino, T. (2006). Prefrontal-hippocampal coupling during memory processing is modulated by COMT val158met genotype. *Biol. Psychiatry* 60, 1250–1258.

Bertram, L., McQueen, M. B., Mullin, K., Blacker, D., and Tanzi, R. E. (2007). Systematic meta-analyses of Alzheimer disease genetic association studies: the AlzGene database. *Nat. Genet.* 39, 17–23.

Bertram, L., and Tanzi, R. E. (2008). Thirty years of Alzheimer's disease genetics: the implications of systematic meta-analyses. *Nat. Rev. Neurosci.* 9, 768–778.

Biswal, B., Yetkin, F. Z., Haughton, V. M., and Hyde, J. S. (1995). Functional connectivity in the motor cortex of resting human brain using echo-planar MRI. *Magn. Reson. Med.* 34, 537–541.

Blasi, G., Lo Bianco, L., Taurisano, P., Gelao, B., Romano, R., Fazio, L., Papazacharias, A., Di Giorgio, A., Caforio, G., Rampino, A., Masellis, R., Papp, A., Ursini, G., Sinibaldi, L., Popolizio, T., Sadee, W., and Bertolino, A. (2009). Functional variation of the dopamine D2 receptor gene is associated with emotional control as well as brain activity and connectivity during emotion processing in humans. *J. Neurosci.* 29, 14812–14819.

Blokland, G. A., McMahon, K. L., Thompson, P. M., Martin, N. G., de Zubicaray, G. I., and Wright, M. J. (2011). Heritability of working memory brain activation. *J. Neurosci.* 31, 10882–10890.

Bluhm, R. L., Miller, J., Lanius, R. A., Osuch, E. A., Boksman, K., Neufeld, R. W., Theberge, J., Schaefer, B., and Williamson, P. (2007). Spontaneous low-frequency fluctuations in the BOLD signal in schizophrenic patients: anomalies in the default network. *Schizophr. Bull.* 33, 1004–1012.

Boomsma, D., Busjahn, A., and Peltonen, L. (2002). Classical twin studies and beyond. *Nat. Rev. Genet.* 3, 872–882.

Bouchard, T. J. Jr. (1998). Genetic and environmental influences on adult intelligence and special mental abilities. *Hum. Biol.* 70, 257–279.

Braitenberg, V., and Schüz, A. (1991). *Anatomy of the Cortex: Statistics and Geometry*. Berlin: Springer.

Bressler, S. L., and Seth, A. K. (2011). Wiener-Granger causality: a well established methodology. *Neuroimage* 58, 323–329.

Buckholtz, J. W., Callicott, J. H., Kolachana, B., Hariri, A. R., Goldberg, T. E., Genderson, M., Egan, M. F., Mattay, V. S., Weinberger, D. R., and Meyer-Lindenberg, A. (2008). Genetic variation in MAOA modulates ventromedial prefrontal circuitry mediating individual differences in human personality. *Mol. Psychiatry* 13, 313–324.

Buckholtz, J. W., Meyer-Lindenberg, A., Honea, R. A., Straub, R. E., Pezawas, L., Egan, M. F., Vakkalanka, R., Kolachana, B., Verchinski, B. A., Sust, S., Mattay, V. S., Weinberger, D. R., and Callicott, J. H. (2007). Allelic variation in RGS4 impacts functional and structural connectivity in the human brain. *J. Neurosci.* 27, 1584–1593.

Buckner, R. L., Andrews-Hanna, J. R., and Schacter, D. L. (2008). The brain's default network: anatomy, function, and relevance to disease. *Ann. N. Y. Acad. Sci.* 1124, 1–38.

Buckner, R. L., Sepulcre, J., Talukdar, T., Krienen, F. M., Liu, H., Hedden, T., Andrews-Hanna, J. R., Sperling, R. A., and Johnson, K. A. (2009). Cortical hubs revealed by intrinsic functional connectivity: mapping, assessment of stability, and relation to Alzheimer's disease. *J. Neurosci.* 29, 1860–1873.

Buckner, R. L., Snyder, A. Z., Shannon, B. J., LaRossa, G., Sachs, R., Fotenos, A. F., Sheline, Y. I., Klunk, W. E., Mathis, C. A., Morris, J. C., and Mintun, M. A. (2005). Molecular, structural, and functional characterization of Alzheimer's disease: evidence for a relationship between default activity, amyloid, and memory. *J. Neurosci.* 25, 7709–7717.

Bullmore, E., Barnes, A., Bassett, D. S., Fornito, A., Kitzbichler, M., Meunier, D., and Suckling, J. (2009). Generic aspects of complexity in brain imaging data and other biological systems. *Neuroimage* 47, 1125–1134.

Bullmore, E., and Sporns, O. (2009). Complex brain networks: graph theoretical analysis of structural and functional systems. *Nat. Rev. Neurosci.* 10, 186–198.

Bullmore, E. T., and Bassett, D. S. (2011). Brain graphs: graphical models of the human brain connectome. *Annu. Rev. Clin. Psychol.* 7, 113–140.

Buzsaki, G., Geisler, C., Henze, D. A., and Wang, X. J. (2004). Interneuron diversity series: circuit complexity and axon wiring economy of cortical interneurons. *Trends Neurosci.* 27, 186–193.

Calhoun, V. D., Adali, T., and Pekar, J. J. (2004). A method for comparing group fMRI data using independent component analysis: application to visual, motor and visuomotor tasks. *Magn. Reson. Imaging* 22, 1181–1191.

Calhoun, V. D., Maciejewski, P. K., Pearlson, G. D., and Kiehl, K. A. (2008). Temporal lobe and "default" hemodynamic brain modes discriminate between schizophrenia and bipolar disorder. *Hum. Brain Mapp.* 29, 1265–1275.

Canli, T., Qiu, M., Omura, K., Congdon, E., Haas, B. W., Amin, Z., Herrmann, M. J., Constable, R. T., and Lesch, K. P. (2006). Neural correlates of epigenesis. *Proc. Natl. Acad. Sci. U.S.A.* 103, 16033–16038.

Cannon, T. D., Kaprio, J., Lönnqvist, J., Huttunen, M., and Koskenvuo, M. (1998). The genetic epidemiology of schizophrenia in a Finnish twin cohort: a population-based modeling study. *Arch. Gen. Psychiatry* 55, 67–74.

Cannon, T. D., and Keller, M. C. (2006). Endophenotypes in the genetic analyses of mental disorders. *Annu. Rev. Clin. Psychol.* 2, 267–290.

Cardno, A. G., Marshall, E. J., Cold, B., MacDonald, A. M., Ribchester, T. R., Davies, N. J., Venturi, P., Jones, L. A., Lewis, S. W., Sham, P. C., Gottesman, I. I., Farmer, A. E., McGuffin, P., Reveley, A. M., and Murray, R. M. (1999). Heritability estimates for psychotic disorders: the Maudsley twin psychosis series. *Arch. Gen. Psychiatry* 56, 162–168.

Caspi, A., Hariri, A. R., Holmes, A., Uher, R., and Moffitt, T. E. (2010). Genetic sensitivity to the environment: the case of the serotonin transporter gene and its implications for studying complex diseases and traits. *Am. J. Psychiatry* 167, 509–527.

Caspi, A., McClay, J., Moffitt, T. E., Mill, J., Martin, J., Craig, I. W., Taylor, A., and Poulton, R. (2002). Role of genotype in the cycle of violence in maltreated children. *Science* 297, 851–854.

Castellanos, F. X., Margulies, D. S., Kelly, C., Uddin, L. Q., Ghaffari, M., Kirsch, A., Shaw, D., Shehzad, Z., Di Martino, A., Biswal, B., Sonuga-Barke, E. J., Rotrosen, J., Adler, L. A., and Milham, M. P. (2008). Cingulate-precuneus interactions: a new locus of dysfunction in adult attention-deficit/hyperactivity disorder. *Biol. Psychiatry* 63, 332–337.

Chen, B. L., Hall, D. H., and Chklovskii, D. B. (2006). Wiring optimization can relate neuronal structure and function. *Proc. Natl. Acad. Sci. U.S.A.* 103, 4723–4728.

Cherniak, C., Changizi, M., and Won Kang, D. (1999). Large-scale optimization of neuron arbors. *Phys. Rev. E Stat. Phys. Plasmas Fluids Relat. Interdiscip. Topics* 59, 6001–6009.

Cherniak, C., Mokhtarzada, Z., Rodriguez-Esteban, R., and Changizi, K. (2004). Global optimization of cerebral cortex layout. *Proc. Natl. Acad. Sci. U.S.A.* 101, 1081–1086.

Chiang, M. C., Barysheva, M., Shattuck, D. W., Lee, A. D., Madsen, S. K., Avedissian, C., Klunder, A. D., Toga, A. W., McMahon, K. L., de Zubicaray, G. I., Wright, M. J., Srivastava, A., Balov, N., and Thompson, P. M. (2009). Genetics of brain fiber architecture and intellectual performance. *J. Neurosci.* 29, 2212–2224.

Chklovskii, D. B. (2004). Synaptic connectivity and neuronal morphology: two sides of the same coin. *Neuron* 43, 609–617.

Chklovskii, D. B., Schikorski, T., and Stevens, C. F. (2002). Wiring optimization in cortical circuits. *Neuron* 34, 341–347.

Chung, H. J., Lee, J. Y., Deocaris, C. C., Min, H., Kim, S. H., and Kim, M. H. (2010). Mouse homologue of the schizophrenia susceptibility gene ZNF804A as a target of Hoxc8. *J. Biomed. Biotechnol.* 2010, 231708.

Clare Kelly, A. M., Uddin, L. Q., Biswal, B. B., Castellanos, F. X., and Milham, M. P. (2008). Competition between functional brain networks mediates behavioral variability. *Neuroimage* 39, 527–537.

Clarke, H., Flint, J., Attwood, A. S., and Munafo, M. R. (2010). Association of the 5-HTTLPR genotype and unipolar depression: a meta-analysis. *Psychol. Med.* 40, 1767–1778.

Curcic-Blake, B., Swart, M., Ter Horst, G. J., Langers, D. R., Kema, I. P., and Aleman, A. (2012). Variation of the gene coding for DARPP-32 (PPP1R1B) and brain connectivity during associative emotional learning. *Neuroimage* 59, 1540–1550.

Damoiseaux, J. S., Rombouts, S. A., Barkhof, F., Scheltens, P., Stam, C. J., Smith, S. M., and Beckmann, C. F. (2006). Consistent resting-state networks across healthy subjects. *Proc. Natl. Acad. Sci. U.S.A.* 103, 13848–13853.

Dennis, N. A., Browndyke, J. N., Stokes, J., Need, A., Burke, J. R., Welsh-Bohmer, K. A., and Cabeza, R. (2010a). Temporal lobe functional activity and connectivity in young adult APOE varepsilon4 carriers. *Alzheimers Dement.* 6, 303–311.

Dennis, N. A., Need, A. C., LaBar, K. S., Waters-Metenier, S., Cirulli, E. T., Kragel, J., Goldstein, D. B., and Cabeza, R. (2010b). COMT val108/158 met genotype affects neural but not cognitive processing in healthy individuals. *Cereb. Cortex* 20, 672–683.

Ellison-Wright, I., and Bullmore, E. (2009). Meta-analysis of diffusion tensor imaging studies in schizophrenia. *Schizophr. Res.* 108, 3–10.

Erhardt, E. B., Allen, E. A., Damaraju, E., and Calhoun, V. D. (2011). On network derivation, classification and visualization: a response to habeck and moeller. *Brain Connect.* 1, 105–110.

Erk, S., Meyer-Lindenberg, A., Schnell, K., Opitz von Boberfeld, C., Esslinger, C., Kirsch, P., Grimm, O., Arnold, C., Haddad, L., Witt, S. H., Cichon, S., Nothen, M. M., Rietschel, M., and Walter, H. (2010). Brain function in carriers of a genome-wide supported bipolar disorder variant. *Arch. Gen. Psychiatry* 67, 803–811.

Esslinger, C., Kirsch, P., Haddad, L., Mier, D., Sauer, C., Erk, S., Schnell, K., Arnold, C., Witt, S. H., Rietschel, M., Cichon, S., Walter, H., and Meyer-Lindenberg, A. (2011). Cognitive state and connectivity effects of the genome-wide significant psychosis variant in ZNF804A. *Neuroimage* 54, 2514–2523.

Esslinger, C., Walter, H., Kirsch, P., Erk, S., Schnell, K., Arnold, C., Haddad, L., Mier, D., Opitz von Boberfeld, C., Raab, K., Witt, S. H., Rietschel, M., Cichon, S., and Meyer-Lindenberg, A. (2009). Neural mechanisms of a genome-wide supported psychosis variant. *Science* 324, 605.

Farrer, L. A., Cupples, L. A., Haines, J. L., Hyman, B., Kukull, W. A., Mayeux, R., Myers, R. H., Pericak-Vance, M. A., Risch, N., and van Duijn, C. M. (1997). Effects of age, sex, and ethnicity on the association between apolipoprotein E genotype and Alzheimer disease. A meta-analysis. APOE and Alzheimer Disease Meta Analysis Consortium. *JAMA* 278, 1349–1356.

Filippini, N., MacIntosh, B. J., Hough, M. G., Goodwin, G. M., Frisoni, G. B., Smith, S. M., Matthews, P. M., Beckmann, C. F., and Mackay, C. E. (2009). Distinct patterns of brain activity in young carriers of the APOE-epsilon4 allele. *Proc. Natl. Acad. Sci. U.S.A.* 106, 7209–7214.

Fleisher, A. S., Sherzai, A., Taylor, C., Langbaum, J. B., Chen, K., and Buxton, R. B. (2009). Resting-state BOLD networks versus task-associated functional MRI for distinguishing Alzheimer's disease risk groups. *Neuroimage* 47, 1678–1690.

Flint, J., and Munafo, M. R. (2007). The endophenotype concept in psychiatric genetics. *Psychol. Med.* 37, 163–180.

Fornito, A., and Bullmore, E. T. (2010). What can spontaneous fluctuations of the blood oxygenation-level-dependent signal tell us about

psychiatric disorders? *Curr. Opin. Psychiatry* 23, 239–249.

Fornito, A., Yoon, J., Zalesky, A., Bullmore, E. T., and Carter, C. S. (2011a). General and specific functional connectivity disturbances in first-episode schizophrenia during cognitive control performance. *Biol. Psychiatry* 70, 64–72.

Fornito, A., Zalesky, A., Bassett, D. S., Meunier, D., Ellison-Wright, I., Yucel, M., Wood, S. J., Shaw, K., O'Connor, J., Nertney, D., Mowry, B. J., Pantelis, C., and Bullmore, E. T. (2011b). Genetic influences on cost-efficient organization of human cortical functional networks. *J. Neurosci.* 31, 3261–3270.

Fornito, A., Yucel, M., Patti, J., Wood, S. J., and Pantelis, C. (2009). Mapping grey matter reductions in schizophrenia: an anatomical likelihood estimation analysis of voxel-based morphometry studies. *Schizophr. Res.* 108, 104–113.

Fornito, A., Zalesky, A., Pantelis, C., and Bullmore, E. T. (2012). Schizophrenia, neuroimaging and connectomics. *Neuroimage*. doi: 10.1016/j.neuroimage.2011.12.090

Fox, M. D., and Raichle, M. E. (2007). Spontaneous fluctuations in brain activity observed with functional magnetic resonance imaging. *Nat. Rev. Neurosci.* 8, 700–711.

Fox, M. D., Snyder, A. Z., Vincent, J. L., and Raichle, M. E. (2007). Intrinsic fluctuations within cortical systems account for intertrial variability in human behavior. *Neuron* 56, 171–184.

Fox, M. D., Snyder, A. Z., Zacks, J. M., and Raichle, M. E. (2006). Coherent spontaneous activity accounts for trial-to-trial variability in human evoked brain responses. *Nat. Neurosci.* 9, 23–25.

Friston, K. J. (1994). Functional and effective connectivity in neuroimaging: a synthesis. *Hum. Brain Mapp.* 2, 56–78.

Friston, K. J., Buechel, C., Fink, G. R., Morris, J., Rolls, E., and Dolan, R. J. (1997). Psychophysiological and modulatory interactions in neuroimaging. *Neuroimage* 6, 218–229.

Friston, K. J., Harrison, L., and Penny, W. (2003). Dynamic causal modelling. *Neuroimage* 19, 1273–1302.

Gai, X., Xie, H. M., Perin, J. C., Takahashi, N., Murphy, K., Wenocur, A. S., D'Arcy, M., O'Hara, R. J., Goldmuntz, E., Grice, D. E., Shaikh, T. H., Hakonarson, H., Buxbaum, J. D., Elia, J., and White, P. S. (2012). Rare structural variation of synapse and neurotransmission genes in autism. *Mol. Psychiatry* 17, 402–411.

Gibbons, A. S., Udawela, M., Jeon, W. J., Seo, M. S., Brooks, L., and Dean, B. (2011). The neurobiology of APOE in schizophrenia and mood disorders. *Front. Biosci.* 16, 962–979.

Glahn, D. C., Winkler, A. M., Kochunov, P., Almasy, L., Duggirala, R., Carless, M. A., Curran, J. C., Olvera, R. L., Laird, A. R., Smith, S. M., Beckmann, C. F., Fox, P. T., and Blangero, J. (2010). Genetic control over the resting brain. *Proc. Natl. Acad. Sci. U.S.A.* 107, 1223–1228.

Gogtay, N., Vyas, N. S., Testa, R., Wood, S. J., and Pantelis, C. (2011). Age of onset of schizophrenia: perspectives from structural neuroimaging studies. *Schizophr. Bull.* 37, 504–513.

Gottesman, I. I. (1991). *Schizophrenia Genesis: The Origins of Madness*. New York: W.H. Freeman and Company.

Gottesman, I. I., and Gould, T. D. (2003). The endophenotype concept in psychiatry: etymology and strategic intentions. *Am. J. Psychiatry* 160, 1–10.

Greicius, M. D., Flores, B. H., Menon, V., Glover, G. H., Solvason, H. B., Kenna, H., Reiss, A. L., and Schatzberg, A. F. (2007). Resting-state functional connectivity in major depression: abnormally increased contributions from subgenual cingulate cortex and thalamus. *Biol. Psychiatry* 62, 429–437.

Greicius, M. D., Srivastava, G., Reiss, A. L., and Menon, V. (2004). Default-mode network activity distinguishes Alzheimer's disease from healthy aging: evidence from functional MRI. *Proc. Natl. Acad. Sci. U.S.A.* 101, 4637–4642.

Habeck, C., and Moeller, J. R. (2011). Intinsic functional-connectivity networks for diagnosis: just beautiful pictures? *Brain Connect.* 1, 99–103.

Hagmann, P., Cammoun, L., Gigandet, X., Meuli, R., Honey, C. J., Wedeen, V. J., and Sporns, O. (2008). Mapping the structural core of human cerebral cortex. *PLoS Biol.* 6, e159. doi:10.1371/journal.pbio.0060159

Hagmann, P., Kurant, M., Gigandet, X., Thiran, P., Wedeen, V. J., Meuli, R., and Thiran, J. P. (2007). Mapping human whole-brain structural networks with diffusion MRI. *PLoS ONE* 2, e597. doi:10.1371/journal.pone.0000597

Hallmayer, J., Cleveland, S., Torres, A., Phillips, J., Cohen, B., Torigoe, T., Miller, J., Fedele, A., Collins, J., Smith, K., Lotspeich, L., Croen, L. A., Ozonoff, S., Lajonchere, C., Grether, J. K., and Risch, N. (2011). Genetic heritability and shared environmental factors among twins pairs with autism. *Arch. Gen. Psychiatry* 68, 1095–1102.

Hariri, A. R., Mattay, V. S., Tessitore, A., Kolachana, B., Fera, F., Goldman, D., Egan, M. F., and Weinberger, D. R. (2002). Serotonin transporter genetic variation and the response of the human amygdala. *Science* 297, 400–403.

Harrison, B. J., Pujol, J., Contreras-Rodriguez, O., Soriano-Mas, C., Lopez-Sola, M., Deus, J., Ortiz, H., Blanco-Hinojo, L., Alonso, P., Hernandez-Ribas, R., Cardoner, N., and Menchon, J. M. (2011). Task-induced deactivation from rest extends beyond the default mode brain network. *PLoS ONE* 6, e22964. doi:10.1371/journal.pone.0022964

Harrison, B. J., Pujol, J., Lopez-Sola, M., Hernandez-Ribas, R., Deus, J., Ortiz, H., Soriano-Mas, C., Yucel, M., Pantelis, C., and Cardoner, N. (2008). Consistency and functional specialization in the default mode brain network. *Proc. Natl. Acad. Sci. U.S.A.* 105, 9781–9786.

Harrison, P. J., and Weinberger, D. R. (2005). Schizophrenia genes, gene expression, and neuropathology: on the matter of their convergence. *Mol. Psychiatry* 10, 40–68.

He, B. J., Snyder, A. Z., Zempel, J. M., Smyth, M. D., and Raichle, M. E. (2008). Electrophysiological correlates of the brain's intrinsic large-scale functional architecture. *Proc. Natl. Acad. Sci. U.S.A.* 105, 16039–16044.

He, Y., Chen, Z. J., and Evans, A. C. (2007). Small-world anatomical networks in the human brain revealed by cortical thickness from MRI. *Cereb. Cortex* 17, 2407–2419.

Heils, A., Teufel, A., Petri, S., Stober, G., Riederer, P., Bengel, D., and Lesch, K. P. (1996). Allelic variation of human serotonin transporter gene expression. *J. Neurochem.* 66, 2621–2624.

Heinz, A., Braus, D. F., Smolka, M. N., Wrase, J., Puls, I., Hermann, D., Klein, S., Grusser, S. M., Flor, H., Schumann, G., Mann, K., and Buchel, C. (2005). Amygdala-prefrontal coupling depends on a genetic variation of the serotonin transporter. *Nat. Neurosci.* 8, 20–21.

Heinz, A., Jones, D. W., Mazzanti, C., Goldman, D., Ragan, P., Hommer, D., Linnoila, M., and Weinberger, D. R. (2000). A relationship between serotonin transporter genotype and in vivo protein expression and alcohol neurotoxicity. *Biol. Psychiatry* 47, 643–649.

Hesselmann, G., Kell, C. A., Eger, E., and Kleinschmidt, A. (2008). Spontaneous local variations in ongoing neural activity bias perceptual decisions. *Proc. Natl. Acad. Sci. U.S.A.* 105, 10984–10989.

Hettema, J. M., Neale, M. C., and Kendler, K. S. (2001). A review and meta-analysis of the genetic epidemiology of anxiety disorders. *Am. J. Psychiatry* 158, 1568–1578.

Hill, M. J., and Bray, N. J. (2011). Allelic differences in nuclear protein binding at a genome-wide significant risk variant for schizophrenia in ZNF804A. *Mol. Psychiatry* 16, 787–789.

Hong, L. E., Hodgkinson, C. A., Yang, Y., Sampath, H., Ross, T. J., Buchholz, B., Salmeron, B. J., Srivastava, V., Thaker, G. K., Goldman, D., and Stein, E. A. (2010). A genetically modulated, intrinsic cingulate circuit supports human nicotine addiction. *Proc. Natl. Acad. Sci. U.S.A.* 107, 13509–13514.

Insel, T. R. (2011). Rethinking schizophrenia. *Nature* 468, 187–193.

Jbabdi, S., and Johansen-Berg, H. (2011). Tractography: where do we go from here? *Brain Connect.* 1, 169–183.

Jedema, H. P., Gianaros, P. J., Greer, P. J., Kerr, D. D., Liu, S., Higley, J. D., Suomi, S. J., Olsen, A. S., Porter, J. N., Lopresti, B. J., Hariri, A. R., and Bradberry, C. W. (2010). Cognitive impact of genetic variation of the serotonin transporter in primates is associated with differences in brain morphology rather than serotonin neurotransmission. *Mol. Psychiatry* 15, 512–522, 446.

Kaiser, M., Gorner, M., and Hilgetag, C. C. (2007). Criticality of spreading dynamics in hierarchical cluster networks without inhibition. *New J. Phys.* 9, 2–13.

Kaiser, M., and Hilgetag, C. C. (2006). Nonoptimal component placement, but short processing paths, due to long-distance projections in neural systems. *PLoS Comput. Biol.* 2, e95. doi:10.1371/journal.pcbi.0020095

Kempf, L., Nicodemus, K. K., Kolachana, B., Vakkalanka, R., Verchinski, B. A., Egan, M. F., Straub, R. E., Mattay, V. A., Callicott, J. H., Weinberger, D. R., and Meyer-Lindenberg, A. (2008). Functional polymorphisms in PRODH are associated with risk and protection for schizophrenia and fronto-striatal structure and function. *PLoS Genet.* 4, e1000252. doi:10.1371/journal.pgen.1000252

Kendler, K. S. (2006). Reflections on the relationship between psychiatric genetics and psychiatric nosology. *Am. J. Psychiatry* 163, 1138–1146.

Kendler, K. S., Gatz, M., Gardner, C. O., and Pedersen, N. L. (2006). A Swedish national twin study of lifetime major depression. *Am. J. Psychiatry* 163, 109–114.

Kendler, K. S., and Neale, M. C. (2010). Endophenotype: a conceptual analysis. *Mol. Psychiatry* 15, 789–797.

Kendler, K. S., Neale, M. C., Kessler, R. C., Heath, A. C., and Eaves, L. J. (1993). The lifetime history of major depression in women. Reliability of diagnosis and heritability. *Arch. Gen. Psychiatry* 50, 863–870.

Kennedy, D. P., and Courchesne, E. (2008). The intrinsic functional organization of the brain is altered in autism. *Neuroimage* 39, 1877–1885.

Kim-Cohen, J., Caspi, A., Taylor, A., Williams, B., Newcombe, R., Craig, I. W., and Moffitt, T. E. (2006). MAOA, maltreatment, and gene-environment interaction predicting children's mental health: new evidence and a meta-analysis. *Mol. Psychiatry* 11, 903–913.

Klyachko, V. A., and Stevens, C. F. (2003). Connectivity optimization and the positioning of cortical areas. *Proc. Natl. Acad. Sci. U.S.A.* 100, 7937–7941.

Konrad, A., Vucurevic, G., Musso, F., Stoeter, P., Dahmen, N., and Winterer, G. (2009). ErbB4 genotype predicts left frontotemporal structural connectivity in human brain. *Neuropsychopharmacology* 34, 641–650.

Koten, J. W. Jr., Wood, G., Hagoort, P., Goebel, R., Propping, P., Willmes, K., and Boomsma, D. I. (2009). Genetic contribution to variation in cognitive function: an FMRI study in twins. *Science* 323, 1737–1740.

Krugel, L. K., Biele, G., Mohr, P. N., Li, S. C., and Heekeren, H. R. (2009). Genetic variation in dopaminergic neuromodulation influences the ability to rapidly and flexibly adapt decisions. *Proc. Natl. Acad. Sci. U.S.A.* 106, 17951–17956.

Latora, V., and Marchiori, M. (2001). Efficient behavior of small-world networks. *Phys. Rev. Lett.* 87, 198701.

Latora, V., and Marchiori, M. (2003). Economic small-world behavior in weighted networks. *Eur. Phys. J. B* 32, 249–263.

Laughlin, S. B., and Sejnowski, T. J. (2003). Communication in neuronal networks. *Science* 301, 1870–1874.

Lesch, K. P., Bengel, D., Heils, A., Sabol, S. Z., Greenberg, B. D., Petri, S., Benjamin, J., Muller, C. R., Hamer, D. H., and Murphy, D. L. (1996). Association of anxiety-related traits with a polymorphism in the serotonin transporter gene regulatory region. *Science* 274, 1527–1531.

Li, D., and He, L. (2007). Meta-analysis supports association between serotonin transporter (5-HTT) and suicidal behavior. *Mol. Psychiatry* 12, 47–54.

Li, Y., Liu, Y., Li, J., Qin, W., Li, K., Yu, C., and Jiang, T. (2009). Brain anatomical network and intelligence. *PLoS Comput. Biol.* 5, e1000395. doi:10.1371/journal.pcbi.1000395

Lips, E. S., Cornelisse, L. N., Toonen, R. F., Min, J. L., Hultman, C. M., Holmans, P. A., O'Donovan, M. C., Purcell, S. M., Smit, A. B., Verhage, M., Sullivan, P. F., Visscher, P. M., and Posthuma, D. (2011). Functional gene group analysis identifies synaptic gene groups as risk factor for schizophrenia. *Mol. Psychiatry*. doi: 10.1038/mp.2011.117

Lo, C. Y., Wang, P. N., Chou, K. H., Wang, J., He, Y., and Lin, C. P. (2010). Diffusion tensor tractography reveals abnormal topological organization in structural cortical networks in Alzheimer's disease. *J. Neurosci.* 30, 16876–16885.

Lynall, M. E., Bassett, D. S., Kerwin, R., McKenna, P. J., Kitzbichler, M., Muller, U., and Bullmore, E. (2010). Functional connectivity and brain networks in schizophrenia. *J. Neurosci.* 30, 9477–9487.

Machulda, M. M., Jones, D. T., Vemuri, P., McDade, E., Avula, R., Przybelski, S., Boeve, B. F., Knopman, D. S., Petersen, R. C., and Jack, C. R. Jr. (2011). Effect of APOE epsilon4 status on intrinsic network connectivity in cognitively normal elderly subjects. *Arch. Neurol.* 68, 1131–1136.

Mahley, R. W., and Rall, S. C. Jr. (2000). Apolipoprotein E: far more than a lipid transport protein. *Annu. Rev. Genomics Hum. Genet.* 1, 507–537.

Margulies, D. S., Bottger, J., Long, X., Lv, Y., Kelly, C., Schafer, A., Goldhahn, D., Abbushi, A., Milham, M. P., Lohmann, G., and Villringer, A. (2010). Resting developments: a review of fMRI post-processing methodologies for spontaneous brain activity. *MAGMA* 23, 289–307.

McClearn, G. E., Johansson, B., Berg, S., Pedersen, N. L., Ahern, F., Petrill, S. A., and Plomin, R. (1997). Substantial genetic influence on cognitive abilities in twins 80 or more years old. *Science* 276, 1560–1563.

McGuffin, P., Rijsdijk, F., Andrew, M., Sham, P., Katz, R., and Cardno, A. (2003). The heritability of bipolar affective disorder and the genetic relationship to unipolar depression. *Arch. Gen. Psychiatry* 60, 497–502.

McHugh, R. K., Hofmann, S. G., Asnaani, A., Sawyer, A. T., and Otto, M. W. (2010). The serotonin transporter gene and risk for alcohol dependence: a meta-analytic review. *Drug Alcohol Depend.* 108, 1–6.

Mennes, M., Zuo, X. N., Kelly, C., Di Martino, A., Zang, Y. F., Biswal, B., Castellanos, F. X., and Milham, M. P. (2011). Linking inter-individual differences in neural activation and behavior to intrinsic brain dynamics. *Neuroimage* 54, 2950–2959.

Menzies, L., Chamberlain, S. R., Laird, A. R., Thelen, S. M., Sahakian, B. J., and Bullmore, E. T. (2008). Integrating evidence from neuroimaging and neuropsychological studies of obsessive-compulsive disorder: the orbitofronto-striatal model revisited. *Neurosci. Biobehav. Rev.* 32, 525–549.

Meunier, D., Lambiotte, R., Fornito, A., Ersche, K. D., and Bullmore, E. T. (2009). Hierarchical modularity in human brain functional networks. *Front. Neuroinformatics* 3, 37.

Meyer-Lindenberg, A. (2009). Neural connectivity as an intermediate phenotype: brain networks under genetic control. *Hum. Brain Mapp.* 30, 1938–1946.

Meyer-Lindenberg, A. (2010). From maps to mechanisms through neuroimaging of schizophrenia. *Nature* 468, 194–202.

Meyer-Lindenberg, A., Straub, R. E., Lipska, B. K., Verchinski, B. A., Goldberg, T., Callicott, J. H., Egan, M. F., Huffaker, S. S., Mattay, V. S., Kolachana, B., Kleinman, J. E., and Weinberger, D. R. (2007). Genetic evidence implicating DARPP-32 in human frontostriatal structure, function, and cognition. *J. Clin. Invest.* 117, 672–682.

Meyer-Lindenberg, A., and Weinberger, D. R. (2006). Intermediate phenotypes and genetic mechanisms of psychiatric disorders. *Nat. Rev. Neurosci.* 7, 818–827.

Meyer-Lindenberg, A. S., Olsen, R. K., Kohn, P. D., Brown, T., Egan, M. F., Weinberger, D. R., and Berman, K. F. (2005). Regionally specific disturbance of dorsolateral prefrontal-hippocampal functional connectivity in schizophrenia. *Arch. Gen. Psychiatry* 62, 379–386.

Minzenberg, M. J., Laird, A. R., Thelen, S., Carter, C. S., and Glahn, D. C. (2009). Meta-analysis of 41 functional neuroimaging studies of executive function in schizophrenia. *Arch. Gen. Psychiatry* 66, 811–822.

Morcom, A. M., and Fletcher, P. C. (2007). Does the brain have a baseline? Why we should be resisting a rest. *Neuroimage* 37, 1073–1082.

Mori, S., and Zhang, J. (2006). Principles of diffusion tensor imaging and its applications to basic neuroscience research. *Neuron* 51, 527–539.

Mukherjee, P., Whalley, H. C., McKirdy, J. W., McIntosh, A. M., Johnstone, E. C., Lawrie, S. M., and Hall, J. (2011). Effects of the BDNF Val66Met polymorphism on neural responses to facial emotion. *Psychiatry Res.* 191, 182–188.

Munafo, M. R., Freimer, N. B., Ng, W., Ophoff, R., Veijola, J., Miettunen, J., Jarvelin, M. R., Taanila, A., and Flint, J. (2009). 5-HTTLPR genotype and anxiety-related personality traits: a meta-analysis and new data. *Am. J. Med. Genet. B Neuropsychiatr. Genet.* 150B, 271–281.

Murthy, N. V., Selvaraj, S., Cowen, P. J., Bhagwagar, Z., Riedel, W. J., Peers, P., Kennedy, J. L., Sahakian, B. J., Laruelle, M. A., Rabiner, E. A., and Grasby, P. M. (2010). Serotonin transporter polymorphisms (SLC6A4 insertion/deletion and rs25531) do not affect the availability of 5-HTT to [11C] DASB binding in the living human brain. *Neuroimage* 52, 50–54.

Nikulina, V., Widom, C. S., and Brzustowicz, L. M. (2012). Child abuse and neglect, MAOA, and mental health outcomes: a prospective examination. *Biol. Psychiatry* 71, 350–357.

O'Donovan, M. C., Craddock, N., Norton, N., Williams, H., Peirce, T., Moskvina, V., Nikolov, I., Hamshere, M., Carroll, L., Georgieva, L., Dwyer, S., Holmans, P., Marchini, J. L., Spencer, C. C., Howie, B., Leung, H. T., Hartmann, A. M., Moller, H. J., Morris, D. W., Shi, Y., Feng, G., Hoffmann, P., Propping, P., Vasilescu, C., Maier, W., Rietschel, M., Zammit, S., Schumacher, J., Quinn, E. M., Schulze, T. G., Williams, N. M., Giegling, I., Iwata, N., Ikeda, M., Darvasi, A., Shifman, S., He, L., Duan, J., Sanders, A. R., Levinson, D. F., Gejman, P. V., Cichon, S., Nothen, M. M., Gill, M., Corvin, A., Rujescu, D., Kirov, G., Owen, M. J., Buccola, N. G., Mowry, B. J., Freedman, R., Amin, F., Black, D. W., Silverman, J. M., Byerley, W. F., and Cloninger, C. R. (2008). Identification of loci associated with schizophrenia by genome-wide association and follow-up. *Nat. Genet.* 40, 1053–1055.

Pacheco, J., Beevers, C. G., Benavides, C., McGeary, J., Stice, E., and Schnyer, D. M. (2009). Frontal-limbic white matter pathway associations with

the serotonin transporter gene promoter region (5-HTTLPR) polymorphism. *J. Neurosci.* 29, 6229–6233.

Pantelis, C., Yucel, M., Bora, E., Fornito, A., Testa, R., Brewer, W. J., Velakoulis, D., and Wood, S. J. (2009). Neurobiological markers of illness onset in psychosis and schizophrenia: the search for a moving target. *Neuropsychol. Rev.* 19, 385–398.

Papagni, S. A., Mechelli, A., Prata, D. P., Kambeitz, J., Fu, C. H., Picchioni, M., Walshe, M., Toulopoulou, T., Bramon, E., Murray, R. M., Collier, D. A., Bellomo, A., and McGuire, P. (2011). Differential effects of DAAO on regional activation and functional connectivity in schizophrenia, bipolar disorder and controls. *Neuroimage* 56, 2283–2291.

Peper, J. S., Brouwer, R. M., Boomsma, D. I., Kahn, R. S., and Hulshoff Pol, H. E. (2007). Genetic influences on human brain structure: a review of brain imaging studies in twins. *Hum. Brain Mapp.* 28, 464–473.

Pettersson-Yeo, W., Allen, P., Benetti, S., McGuire, P., and Mechelli, A. (2011). Dysconnectivity in schizophrenia: where are we now? *Neurosci. Biobehav. Rev.* 35, 1110–1124.

Pezawas, L., Meyer-Lindenberg, A., Drabant, E. M., Verchinski, B. A., Munoz, K. E., Kolachana, B. S., Egan, M. F., Mattay, V. S., Hariri, A. R., and Weinberger, D. R. (2005). 5-HTTLPR polymorphism impacts human cingulate-amygdala interactions: a genetic susceptibility mechanism for depression. *Nat. Neurosci.* 8, 828–834.

Phillips, M. L., Drevets, W. C., Rauch, S. L., and Lane, R. (2003a). Neurobiology of emotion perception I: the neural basis of normal emotion perception. *Biol. Psychiatry* 54, 504–514.

Phillips, M. L., Drevets, W. C., Rauch, S. L., and Lane, R. (2003b). Neurobiology of emotion perception II: implications for major psychiatric disorders. *Biol. Psychiatry* 54, 515–528.

Potkin, S. G., Turner, J. A., Fallon, J. A., Lakatos, A., Keator, D. B., Guffanti, G., and Macciardi, F. (2009). Gene discovery through imaging genetics: identification of two novel genes associated with schizophrenia. *Mol. Psychiatry* 14, 416–428.

Prata, D. P., Papagni, S. A., Mechelli, A., Fu, C. H., Kambeitz, J., Picchioni, M., Kane, F., Kalidindi, S., McDonald, C., Kravariti, E., Toulopoulou, T., Bramon, E., Walshe, M., Murray, R., Collier, D. A., and McGuire, P. K. (2012). Effect of D-amino acid oxidase activator (DAOA; G72) on brain function during verbal fluency. *Hum. Brain Mapp.* 33, 143–153.

Purcell, S. M., Wray, N. R., Stone, J. L., Visscher, P. M., O'Donovan, M. C., Sullivan, P. F., and Sklar, P. (2009). Common polygenic variation contributes to risk of schizophrenia and bipolar disorder. *Nature* 460, 748–752.

Ramón y Cajal, S. (1995). *Histology of the Nervous System.* New York: Oxford University Press.

Rasch, B., Spalek, K., Buholzer, S., Luechinger, R., Boesiger, P., de Quervain, D. J., and Papassotiropoulos, A. (2010). Aversive stimuli lead to differential amygdala activation and connectivity patterns depending on catechol-O-methyltransferase Val158Met genotype. *Neuroimage* 52, 1712–1719.

Rasch, B., Spalek, K., Buholzer, S., Luechinger, R., Boesiger, P., Papassotiropoulos, A., and de Quervain, D. J. (2009). A genetic variation of the noradrenergic system is related to differential amygdala activation during encoding of emotional memories. *Proc. Natl. Acad. Sci. U.S.A.* 106, 19191–19196.

Rasetti, R., Sambataro, F., Chen, Q., Callicott, J. H., Mattay, V. S., and Weinberger, D. R. (2011). Altered cortical network dynamics: a potential intermediate phenotype for schizophrenia and association with ZNF804A. *Arch. Gen. Psychiatry* 68, 1207–1217.

Riley, B., Thiselton, D., Maher, B. S., Bigdeli, T., Wormley, B., McMichael, G. O., Fanous, A. H., Vladimirov, V., O'Neill, F. A., Walsh, D., and Kendler, K. S. (2010). Replication of association between schizophrenia and ZNF804A in the Irish Case-Control Study of schizophrenia sample. *Mol. Psychiatry* 15, 29–37.

Robinson, E. B., Koenen, K. C., McCormick, M. C., Munir, K., Hallett, V., Happè, F., Plomin, R., and Ronald, A. (2012). A mutlivariate twin study of autistic traits in 12-year olds: testing the fractionable autism triad hypothesis. *Behav. Genet.* 42, 245–255.

Rubinov, M., and Sporns, O. (2010). Complex network measures of brain connectivity: uses and interpretations. *Neuroimage* 52, 1059–1069.

Rubinov, M., Sporns, O., Thivierge, J. P., and Breakspear, M. (2011). Neurobiologically realistic determinants of self-organized criticality in networks of spiking neurons. *PLoS Comput. Biol.* 7, e1002038. doi:10.1371/journal.pcbi.1002038

Sabol, S. Z., Hu, S., and Hamer, D. (1998). A functional polymorphism in the monoamine oxidase A gene promoter. *Hum. Genet.* 103, 273–279.

Schardt, D. M., Erk, S., Nusser, C., Nothen, M. M., Cichon, S., Rietschel, M., Treutlein, J., Goschke, T., and Walter, H. (2010). Volition diminishes genetically mediated amygdala hyperreactivity. *Neuroimage* 53, 943–951.

Seeley, W. W. (2011). Divergent network connectivity changes in healthy APOE epsilon4 carriers: disinhibition or compensation? *Arch. Neurol.* 68, 1107–1108.

Seeley, W. W., Crawford, R. K., Zhou, J., Miller, B. L., and Greicius, M. D. (2009). Neurodegenerative diseases target large-scale human brain networks. *Neuron* 62, 42–52.

Shehzad, Z., Kelly, A. M., Reiss, P. T., Gee, D. G., Gotimer, K., Uddin, L. Q., Lee, S. H., Margulies, D. S., Roy, A. K., Biswal, B. B., Petkova, E., Castellanos, F. X., and Milham, M. P. (2009). The resting brain: unconstrained yet reliable. *Cereb. Cortex* 19, 2209–2229.

Sheline, Y. I., Morris, J. C., Snyder, A. Z., Price, J. L., Yan, Z., D'Angelo, G., Liu, C., Dixit, S., Benzinger, T., Fagan, A., Goate, A., and Mintun, M. A. (2010a). APOE4 allele disrupts resting state fMRI connectivity in the absence of amyloid plaques or decreased CSF Abeta42. *J. Neurosci.* 30, 17035–17040.

Sheline, Y. I., Raichle, M. E., Snyder, A. Z., Morris, J. C., Head, D., Wang, S., and Mintun, M. A. (2010b). Amyloid plaques disrupt resting state default mode network connectivity in cognitively normal elderly. *Biol. Psychiatry* 67, 584–587.

Shmuel, A., and Leopold, D. A. (2008). Neuronal correlates of spontaneous fluctuations in fMRI signals in monkey visual cortex: Implications for functional connectivity at rest. *Hum. Brain Mapp.* 29, 751–761.

Shulman, G. L., Fiez, J. A., Corbetta, M., Buckner, R. L., Miezin, F. M., Raichle, M. E., and Petersen, S. E. (1997). Common blood flow changes across visual tasks: II. Decreases in cerebral cortex. *J. Cogn. Neurosci.* 9, 648–663.

Smit, D. J., Stam, C. J., Posthuma, D., Boomsma, D. I., and de Geus, E. J. (2008). Heritability of "small-world" networks in the brain: a graph theoretical analysis of resting-state EEG functional connectivity. *Hum. Brain Mapp.* 29, 1368–1378.

Smith, S. M., Fox, P. T., Miller, K. L., Glahn, D. C., Fox, P. M., Mackay, C. E., Filippini, N., Watkins, K. E., Toro, R., Laird, A. R., and Beckmann, C. F. (2009). Correspondence of the brain's functional architecture during activation and rest. *Proc. Natl. Acad. Sci. U.S.A.* 106, 13040–13045.

Smith, S. M., Jenkinson, M., Johansen-Berg, H., Rueckert, D., Nichols, T. E., Mackay, C. E., Watkins, K. E., Ciccarelli, O., Cader, M. Z., Matthews, P. M., and Behrens, T. E. (2006). Tract-based spatial statistics: voxelwise analysis of multi-subject diffusion data. *Neuroimage* 31, 1487–1505.

Sonuga-Barke, E. J., and Castellanos, F. X. (2007). Spontaneous attentional fluctuations in impaired states and pathological conditions: a neurobiological hypothesis. *Neurosci. Biobehav. Rev.* 31, 977–986.

Sporns, O. (2011). The human connectome: a complex network. *Ann. N. Y. Acad. Sci.* 1224, 109–125.

Sporns, O., Tononi, G., and Edelman, G. M. (2000). Theoretical neuroanatomy: relating anatomical and functional connectivity in graphs and cortical connection matrices. *Cereb. Cortex* 10, 127–141.

Sporns, O., Tononi, G., and Kotter, R. (2005). The human connectome: a structural description of the human brain. *PLoS Comput. Biol.* 1, e42. doi:10.1371/journal.pcbi.0010042

Stefansson, H., Ophoff, R. A., Steinberg, S., Andreassen, O. A., Cichon, S., Rujescu, D., Werge, T., Pietilainen, O. P., Mors, O., Mortensen, P. B., Sigurdsson, E., Gustafsson, O., Nyegaard, M., Tuulio-Henriksson, A., Ingason, A., Hansen, T., Suvisaari, J., Lonnqvist, J., Paunio, T., Borglum, A. D., Hartmann, A., Fink-Jensen, A., Nordentoft, M., Hougaard, D., Norgaard-Pedersen, B., Bottcher, Y., Olesen, J., Breuer, R., Moller, H. J., Giegling, I., Rasmussen, H. B., Timm, S., Mattheisen, M., Bitter, I., Rethelyi, J. M., Magnusdottir, B. B., Sigmundsson, T., Olason, P., Masson, G., Gulcher, J. R., Haraldsson, M., Fossdal, R., Thorgeirsson, T. E., Thorsteinsdottir, U., Ruggeri, M., Tosato, S., Franke, B., Strengman, E., Kiemeney, L. A., Melle, I., Djurovic, S., Abramova, L., Kaleda, V., Sanjuan, J., de Frutos, R., Bramon, E., Vassos, E., Fraser, G., Ettinger, U., Picchioni, M., Walker, N., Toulopoulou, T., Need, A. C., Ge, D., Yoon, J. L., Shianna, K. V., Freimer, N. B., Cantor, R. M., Murray, R., Kong, A., Golimbet, V., Carracedo, A., Arango, C., Costas, J., Jonsson, E. G., Terenius, L., Agartz, I., Petursson, H., Nothen, M. M., Rietschel, M., Matthews, P. M., Muglia, P., Peltonen, L., St Clair, D., Goldstein, D. B., Stefansson, K., and Collier, D. A. (2009). Common variants conferring risk of schizophrenia. *Nature* 460, 744–747.

Steinberg, S., Mors, O., Borglum, A. D., Gustafsson, O., Werge, T., Mortensen, P. B., Andreassen, O. A., Sigurdsson, E., Thorgeirsson, T. E., Bottcher, Y., Olason, P., Ophoff, R. A., Cichon, S., Gudjonsdottir, I. H., Pietilainen, O. P., Nyegaard, M., Tuulio-Henriksson, A., Ingason, A., Hansen, T., Athanasiu, L., Suvisaari, J., Lonnqvist, J., Paunio, T., Hartmann, A., Jurgens, G., Nordentoft, M., Hougaard, D., Norgaard-Pedersen, B., Breuer, R., Moller, H. J., Giegling, I., Glenthoj, B., Rasmussen, H. B., Mattheisen, M., Bitter, I., Rethelyi, J. M., Sigmundsson, T., Fossdal, R., Thorsteinsdottir, U., Ruggeri, M., Tosato, S., Strengman, E., Kiemeney, L. A., Melle, I., Djurovic, S., Abramova, L., Kaleda, V., Walshe, M., Bramon, E., Vassos, E., Li, T., Fraser, G., Walker, N., Toulopoulou, T., Yoon, J., Freimer, N. B., Cantor, R. M., Murray, R., Kong, A., Golimbet, V., Jonsson, E. G., Terenius, L., Agartz, I., Petursson, H., Nothen, M. M., Rietschel, M., Peltonen, L., Rujescu, D., Collier, D. A., Stefansson, H., St Clair, D., and Stefansson, K. (2011). Expanding the range of ZNF804A variants conferring risk of psychosis. *Mol. Psychiatry* 16, 59–66.

Sullivan, P. F., Neale, M. C., and Kendler, K. S. (2000). Genetic epidemiology of major depression: review and meta-analysis. *Am. J. Psychiatry* 157, 1552–1562.

Tan, H. Y., Chen, Q., Sust, S., Buckholtz, J. W., Meyers, J. D., Egan, M. F., Mattay, V. S., Meyer-Lindenberg, A., Weinberger, D. R., and Callicott, J. H. (2007). Epistasis between catechol-O-methyltransferase and type II metabotropic glutamate receptor 3 genes on working memory brain function. *Proc. Natl. Acad. Sci. U.S.A.* 104, 12536–12541.

Thompson, P. M., Cannon, T. D., Narr, K. L., Van Erp, T. G. M., Poutanen, V.-P., Huttunen, M., Lönnqvist, J., Standertskjöld-Nordenstam, C. G., Kaprio, J., Khaledy, M., Dail, R., Zoumalan, C. I., and Toga, A. W. (2001). Genetic influences on brain structure. *Nat. Neurosci.* 4, 1253–1258.

van den Heuvel, M. P., Mandl, R. C., Stam, C. J., Kahn, R. S., and Hulshoff Pol, H. E. (2010). Aberrant frontal and temporal complex network structure in schizophrenia: a graph theoretical analysis. *J. Neurosci.* 30, 15915–15926.

van den Heuvel, M. P., Stam, C. J., Kahn, R. S., and Hulshoff Pol, H. E. (2009). Efficiency of functional brain networks and intellectual performance. *J. Neurosci.* 29, 7619–7624.

Van Essen, D. C. (1997). A tension-based theory of morphogenesis and compact wiring in the central nervous system. *Nature* 385, 313–318.

van Grootheest, D. S., Cath, D. C., Beekman, A. T., and Boomsma, D. I. (2005). Twin studies on obsessive-compulsive disorder: a review. *Twin Res. Hum. Genet.* 8, 450–458.

Walters, J. T., and Owen, M. J. (2007). Endophenotypes in psychiatric genetics. *Mol. Psychiatry* 12, 886–890.

Wang, L., Zhu, C., He, Y., Zang, Y., Cao, Q., Zhang, H., Zhong, Q., and Wang, Y. (2009). Altered small-world brain functional networks in children with attention-deficit/hyperactivity disorder. *Hum. Brain Mapp.* 30, 638–649.

Wei, L., Li, Y., Tang, Y., and Wang, J. (2010). Brain functional connectivity in depression during emotion processing. *Sheng Wu Yi Xue Gong Cheng Xue Za Zhi* 27, 961–967.

Weinberger, D. R., Berman, K. F., Suddath, R., and Torrey, E. F. (1992). Evidence of dysfunction of a prefrontal-limbic network in schizophrenia: a magnetic resonance imaging and regional cerebral blood flow study of discordant monozygotic twins. *Arch. Gen. Psychiatry* 149, 890–897.

Westlye, E. T., Lundervold, A., Rootwelt, H., Lundervold, A. J., and Westlye, L. T. (2011). Increased hippocampal default mode synchronization during rest in middle-aged and elderly APOE epsilon4 carriers: relationships with memory performance. *J. Neurosci.* 31, 7775–7783.

Whitfield-Gabrieli, S., Thermenos, H. W., Milanovic, S., Tsuang, M. T., Faraone, S. V., McCarley, R. W., Shenton, M. E., Green, A. I., Nieto-Castanon, A., LaViolette, P., Wojcik, J., Gabrieli, J. D., and Seidman, L. J. (2009). Hyperactivity and hyperconnectivity of the default network in schizophrenia and in first-degree relatives of persons with schizophrenia. *Proc. Natl. Acad. Sci. U.S.A.* 106, 1279–1284.

Williams, H. J., Norton, N., Dwyer, S., Moskvina, V., Nikolov, I., Carroll, L., Georgieva, L., Williams, N. M., Morris, D. W., Quinn, E. M., Giegling, I., Ikeda, M., Wood, J., Lencz, T., Hultman, C., Lichtenstein, P., Thiselton, D., Maher, B. S., Malhotra, A. K., Riley, B., Kendler, K. S., Gill, M., Sullivan, P., Sklar, P., Purcell, S., Nimgaonkar, V. L., Kirov, G., Holmans, P., Corvin, A., Rujescu, D., Craddock, N., Owen, M. J., and O'Donovan, M. C. (2011). Fine mapping of ZNF804A and genome-wide significant evidence for its involvement in schizophrenia and bipolar disorder. *Mol. Psychiatry* 16, 429–441.

Winterer, G., Konrad, A., Vucurevic, G., Musso, F., Stoeter, P., and Dahmen, N. (2008). Association of 5′ end neuregulin-1 (NRG1) gene variation with subcortical medial frontal microstructure in humans. *Neuroimage* 40, 712–718.

Xu, L., Groth, K. M., Pearlson, G., Schretlen, D. J., and Calhoun, V. D. (2009a). Source-based morphometry: the use of independent component analysis to identify gray matter differences with application to schizophrenia. *Hum. Brain Mapp.* 30, 711–724.

Xu, L., Pearlson, G., and Calhoun, V. D. (2009b). Joint source based morphometry identifies linked gray and white matter group differences. *Neuroimage* 44, 777–789.

Zalesky, A., and Fornito, A. (2009). A DTI-derived measure of cortico-cortical connectivity. *IEEE Trans. Med. Imaging* 28, 1023–1036.

Zalesky, A., Fornito, A., Harding, I. H., Cocchi, L., Yucel, M., Pantelis, C., and Bullmore, E. T. (2010). Whole-brain anatomical networks: does the choice of nodes matter? *Neuroimage* 50, 970–983.

Zalesky, A., Fornito, A., Seal, M. L., Cocchi, L., Westin, C. F., Bullmore, E. T., Egan, G. F., and Pantelis, C. (2011). Disrupted axonal fiber connectivity in schizophrenia. *Biol. Psychiatry* 69, 80–89.

Zhang, D., and Raichle, M. E. (2010). Disease and the brain's dark energy. *Nat. Rev. Neurol.* 6, 15–28.

Conflict of Interest Statement: Edward T. Bullmore is employed half-time by GlaxoSmithKline.

Received: 25 November 2011; accepted: 23 March 2012; published online: 19 April 2012.

Citation: Fornito A and Bullmore ET (2012) Connectomic intermediate phenotypes for psychiatric disorders. Front. Psychiatry ***3****:32. doi: 10.3389/fpsyt.2012.00032*

This article was submitted to Frontiers in Neuropsychiatric Imaging and Stimulation, a specialty of Frontiers in Psychiatry.

frontiers in
PSYCHIATRY

REVIEW ARTICLE
published: 05 January 2012
doi: 10.3389/fpsyt.2011.00077

Mapping the Alzheimer's brain with connectomics

Teng Xie and Yong He*

State Key Laboratory of Cognitive Neuroscience and Learning, Beijing Normal University, Beijing, China

Edited by:
Alex Fornito, University of Melbourne, Australia

Reviewed by:
Aristotle Voineskos, Centre for Addiction and Mental Health, Canada
Christian Sorg, Klinikum rechts der Isar Technische Universität München, Germany

****Correspondence:***
Yong He, State Key Laboratory of Cognitive Neuroscience and Learning, Beijing Normal University, Beijing 100875, China.
e-mail: yong.he@bnu.edu.cn

Alzheimer's disease (AD) is the most common form of dementia. As an incurable, progressive, and neurodegenerative disease, it causes cognitive and memory deficits. However, the biological mechanisms underlying the disease are not thoroughly understood. In recent years, non-invasive neuroimaging and neurophysiological techniques [e.g., structural magnetic resonance imaging (MRI), diffusion MRI, functional MRI, and EEG/MEG] and graph theory based network analysis have provided a new perspective on structural and functional connectivity patterns of the human brain (i.e., the human connectome) in health and disease. Using these powerful approaches, several recent studies of patients with AD exhibited abnormal topological organization in both global and regional properties of neuronal networks, indicating that AD not only affects specific brain regions, but also alters the structural and functional associations between distinct brain regions. Specifically, disruptive organization in the whole-brain networks in AD is involved in the loss of small-world characters and the re-organization of hub distributions. These aberrant neuronal connectivity patterns were associated with cognitive deficits in patients with AD, even with genetic factors in healthy aging. These studies provide empirical evidence to support the existence of an aberrant connectome of AD. In this review we will summarize recent advances discovered in large-scale brain network studies of AD, mainly focusing on graph theoretical analysis of brain connectivity abnormalities. These studies provide novel insights into the pathophysiological mechanisms of AD and could be helpful in developing imaging biomarkers for disease diagnosis and monitoring.

Keywords: connectome, graph theory, small-world, cortical thickness, genetics, DTI, fMRI, EEG/MEG

INTRODUCTION

Alzheimer's disease (AD) is the most common form of dementia, comprising 50–70% of all dementia cases (Kukull and Bowen, 2002). Currently, 35.6 million people suffer from AD globally and the number is predicted to rise to 115.4 million by 2050[1]. As an incurable, progressive, and neurodegenerative disease, it causes memory loss and other cognitive deficits.

In recent years, modern magnetic resonance imaging [MRI; e.g., structural MRI (sMRI), functional MRI (fMRI), and diffusion MRI] and neurophysiological (e.g., electroencephalograph and magnetoencephalograph, usually referred as EEG/MEG) techniques have provided an efficient, feasible, and non-invasive way to investigate the biological mechanisms of AD *in vivo*. A large quantity of studies have found focal structural and functional abnormalities of the brains of patients with AD, including disturbed functional activation and reduced gray matter volume or thickness in regions of the brain including the posterior cingulate, the medial temporal lobe, the hippocampus, and the parahippocampal gyrus (Rombouts et al., 2000; Frisoni et al., 2002; Busatto et al., 2003; Sperling et al., 2003). Recent studies have suggested that AD is not only associated with regional disturbance of brain structure and function but also with abnormalities in the connections between different regions. De Lacoste and White (1993) suggested that neurofibrillary tangles and neuritic plaques (the two principle neuropathological biomarkers of AD) are usually distributed in the regions where corticocortical connections begin or end. Disruptive alterations in white matter tracts have been observed in AD and involve the cingulum, the uncinate fasciculus, the splenium, and the genu of the corpus callosum (Rose et al., 2000; Bozzali et al., 2002; Naggara et al., 2006; Xie et al., 2006; Fellgiebel et al., 2008; Ukmar et al., 2008; Kiuchi et al., 2009). Abnormal functional connectivities have also been found, including abnormal interhemispheric and intrahemispheric (frontoparietal, frontotemporal, and temporoparietal) connections (Wada et al., 1998a,b; Berendse et al., 2000; Grady et al., 2001; Greicius et al., 2004; Pijnenburg et al., 2004; Koenig et al., 2005; Celone et al., 2006; Stam et al., 2006; Wang et al., 2007). All of these studies proposed that AD is a syndrome of disconnection in neuronal networks (for reviews, see Delbeuck et al., 2003; He et al., 2009a; Filippi and Agosta, 2011).

Despite the number of studies of AD-related alterations in structural and functional connections between brain regions, there is increasing evidence that AD is also characterized by large-scale brain system disruptions. Sporns et al. (2005) proposed the notion of the "connectome" to describe the detailed structural and functional connectivity pattern of the human brain. Since then, many studies have utilized multi-modal neuroimaging and neurophysiological techniques as well as advanced graph theoretical approaches to investigate the human brain connectome in health and disease. These studies have discovered many important

[1]http://www.alz.co.uk/

topological characteristics of the brain system such as efficient small-worldness and distributed network hubs in the medial frontal and parietal regions (for reviews, see Bullmore and Sporns, 2009; He and Evans, 2010; Stam, 2010; Sporns, 2011). Such topology-based approaches have also been used to study the neuronal systems of patients with AD and have revealed a disruption of the typical organizational pattern of brain networks, including shifts in small-world topology and redistribution of hub regions (Stam et al., 2007a, 2009; He et al., 2008; Supekar et al., 2008; De Haan et al., 2009; Lo et al., 2010; Sanz-Arigita et al., 2010; Yao et al., 2010). Moreover, these methods have also been used to study topological organization of brain networks in the apolipoprotein E epsilon 4 allele (APOE-4) carriers (APOE-4 is a major genetic determinant for AD; Brown et al., 2011). These findings have provided new insights into the understanding of the biological mechanism of AD and could lead to the use of a network based imaging biomarker for disease diagnosis and monitoring.

In this review, we will summarize recent advances on graph theory based network analysis of the brain connectome in AD. First, we will briefly introduce several basic concepts of graph-based network analysis and human connectomics. Then we will review recent studies of graph theoretical analysis of AD brain networks derived from different imaging modalities including sMRI, diffusion MRI, EEG/MEG, and fMRI. Next we will have a short discussion regarding the effects of genetics on brain connectome in AD. Finally, we will propose further considerations for future studies of AD connectomics.

GRAPH THEORY AND HUMAN CONNECTOMICS

GRAPH THEORY

Generally speaking, a graph G (or a network) consists of N nodes linked by K edges. Depending on whether the edges have a direction or not, the graphs can be classified into directed or undirected. Furthermore, the graph is classified as weighted or unweighted based on whether the edges are weighted. Graphs (networks) can be described by an adjacent matrix $A(n, n)$ in which n is the number of nodes and the value of A_{ij} refers to the edge linking node i and node j.

There are many graph metrics that can be used to describe the topological properties of a network, including cost/sparsity, clustering coefficient (C_p), characteristic path length (L_p), normalized clustering coefficient (γ), normalized characteristic path length (λ), small-worldness (σ), global efficiency (E_g), local efficiency (E_{loc}), degree (k), nodal efficiency (E_{nodal}), and betweenness centrality (B_c; **Table 1**). In this review we will only focus on undirected and unweighted networks. For a detailed description of network metrics in directed or weighted networks, please see Boccaletti et al. (2006) and Rubinov and Sporns (2010).

The cost/sparsity of a network is the ratio of K to the possible maximum number of edges in the network K_{max}, which equals $N(N-1)/2$. The C_p of node i is the cost/sparsity of the subgraph G_i consisting of the nodes directly linked with i (the neighbors of node i). The C_p of a network is the mean C_p across all the nodes. The distance between node i and j (noted as d_{ij}), also known as the shortest path length, refers to the minimum number of edges that must be passed from i to j, and L_p is the arithmetic mean or

Table 1 | Network indices.

Index	Definition	Interpretation	Meaning
Cost/sparsity	$\text{Cost}(G) = K/K_{max}$	G: the network, or the graph to be studied K: the number of edges in the network K_{max}: the maximum possible number of edges in the network	The cost of constructing the network
Degree (k)		The number of edges linked to a certain node	The accessibility of a certain node
Clustering coefficient (C_p)	$C_p^i = \text{Cost}(G_i)$ $C_p = \frac{1}{N}\sum_{i=1}^{N} C_p^i$	G_i: the subgraph comprising of neighbors of node i and the connections between them C_p^i: the clustering coefficient of node i, i.e., the cost of G_i N: the number of nodes in graph G	A high C_p of indicates that the nodes tend to form dense regional cliques, implying that the efficiency in local information transfer and processing are high
Characteristic path length (L_p)	$L_p = \frac{N(N-1)}{\sum_{1\le i\ne j\le N}\frac{1}{d_{ij}}}$	d_{ij}: the minimal number of edges that must be passed from node i to node j L_p: the arithmetic or harmonic mean of d_{ij} of all the node pairs. Here the equation presents the harmonic mean	A low L_p indicates high transfer speed through the overall network, implying that the network has a high global efficiency
Global efficiency (E_g)	$E_g = \frac{1}{L_p}$	E_g: equals $1/L_p$ if L_p is the harmonic mean defined as above	The overall information transfer efficiency across the whole network
Local efficiency (E_{loc})	$E_{loc} = \frac{1}{N}\sum_{i=1}^{N} E_g(G_i)$	E_{loc}: the mean of the global efficiencies of G_i across all the nodes in the network	A higher E_{loc} value reflects higher efficiency of regional information processing
Betweenness centrality [$B_c(i)$]	$B_c(i) = \sum_{j\ne m\ne i\in G}\frac{e_{jim}}{e_{jm}}$	e_{jim}: the number of shortest paths between node j and m which pass through node i e_{jm}: the number of shortest paths between node j and m $B_c(i)$: equals the sum of e_{jim}/e_{jm} across all the node pairs except for those including i	A node with high betweenness plays a critical role in the information processing of the network because its abnormality would widely affect the shortest paths and thus influence the whole network efficiency

the harmonic mean of the shortest path lengths between all pairs of nodes in G. The C_p and L_p of a network reveals the local and global efficiency of information transfer and processing, respectively. According to C_p and L_p, networks can be assigned to three different categories: regular networks with high C_p and L_p, random networks with low C_p and L_p, and small-world networks with high C_p ($\gg C_p^{rand}$, the mean C_p of a number of matched random networks) and low L_p ($\sim L_p^{rand}$, the mean L_p of a number of matched random networks; Watts and Strogatz, 1998). Small-world is a common organizational structure of networks in lots of fields such as airline networks, social networks, physiological networks, and neuronal networks and has been proved to support highly efficient segregated and integrated information processing with low wiring costs (Watts and Strogatz, 1998). Three secondary parameters, γ (C_p/C_p^{rand}), λ (L_p/L_p^{rand}), and σ (γ/λ) can reveal the network's small-worldness (Watts and Strogatz, 1998; Humphries et al., 2006). The efficiency of information processing in a graph can be measured with E_g and E_{loc} (Latora and Marchiori, 2001). E_g equals the inverse of L_p if L_p is the harmonic mean of distances over all pairs of nodes and E_{loc} is the average of $E_g(G_i)$ in which i ranges from 1 to N.

While the metrics mentioned above contain information about the organizational properties of the comprehensive network, several nodal metrics such as k, E_{nodal}, and B_c can be further used to indicate the different roles of the nodes. The degree, k, refers to the number of edges linking to a particular node and reveals the accessibility of the node. E_{nodal} of node i is the inverse of the harmonic mean distance between i and all other nodes (Achard and Bullmore, 2007). The definition of B_c is much more complex. To get the B_c of a certain node i [i.e., $B_c(i)$ in **Table 1**], we should first select a pair of nodes, noted as m and n, calculate the number of shortest paths between them passing through i, divide that number by the total number of shortest paths between m and n, and then sum the ratios across all pairs of nodes in the network (Freeman, 1977). $B_c(i)$ measures the extent to which the node i is a necessity of the shortest paths between any pair of nodes excluding i in the network. Nodes with high k, B_c, or with short average path length to other nodes (and thus with high E_{nodal}) are considered of high importance to the information processing efficiency of the network and are called hubs. Because the hubs tend to have lots of connections to other nodes or on the way of lots of shortest paths, removal of hubs can cause significant changes in the organization of the network.

HUMAN CONNECTOMICS

Human connectomics is an emerging scientific concept that is used to represent the comprehensive descriptions of structural and functional connectivity patterns of the human brain (Sporns et al., 2005). The human connectome can be constructed on different scales: the microscale, the mesoscale, and the macroscale. The main difference between the three scales is the definition of the network node. A single neuron represents the node when using the microscale. For the mesoscale the nodes are a group of neurons and for the macroscale the nodes are anatomically separate brain regions (Sporns et al., 2005). The edges are then determined by analyzing multi-modal imaging data, for example by measuring the properties of white matter tracts derived from diffusion MRI images, the correlations of time courses from EEG/MEG/fMRI data and the association of brain morphometry obtained from sMRI. Currently, it is hard to obtain microscale and mesoscale network data on the human brain *in vivo*. To date, existing studies mainly focused on undirected and unweighted macroscale matrices. All the networks mentioned in this review are undirected and unweighted brain networks if not noted specifically. Once the brain networks are constructed using neuroimaging data, a threshold is usually used to transform the initial connectivity matrix into a binary adjacent matrix. Either the correlation coefficient or the cost/sparsity can be used to set the threshold. The flowchart of brain network construction is shown in **Figure 1**.

On the basis of the connectome analysis, many studies have demonstrated that healthy human brain networks derived from different modalities are small-world networks with high C_p and short L_p (for reviews, see Reijneveld et al., 2007; Stam and Reijneveld, 2007; Bullmore and Sporns, 2009; He and Evans, 2010; Sporns, 2011). Considering the traits of a small-world network, it can be inferred that the human brain has evolved into the optimal architecture that maximizes the local and global information processing efficiency in the human brain while lowering the wiring cost. Existing studies also have demonstrated coincident areas as hubs in human brain networks such as the precuneus, the posterior cingulate cortex, the dorsal superior frontal gyrus, the precentral gyrus, and the middle and superior occipital gyri (Achard et al., 2006; He et al., 2007; Hagmann et al., 2008; Buckner et al., 2009; Gong et al., 2009; Tomasi and Volkow, 2010). In addition, significant genetic effects on the brain connectome of healthy people have been demonstrated by two recent studies on twins. Using

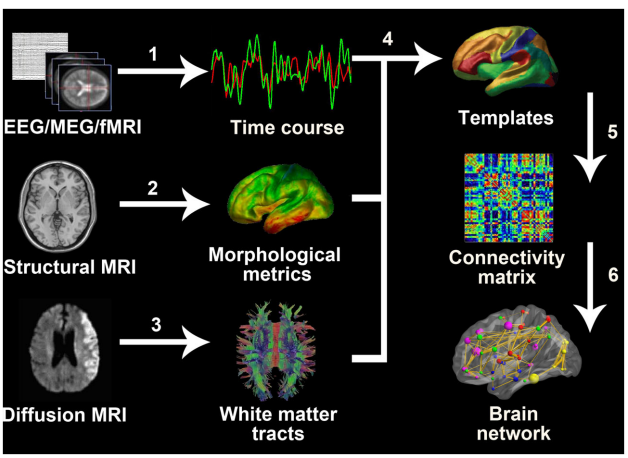

FIGURE 1 | General process of whole-brain network construction. 1, Extract time course from EEG/MEG records or fMRI images. 2, Calculate morphological metrics such as cortical thickness (the picture showed in **Figure 1**) and gray matter volume. 3, Define white matter fiber bundles using tractography. 4, Extract regional information from the original voxel- or vertex-based MRI data according to templates. 5, For EEG/MEG, fMRI, and sMRI, the connectivity matrix usually refers to the correlation matrix; for diffusion MRI, it can be a matrix consisting of numbers of fibers regions or the connectivity strength. 6, Generate the whole-brain network using further modification of the connectivity matrix, for example by using thresholds.

resting-state fMRI, Fornito et al. (2011) illustrated that in functional brain network, 60% of the variation of the cost–efficiency, which is an index measuring the difference between the network cost and efficiency, was attributed to additive genetic effects. Using sMRI, Schmitt et al. (2008) demonstrated that genetically mediated neuroanatomic network derived from cortical thickness correlations follows a small-world architecture, suggesting that genetic factors are involved in the correlative patterning of the human cortex in this manner.

BRAIN CONNECTOMICS IN AD

STRUCTURAL CONNECTOMICS IN AD

Using sMRI and diffusion tensor imaging (DTI), several studies have demonstrated abnormal topological properties in the structural brain networks of patients with AD. In this section, we will review the existing studies of AD structural connectomics.

Gray matter networks

Gray matter morphometric information (gray matter density, gray matter volume, and cortical thickness) revealed by sMRI provides a promising way to explore human brain anatomy. Coordinate variations of brain morphometry measurements between functionally- or anatomically-connected areas have been found in recent sMRI studies, in the visual areas (Andrews et al., 1997) and in the frontotemporal (Bullmore et al., 1998; Lerch et al., 2006), frontoparietal (Wright et al., 1999), and symmetrical interhemispheric regions (Mechelli et al., 2005; He et al., 2007; Zielinski et al., 2010). Human brain structural networks can be established from sMRI images based on gray matter volume or cortical thickness correlations between different areas. He et al. (2007) used graph theoretical network analysis (GRETNA) to examine the macroscale cortical thickness correlation network of 124 normal adults and described it as small-world. Networks based on gray matter volume correlations also revealed a similar topology (Bassett et al., 2008). Gray matter-based network analysis technique has gained more and more attention in the AD research field.

He et al. (2008) was the first group to use sMRI and graph theory tools to investigate structural brain networks in AD patients. Their study included 97 healthy older adults and 92 AD patients. The cortical thickness coordination networks at large-scale were constructed for both groups. The networks consisted of 54 nodes each, referring to 54 regions from the automated non-linear image matching and anatomical labeling (ANIMAL) template. GRETNA, as used in their previous study (He et al., 2007), was then applied to the two structural networks. They found that the AD group had decreased interregional correlations of cortical thickness between the bilateral postcentral gyri and between the bilateral superior parietal lobes. Increased correlations were also discovered within regions such as the medial prefrontal cortex, the cingulate regions, the supramarginal gyrus, the superior temporal gyrus, and the inferior temporal gyrus. These regions were mostly located in the so-called default mode network (DMN), which is a neuronal network closely related to episodic memory, comprising of the posterior cingulate cortex/precuneus, the lateral temporal and parietal cortex, the hippocampus, and the medial frontal cortex regions (Raichle et al., 2001). While the networks derived from both groups demonstrated small-world characteristics, significant differences in network parameters were observed over binary networks using a wide range of sparsity thresholds (**Figures 2A,B**). The brain networks in AD showed increased C_p and L_p compared with those of healthy adults, indicating a less optimal topological structure. They also found decreased betweenness centrality in the right superior temporal gyrus and the bilateral angular gyri. Increases were also found in the left lingual gyrus, the left lateral occipitotemporal gyrus, and the right cingulate gyrus in the network of patients with AD (**Figure 2C**). All of these regions were identified as hubs in either the health network or in the AD network by this study. In addition, they discovered that the AD network was more vulnerable to targeted attack, that is, the absence of hub regions had a greater influence on the AD network.

Another recent study explored changes in the topological properties of the structural brain network in patients with AD and mild cognitive impairment (MCI; Yao et al., 2010). MCI is considered an intermediate stage between normal aging and AD, and people with MCI are at high risk developing AD. The dataset for this study was acquired from the Alzheimer's Disease Neuroimaging Initiative[2,3] and included 98 normal controls, 113 subjects with MCI, and 91 AD patients. In this work, Yao and colleagues constructed a 90 by 90 gray matter volume correlation network for each of the three groups using an automated anatomical labeling (AAL) template with multiple sparsity thresholds ranging from 15 to 30%. Permutation testing revealed a significant increase in C_p over a wide range of thresholds and a larger L_p on higher thresholds in the AD networks compared with the healthy networks, implying a weakening of small-worldness. This result was consistent with previous study based on cortical thickness correlation networks (He et al., 2008). The C_p and L_p values of MCI network were intermediate between AD group and normal control group but no significant changes were found. They further identified the middle temporal gyrus, temporal pole, lingual gyrus, orbital frontal gyrus, and superior parietal gyrus as hub regions in the network of the normal control group, and the orbital frontal gyrus, inferior frontal gyrus, cingulate, and medial orbital frontal gyrus in the AD group. The hubs of MCI network largely overlapped with AD network. The alteration in hub regions revealed the disturbed large-scale brain connectome integration in AD. Regions including the parahippocampal gyrus, temporal pole, fusiform, cingulate, superior parietal region, and orbital frontal gyrus showed significant changes in the interregional correlations between the normal control and AD groups.

In summary, these sMRI-based studies have consistently demonstrated that patients with AD had aberrant morphological organization in gray matter structural networks. Specifically, the patients were found to have higher C_p and L_p in the brain structural networks, suggesting a tendency from the optimal small-world organization toward a regular-like connectivity pattern in the AD brain connectome. However, it needs to note that the biological mechanisms underlying topological alterations of morphological networks in AD remain largely unclear, although

[2]http://adni.loni.ucla.edu/
[3]http://adni-info.org

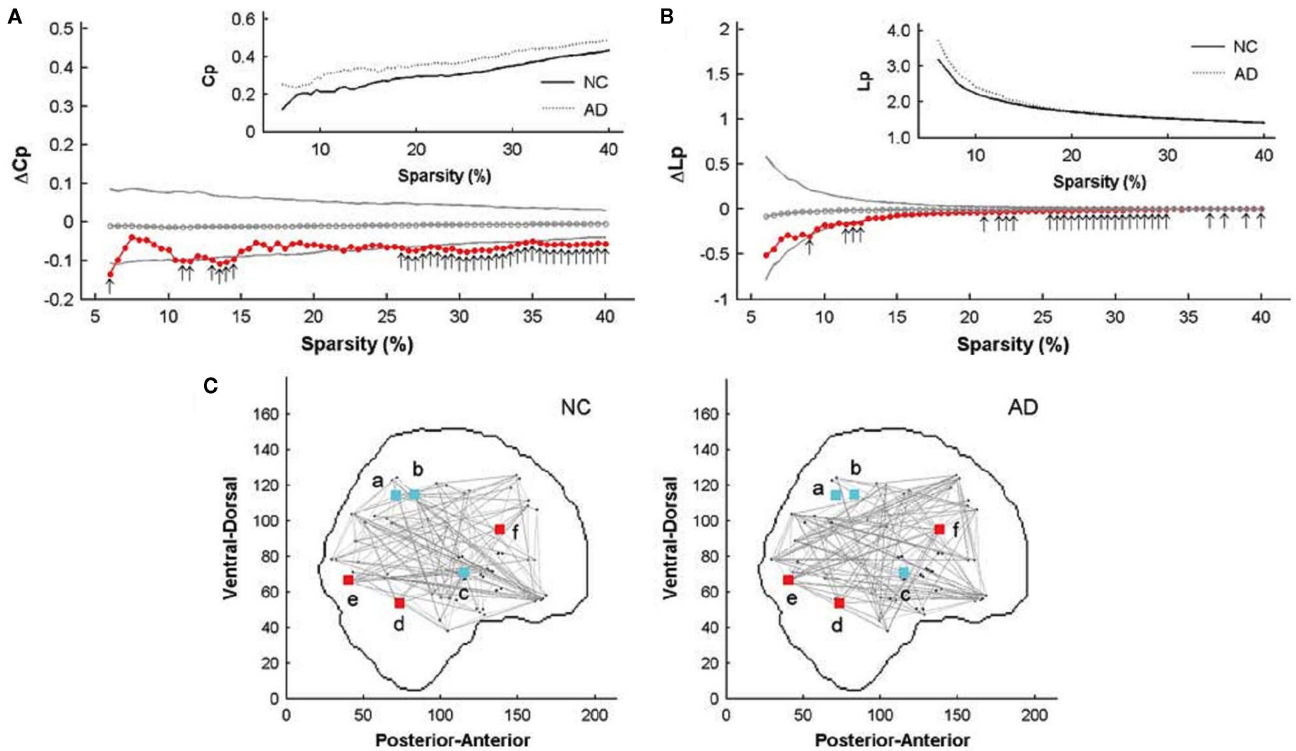

FIGURE 2 | Comparison of structural connectome between patients with AD and healthy controls (He et al., 2008). Significant differences ($p < 0.05$) in C_p and L_p between patients with AD and healthy controls with different sparsity thresholds are shown in **(A,B)** with arrows. The gray lines represent mean values and 95% confidence intervals of between-group differences obtained by permutation tests, while red dots show the real value of the differences. **(C)** Shows hub regions with significantly different betweenness in the AD group compared with the healthy control group. Red regions have significantly increased betweenness in the AD group and cyan regions have decreased values of betweenness. The small letters a through *f* represented the right angular gyrus, the left angular gyrus, the right superior temporal gyrus, the left lateral occipitotemporal gyrus, the right lingual gyrus, and the left cingulate gyrus, respectively.

several previous studies have suggested that these morphological correlations among regions might be associated with the mutually tropic effects, environment-related plasticity, and genetic effects (Mechelli et al., 2005; He et al., 2007).

White matter networks

Different from sMRI, diffusion MRI captures the movement of water molecule in brain tissues, revealing the orientation of white matter fiber bundles by deterministic (Mori et al., 1999) or probabilistic (Behrens et al., 2003) tractography. Studies using the DTI technique have found faithful white matter fiber bundles known as real anatomical connections (Catani et al., 2002; Wakana et al., 2004). Relating to the AD research, DTI-based studies have reported widespread disruptions of white matter integrity in the corpus callosum, the superior longitudinal fasciculus, and cingulum (Rose et al., 2000; Bozzali et al., 2002; Naggara et al., 2006; Xie et al., 2006; Fellgiebel et al., 2008; Ukmar et al., 2008; Kiuchi et al., 2009).

Studies on the brain's white matter are extremely important for the human connectome because white matter tracts connect functionally related regions and therefore might underlie functional states of the brain. Several recent studies have utilized DTI to construct human whole-brain white matter networks and demonstrated small-world topological properties (Hagmann et al., 2007; Iturria-Medina et al., 2008; Gong et al., 2009). Several hub regions have also been identified in the white matter structural networks in healthy adults, including the precuneus, the medial frontal cortex, the middle occipital gyrus, and the cingulate gyrus (Hagmann et al., 2008; Gong et al., 2009).

Lo et al. (2010) published the first research on the AD network based on the DTI technique. They used a dataset of 25 AD patients and 30 age- and gender-matched normal controls. They performed fiber tracking via the fiber assignment by continuous tracking algorithm (Mori et al., 1999). The fiber number between two cortical regions multiplied by the mean fractional anisotropy of the fiber bundles was calculated as the weight of edge. After constructing an undirected weighted network for each participant according to the AAL template, they calculated the C_p, L_p, γ, λ, σ, E_g, E_{loc}, and E_{nodal} to investigate the topological differences between the normal control group and the AD group. It turned out that both normal and AD networks showed prominent small-worldness. No significant differences were found for the values of C_p, γ, and σ between the two groups. However the AD group did have larger L_p and λ values. The increased L_p was in accordance with previous structural connectomics studies of AD (He et al., 2008; Yao et al., 2010). As to the efficiency

measurements, E_g was significantly reduced in AD network, while E_{loc} was not significantly different. These differences revealed a less optimal organization of the brain network in patients with AD. The researchers further identified nodes with high E_{nodal} values as hubs and compared the E_{nodal} of the hubs in AD with those of normal controls. They found that AD-related E_{nodal} reduction was limited to several prefrontal areas including the medial superior frontal gyrus, the middle frontal gyrus, the orbital part of the inferior frontal gyrus, and the temporal pole of the middle temporal gyrus in the temporal lobe (**Figure 3**). The researchers correlated the network properties with the cognitive performance of the patients with AD and found significant correlations between some of the network metrics and memory test scores.

FUNCTIONAL CONNECTOMICS IN AD

Modern functional neuroimaging (e.g., fMRI) and neurophysiological techniques (e.g., EEG/MEG) can non-invasively measure human brain activities and provides valuable information about human brain networks. In this section we will summarize recent advances in AD functional connectomics.

EEG/MEG networks

EEG/MEG records the electric and magnetic field changes caused by the neuronal activities during a task or during the resting-state. These neurophysiological techniques also provide powerful approaches with high temporal resolution to investigate human brain function in health and disease. Functional brain connectome analysis based on EEG/MEG data have uncovered small-world topology in healthy people (Stam, 2004; Bassett et al., 2006; Micheloyannis et al., 2006; Ferri et al., 2007; Smit et al., 2008). The techniques have also been applied studies of AD and have demonstrated abnormal functional connectivity, both in inter-hemispheric and intrahemispheric connections (Berendse et al., 2000; Knott et al., 2000; Adler et al., 2003; Pijnenburg et al., 2004; Koenig et al., 2005; Stam et al., 2006).

Stam et al. (2007a) used EEG to conduct brain network analysis on 15 patients with AD and 13 control subjects with only subjective memory complains. They computed synchronization likelihood in the beta band (13–30 Hz) between any pairs of 21 nodes and constructed a binary brain network for each participant. Their study showed that the AD group had significant increases in L_p both under synchronization likelihood thresholds and sparsity thresholds, implying impaired large-scale brain functional integration. However, they barely found significant changes in C_p below either type of the thresholds. This might imply that the local connectivity of the brain network in AD was relatively spared. Further analysis revealed significant negative Pearson's correlations between L_p and the mini mental state examination (MMSE) score. The results demonstrated the altered brain functional connectivity pattern associated with AD.

In a later work, Stam et al. (2009) used resting-state MEG data to investigate the human brain connectomics in AD. The study included 18 healthy people and 18 patients with AD. They produced a 149-node weighted brain network based on the phase lag index (PLI, see Stam et al., 2007b). The AD group showed significant mean PLI reduction in the beta band and the lower alpha band (8–10 Hz). Significant decreases were also observed in the left frontoparietal, the frontotemporal, the parietooccipital, and the temporooccipital PLIs in the lower alpha band, and in the interhemispheric frontal and right frontoparietal PLIs in the beta band. The findings supported AD as a disconnection syndrome. Statistical analysis on small-world indices revealed significantly higher L_p and lower C_p, γ, and λ in the brain networks of the lower alpha band of patients with AD, leaving no discovery in the beta band. The alteration of small-world indices showed that the AD brain network exhibited a random-like pattern. Putting all the participants together, the MMSE score was positively correlated with mean PLI in the beta band and γ in the lower alpha band.

De Haan et al. (2009) conducted another EEG study of AD and frontotemporal dementia. They acquired resting-state EEG records from 20 patients with AD and 23 healthy people with only subjective cognitive complaints. Binary synchronization likelihood brain networks were constructed with synchronization likelihood thresholds and sparsity thresholds. In the beta band, σ was significantly decreased in AD networks while small-worldness was demonstrated both in healthy and AD networks across all band frequencies. C_p and γ decreased in the AD group in the lower alpha and beta bands. The λ value of AD networks also decreased in the lower alpha and gamma (30–45 Hz) bands. These results implied a disturbance in the balance of localized and integrated information processing and a random-oriented shift of the AD brain networks. The degree correlation, which refers to the mean Pearson correlation coefficient of the degree between each pair of directly linked nodes, was decreased in AD in the lower and upper (10–13 Hz) alpha bands. Taken together, all of these findings supported the conclusion that AD is a disconnection syndrome. The researchers also found that λ was positively correlated with MMSE score in AD patients in the lower alpha band.

More recently, Ahmadlou et al. (2010) studied EEG networks in AD using a visibility graph method (Lacasa et al., 2008). The basic idea of visibility graph is to transform time series into a network whose structure is related to the self-similarity and complexity of the time series. The complexity in the visibility graph of AD patients was significantly decreased in the alpha and delta bands compared with the normal elderly group. They further derived classifiers based on the discriminative complexity measurements and yielded an average accuracy of 97.75% at best. This study demonstrated the possibility of using graph metrics as biomarkers for the diagnosis of AD.

In summary, the EEG/MEG network analysis demonstrated abnormal brain connectome from a functional perspective. All the networks presented a random-like reconstruction in patients with AD, characterized by lower C_p/γ or shorter L_p. The alpha and beta bands showed the highest consistency in detecting AD-related changes in network metrics. A previous study combining EEG and fMRI (Laufs et al., 2003) indicated that the power of the alpha band (8–12 Hz) was correlated with spontaneous neuronal activities of attention-related brain regions, and the power of part of the beta band (17–23 Hz) was correlated with activities in DMN regions. Thus, we speculate that the alterations of network indices in the alpha and beta bands might reflect the underlying mechanism of functional deficits observed in patients with AD.

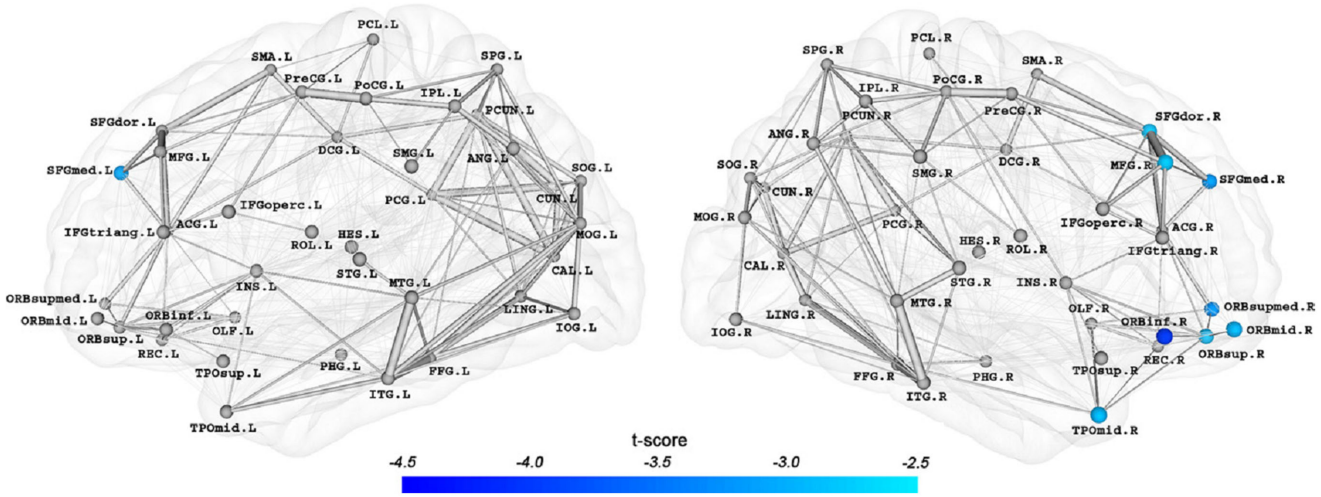

FIGURE 3 | Brain regions with significant differences ($p < 0.05$, FDR corrected) in E_{nodal} in the AD networks (Lo et al., 2010). The regions included the medial part of the superior frontal gyrus (SFGmed.F and SFGmed.R), the right dorsolateral part of the superior frontal gyrus (SFGdor.R), the right middle frontal gyrus (MFG.R), the right orbital part of the inferior frontal gyrus (ORBinf.R), the orbital and the medial orbital part of the superior frontal gyrus (ORBsup.R and ORBsupmed.R), the orbital part of the middle frontal gyrus (ORBmid.R), and the right temporal pole of the middle temporal gyrus (TPOmid.R). The connection strengths between nodes were represented by the edge widths, removing the effects of age and gender.

Functional MRI networks

Functional MRI captures blood–oxygen level dependent signal and indirectly describe the brain activity. fMRI has a relatively low temporal resolution (∼2 s) but a high special resolution (∼2 mm). Using resting-state fMRI (R-fMRI; Biswal et al., 1995), Salvador et al. (2005) first performed the graph theoretical analysis of the functional networks of the human brain. They constructed a 90-node undirected binary network for each participant. Graph theoretical analysis showed that the healthy human brain connectome is a small-world network with hierarchical organization. Later studies found similar topological structure in the human brain, studied the efficiency of the connectome (Achard and Bullmore, 2007) and identified several hub regions such as the precuneus, the middle temporal gyrus, the middle frontal gyrus, and the medial superior frontal gyrus (Achard et al., 2006; Buckner et al., 2009; He et al., 2009b; Zuo et al., 2011; for a review, see Wang et al., 2010). These findings made the understanding of brain network topology more clear and detailed.

Studies of AD based on R-fMRI data have found altered brain functional connectivity in patients with AD (Wang et al., 2006; Allen et al., 2007). Some task-based fMRI studies also found aberrant brain activity in the DMN of patients with AD during simple motor tasks (Greicius et al., 2004) and tasks of associative memory (Celone et al., 2006). Buckner et al. (2009) found a correlation between the locations of hub regions of fMRI brain networks in healthy adults and the sites of Aβ deposition in the brains of patients with AD. These regions included the inferior/superior parietal lobule, the medial superior frontal cortex, the medial prefrontal cortex, and the posterior cingulate/precuneus (**Figure 4**), implying that the hubs are preferentially affected in the progress of AD.

Supekar et al. (2008) published the first R-fMRI study of the functional brain connectome in AD using the topological network analysis method. The researchers recruited 21 patients with AD and 18 healthy volunteers matched for age, gender, and education. R-fMRI brain networks were established using wavelet correlation. The researchers computed small-world metrics of the 90-node networks based on the AAL template and found that both γ and σ of the functional networks were significantly lower in the AD group, indicating that the functional network in AD lost small-worldness. Further investigation showed that using γ as a biomarker to diagnose AD would yield 72% sensitivity and 78% specificity at best, suggesting that the topological network indices could serve as biomarkers of AD. Nodal C_p values were significantly decreased in the hippocampus bilaterally, demonstrating that intrinsic brain functional organization was disrupted. The researchers also found decreased intratemporal connections and weakened connectivity strength (i.e., correlation coefficients) between the thalamus and the frontal, temporal, and occipital lobes. Conversely, the connections within the frontal lobe were enhanced. The analysis was repeated on a second fMRI dataset acquired from the same subjects and produced similar results, suggesting that this analysis technique is reproducible.

In a more recent study, Sanz-Arigita et al. (2010) compared 18 patients with mild AD to 21 healthy controls to explore the loss of small-worldness in AD brain networks. According to the AAL template, a region-based synchronization likelihood matrix was established for each subject and then binarized by a series of thresholds ranged from 0.01 to 0.05 with increments of 0.01. C_p and L_p, along with γ and λ were calculated as the indices of small-worldness. The C_p of patients with AD did not show significant differences from the healthy control group, but the L_p was significantly decreased in the AD group across a wide range

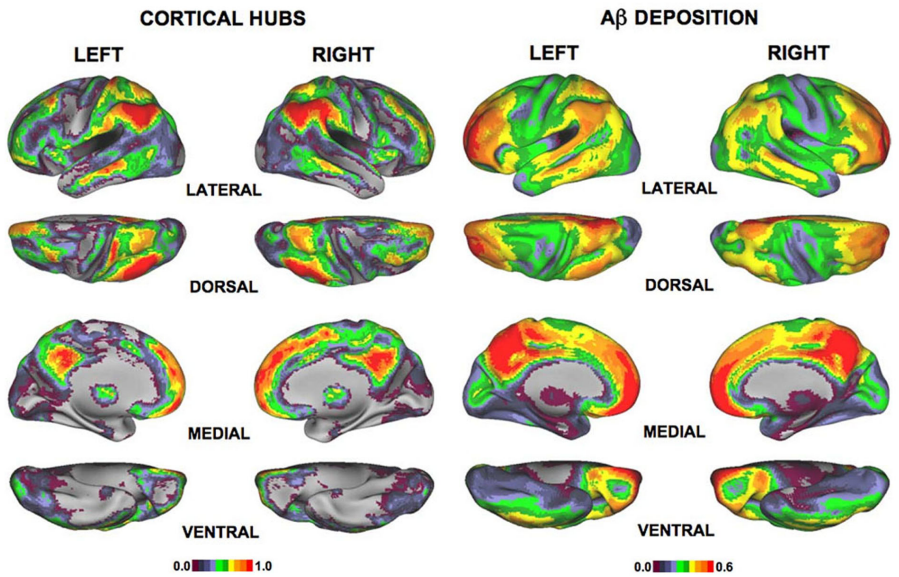

FIGURE 4 | The spatial distribution of functional brain hubs in normal controls (the two columns on the left) and Aβ deposition in AD (the two columns on the right; Buckner et al., 2009). The left color bar shows the *Z* score of degree. The right color bar reveals the extent of Aβ deposition.

of thresholds, implying a trend toward random networks. They found significant synchronization differences between the AD and control groups. Similar to the findings of Supekar et al. (2008), these changes included increases in the functional connectivity within the frontal cortices, between the frontal cortices and the corpus striatum and between the frontal cortices and the thalamus, as revealed by synchronization likelihood and decreases between the temporal lobe, the parietal cortex and the occipital cortex. The long-distance connectivity loss supported the conclusion that AD is a disconnection syndrome, while the strengthened connections suggested that a compensatory mechanism might be responsible for reserving cognitive functions.

Other than the whole-brain network analysis studies, several graph theoretical DMN studies based on fMRI have been conducted. Ciftci (2011) utilized the minimum spanning tree (the subgraph of a network with the minimum cost while connecting all the nodes) to investigate the alteration of DMN connectivity during AD. Their study included 14 young subjects, 14 healthy elderly subjects, and 13 subjects with AD. Significantly lower connection density was observed in the AD and elderly groups compared with the younger group, although the minimum spanning tree of the three groups all presented a similar chain-like structure. Cluster analysis on the three spanning trees revealed much more fragmented functioning organization in AD, which was most notable in the hippocampus/parahippocampus and the precuneus/posterior cingulate complex. They also found a decreased correlation coefficient between the hippocampus/parahippocampus and the inferior temporal gyrus and between the precuneus/posterior cingulate gyrus and the angular gyrus. Another study by Miao et al. (2011) used independent component analysis to identify DMN in 12 normal young adults, 16 older adult controls, and 15 patients with AD. The researchers further constructed directed brain networks using Granger causality modeling and examined the proportion of edges connected with hubs compared to all edges. They found the proportion to be significantly decreased in patients with AD, implying impaired directed DMN connectivity in AD. Utilizing this ratio as a diagnostic tool for AD yielded a specificity of 81.25% and a sensitivity of 80.00%.

In summary, the AD brain connectome studies based on fMRI data demonstrated disrupted network connectivity pattern in patients with AD. The lower C_p, L_p, γ, or λ revealed a random-toward transition of brain connectome in the disease, which were consistent with EEG/MEG studies (Stam et al., 2007a, 2009; De Haan et al., 2009). These less optimized reconfigurations of functional brain network supported the theory that AD is a disconnection syndrome and might imply the functional basis of cognitive deficits.

The studies of structural and functional brain connectomics in AD have illustrated that the brain network configuration in patients with AD was significantly altered compared with normal controls. However, it needs to note that the alterations of topological metrics in the brain networks such as C_p and L_p showed distinct patterns in different modalities (see **Table 2** for detail information). These discrepancies could be attributed to different imaging modality, network size, and population size applied in these studies (**Table 2**). In spite of these differences, we noticed that all of the studies pointed to a less optimized connectivity pattern in AD brain networks. Correlation analysis also revealed that cognitive performances of patients with AD were correlated to topological network indices. As to the nodal properties, the existing studies found aberrant changes in B_c and connectivity strength involving DMN regions. These regions were closely associated with episodic memory and showed significant gray matter atrophy and abnormal functional activities in AD (Rombouts et al., 2000; Frisoni et al., 2002; Busatto et al., 2003; Sperling et al., 2003; Buckner et al., 2005). Although the biological mechanism underlying disrupted

Table 2 | Alzheimer's disease-related alterations of topological properties.

Study	Modality	Connectivity method	Network type	Matrix size	Main findings					
					C_p	L_p	γ	λ	E_g	E_{loc}
He et al. (2008)	sMRI	Partial correlation of cortical thickness	Binary	54	+	+	/	/	/	/
Yao et al. (2010)	sMRI	Pearson correlation of gray matter volume	Binary	90	+	+	/	/	/	/
Lo et al. (2010)	DTI	Deterministic fiber tracking	Weighted	78	NS	+	NS	+	–	NS
Stam et al. (2007a)	EEG	Synchronization likelihood	Binary	21	NS	+	NS	+	/	/
Stam et al. (2009)	MEG	Phase lag index	Weighted	149	–	+	–	–	/	/
De Haan et al. (2009)	EEG	Synchronization likelihood	Binary	21	/	/	–	–	/	/
Supekar et al. (2008)	fMRI	Wavelet correlation	Binary	90	/	/	–	NS	/	/
Sanz-Arigita et al. (2010)	fMRI	Synchronization likelihood	Binary	116/90	NS	–	/	/	/	/

This table was modified from Table 5 in Lo et al. (2010).

+, AD > NC; –, AD < NC; NS, none significance.

topological properties in AD brain networks still remains unclear, we speculate that the disruption could be attributed to the neuron loss, amyloid deposition, or metabolic abnormalities.

AD CONNECTOME AND GENETICS

Researchers have demonstrated that numerous genes have been associated with late-onset AD, including amyloid precursor protein, presenilin 1, presenilin 2, and APOE (for reviews, see Bookheimer and Burggren, 2009; Bekris et al., 2010). Of these genes, APOE is one of the major genetic risk factors for developing AD. Studies on normal people have revealed APOE-4 effects on the brain structure and function but controversy exists. For example, some studies reported smaller gray matter volume or thinner cortex in APOE-4 carriers in the hippocampus (Tohgi et al., 1997; Den Heijer et al., 2002; Honea et al., 2009) and the entorhinal cortex (Shaw et al., 2007; Burggren et al., 2008), yet others found no such differences (Reiman et al., 1998; Jak et al., 2007; Cherbuin et al., 2008). As to the studies of brain function, decreased activities were reported in the APOE-4 carriers in regions such as the medial prefrontal cortex, the hippocampus, and the posterior cingulate (Reiman et al., 1996; Small et al., 2000; Persson et al., 2008; Pihlajamaki and Sperling, 2009; Adamson et al., 2011), but enhanced activities were also found in these regions (Bookheimer et al., 2000; Wishart et al., 2006; Han et al., 2007; Filippini et al., 2009). Notably, APOE was also found to modulate disease phenotype. For example, several studies have demonstrated greater gray matter atrophy in the hippocampus and entorhinal cortex in APOE-4 carriers with AD as compared to APOE-4 non-carriers with AD (Lehtovirta et al., 1996; Geroldi et al., 1999; Bigler et al., 2000; Hashimoto et al., 2001; Wolk and Dickerson, 2010), while evidences for non-significant volume differences in hippocampus were also reported (Jack et al., 1998; Drzezga et al., 2009). The discrepancies of the results could be attributable to the sample size and the demographic differences of subjects.

There are also evidences indicating that APOE-4 alters the brain connectivity in normal participants. For example, several studies magnified abnormal functional connectivity associated with APOE-4 in DMN (Filippini et al., 2009; Fleisher et al., 2009; Sheline et al., 2010; Machulda et al., 2011). DTI studies found aberrant white matter tracts with descended fractional anisotropy in APOE-4 carriers, including the posterior corpus callosum and the medial temporal lobe (Persson et al., 2006) and the parahippocampal white matter (Nierenberg et al., 2005; Honea et al., 2009). So far, there's only one study using graph theoretical analysis to explore the APOE-4 effects on whole-brain networks. Brown et al. (2011) utilized DTI tractography methods to investigate the relationship between the age and the topology of human brain structural network in normal elderly people. They found that only in the APOE-4 group the cost, C_p and σ showed significant negative correlation with age, while only in the APOE-4 non-carriers group L_p showed significant positive correlation with age. The nodal C_p of APOE-4 carriers decreased more sharply along with age in the right precuneus, the left orbitofrontal cortex, the left supramarginal gyrus, and right inferior temporal gyrus. This study demonstrated that APOE mediated the topological organization of human brain structural connectome in aging. Further studies would be important to combine different imaging modalities to systematically explore how the APOE-4 and other genetic risk factors of AD affect the topology of human connectome in health and AD.

FUTURE PERSPECTIVES

Despite the abundance of findings already obtained from the method, graph theoretical analysis of the AD network is only in its infancy and still has some problems. Future studies should take in account a number of considerations, which will be discussed in this section.

First, the existing works on AD brain networks are at the macroscale. The interplay between macroscale network property alterations associated with AD and the biological and pathological mechanisms of AD have not been studied thoroughly. AD could cause neuron loss and white matter aberrance, which may be account for the gray matter atrophy revealed by volume loss or cortical thinning and the white matter fiber changes found in diffusion studies. Also, one study demonstrated that Aβ deposition locations corresponded with hub regions of healthy brain networks (Buckner et al., 2009). However, the relationship between these pathological changes and network abnormalities still needs further exploration. Empirical studies of AD pathology and neuroimaging would be helpful in clarifying this issue.

Second, multi-modal analysis represents one potential avenue for future research on connectomics. Data from sMRI, diffusion MRI, fMRI, and EEG/MEG all reveal meaningful information about human brain connectome from different perspectives, the combination of datasets from various modalities would thus give us a full view of human connectome in health and disease. For example, Villain et al. (2008) showed that the hippocampal atrophy in patients with AD was specifically related to cingulum bundle atrophy, which is in turn highly correlated to hypometabolism of the posterior cingulate cortex, suggesting the hypometabolism might result from hippocampal atrophy via cingulum bundle disruption.

Third, little is known about the dynamic progress of AD. Most of the AD network studies focus on comparing indices to those of normal controls and demonstrating significant differences between the two groups. We have little knowledge of longitudinal changes in brain connectomics. An R-fMRI study (Zhang et al., 2010) compared the posterior cingulate cortex connectivity of healthy controls to those of patients with mild, moderate ad severe AD. The researchers suggested that the patients with AD had abnormal posterior cingulate cortex connectivity patterns and that the disruption intensified with disease progression. This study demonstrated the dynamic changes in brain connectivity in AD, but the relationship between the network and the disease progression remains unclear. Continuous longitudinal observations of AD development are needed to characterize the developmental changes.

Fourth, further studies are necessary to determine whether the abnormalities found in network studies are specific to AD. De Haan et al. (2009) demonstrated that network property alterations such as decreases in C_p and L_p were not observed in patients with frontotemporal lobar degeneration and that degree correlation decreased in AD but increased in frontotemporal lobar degeneration. Still many more studies are needed to compare the disruptions of brain connectivity patterns between AD and other dementia, such as dementia with Lewy bodies.

Fifth, the reliability of network property changes as a biomarker of AD needs to be examined, given that controversial results were obtained from different studies mentioned in this review (**Table 2**). Several studies on the reliability of network topological metrics of healthy people have been done in MEG (Deuker et al., 2009), fMRI (Telesford et al., 2010; Wang et al., 2011), and diffusion MRI (Vaessen et al., 2010; Bassett et al., 2011), but little is known about using these indices to diagnose AD. This is an important issue in establishing a topological biomarker for diagnosing and monitoring AD.

Finally, some individuals are at high risk of developing AD, such as those with the APOE-4 genotype and patients with amnesia MCI. Sorg et al. (2007) demonstrated that patients with amnesia MCI have reduced connectivity in the DMN and the executive attention network. In addition, Yao et al. (2010) discovered that the brain networks of patients with amnesia MCI and the patients with AD of both group demonstrated similar alterations compared to healthy controls, while the differences between the network topologies of the two patient groups were not significant. Some progress has been made in this field, but further studies are needed to clarify the AD-like topological alterations in people with AD risk factors.

CONCLUSION

To summarize, brain connectome analysis of adults with AD has provided an important methodology for studies of AD. All of the studies mentioned above demonstrated that AD brain networks are less optimally constructed and have decreased information processing efficiency. These alterations in brain connectivity patterns reveal the underlying brain structural and functional disruptions that cause the cognitive deficits of AD. Thus, these studies provide further support for the description of AD as a disconnection syndrome. The graph theory analysis methods have proved to be powerful tools for exploring the structural and functional architecture of the human brain and have provided new understanding of the biological mechanisms of AD and have uncovered potential biomarkers of early diagnosis and disease progression.

ACKNOWLEDGMENTS

This work was supported by the Natural Science Foundation of China (Grant Nos. 81030028 and 30870667), Beijing Natural Science Foundation (Grant No. 7102090), and the Scientific Research Foundation for the Returned Overseas Chinese Scholars (State Education Ministry, Yong He).

REFERENCES

Achard, S., and Bullmore, E. (2007). Efficiency and cost of economical brain functional networks. *PLoS Comput. Biol.* 3, e17. doi:10.1371/journal.pcbi.0030017

Achard, S., Salvador, R., Whitcher, B., Suckling, J., and Bullmore, E. (2006). A resilient, low-frequency, small-world human brain functional network with highly connected association cortical hubs. *J. Neurosci.* 26, 63–72.

Adamson, M. M., Hutchinson, J. B., Shelton, A. L., Wagner, A. D., and Taylor, J. L. (2011). Reduced hippocampal activity during encoding in cognitively normal adults carrying the APOE varepsilon4 allele. *Neuropsychologia* 49, 2448–2455.

Adler, G., Brassen, S., and Jajcevic, A. (2003). EEG coherence in Alzheimer's dementia. *J. Neural Transm.* 110, 1051–1058.

Ahmadlou, M., Adeli, H., and Adeli, A. (2010). New diagnostic EEG markers of the Alzheimer's disease using visibility graph. *J. Neural Transm.* 117, 1099–1109.

Allen, G., Barnard, H., Mccoll, R., Hester, A. L., Fields, J. A., Weiner, M. F., Ringe, W. K., Lipton, A. M., Brooker, M., Mcdonald, E., Rubin, C. D., and Cullum, C. M. (2007). Reduced hippocampal functional connectivity in Alzheimer disease. *Arch. Neurol.* 64, 1482–1487.

Andrews, T. J., Halpern, S. D., and Purves, D. (1997). Correlated size variations in human visual cortex, lateral geniculate nucleus, and optic tract. *J. Neurosci.* 17, 2859–2868.

Bassett, D. S., Brown, J. A., Deshpande, V., Carlson, J. M., and Grafton, S. T. (2011). Conserved and variable architecture of human white matter connectivity. *Neuroimage* 54, 1262–1279.

Bassett, D. S., Bullmore, E., Verchinski, B. A., Mattay, V. S., Weinberger, D. R., and Meyer-Lindenberg, A. (2008). Hierarchical organization of human cortical networks in health and schizophrenia. *J. Neurosci.* 28, 9239–9248.

Bassett, D. S., Meyer-Lindenberg, A., Achard, S., Duke, T., and Bullmore, E. (2006). Adaptive reconfiguration of fractal small-world human brain functional networks. *Proc. Natl. Acad. Sci. U.S.A.* 103, 19518–19523.

Behrens, T. E., Woolrich, M. W., Jenkinson, M., Johansen-Berg, H., Nunes, R. G., Clare, S., Matthews, P. M., Brady, J. M., and Smith, S. M. (2003). Characterization and propagation of uncertainty in diffusion-weighted MR imaging. *Magn. Reson. Med.* 50, 1077–1088.

Bekris, L. M., Yu, C. E., Bird, T. D., and Tsuang, D. W. (2010). Genetics of Alzheimer disease. *J. Geriatr. Psychiatry Neurol.* 23, 213–227.

Berendse, H. W., Verbunt, J. P., Scheltens, P., Van Dijk, B. W., and Jonkman, E. J. (2000). Magnetoencephalographic analysis of cortical activity in Alzheimer's disease: a pilot study. *Clin. Neurophysiol.* 111, 604–612.

Bigler, E. D., Lowry, C. M., Anderson, C. V., Johnson, S. C., Terry, J., and Steed, M. (2000). Dementia, quantitative neuroimaging, and apolipoprotein E genotype. *AJNR Am. J. Neuroradiol.* 21, 1857–1868.

Biswal, B., Yetkin, F. Z., Haughton, V. M., and Hyde, J. S. (1995). Functional connectivity in the motor cortex of resting human brain using echo-planar MRI. *Magn. Reson. Med.* 34, 537–541.

Boccaletti, S., Latora, V., Moreno, Y., Chavez, M., and Hwang, D. U. (2006). Complex networks: structure and dynamics. *Phys. Rep.* 424, 175–308.

Bookheimer, S., and Burggren, A. (2009). APOE-4 genotype and neurophysiological vulnerability to Alzheimer's and cognitive aging. *Annu. Rev. Clin. Psychol.* 5, 343–362.

Bookheimer, S. Y., Strojwas, M. H., Cohen, M. S., Saunders, A. M., Pericak-Vance, M. A., Mazziotta, J. C., and Small, G. W. (2000). Patterns of brain activation in people at risk for Alzheimer's disease. *N. Engl. J. Med.* 343, 450–456.

Bozzali, M., Falini, A., Franceschi, M., Cercignani, M., Zuffi, M., Scotti, G., Comi, G., and Filippi, M. (2002). White matter damage in Alzheimer's disease assessed in vivo using diffusion tensor magnetic resonance imaging. *J. Neurol. Neurosurg. Psychiatr.* 72, 742–746.

Brown, J. A., Terashima, K. H., Burggren, A. C., Ercoli, L. M., Miller, K. J., Small, G. W., and Bookheimer, S. Y. (2011). Brain network local interconnectivity loss in aging APOE-4 allele carriers. *Proc. Natl. Acad. Sci. U.S.A.* 108, 20760–20765.

Buckner, R. L., Sepulcre, J., Talukdar, T., Krienen, F. M., Liu, H., Hedden, T., Andrews-Hanna, J. R., Sperling, R. A., and Johnson, K. A. (2009). Cortical hubs revealed by intrinsic functional connectivity: mapping, assessment of stability, and relation to Alzheimer's disease. *J. Neurosci.* 29, 1860–1873.

Buckner, R. L., Snyder, A. Z., Shannon, B. J., LaRossa, G., Sachs, R., Fotenos, A. F., Sheline, Y. I., Klunk, W. E., Mathis, C. A., Morris, J. C., and Mintun, M. A. (2005). Molecular, structural, and functional characterization of Alzheimer's disease: evidence for a relationship between default activity, amyloid, and memory. *J. Neurosci.* 25, 7709–7717.

Bullmore, E., and Sporns, O. (2009). Complex brain networks: graph theoretical analysis of structural and functional systems. *Nat. Rev. Neurosci.* 10, 186–198.

Bullmore, E. T., Woodruff, P. W., Wright, I. C., Rabe-Hesketh, S., Howard, R. J., Shuriquie, N., and Murray, R. M. (1998). Does dysplasia cause anatomical dysconnectivity in schizophrenia? *Schizophr. Res.* 30, 127–135.

Burggren, A. C., Zeineh, M. M., Ekstrom, A. D., Braskie, M. N., Thompson, P. M., Small, G. W., and Bookheimer, S. Y. (2008). Reduced cortical thickness in hippocampal subregions among cognitively normal apolipoprotein E e4 carriers. *Neuroimage* 41, 1177–1183.

Busatto, G. F., Garrido, G. E., Almeida, O. P., Castro, C. C., Camargo, C. H., Cid, C. G., Buchpiguel, C. A., Furuie, S., and Bottino, C. M. (2003). A voxel-based morphometry study of temporal lobe gray matter reductions in Alzheimer's disease. *Neurobiol. Aging* 24, 221–231.

Catani, M., Howard, R. J., Pajevic, S., and Jones, D. K. (2002). Virtual in vivo interactive dissection of white matter fasciculi in the human brain. *Neuroimage* 17, 77–94.

Celone, K. A., Calhoun, V. D., Dickerson, B. C., Atri, A., Chua, E. F., Miller, S. L., Depeau, K., Rentz, D. M., Selkoe, D. J., Blacker, D., Albert, M. S., and Sperling, R. A. (2006). Alterations in memory networks in mild cognitive impairment and Alzheimer's disease: an independent component analysis. *J. Neurosci.* 26, 10222–10231.

Cherbuin, N., Anstey, K. J., Sachdev, P. S., Maller, J. J., Meslin, C., Mack, H. A., Wen, W., and Easteal, S. (2008). Total and regional gray matter volume is not related to APOE∗E4 status in a community sample of middle-aged individuals. *J. Gerontol. A Biol. Sci. Med. Sci.* 63, 501–504.

Ciftci, K. (2011). Minimum spanning tree reflects the alterations of the default mode network during Alzheimer's disease. *Ann. Biomed. Eng.* 39, 1493–1504.

De Haan, W., Pijnenburg, Y. A., Strijers, R. L., Van Der Made, Y., Van Der Flier, W. M., Scheltens, P., and Stam, C. J. (2009). Functional neural network analysis in frontotemporal dementia and Alzheimer's disease using EEG and graph theory. *BMC Neurosci.* 10, 101. doi:10.1186/1471-2202-10-101

De Lacoste, M. C., and White, C. L. III. (1993). The role of cortical connectivity in Alzheimer's disease pathogenesis: a review and model system. *Neurobiol. Aging* 14, 1–16.

Delbeuck, X., Van Der Linden, M., and Collette, F. (2003). Alzheimer's disease as a disconnection syndrome? *Neuropsychol. Rev.* 13, 79–92.

Den Heijer, T., Oudkerk, M., Launer, L. J., Van Duijn, C. M., Hofman, A., and Breteler, M. M. (2002). Hippocampal, amygdalar, and global brain atrophy in different apolipoprotein E genotypes. *Neurology* 59, 746–748.

Deuker, L., Bullmore, E. T., Smith, M., Christensen, S., Nathan, P. J., Rockstroh, B., and Bassett, D. S. (2009). Reproducibility of graph metrics of human brain functional networks. *Neuroimage* 47, 1460–1468.

Drzezga, A., Grimmer, T., Henriksen, G., Muhlau, M., Perneczky, R., Miederer, I., Praus, C., Sorg, C., Wohlschlager, A., Riemenschneider, M., Wester, H. J., Foerstl, H., Schwaiger, M., and Kurz, A. (2009). Effect of APOE genotype on amyloid plaque load and gray matter volume in Alzheimer disease. *Neurology* 72, 1487–1494.

Fellgiebel, A., Schermuly, I., Gerhard, A., Keller, I., Albrecht, J., Weibrich, C., Muller, M. J., and Stoeter, P. (2008). Functional relevant loss of long association fibre tracts integrity in early Alzheimer's disease. *Neuropsychologia* 46, 1698–1706.

Ferri, R., Rundo, F., Bruni, O., Terzano, M. G., and Stam, C. J. (2007). Small-world network organization of functional connectivity of EEG slow-wave activity during sleep. *Clin. Neurophysiol.* 118, 449–456.

Filippi, M., and Agosta, F. (2011). Structural and functional network connectivity breakdown in Alzheimer's disease studied with magnetic resonance imaging techniques. *J. Alzheimers Dis.* 24, 455–474.

Filippini, N., Macintosh, B. J., Hough, M. G., Goodwin, G. M., Frisoni, G. B., Smith, S. M., Matthews, P. M., Beckmann, C. F., and Mackay, C. E. (2009). Distinct patterns of brain activity in young carriers of the APOE-epsilon4 allele. *Proc. Natl. Acad. Sci. U.S.A.* 106, 7209–7214.

Fleisher, A. S., Sherzai, A., Taylor, C., Langbaum, J. B., Chen, K., and Buxton, R. B. (2009). Resting-state BOLD networks versus task-associated functional MRI for distinguishing Alzheimer's disease risk groups. *Neuroimage* 47, 1678–1690.

Fornito, A., Zalesky, A., Bassett, D. S., Meunier, D., Ellison-Wright, I., Yucel, M., Wood, S. J., Shaw, K., O'Connor, J., Nertney, D., Mowry, B. J., Pantelis, C., and Bullmore, E. T. (2011). Genetic influences on cost-efficient organization of human cortical functional networks. *J. Neurosci.* 31, 3261–3270.

Freeman, L. C. (1977). A set of measures of centrality based on betweenness. *Sociometry* 40, 35–41.

Frisoni, G. B., Testa, C., Zorzan, A., Sabattoli, F., Beltramello, A., Soininen, H., and Laakso, M. P. (2002). Detection of grey matter loss in mild Alzheimer's disease with voxel based morphometry. *J. Neurol. Neurosurg. Psychiatr.* 73, 657–664.

Geroldi, C., Pihlajamaki, M., Laakso, M. P., Decarli, C., Beltramello, A., Bianchetti, A., Soininen, H., Trabucchi, M., and Frisoni, G. B. (1999). APOE-epsilon4 is associated with less frontal and more medial temporal lobe atrophy in AD. *Neurology* 53, 1825–1832.

Gong, G., He, Y., Concha, L., Lebel, C., Gross, D. W., Evans, A. C., and Beaulieu, C. (2009). Mapping anatomical connectivity patterns of human cerebral cortex using in vivo diffusion tensor imaging tractography. *Cereb. Cortex* 19, 524–536.

Grady, C. L., Furey, M. L., Pietrini, P., Horwitz, B., and Rapoport, S. I. (2001). Altered brain functional connectivity and impaired short-term memory in Alzheimer's disease. *Brain* 124, 739–756.

Greicius, M. D., Srivastava, G., Reiss, A. L., and Menon, V. (2004). Default-mode network activity distinguishes Alzheimer's disease from healthy aging: evidence from functional MRI. *Proc. Natl. Acad. Sci. U.S.A.* 101, 4637–4642.

Hagmann, P., Cammoun, L., Gigandet, X., Meuli, R., Honey, C. J., Wedeen, V. J., and Sporns, O. (2008). Mapping the structural core of human cerebral cortex. *PLoS Biol.* 6, e159. doi:10.1371/journal.pbio.0060159

Hagmann, P., Kurant, M., Gigandet, X., Thiran, P., Wedeen, V. J., Meuli, R., and Thiran, J. P. (2007). Mapping human whole-brain structural networks with diffusion MRI. *PLoS ONE* 2, e597. doi:10.1371/journal.pone.0000597

Han, S. D., Houston, W. S., Jak, A. J., Eyler, L. T., Nagel, B. J., Fleisher, A. S., Brown, G. G., Corey-Bloom, J., Salmon, D. P., Thal, L. J., and Bondi, M. W. (2007). Verbal paired-associate learning by APOE genotype in non-demented older adults: fMRI evidence of a right hemispheric compensatory response. *Neurobiol. Aging* 28, 238–247.

Hashimoto, M., Yasuda, M., Tanimukai, S., Matsui, M., Hirono, N., Kazui, H., and Mori, E. (2001). Apolipoprotein E epsilon 4 and the pattern of regional brain atrophy in Alzheimer's disease. *Neurology* 57, 1461–1466.

He, Y., Chen, Z., and Evans, A. (2008). Structural insights into aberrant topological patterns of large-scale cortical networks in Alzheimer's disease. *J. Neurosci.* 28, 4756–4766.

He, Y., Chen, Z., Gong, G., and Evans, A. (2009a). Neuronal networks in Alzheimer's disease. *Neuroscientist* 15, 333–350.

He, Y., Wang, J., Wang, L., Chen, Z. J., Yan, C., Yang, H., Tang, H., Zhu, C., Gong, Q., Zang, Y., and Evans, A. C. (2009b). Uncovering intrinsic modular organization of spontaneous brain activity in humans. *PLoS ONE* 4, e5226. doi:10.1371/journal.pone.0005226

He, Y., Chen, Z. J., and Evans, A. C. (2007). Small-world anatomical networks in the human brain revealed by cortical thickness from MRI. *Cereb. Cortex* 17, 2407–2419.

He, Y., and Evans, A. (2010). Graph theoretical modeling of brain connectivity. *Curr. Opin. Neurol.* 23, 341–350.

Honea, R. A., Vidoni, E., Harsha, A., and Burns, J. M. (2009). Impact of APOE on the healthy aging brain: a voxel-based MRI and DTI study. *J. Alzheimers Dis.* 18, 553–564.

Humphries, M. D., Gurney, K., and Prescott, T. J. (2006). The brainstem reticular formation is a small-world, not scale-free, network. *Proc. Biol. Sci.* 273, 503–511.

Iturria-Medina, Y., Sotero, R. C., Canales-Rodriguez, E. J., Aleman-Gomez, Y., and Melie-Garcia, L. (2008). Studying the human brain anatomical network via diffusion-weighted MRI and graph theory. *Neuroimage* 40, 1064–1076.

Jack, C. R. Jr., Petersen, R. C., Xu, Y. C., O'Brien, P. C., Waring, S. C., Tangalos, E. G., Smith, G. E., Ivnik, R. J., Thibodeau, S. N., and Kokmen, E. (1998). Hippocampal atrophy and apolipoprotein E genotype are independently associated with Alzheimer's disease. *Ann. Neurol.* 43, 303–310.

Jak, A. J., Houston, W. S., Nagel, B. J., Corey-Bloom, J., and Bondi, M. W. (2007). Differential cross-sectional and longitudinal impact of APOE genotype on hippocampal volumes in nondemented older adults. *Dement. Geriatr. Cogn. Disord.* 23, 382–389.

Kiuchi, K., Morikawa, M., Taoka, T., Nagashima, T., Yamauchi, T., Makinodan, M., Norimoto, K., Hashimoto, K., Kosaka, J., Inoue, Y., Inoue, M., Kichikawa, K., and Kishimoto, T. (2009). Abnormalities of the uncinate fasciculus and posterior cingulate fasciculus in mild cognitive impairment and early Alzheimer's disease: a diffusion tensor tractography study. *Brain Res.* 1287, 184–191.

Knott, V., Mohr, E., Mahoney, C., and Ilivitsky, V. (2000). Electroencephalographic coherence in Alzheimer's disease: comparisons with a control group and population norms. *J. Geriatr. Psychiatry Neurol.* 13, 1–8.

Koenig, T., Prichep, L., Dierks, T., Hubl, D., Wahlund, L. O., John, E. R., and Jelic, V. (2005). Decreased EEG synchronization in Alzheimer's disease and mild cognitive impairment. *Neurobiol. Aging* 26, 165–171.

Kukull, W. A., and Bowen, J. D. (2002). Dementia epidemiology. *Med. Clin. North Am.* 86, 573–590.

Lacasa, L., Luque, B., Ballesteros, F., Luque, J., and Nuno, J. C. (2008). From time series to complex networks: the visibility graph. *Proc. Natl. Acad. Sci. U.S.A.* 105, 4972–4975.

Latora, V., and Marchiori, M. (2001). Efficient behavior of small-world networks. *Phys. Rev. Lett.* 87, 198701.

Laufs, H., Krakow, K., Sterzer, P., Eger, E., Beyerle, A., Salek-Haddadi, A., and Kleinschmidt, A. (2003). Electroencephalographic signatures of attentional and cognitive default modes in spontaneous brain activity fluctuations at rest. *Proc. Natl. Acad. Sci. U.S.A.* 100, 11053–11058.

Lehtovirta, M., Soininen, H., Laakso, M. P., Partanen, K., Helisalmi, S., Mannermaa, A., Ryynanen, M., Kuikka, J., Hartikainen, P., and Riekkinen, P. J. Sr. (1996). SPECT and MRI analysis in Alzheimer's disease: relation to apolipoprotein E epsilon 4 allele. *J. Neurol. Neurosurg. Psychiatr.* 60, 644–649.

Lerch, J. P., Worsley, K., Shaw, W. P., Greenstein, D. K., Lenroot, R. K., Giedd, J., and Evans, A. C. (2006). Mapping anatomical correlations across cerebral cortex (MACACC) using cortical thickness from MRI. *Neuroimage* 31, 993–1003.

Lo, C. Y., Wang, P. N., Chou, K. H., Wang, J., He, Y., and Lin, C. P. (2010). Diffusion tensor tractography reveals abnormal topological organization in structural cortical networks in Alzheimer's disease. *J. Neurosci.* 30, 16876–16885.

Machulda, M. M., Jones, D. T., Vemuri, P., Mcdade, E., Avula, R., Przybelski, S., Boeve, B. F., Knopman, D. S., Petersen, R. C., and Jack, C. R. Jr. (2011). Effect of APOE epsilon4 status on intrinsic network connectivity in cognitively normal elderly subjects. *Arch. Neurol.* 68, 1131–1136.

Mechelli, A., Friston, K. J., Frackowiak, R. S., and Price, C. J. (2005). Structural covariance in the human cortex. *J. Neurosci.* 25, 8303–8310.

Miao, X., Wu, X., Li, R., Chen, K., and Yao, L. (2011). Altered connectivity pattern of hubs in default-mode network with Alzheimer's disease: an granger causality modeling approach. *PLoS ONE* 6, e25546. doi:10.1371/journal.pone.0025546

Micheloyannis, S., Pachou, E., Stam, C. J., Breakspear, M., Bitsios, P., Vourkas, M., Erimaki, S., and Zervakis, M. (2006). Small-world networks and disturbed functional connectivity in schizophrenia. *Schizophr. Res.* 87, 60–66.

Mori, S., Crain, B. J., Chacko, V. P., and Van Zijl, P. C. (1999). Three-dimensional tracking of axonal projections in the brain by magnetic resonance imaging. *Ann. Neurol.* 45, 265–269.

Naggara, O., Oppenheim, C., Rieu, D., Raoux, N., Rodrigo, S., Dalla Barba, G., and Meder, J. F. (2006). Diffusion tensor imaging in early Alzheimer's disease. *Psychiatry Res.* 146, 243–249.

Nierenberg, J., Pomara, N., Hoptman, M. J., Sidtis, J. J., Ardekani, B. A., and Lim, K. O. (2005). Abnormal white matter integrity in healthy apolipoprotein E epsilon4 carriers. *Neuroreport* 16, 1369–1372.

Persson, J., Lind, J., Larsson, A., Ingvar, M., Cruts, M., Van Broeckhoven, C., Adolfsson, R., Nilsson, L. G., and Nyberg, L. (2006). Altered brain white matter integrity in healthy carriers of the APOE epsilon4 allele: a risk for AD? *Neurology* 66, 1029–1033.

Persson, J., Lind, J., Larsson, A., Ingvar, M., Sleegers, K., Van Broeckhoven, C., Adolfsson, R., Nilsson, L. G., and Nyberg, L. (2008). Altered deactivation in individuals with genetic risk for Alzheimer's disease. *Neuropsychologia* 46, 1679–1687.

Pihlajamaki, M., and Sperling, R. A. (2009). Functional MRI assessment of task-induced deactivation of the default mode network in Alzheimer's disease and at-risk older individuals. *Behav. Neurol.* 21, 77–91.

Pijnenburg, Y. A., V D Made, Y., Van Cappellen Van Walsum, A. M., Knol, D. L., Scheltens, P., and Stam, C. J. (2004). EEG synchronization likelihood in mild cognitive impairment and Alzheimer's disease during a working memory task. *Clin. Neurophysiol.* 115, 1332–1339.

Raichle, M. E., Macleod, A. M., Snyder, A. Z., Powers, W. J., Gusnard, D. A., and Shulman, G. L. (2001). A default mode of brain function. *Proc. Natl. Acad. Sci. U.S.A.* 98, 676–682.

Reijneveld, J. C., Ponten, S. C., Berendse, H. W., and Stam, C. J. (2007). The application of graph theoretical analysis to complex networks in the brain. *Clin. Neurophysiol.* 118, 2317–2331.

Reiman, E. M., Caselli, R. J., Yun, L. S., Chen, K., Bandy, D., Minoshima, S., Thibodeau, S. N., and Osborne, D. (1996). Preclinical evidence of Alzheimer's disease in persons homozygous for the epsilon 4 allele for apolipoprotein E. *N. Engl. J. Med.* 334, 752–758.

Reiman, E. M., Uecker, A., Caselli, R. J., Lewis, S., Bandy, D., De Leon, M. J., De Santi, S., Convit, A., Osborne, D., Weaver, A., and Thibodeau, S. N. (1998). Hippocampal volumes in cognitively normal persons at genetic risk for Alzheimer's disease. *Ann. Neurol.* 44, 288–291.

Rombouts, S. A., Barkhof, F., Veltman, D. J., Machielsen, W. C., Witter, M. P., Bierlaagh, M. A., Lazeron, R. H., Valk, J., and Scheltens, P. (2000). Functional MR imaging in Alzheimer's disease during memory encoding. *AJNR Am. J. Neuroradiol.* 21, 1869–1875.

Rose, S. E., Chen, F., Chalk, J. B., Zelaya, F. O., Strugnell, W. E., Benson, M., Semple, J., and Doddrell, D. M. (2000). Loss of connectivity in Alzheimer's disease: an evaluation of white matter tract integrity with colour coded MR diffusion tensor imaging. *J. Neurol. Neurosurg. Psychiatr.* 69, 528–530.

Rubinov, M., and Sporns, O. (2010). Complex network measures of brain connectivity: uses and interpretations. *Neuroimage* 52, 1059–1069.

Salvador, R., Suckling, J., Coleman, M. R., Pickard, J. D., Menon, D., and Bullmore, E. (2005). Neurophysiological architecture of functional magnetic resonance images of human brain. *Cereb. Cortex* 15, 1332–1342.

Sanz-Arigita, E. J., Schoonheim, M. M., Damoiseaux, J. S., Rombouts, S. A., Maris, E., Barkhof, F., Scheltens, P., and Stam, C. J. (2010). Loss of "small-world" networks in Alzheimer's disease: graph analysis of FMRI resting-state functional

connectivity. *PLoS ONE* 5, e13788. doi:10.1371/journal.pone.0013788

Schmitt, J. E., Lenroot, R. K., Wallace, G. L., Ordaz, S., Taylor, K. N., Kabani, N., Greenstein, D., Lerch, J. P., Kendler, K. S., Neale, M. C., and Giedd, J. N. (2008). Identification of genetically mediated cortical networks: a multivariate study of pediatric twins and siblings. *Cereb. Cortex* 18, 1737–1747.

Shaw, P., Lerch, J. P., Pruessner, J. C., Taylor, K. N., Rose, A. B., Greenstein, D., Clasen, L., Evans, A., Rapoport, J. L., and Giedd, J. N. (2007). Cortical morphology in children and adolescents with different apolipoprotein E gene polymorphisms: an observational study. *Lancet Neurol.* 6, 494–500.

Sheline, Y. I., Morris, J. C., Snyder, A. Z., Price, J. L., Yan, Z., D'Angelo, G., Liu, C., Dixit, S., Benzinger, T., Fagan, A., Goate, A., and Mintun, M. A. (2010). APOE4 allele disrupts resting state fMRI connectivity in the absence of amyloid plaques or decreased CSF Abeta42. *J. Neurosci.* 30, 17035–17040.

Small, G. W., Ercoli, L. M., Silverman, D. H., Huang, S. C., Komo, S., Bookheimer, S. Y., Lavretsky, H., Miller, K., Siddarth, P., Rasgon, N. L., Mazziotta, J. C., Saxena, S., Wu, H. M., Mega, M. S., Cummings, J. L., Saunders, A. M., Pericak-Vance, M. A., Roses, A. D., Barrio, J. R., and Phelps, M. E. (2000). Cerebral metabolic and cognitive decline in persons at genetic risk for Alzheimer's disease. *Proc. Natl. Acad. Sci. U.S.A.* 97, 6037–6042.

Smit, D. J., Stam, C. J., Posthuma, D., Boomsma, D. I., and De Geus, E. J. (2008). Heritability of "small-world" networks in the brain: a graph theoretical analysis of resting-state EEG functional connectivity. *Hum. Brain Mapp.* 29, 1368–1378.

Sorg, C., Riedl, V., Muhlau, M., Calhoun, V. D., Eichele, T., Laer, L., Drzezga, A., Forstl, H., Kurz, A., Zimmer, C., and Wohlschlager, A. M. (2007). Selective changes of resting-state networks in individuals at risk for Alzheimer's disease. *Proc. Natl. Acad. Sci. U.S.A.* 104, 18760–18765.

Sperling, R. A., Bates, J. F., Chua, E. F., Cocchiarella, A. J., Rentz, D. M., Rosen, B. R., Schacter, D. L., and Albert, M. S. (2003). fMRI studies of associative encoding in young and elderly controls and mild Alzheimer's disease. *J. Neurol. Neurosurg. Psychiatr.* 74, 44–50.

Sporns, O. (2011). The human connectome: a complex network. *Ann. N. Y. Acad. Sci.* 1224, 109–125.

Sporns, O., Tononi, G., and Kotter, R. (2005). The human connectome: a structural description of the human brain. *PLoS Comput. Biol.* 1, e42. doi:10.1371/journal.pcbi.0010042

Stam, C. J. (2004). Functional connectivity patterns of human magnetoencephalographic recordings: a "small-world" network? *Neurosci. Lett.* 355, 25–28.

Stam, C. J. (2010). Use of magnetoencephalography (MEG) to study functional brain networks in neurodegenerative disorders. *J. Neurol. Sci.* 289, 128–134.

Stam, C. J., De Haan, W., Daffertshofer, A., Jones, B. F., Manshanden, I., Van Cappellen Van Walsum, A. M., Montez, T., Verbunt, J. P., De Munck, J. C., Van Dijk, B. W., Berendse, H. W., and Scheltens, P. (2009). Graph theoretical analysis of magnetoencephalographic functional connectivity in Alzheimer's disease. *Brain* 132, 213–224.

Stam, C. J., Jones, B. F., Manshanden, I., Van Cappellen Van Walsum, A. M., Montez, T., Verbunt, J. P., De Munck, J. C., Van Dijk, B. W., Berendse, H. W., and Scheltens, P. (2006). Magnetoencephalographic evaluation of resting-state functional connectivity in Alzheimer's disease. *Neuroimage* 32, 1335–1344.

Stam, C. J., Jones, B. F., Nolte, G., Breakspear, M., and Scheltens, P. (2007a). Small-world networks and functional connectivity in Alzheimer's disease. *Cereb. Cortex* 17, 92–99.

Stam, C. J., Nolte, G., and Daffertshofer, A. (2007b). Phase lag index: assessment of functional connectivity from multi channel EEG and MEG with diminished bias from common sources. *Hum. Brain Mapp.* 28, 1178–1193.

Stam, C. J., and Reijneveld, J. C. (2007). Graph theoretical analysis of complex networks in the brain. *Nonlinear Biomed. Phys.* 1, 3.

Supekar, K., Menon, V., Rubin, D., Musen, M., and Greicius, M. D. (2008). Network analysis of intrinsic functional brain connectivity in Alzheimer's disease. *PLoS Comput. Biol.* 4, e1000100. doi:10.1371/journal.pcbi.1000100

Telesford, Q. K., Morgan, A. R., Hayasaka, S., Simpson, S. L., Barret, W., Kraft, R. A., Mozolic, J. L., and Laurienti, P. J. (2010). Reproducibility of graph metrics in FMRI networks. *Front. Neuroinform.* 4:117. doi:10.3389/fninf.2010.00117

Tohgi, H., Takahashi, S., Kato, E., Homma, A., Niina, R., Sasaki, K., Yonezawa, H., and Sasaki, M. (1997). Reduced size of right hippocampus in 39- to 80-year-old normal subjects carrying the apolipoprotein E epsilon4 allele. *Neurosci. Lett.* 236, 21–24.

Tomasi, D., and Volkow, N. D. (2010). Functional connectivity density mapping. *Proc. Natl. Acad. Sci. U.S.A.* 107, 9885–9890.

Ukmar, M., Makuc, E., Onor, M. L., Garbin, G., Trevisiol, M., and Cova, M. A. (2008). Evaluation of white matter damage in patients with Alzheimer's disease and in patients with mild cognitive impairment by using diffusion tensor imaging. *Radiol. Med.* 113, 915–922.

Vaessen, M. J., Hofman, P. A., Tijssen, H. N., Aldenkamp, A. P., Jansen, J. F., and Backes, W. H. (2010). The effect and reproducibility of different clinical DTI gradient sets on small world brain connectivity measures. *Neuroimage* 51, 1106–1116.

Villain, N., Desgranges, B., Viader, F., De La Sayette, V., Mezenge, F., Landeau, B., Baron, J. C., Eustache, F., and Chetelat, G. (2008). Relationships between hippocampal atrophy, white matter disruption, and gray matter hypometabolism in Alzheimer's disease. *J. Neurosci.* 28, 6174–6181.

Wada, Y., Nanbu, Y., Kikuchi, M., Koshino, Y., Hashimoto, T., and Yamaguchi, N. (1998a). Abnormal functional connectivity in Alzheimer's disease: intrahemispheric EEG coherence during rest and photic stimulation. *Eur. Arch. Psychiatry Clin. Neurosci.* 248, 203–208.

Wada, Y., Nanbu, Y., Koshino, Y., Yamaguchi, N., and Hashimoto, T. (1998b). Reduced interhemispheric EEG coherence in Alzheimer disease: analysis during rest and photic stimulation. *Alzheimer Dis. Assoc. Disord.* 12, 175–181.

Wakana, S., Jiang, H., Nagae-Poetscher, L. M., Van Zijl, P. C., and Mori, S. (2004). Fiber tract-based atlas of human white matter anatomy. *Radiology* 230, 77–87.

Wang, J., Zuo, X., and He, Y. (2010). Graph-based network analysis of resting-state functional MRI. *Front. Syst. Neurosci.* 4:16. doi:10.3389/fnsys.2010.00016

Wang, J. H., Zuo, X. N., Gohel, S., Milham, M. P., Biswal, B. B., and He, Y. (2011). Graph theoretical analysis of functional brain networks: test-retest evaluation on short- and long-term resting-state functional MRI data. *PLoS ONE* 6, e21976. doi:10.1371/journal.pone.0021976

Wang, K., Liang, M., Wang, L., Tian, L., Zhang, X., Li, K., and Jiang, T. (2007). Altered functional connectivity in early Alzheimer's disease: a resting-state fMRI study. *Hum. Brain Mapp.* 28, 967–978.

Wang, L., Zang, Y., He, Y., Liang, M., Zhang, X., Tian, L., Wu, T., Jiang, T., and Li, K. (2006). Changes in hippocampal connectivity in the early stages of Alzheimer's disease: evidence from resting state fMRI. *Neuroimage* 31, 496–504.

Watts, D. J., and Strogatz, S. H. (1998). Collective dynamics of "small-world" networks. *Nature* 393, 440–442.

Wishart, H. A., Saykin, A. J., Rabin, L. A., Santulli, R. B., Flashman, L. A., Guerin, S. J., Mamourian, A. C., Belloni, D. R., Rhodes, C. H., and Mcallister, T. W. (2006). Increased brain activation during working memory in cognitively intact adults with the APOE epsilon4 allele. *Am. J. Psychiatry* 163, 1603–1610.

Wolk, D. A., and Dickerson, B. C. (2010). Apolipoprotein E (APOE) genotype has dissociable effects on memory and attentional-executive network function in Alzheimer's disease. *Proc. Natl. Acad. Sci. U.S.A.* 107, 10256–10261.

Wright, I. C., Sharma, T., Ellison, Z. R., Mcguire, P. K., Friston, K. J., Brammer, M. J., Murray, R. M., and Bullmore, E. T. (1999). Supra-regional brain systems and the neuropathology of schizophrenia. *Cereb. Cortex* 9, 366–378.

Xie, S., Xiao, J. X., Gong, G. L., Zang, Y. F., Wang, Y. H., Wu, H. K., and Jiang, X. X. (2006). Voxel-based detection of white matter abnormalities in mild Alzheimer disease. *Neurology* 66, 1845–1849.

Yao, Z., Zhang, Y., Lin, L., Zhou, Y., Xu, C., and Jiang, T. (2010). Abnormal cortical networks in mild cognitive impairment and Alzheimer's disease. *PLoS Comput. Biol.* 6, e1001006. doi:10.1371/journal.pcbi.1001006

Zhang, H. Y., Wang, S. J., Liu, B., Ma, Z. L., Yang, M., Zhang, Z. J., and Teng, G. J. (2010). Resting brain connectivity: changes during the progress of Alzheimer disease. *Radiology* 256, 598–606.

Zielinski, B. A., Gennatas, E. D., Zhou, J., and Seeley, W. W. (2010). Network-level structural covariance in the developing brain. *Proc. Natl. Acad. Sci. U.S.A.* 107, 18191–18196.

Zuo, X. N., Ehmke, R., Mennes, M., Imperati, D., Castellanos, F.

X., Sporns, O., and Milham, M. P. (2011). Network centrality in the uman functional connectome. *Cereb. Cortex.* doi: 10.1093/cercor/bhr269. [Epub ahead of print].

Conflict of Interest Statement: The authors declare that the research was conducted in the absence of any commercial or financial relationships that could be construed as a potential conflict of interest.

Received: 27 October 2011; accepted: 19 December 2011; published online: 05 January 2012.

Citation: Xie T and He Y (2012) Mapping the Alzheimer's brain with connectomics. Front. Psychiatry ***2****:77. doi: 10.3389/fpsyt.2011.00077*

This article was submitted to Frontiers in Neuropsychiatric Imaging and Stimulation, a specialty of Frontiers in Psychiatry.

frontiers in
PSYCHIATRY

ORIGINAL RESEARCH ARTICLE
published: 10 January 2012
doi: 10.3389/fpsyt.2011.00075

Exploring the psychosis functional connectome: aberrant intrinsic networks in schizophrenia and bipolar disorder

Vince D Calhoun[1,2,3,4]*, Jing Sui[1], Kent Kiehl[1,5], Jessica Turner[1], Elena Allen[1] and Godfrey Pearlson[3,4]

[1] *The Mind Research Network, Albuquerque, NM, USA*
[2] *Department of ECE, University of New Mexico, Albuquerque, NM, USA*
[3] *Olin Neuropsychiatry Research Center, Hartford, CT, USA*
[4] *Department of Psychiatry, Yale University, New Haven, CT, USA*
[5] *Department of Psychology, University of New Mexico, Albuquerque, NM, USA*

Edited by:
Alex Fornito, University of Melbourne, Australia

Reviewed by:
Christopher A. Wall, Mayo Clinic, USA
Martijn Van Den Heuvel, University Medical Center Utrecht, Netherlands

****Correspondence:***
Vince D Calhoun, The Mind Research Network, 1101 Yale Blvd NE, Albuquerque, NM 87106, USA.
e-mail: vcalhoun@unm.edu

Intrinsic functional brain networks (INs) are regions showing temporal coherence with one another. These INs are present in the context of a task (as opposed to an undirected task such as rest), albeit modulated to a degree both spatially and temporally. Prominent networks include the default mode, attentional fronto-parietal, executive control, bilateral temporal lobe, and motor networks. The characterization of INs has recently gained considerable momentum, however; most previous studies evaluate only a small subset of the INs (e.g., default mode). In this paper we use independent component analysis to study INs decomposed from functional magnetic resonance imaging data collected in a large group of schizophrenia patients, healthy controls, and individuals with bipolar disorder, while performing an auditory oddball task. Schizophrenia and bipolar disorder share significant overlap in clinical symptoms, brain characteristics, and risk genes which motivates our goal of identifying whether functional imaging data can differentiate the two disorders. We tested for group differences in properties of all identified INs including spatial maps, spectra, and functional network connectivity. A small set of default mode, temporal lobe, and frontal networks with default mode regions appearing to play a key role in all comparisons. Bipolar subjects showed more prominent changes in ventromedial and prefrontal default mode regions whereas schizophrenia patients showed changes in posterior default mode regions. Anti-correlations between left parietal areas and dorsolateral prefrontal cortical areas were different in bipolar and schizophrenia patients and amplitude was significantly different from healthy controls in both patient groups. Patients exhibited similar frequency behavior across multiple networks with decreased low frequency power. In summary, a comprehensive analysis of INs reveals a key role for the default mode in both schizophrenia and bipolar disorder.

Keywords: fMRI, connectivity, networks, intrinsic activity, independent component analysis, ICA, default mode network

INTRODUCTION

Schizophrenia (SZ) is a psychotic disorder characterized by altered perception, cognition, thought processes, and behaviors whereas bipolar (BP) illness is a mood disorder involving prolonged states of depression and mania (Goodwin and Jamison, 2007). Clinicians have noted for many years that there are extensive commonalities between them, for a recent review see (Keshavan et al., in press). Specifically, the two brain diseases have overlapping symptoms (e.g., 60% of bipolar 1 patients have psychotic features (Guze et al., 1975; Goes et al., 2007), both types of patients show persistent neurocognitive deficits (Glahn et al., 2004), similar risk genes (Bahn, 2002), and co-occurrence within relatives (Lichtenstein et al., 2009); however, the common and distinct neural mechanisms underlying these disorders remain unclear.

Over the past decade there has been increasing study of functional connectivity in mental illness. Two of the more widely used methods include seed-based approaches (Greicius et al., 2004) and investigations based on independent component analysis (ICA; Calhoun et al., 2004, 2009a). These approaches both capitalize on underlying temporal coherence in the functional magnetic resonance imaging (fMRI) timecourses (TCs) which appears to reflect functionally relevant activity and is present both at rest and during a task (Biswal et al., 1995; Calhoun et al., 2008a). Intrinsic functional brain networks (INs) are sets of brain regions of the brain showing temporal coherence with one another; they provide a key way of evaluating the human (macro) functional connectome (Biswal et al., 2010; Allen et al., 2011; Sporns, 2011). The INs are quite robust and as we have shown in a direct comparison of extended rest data and auditory oddball data, the task essentially gives us a controlled way to study how these networks are modulated both spatially and temporally by a directed task (versus an undirected task such as resting; Calhoun et al., 2008a). Numerous INs have been identified consistently by many groups, such as the default mode network, the attentional fronto-parietal networks,

the executive control network (or salience network), and bilateral temporal lobe and motor cortex. The INs are likely critical components of healthy and aberrant brain functions given the many studies showing important cognitive processes which appear to be localized to these networks such as prediction of errors (Eichele et al., 2008) and studies showing dysfunction in INs in various mental illness (Greicius et al., 2004; Calhoun et al., 2008b, 2009a; Broyd et al., 2009).It is also important to note that INs comprise most of the variance of the fMRI data (Calhoun et al., 2008a).

Evaluating characteristics of INs in health and disease has gained considerable momentum in recent years. However, most previous studies have evaluated only a small subset of the INs (e.g., default mode). While this approach has revealed significant differences in, e.g., schizophrenia and bipolar disorder (Calhoun et al., 2008b), it does not enable us to evaluate the underlying functional brain changes in a comprehensive manner. We have recently developed a multivariate testing framework that allows us to test multiple INs and multiple aspects of each network while also controlling the false positive rate associated with the multiple testing (Allen et al., 2011).

In this paper we use ICA to study INs from a large group of schizophrenia patients, healthy controls, and individuals with bipolar disorder. ICA is increasingly utilized as a tool for evaluating the hidden spatiotemporal structure contained within brain imaging data and is often applied to fMRI data in a group framework to enable inference about individual variation within groups of subjects (Calhoun et al., 2001; Allen et al., in press; Erhardt et al., in press). Following application of group ICA to fMRI data from all subjects, we then identify all plausible INs and use a comprehensive approach to test for group differences in all identified INs. Within a rigorous statistical framework, we evaluate multiple parameters of these networks and their relationship with disease group, including spatial maps (SMs), spectra, and functional network connectivity (FNC). We also discuss the potential of using these parameters for classification of disease and differentiation of the bipolar and schizophrenia groups.

Results reveal a key role for the default mode network in that these regions show significant and specific differences between healthy subjects, patients with schizophrenia, and patients with bipolar disorder. These regions are somewhat similar to a model previously proposed by Williamson (Williamson, 2007; Williamson and Allman, 2011) with anterior regions involved in emotional processing more relevant in comparisons between healthy subjects and those with bipolar disorder and posterior and temporal lobe dysfunction more specific to schizophrenia patients. Results are also consistent with findings reported in Lynall et al. (2010).

MATERIALS AND METHODS

PARTICIPANTS

Sixty-two healthy controls [HC, age 38 ± 17 (range), 30 females], 54 patients with schizophrenia (SZ, age 37 ± 12, 22 females), and 48 patients with bipolar disorder (BP, age 37 ± 14, 26 females) were recruited at the Olin Neuropsychiatric Research Center and were scanned with fMRI while performing an auditory oddball task (Kiehl and Liddle, 2001). These data have been analyzed jointly with diffusion tensor imaging in another study (Sui et al., in press). All subjects gave written, informed, Hartford Hospital, and Yale University IRB-approved consent. Schizophrenia or bipolar disorder was diagnosed according to DSM-IV–TR criteria on the basis of a structured clinical interview (First et al., 1995) administered by a research nurse and review of the medical file. Bipolar patients with further sub-classified into those who were historically psychotic or non-psychotic based on previously published criteria (Strasser et al., 2005); 48% of bipolar patients were thus classified as psychotic in one or more illness episodes, including the current one. All patients were stabilized on medication for at least 4 weeks prior to the scan session in this study. Healthy participants were screened to ensure they were free from DSM-IV Axis I or Axis II psychopathology (assessed using the SCID; Spitzer et al., 1996) and also interviewed to determine that there was no history of psychosis or major mood disorder in any first-degree relatives). All subjects were urine-screened to eliminate those who were positive for abused substances, or currently pregnant in the case of females. Patients and controls were age and sex matched, with no significant differences among three groups, where age: $p = 0.93$, $F = 0.07$, $DF = 2$. Sex: $p = 0.99$, $\chi^2 = 0.017$, $DF = 2$. All participants had normal hearing, and were able to perform the oddball task successfully during practice prior to the scanning session. Bipolar subjects were also assessed for current psychosis at the time of scanning based on a criterion of scoring 3 or higher in one or more of the following PANSS (Kay et al., 1987) positive subscale items: P1 (delusions), P2 (conceptual disorganization), P3 (hallucinations), and P6 (suspiciousness/persecutory). Other positive symptoms such as grandiosity and excitement (P4, 5) did not qualify as psychosis. Based on these criteria 48% (23/48) of bipolar subject met the criterion of current psychosis at the time of scanning.

IMAGING PARAMETERS

Scans were acquired at the Institute of Living, Hartford, CT, USA on a 3 T dedicated head scanner (Siemens Allegra) equipped with 40 mT/m gradients and a standard quadrature head coil. The functional scans were acquired using gradient-echo echo planar imaging (EPI) with the following parameters: repeat time (TR) = 1.5 s, echo time (TE) = 27 ms, field of view = 24 cm, acquisition matrix = 64×64, flip angle = 70°, voxel size = 3.75 mm × 3.75 mm × 4 mm, slice thickness = 4 mm, gap = 1 mm, number of slices = 29; ascending acquisition. Six dummy scans were carried out at the beginning to allow for longitudinal equilibrium, after which the paradigm was automatically triggered to start by the scanner.

TASK

The auditory oddball task involved subjects encountering three frequencies of sounds: target (1200 Hz with probability, $p = 0.09$), novel (computer generated complex tones, $p = 0.09$), and standard (1000 Hz, $p = 0.82$) presented through a computer system via sound insulated, MR-compatible earphones. Stimuli were presented sequentially in pseudorandom order for 200 ms each with inter-stimulus interval (ISI) varying randomly from 500 to 2050 ms. Subjects were asked to make a quick button–press response with their right index finger upon each presentation of each target stimulus; no response was required for the other two stimuli. Two runs of 244 stimuli were presented (Kiehl et al., 2005).

PREPROCESSING

Functional magnetic resonance imaging data were preprocessed using an automated preprocessing pipeline and neuroinformatics system developed at MRN (Bockholt et al., 2010) and based around SPM5[1]. Following the completion of a scan, data are automatically archived and copied to an analysis directory where preprocessing is performed. In the functional data pipeline, the first four volumes are discarded to remove T1 equilibration effects, images are realigned using INRIalign, and slice-timing correction is applied using the middle slice as the reference frame. Data are then spatially normalized into the standard Montreal Neurological Institute (MNI) space (Friston et al., 1995), resliced to 3 mm × 3 mm × 3 mm voxels, and smoothed using a Gaussian kernel with a full-width at half-maximum (FWHM) of 10 mm.

Group ICA

Group independent components analysis was performed using the GIFT toolbox[2]. Our analysis followed a similar approach as described in a recent study performed on a large ($N = 603$) analysis of resting fMRI data (Allen et al., 2011). We chose relatively high model order ICA (75 components) as previous studies have demonstrated that such models yield refined components that correspond to known anatomical and functional segmentations (Kiviniemi et al., 2009; Abou-Elseoud et al., 2010). Subject-specific data reduction principal components analysis (PCA) retained 100 principal components (PCs). Group data reduction retained 75 PCs using the expectation–maximization (EM) algorithm, included in GIFT. The Infomax ICA algorithm (Bell and Sejnowski, 1995) was used to estimate the independent components. Subject-specific SMs and TCs were estimated using a back-reconstruction method based on PCA compression and projection (Calhoun et al., 2001; Erhardt et al., in press).

Feature identification

IN selection. We identified a subset of components considered to be INs (as opposed to physiological artifacts) by inspecting the aggregate SMs and average power spectra. Components were evaluated based on expectations that INs should exhibit peak activations in gray matter, low spatial overlap with known vascular, ventricular, motion, and susceptibility artifacts, and TCs dominated by low frequency fluctuations (Cordes et al., 2001; Allen et al., 2011). From the 75 decomposed components, we identified $c_1 = 47$ putative INs for further study.

Outcome measures. For the set of selected INs, we considered three outcome variables: (1) component power spectra, (2) component SMs, and (3) between component connectivity (FNC). We additionally evaluated the task-relatedness of the ICA time courses by the task stimuli. Component SMs were thresholded based on the distribution of voxel-wise t-statistics to identify voxels with strong and consistent activation across subjects to focus our analysis on the subset of voxels most representative of each network (Allen et al., 2011). From this point forward, descriptions of component SMs refer to the thresholded maps, which include regions most associated with component TCs. FNC was estimated as the Pearson's correlation coefficient between pairs of TCs (Jafri et al., 2008). Subject-specific TCs were detrended and despiked based on the median absolute deviation as implemented in 3dDespike[3], then filtered using a fifth-order Butterworth low-pass filter with a high frequency cutoff of 0.15 Hz. Pairwise correlations were computed between RSN TCs, resulting in a symmetric $c_1 \times c_1$ correlation matrix for each subject. For all FNC analyses, correlations were transformed to z-scores using Fisher's transformation, $z = \text{atanh}(k)$, where k is the correlation between two component TCs.

Statistical analyses

Overview. We utilize a recently published multivariate model selection strategy optimized for the large dimensions of the three ICA-derived outcome measures (Allen et al., 2011). Such an approach reduces the total number of statistical tests performed and facilitates testing predictors on the response matrices as a whole. We utilize a multivariate analysis of covariance (MANCOVA) to identify factors that influence the response matrix. We then proceed to perform univariate tests with a reduced design matrix and correct for multiple comparisons using the false discovery rate (FDR; Genovese et al., 2002). The design matrix included regressors for group membership (bipolar, schizophrenia, healthy) as well as group interactions.

Response variables. For each of $I = 1,\ldots, N$ subjects, we have $c = 1,\ldots, c_1$ power spectra (P_{ic}) each with 150 spectral bins, $c = 1,\ldots,$ CSMs (S_{ic}), and a single vector of FNC pairwise correlations between the C components (K_{i}). Each of these response variables is modeled separately. Prior to modeling, response variables are transformed and dimension reduced. Spectra are element wise log-transformed, which is useful because it normalizes the highly skewed power distribution. Similarly, FNC correlations are Fisher-transformed [$z = \text{atanh}(k)$]. We perform a PCA dimension reduction on each matrix using 15 dimensions (several different dimensions were compared with similar results). Those reduced components are used as input to the MANCOVAs, to capture the primary effects.

Univariate tests. Following the MANCOVA on the reduced response variables to determine whether diagnosis has a significant effect, we perform univariate tests on the original response variables to determine which spectral bins, SM voxels, or FNC correlations are associated with diagnosis. Associations are visualized by plotting the log of the p-value with the sign of the associated t-statistic, $-\text{sign}(t)\log_{10}(p)$, which provides information on both the directionally and statistical strength of the result. Univariate tests were corrected for multiple comparisons at an alpha = 0.05 significance level using FDR.

We also report the task modulation of each of the identified IN components by performing a multiple regression of the hemodynamic model (creating using the default SPM hemodynamic response function). This provides a beta for each regressor and

[1] http://www.fil.ion.ucl.ac.uk/spm/software/spm5
[2] http://mialab.mrn.org/software
[3] http://afni.nimh.nih.gov/

each component, and these betas are then subjected to one-sample *t*-tests to evaluate whether a given component is modulated by a particular task stimulus. A two-sample *t*-test is used to test for group differences in the task modulation (Calhoun et al., 2009b).

RESULTS

Behaviorally (see **Table 1**) all subjects performed with comparable accuracy on the auditory oddball task; schizophrenia; and bipolar patients however performed significantly more slowly than healthy controls, consistent with multiple prior studies (Muller et al., 2001).

Table 1 | Auditory oddball behavioral results: mean reaction time and percent correct hits are presented for each group.

Mean ± SD	Mean reaction time (ms)	Percent of correct hits
HC	404 ± 88	99.3 ± 2.4%
SZ	480 ± 91	98.1 ± 3.8%
BP	443 ± 60	98.9 ± 2.7%
ANOVA test of group difference	$p < 0.0002$	$p < 0.14$

Healthy controls reacted the fastest, followed by bipolar patients and then schizophrenia patients. All subjects were performing the task well with near perfect accuracy (with slight differences in the same order as mentioned before).

We performed a 75-component GICA. Based on visual inspection of SMs and power spectra, we identified 47 components as plausible INs. The MANCOVA yielded significant effects of diagnosis within multiple components and within all response variables of the group ICA including voxel-wise SMs, FNC, and spectra. In addition, we found significant differences in task modulation between groups as well. In the following we summarize each set of results, starting with the SMs.

Six components out of 47 were found to show SM group differences using a threshold of $p < 0.05$ within the MANCOVA framework. Univariate tests revealed significant voxels in all six components for each of the pairwise group contrasts. Results are summarized in **Figure 1**. The INs showing group differences can be grouped into three categories, comprised of default mode, frontal, and temporal components.

The first category includes two networks [Components (C)55 and C38] showing posterior cingulate regions. These regions in addition to a left parietal network (C43) are implicated as being part of the default mode network (Raichle et al., 2001). All three of these components are significantly negatively modulated by the

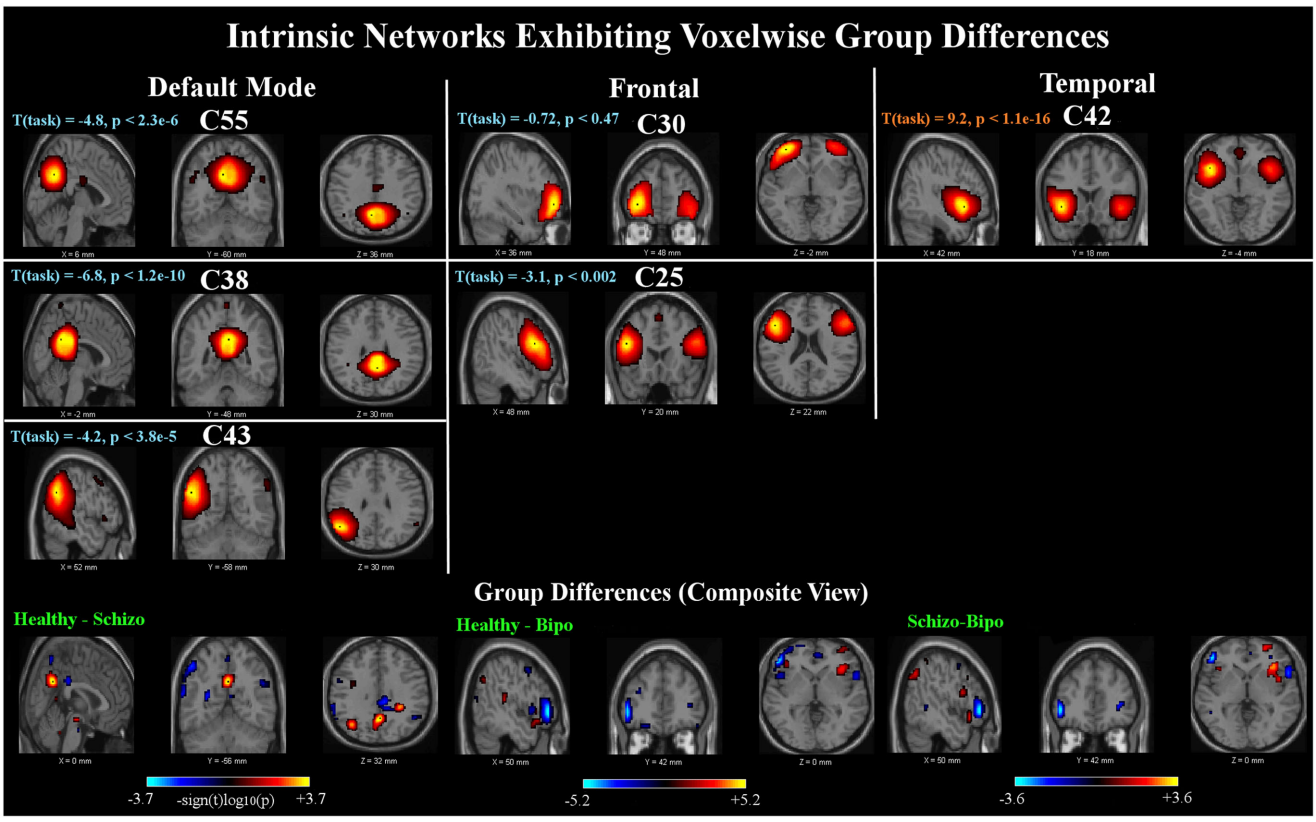

FIGURE 1 | Spatial maps: top panels show sagittal, coronal, and axial slices of the six components found to have group differences. In this and subsequent figures, component spatial maps are thresholded at $T > 1$. *T* (task) indicates the task-relatedness of each component, as assessed with a one-sample *t*-test of the subject beta values. Bottom panels show composite maps of the group differences for the Healthy – Schizo (left), Healthy – Bipo (middle), and Schizo – Bipo (right) contrasts (thresholded at $p < 0.05$, corrected for multiple comparisons). Composite maps for each contrast are created by taking the maximum significant value (over the six components) at each voxel.

target stimuli. The second category includes two frontal lobe networks (C30 and C25) mostly in superior and inferior frontal lobe and inclusive of dorsolateral prefrontal cortex (DLPFC). Both INs in our study are slightly left lateralized and neither shows significant modulation by the target stimuli. The third category includes one component (C42) in bilateral temporal lobe, mostly superior temporal gyrus, and insula but also the anterior cingulate; this component is also very strongly positively modulated by the target stimuli.

A composite view of the univariate contrasts showing group differences in any of the six components are shown in **Figure 1**. To create the composite, the maximum significant value over all comparisons is shown at each voxel. Voxel-wise differences show primarily posterior parietal, default mode regions differentiate schizophrenia from healthy individuals, with additional parietal and inferior frontal regions showing stronger measures in subjects with schizophrenia than in healthy individuals. Subject with bipolar disease show similar increased measures in the frontal cortex, and weaker measures in the precuneus and posterior default mode areas, as well as additional lateral frontal and temporal regions. The largest differences between healthy controls and schizophrenia patients include the inferior frontal triangle (including Brodman 44, 45, and 46) and regions in the temporal lobe. A full listing of the regions is provided in **Table 2**.

Functional network connectivity results are shown in **Figure 2**. All significant FNC differences ($p < 0.05$ FDR corrected) are shown on the left. In addition, the FNC matrix (uncorrected for multiple comparisons) is shown on the right. In comparisons between the groups, the default mode regions played a primary role. Group differences between schizophrenia and healthy controls are found between the posterior cingulate (C14) and both right cerebellum (C7) and posterior temporal lobe (C8). Differences between healthy controls and bipolar patients revealed two pairs, the first being posterior cingulate (C14) linked to a visual component including the temporo-occipital–parietal junction (C24) and the second being a link between the anterior default mode (C44) with the inferior parietal lobule and angular gyri in addition to the posterior portion of the superior temporal lobe (C1). Differences between schizophrenia and bipolar patients manifested as a pair of links between the anterior cingulate (C68) and bilateral superior temporal gyrus (C42) and also the temporal pole (mostly right lateralized; C22). In addition, FNC difference between patient groups were significant for lateral frontal (C25) and lateral parietal (C43), both left lateralized. Three of the same networks showing voxel-wise SM differences (C42, C43, C25) were also demonstrated FNC differences between schizophrenia and bipolar disorder.

The right portion of **Figure 2** shows the full FNC difference matrices for all pairs of components. Generally, healthy controls show more positive correlations among ICA TCs across networks than do either schizophrenia or bipolar patients (more orange/red in the figure) whereas schizophrenia patients show more FNC than bipolar patients.

Finally, we also evaluated group differences in spectral power. **Figure 3** (left and middle) shows a spectral image of components (y axis) by spectra (x axis) with significant differences shown in orange (HC < SZ or BP) or blue (HC < SZ or BP). On the right is the average spectra across all components for each group. Consistent with previous work we found healthy controls showed more spectral power at lower frequencies whereas patients showed more spectral power at higher frequencies (Garrity et al., 2007; Calhoun et al., 2008a). In addition, we saw a similar pattern in the bipolar patients: there were no significant differences in spectral profiles between schizophrenia patients and bipolar patients. It is clear from this that controls have greater power in the low frequency bands that do the patients and both patients groups have more power in the high frequencies. The general tendency off all component spectra tended to be similar, with some showing slightly stronger effects which passed significance.

A recurring finding in these analyses is the implication of the regions from the posterior cingulate into precuneus region of the default mode network, showing lower coherence and connectivity in the patients than in the healthy individuals. However, the distinctions between the patient groups implicate relatively less of the posterior areas and more of the frontal regions, as summarized in **Figure 4**.

DISCUSSION

In this paper we have performed, to our knowledge, the first comprehensive comparative analysis of INs to identify those which differentiate schizophrenia and bipolar disorder from healthy controls. We performed a relatively high model order ICA decomposition in order to evaluate the relationship among sub-nodes of INs in a simple auditory oddball task. We evaluated three different properties of the extracted INs, focused on group differences. The first property we evaluated was within-network voxel-wise differences, providing a measure of the *strength* of the connectivity differences in a given region. This property was significantly different in anterior and posterior cingulate and parietal default mode regions, temporal lobe, and lateral frontal/DLPFC. Results are consistent with those reported in a recent graph theoretic study (Lynall et al., 2010).

Group variations in the strength of connectivity were observed in temporal gyrus (BA 21 22 41 42) which is responsible for processing of auditory information, as has been found previously both in these data and others (Kim et al., 2009; Sui et al., in press), and is in keeping with auditory oddball processing differences in SZ and BP found using other modalities (Ford et al., 1994; Schulze et al., 2008; Calhoun et al., 2010). Structural and functional abnormalities in the superior temporal gyrus, particularly on the left side, have been demonstrated in schizophrenia patients in multiple studies as well as in psychotic bipolar disorder and constitute the best-replicated brain differences correlating with the severity of psychotic symptoms in schizophrenia, most specifically auditory hallucinations and formal thought disorder collectively; abnormalities in these regions likely underpin psychotic phenomena (Swerdlow, 2010; Fusar-Poli et al., 2011). This supports the idea that aberrant patterns of coherence in temporal lobe may be a cardinal abnormality in both schizophrenia, and to a lesser extent in bipolar disorder (Pearlson, 1997; Calhoun et al., 2008b; Chance et al., 2008). The insula has a role in emotional regulation, as reviewed by (McIntosh et al., 2008; Kempton et al., 2009) who discuss differential insula response in BP compared to HC and SZ.

Table 2 | Summary of regions showing group differences in spatial maps: clusters of significant between-group differences (cluster size > 27 voxels; $p < 0.05$ corrected for multiple comparisons within each component) from components C55, C38, C43, C30, C25, and C42 (which are displayed in Figure 1).

Area	Brodmann area	Volume (cc)(L/R)	Random effects: max $\log_{10}$ p (x, y, z)(L/R)
HC–SZ POSITIVE			
Precuneus	7, 19, 31, 39	3.7/0.9	3.9 (0, −54, 33)/3.0 (3, −51, 33)
Angular gyrus	39	1.1/0.0	3.5 (−39, −62, 34)/NA
Cingulate gyrus	31	0.4/0.1	2.3 (−3, −57, 28)/1.5 (3, −51, 27)
Inferior parietal lobule	39	0.3/0.0	2.2 (−39, −62, 39)/NA
Superior temporal gyrus	22, 38, 41	0.9/0.0	2.2 (−56, −32, 7)/NA
Inferior frontal gyrus	9, 45, 46, 47	0.6/0.7	1.7 (−36, 32, 7)/2.0 (48, 24, 10)
Culmen	NA	0.0/0.3	NA/1.9 (21, −30, −21)
Middle frontal gyrus	10, 11	0.5/0.3	1.9 (−48, 43, −7)/1.6 (36, 53, 6)
Parahippocampal gyrus	28, 35, 36	0.2/0.3	1.8 (−18, −18, −12)/1.7 (27, −33, −16)
Middle temporal gyrus	22	0.4/0.0	1.7 (−56, −35, 5)/NA
Cuneus	7	0.2/0.0	1.6 (−6, −68, 31)/NA
Precentral gyrus	NA	0.2/0.0	1.6 (−42, −5, 22)/NA
Anterior cingulate	NA	0.1/0.0	1.4 (−18, 41, −5)/NA
Medial frontal gyrus	NA	0.1/0.0	1.4 (−18, 46, −5)/NA
HC–SZ NEGATIVE			
Supramarginal gyrus	40	0.8/0.3	3.0 (−62, −51, 25)/1.9 (48, −51, 30)
Inferior parietal lobule	40	2.3/0.0	2.9 (−65, −42, 24)/NA
Precentral gyrus	6, 9, 44	0.8/0.3	2.9 (−39, 13, 35)/1.8 (45, 3, 8)
Middle frontal gyrus	8, 9, 10, 46	3.5/0.0	2.8 (−42, 53, 8)/NA
Superior temporal gyrus	22, 39, 42	1.3/0.1	2.7 (−65, −34, 21)/1.4 (48, 6, 2)
Inferior frontal gyrus	9, 44, 45, 46, 47	5.9/0.3	2.6 (−56, 15, 16)/1.5 (53, 35, 7)
Cingulate gyrus	23, 31	0.3/2.1	1.9 (0, −28, 32)/2.5 (6, −28, 32)
Insula	13	1.5/2.0	2.3 (−33, 18, 5)/2.4 (42, 6, 2)
Superior frontal gyrus	10	0.4/0.7	1.9 (−36, 53, 14)/2.1 (24, 61, −3)
Superior parietal lobule	7	0.3/0.0	2.1 (−36, −65, 50)/NA
Posterior cingulate	31	0.1/0.1	1.3 (−9, −57, 25)/2.0 (3, −52, 16)
Uncus	28, 34	0.1/0.0	1.8 (−15, −7, −22)/NA
Culmen	NA	0.4/0.1	1.7 (−15, −44, −13)/1.6 (18, −45, −20)
Precuneus	7, 31	0.2/0.1	1.6 (−3, −56, 55)/1.4 (15, −42, 44)
Parahippocampal gyrus	28	0.1/0.2	1.4 (−18, −10, −22)/1.5 (30, −19, −22)
Lentiform nucleus	NA	0.1/0.0	1.5 (−21, 17, −1)/NA
Middle temporal gyrus	NA	0.1/0.0	1.4 (−56, −58, 3)/NA
Claustrum	NA	0.0/0.1	NA/1.4 (36, 0, 3)
Postcentral gyrus	NA	0.1/0.0	1.4 (−50, −11, 17)/NA
HC–BP POSITIVE			
Precuneus	7, 19, 31, 39	9.9/2.4	5.3 (−3, −60, 31)/4.1 (3, −60, 31)
Cingulate gyrus	31	1.3/0.2	4.1 (0, −60, 28)/2.8 (3, −57, 28)
Cuneus	7	0.3/0.3	3.9 (−3, −65, 31)/3.2 (3, −65, 31)
Posterior cingulate	29, 30, 31	1.5/0.1	3.3 (−6, −46, 13)/1.7 (3, −60, 25)
Inferior frontal gyrus	10, 44, 45, 47	2.6/3.8	2.3 (−45, 23, −14)/3.3 (33, 23, −4)
Insula	13, 47	0.5/0.8	2.2 (−42, 12, 13)/2.7 (36, 23, 2)
Superior temporal gyrus	38, 41	1.0/0.0	2.5 (−48, −29, 12)/NA
Middle frontal gyrus	9, 10	0.3/1.2	1.6 (−39, 25, 32)/2.4 (33, 55, 3)
Angular gyrus	39	1.2/0.0	2.2 (−39, −62, 36)/NA
Culmen	NA	0.7/0.0	2.0 (−30, −42, −21)/NA
Precentral gyrus	44	0.3/0.2	1.6 (−36, 22, 35)/2.0 (45, 18, 7)
Superior parietal lobule	7	0.1/0.0	1.9 (−24, −53, 44)/NA
Superior frontal gyrus	10	0.0/0.4	NA/1.9 (30, 55, 0)
Claustrum	NA	0.0/0.1	NA/1.7 (30, 17, −1)

(Continued)

Table 2 | Continued

Area	Brodmann area	Volume (cc)(L/R)	Random effects: max $\log_{10}$ p (x, y, z)(L/R)
Postcentral gyrus	40	0.1/0.0	1.7 (−50, −25, 18)/NA
Middle temporal gyrus	NA	0.1/0.0	1.7 (−59, 0, −5)/NA
Inferior parietal lobule	39	0.4/0.0	1.5 (−36, −62, 39)/NA
Fusiform gyrus	20	0.1/0.0	1.5 (−30, −39, −18)/NA
Parahippocampal gyrus	NA	0.1/0.0	1.4 (−30, −30, −14)/NA
HC–BP NEGATIVE			
Inferior frontal gyrus	9, 10, 44, 45, 46, 47	6.3/1.1	6.0 (−53, 38, 1)/2.2 (53, 15, 5)
Middle frontal gyrus	6, 8, 10, 11, 47	3.4/0.2	5.2 (−50, 38, −4)/1.7 (36, 44, 6)
Superior temporal gyrus	22, 38	0.7/0.4	3.2 (−36, 5, −15)/2.1 (56, 12, −1)
Cingulate gyrus	23, 31	0.7/1.4	2.7 (0, −30, 35)/3.0 (6, −33, 40)
Precuneus	7, 31	0.2/0.4	1.8 (−6, −60, 22)/2.4 (6, −36, 43)
Posterior cingulate	23, 29	0.0/0.7	NA/2.1 (9, −52, 16)
Anterior cingulate	32	0.0/0.4	NA/2.0 (3, 46, −5)
Precentral gyrus	44	0.0/0.2	NA/1.9 (53, 12, 8)
Superior frontal gyrus	10	0.4/0.1	1.8 (−24, 40, −17)/1.3 (24, 58, −10)
Caudate	NA	0.0/0.1	NA/1.8 (21, −34, 16)
paracentral lobule	31	0.0/0.1	NA/1.7 (6, −30, 43)
Medial frontal gyrus	10	0.1/0.0	1.6 (−18, 61, −3)/NA
Supramarginal gyrus	NA	0.0/0.1	NA/1.5 (56, −45, 33)
Middle temporal gyrus	NA	0.1/0.0	1.5 (−45, −72, 15)/NA
Parahippocampal gyrus	35	0.1/0.0	1.5 (−18, −30, −9)/NA
Insula	NA	0.1/0.0	1.3 (−45, 12, −1)/NA
SZ–BP POSITIVE			
Supramarginal gyrus	40	0.6/0.0	3.9 (−62, −48, 22)/NA
Inferior frontal gyrus	44, 47	2.9/3.1	2.8 (−42, 23, −6)/3.6 (36, 26, −9)
Precentral gyrus	9, 44	0.6/0.1	3.4 (−39, 19, 35)/1.5 (45, 0, 6)
Superior temporal gyrus	22, 39, 42	1.2/0.0	3.3 (−62, −51, 19)/NA
Posterior cingulate	29	0.4/0.1	2.8 (−9, −43, 8)/1.4 (6, −49, 11)
Superior frontal gyrus	10	0.0/1.0	NA/2.7 (21, 55, 0)
Middle frontal gyrus	9, 10, 46	1.0/0.3	2.5 (−39, 22, 32)/2.2 (24, 56, 6)
Precuneus	7, 19, 31	3.6/1.2	2.4 (−18, −48, 36)/2.3 (9, −66, 28)
Cuneus	7	0.1/0.3	1.9 (0, −65, 31)/2.4 (6, −65, 31)
Insula	13, 47	1.2/1.6	2.1 (−36, 15, 13)/2.3 (33, 23, 2)
Culmen	NA	0.8/0.0	2.2 (−27, −39, −21)/NA
Uncus	28, 34	0.1/0.0	2.0 (−15, −7, −22)/NA
Inferior parietal lobule	39, 40	1.3/0.0	1.9 (−59, −33, 40)/NA
Cingulate gyrus	31	0.8/0.3	1.9 (−18, −39, 32)/1.6 (21, −39, 32)
Claustrum	NA	0.0/0.1	NA/1.8 (30, 17, −1)
Angular gyrus	39	0.3/0.0	1.8 (−50, −68, 37)/NA
Superior parietal lobule	7	0.2/0.0	1.8 (−24, −53, 44)/NA
Medial frontal gyrus	NA	0.1/0.0	1.7 (−6, 45, 34)/NA
Parahippocampal gyrus	28	0.1/0.0	1.7 (−15, −10, −20)/NA
Middle temporal gyrus	NA	0.1/0.0	1.7 (−56, −3, −7)/NA
Fusiform gyrus	20	0.1/0.0	1.4 (−30, −39, −18)/NA
Postcentral gyrus	40	0.1/0.0	1.3 (−59, −28, 21)/NA
SZ–BP NEGATIVE			
Inferior frontal gyrus	10, 45, 46, 47	2.0/1.3	3.8 (−50, 41, −2)/2.5 (53, 15, −1)
Middle frontal gyrus	6, 10, 47	1.6/0.3	3.5 (−50, 38, −4)/2.2 (33, 44, 6)
Culmen	NA	0.0/1.0	NA/2.6 (24, −30, −26)
Posterior cingulate	29	0.0/0.3	NA/2.3 (12, −57, 17)
Lentiform nucleus	NA	0.1/0.0	1.9 (−27, 0, −5)/NA

(Continued)

Table 2 | Continued

Area	Brodmann area	Volume (cc)(L/R)	Random effects: max $\log_{10}$ p (x, y, z)(L/R)
Superior temporal gyrus	22	0.2/0.4	1.5 (−33, 2, −13)/1.8 (56, 12, −1)
Precentral gyrus	44	0.0/0.1	NA/1.7 (56, 15, 8)
Thalamus	NA	0.0/0.3	NA/1.7 (9, −23, 9)
Middle temporal gyrus	NA	0.2/0.0	1.5 (−42, −69, 15)/NA
Precuneus	7	0.0/0.1	NA/1.5 (12, −60, 20)
Parahippocampal gyrus	NA	0.0/0.1	NA/1.4 (24, −30, −16)
Inferior parietal lobule	NA	0.1/0.0	1.4 (−39, −42, 41)/NA
Anterior cingulate	32	0.0/0.1	NA/1.4 (3, 47, −2)

Cluster extent and maximum t-statistic are given separately for each hemisphere (L/R) when applicable.

Intrinsic functional brain networks showing group differences include C55 and C38, comprising posterior cingulate regions together with a left parietal network (C43) constituting part of the default mode network. The finding that DMN subcomponents exhibit differential behavior in schizophrenia (Skudlarski et al., 2010) further validates earlier conclusions that the DMN should be seen not as a single unit but as composed of substructures that all contribute to resting state activation while varying substantially in connectivity patterns. Here such a distinction is shown to be clinically relevant in identifying distinctions between SZ and BP.

A second network set includes two frontal lobe networks (C30 and C25) mostly located in superior and inferior frontal lobe, including DLPFC. DLPFC plays an important role in the integration of sensory and mnemonic information, executive function, planning and regulation of cognitive function and action. Researchers have frequently reported dysfunction and lack of functional connectivity of this region in patients with schizophrenia (Badcock et al., 2005; Hamilton et al., 2009) and bipolar disorder (Curtis et al., 2001; Glahn et al., 2010). Our results are consistent with the above findings and suggest that these deficits might be related to shared risk factors and disease mechanisms common to both disorders.

The second property we evaluated was FNC, evaluating differences in the pairwise correlation among component TCs. Default mode regions again proved to play a major role with schizophrenia subjects differentiated from bipolar subjects via a greater association between anterior default mode and two temporal lobe INs, and from healthy controls via a weaker association between the posterior default mode and a more inferior posterior temporal lobe IN and a cerebellar IN. In contrast, bipolar subjects were differentiated from healthy subjects via a posterior default mode – right visual IN as well as an anterior default mode – right parietal IN.

Strakowski et al. (2005) supports a model of bipolar disorder that involves dysfunction within subcortical (striatal–thalamic) – prefrontal networks and the associated limbic modulating regions (amygdala, midline cerebellum). These studies suggest that, in bipolar disorder, there may be diminished prefrontal modulation of subcortical and medial temporal structures within the anterior limbic network (e.g., amygdala, anterior striatum, and thalamus) that results in dysregulation of mood.

The fact that both ventral anterior cingulate DMN regions as well as medial PFC regions were prevalent in the comparisons with bipolar disorder is consistent with the role of both these regions in emotional processing (Bush et al., 2000; Laird et al., 2009; Uddin et al., 2009; Ongur et al., 2010) as well as with a predicted model of bipolar disorder implicating the emotional encoding network (Williamson and Allman, 2011). It is notable that in the comparison of HC–SZ negative and HC–BP negative voxels, anterior cingulate BA 32 is one of the few regions that distinguishes the two pathologic diagnostic groups, as reflected in the final part of **Table 2** (SZ − BP negative voxels) BA 32 constitutes an important part of the "affective anterior cingulate," together with regions BA 24 and 25, which is connected to portions of emotional processing circuitry including amygdala and orbitofrontal cortex (Bush et al., 2000).

The key role that DMN plays in both schizophrenia and bipolar disorder is also consistent with the hypothesis that DMN plays a sentinel role in monitoring the external environment. The default network is hypothesized to support internally focused cognition that relies on mnemonic systems (Buckner et al., 2008). Hahn and colleague suggest that activity at rest "may reflect, among other functions, the continuous provision of resources for spontaneous, broad, and exogenously driven information gathering." Their results also suggest that nicotine improved attentional performance by down-regulating resting brain function in response to task-related cues (Hahn et al., 2007).

Schizophrenia has been associated with overactive (more rapidly fluctuating) default mode activity (Garrity et al., 2007), which when connected to Hahn's results, could explain the higher prevalence of smoking in patients with schizophrenia. In this study we also evaluated the spectra of the INs, providing a measure of differences in the *fluctuations in the intrinsic activity* (at least within the frequencies captured by fMRI data). Consistent with previous results, schizophrenia patients reliably show significantly less low frequency power and more high frequency power (Garrity et al., 2007; Calhoun et al., 2008a; Ongur et al., 2010; Turner et al., in press). In addition, the frequency content of INs from the bipolar patients showed a similar behavior, indeed, bipolar, and schizophrenia spectra did not show significant differences from one another. This may reflect the fact that the spectra are just sensitive to amplitude differences, not connectivity differences, so it is perhaps not surprising that they appear to be less sensitive

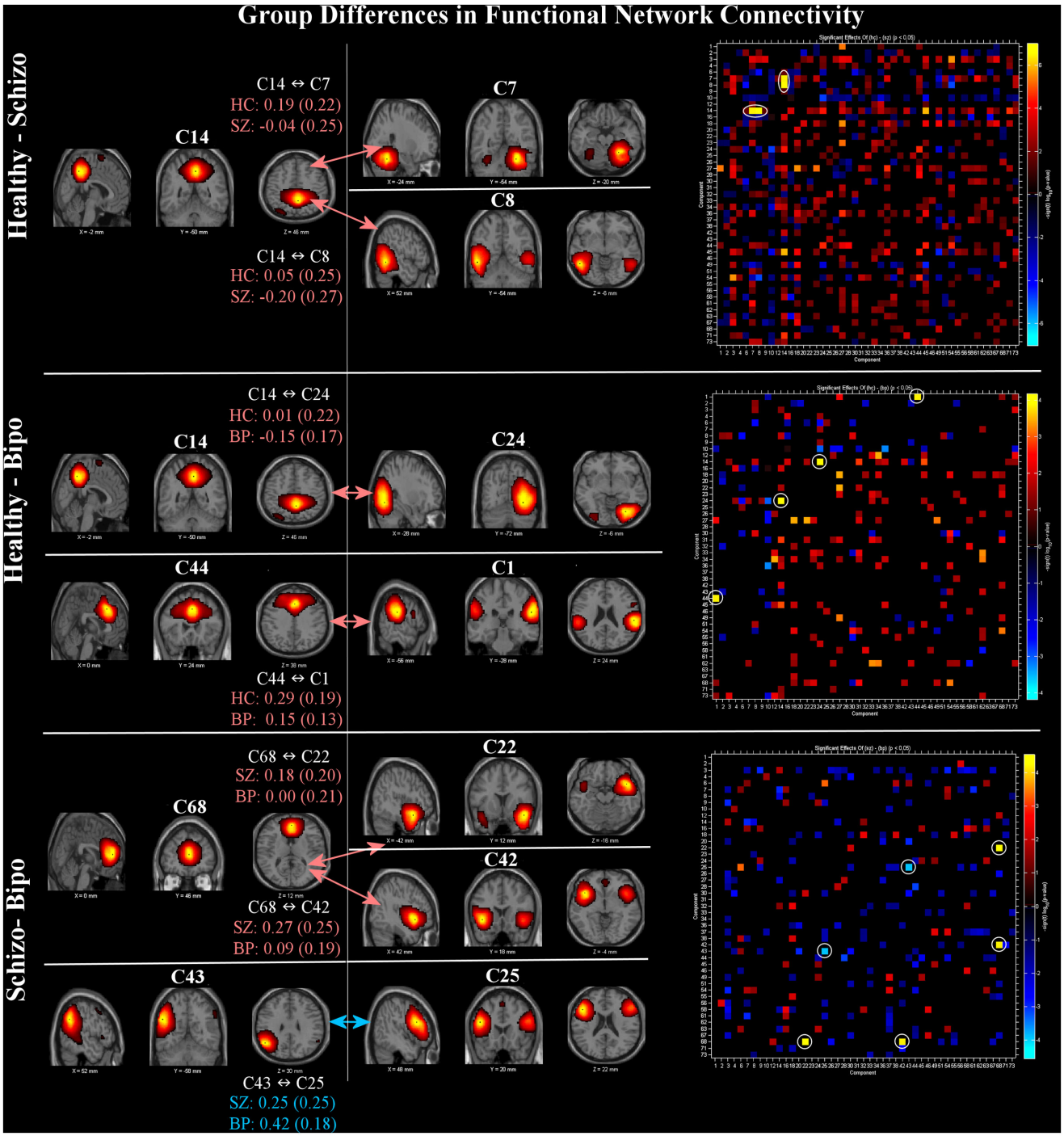

FIGURE 2 | Functional network connectivity (FNC): significant between-group differences (thresholded at $p < 0.05$, corrected for multiple comparisons) in FNC (left) and full difference matrices (thresholded at $p < 0.05$, not corrected, to provide additional context) for Healthy – Schizo (top), Healthy – Bipo (middle), and Schizo – Bipo (bottom) contrasts (right). Significant FNC differences are highlighted with white circles in the matrices. For each example, the FNC values (temporal correlations between components) within each group are displayed as mean (SD).

to discriminate between these two disorders. Numerous recent papers have stressed the similarities between bipolar disorder with psychotic symptoms and schizophrenia, e.g., as reviewed in (Keshavan et al., in press). Multiple regions implicated as abnormal in both schizophrenia and bipolar disorder, differed in turn from each other, as shown in the lower part of **Table 2**, with many more

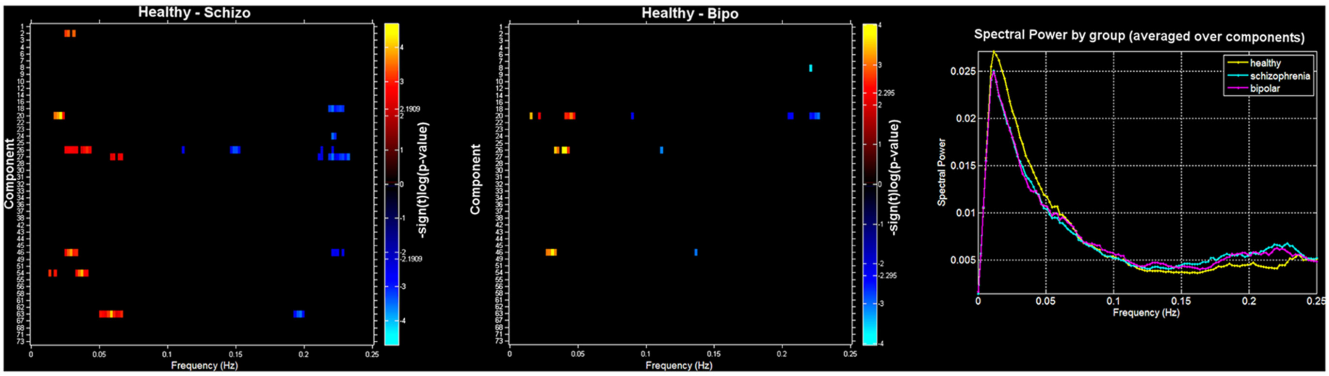

FIGURE 3 | Spectra: between-group differences in spectral power (thresholded at $p < 0.05$, corrected for multiple comparisons) for Healthy – Schizo (top) and Healthy – Bipo (middle) contrasts. Note that the Schizo – Bipo contrast showed no significant differences. Color maps in left and middle panels show the power differences at each frequency over each component separately. Rightmost panel shows the mean power spectra for each group, averaged over all components.

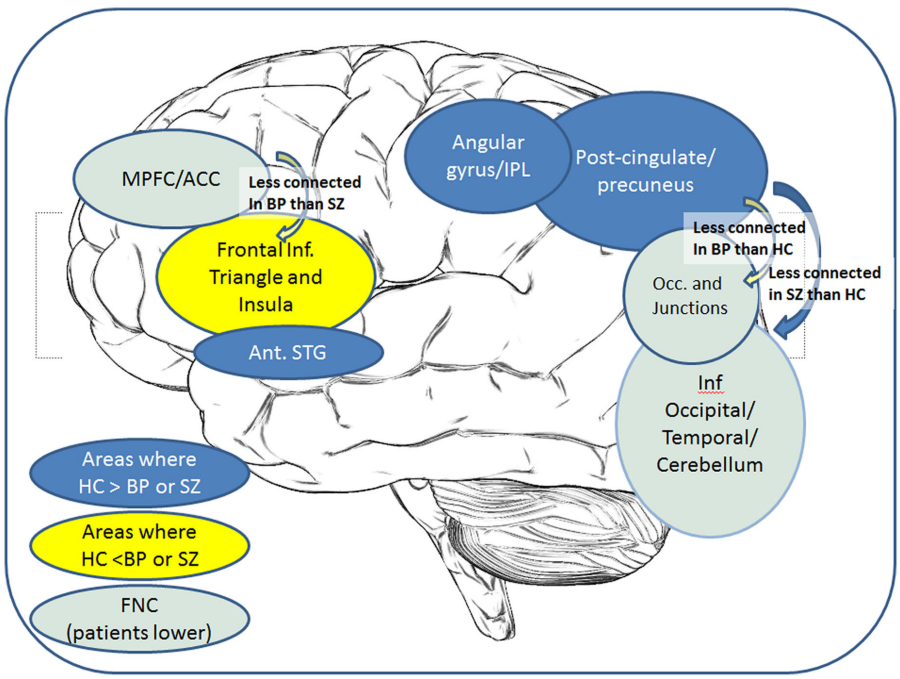

FIGURE 4 | Overall summary of results: a cartoon depicting the key regions showing group differences in either voxel-wise maps or FNC correlations.

temporal lobe regions implicated as abnormal in the (SZ–BP positive) category, perhaps consistent with proposed developmentally based extensive temporal connectivity differences in schizophrenia reviewed by (Swerdlow, 2010).

Results described in this paper may also be useful in direction classification work. Using a comprehensive approach, we have found that connectivity with posterior cingulate and precuneus regions may be the most important in future diagnostic classification and for potential biomarker identification. This is a focus of future work. In addition, recent network studies of structural MRI data have shown some similarities with the functional data and suggest that a direct combination of structural and functional findings will prove useful (Calhoun et al., 2006; Calhoun and Adali, 2009; van den Heuvel et al., 2009; Michael et al., 2010; Segall and Calhoun, 2011; Sui and Calhoun, 2011; Wang et al., 2011; Zalesky et al., 2011). Finally, the use of graph theoretic measures on the ICA output (either using the TCs, Yu et al., 2011, or the maps, Ma et al., in press, as nodes) is straightforward and is a promising direction to pursue for this work.

CONCLUSION

We have performed a comprehensive analysis of differences in multiple aspects of INs in schizophrenia, bipolar disorder, and healthy controls. One key finding was the prevalence of regions implicated in the default mode network, substructures of which played different roles in identifying distinctions between schizophrenia and bipolar disorder.

ACKNOWLEDGMENTS

This work was supported by the National Institutes of Health grants R01MH072681 (to K. A. Kiehl), R01EB006841, 5P20RR021938, and R01EB005846 (to V. D. Calhoun), and R01MH43775, R01MH074797, and R01MH077945 (to G. D. Pearlson). We thank the research staff at the Olin Neuropsychiatric Research Center who helped collect and check the data.

REFERENCES

Abou-Elseoud, A., Starck, T., Remes, J., Nikkinen, J., Tervonen, O., and Kiviniemi, V. (2010). The effect of model order selection in group PICA. *Hum. Brain Mapp.* 31, 1207–1216.

Allen, E., Erhardt, E., Damaraju, E., Gruner, W., Segall, J., Silva, R., Havlicek, M., Rachakonda, S., Fries, J., Kalyanam, R., Michael, A., Turner, J., Eichele, T., Adelsheim, S., Bryan, A., Bustillo, J. R., Clark, V. P., Feldstein, S., Filbey, F. M., Ford, C., Hutchison, K., Jung, R., Kiehl, K. A., Kodituwakku, P., Komesu, Y., Mayer, A. R., Pearlson, G. D., Phillips, J., Sadek, J., Stevens, M., Teuscher, U., Thoma, R. J., and Calhoun, V. D. (2011). A baseline for the multivariate comparison of resting state networks. *Front. Hum. Neurosci.* 1, 12.

Allen, E. A., Erhardt, E., Wei, Y., Eichele, T., and Calhoun, V. D. (in press). Capturing inter-subject variability with group independent component analysis of fMRI data: a simulation study. *Neuroimage.*

Badcock, J. C., Michiel, P. T., and Rock, D. (2005). Spatial working memory and planning ability: contrasts between schizophrenia and bipolar I disorder. *Cortex* 41, 753–763.

Bahn, S. (2002). Gene expression in bipolar disorder and schizophrenia: new approaches to old problems. *Bipolar. Disord.* 4(Suppl. 1), 70–72.

Bell, A. J., and Sejnowski, T. J. (1995). An information maximisation approach to blind separation and blind deconvolution. *Neural Comput.* 7, 1129–1159.

Biswal, B., Yetkin, F. Z., Haughton, V. M., and Hyde, J. S. (1995). Functional connectivity in the motor cortex of resting human brain using echo-planar MRI. *Magn. Reson. Med.* 34, 537–541.

Biswal, B. B., Mennes, M., Zuo, X. N., Gohel, S., Kelly, C., Smith, S. M., Beckmann, C. F., Adelstein, J. S., Buckner, R. L., Colcombe, S., Dogonowski, A. M., Ernst, M., Fair, D., Hampson, M., Hoptman, M. J., Hyde, J. S., Kiviniemi, V. J., Kotter, R., Li, S. J., Lin, C. P., Lowe, M. J., Mackay, C., Madden, D. J., Madsen, K. H., Margulies, D. S., Mayberg, H. S., McMahon, K., Monk, C. S., Mostofsky, S. H., Nagel, B. J., Pekar, J. J., Peltier, S. J., Petersen, S. E., Riedl, V., Rombouts, S. A., Rypma, B., Schlaggar, B. L., Schmidt, S., Seidler, R. D., Siegle, G. J., Sorg, C., Teng, G. J., Veijola, J., Villringer, A., Walter, M., Wang, L., Weng, X. C., Whitfield-Gabrieli, S., Williamson, P., Windischberger, C., Zang, Y. F., Zhang, H. Y., Castellanos, F. X., and Milham, M. P. (2010). Toward discovery science of human brain function. *Proc. Natl. Acad. Sci. U.S.A.* 107, 4734–4739.

Bockholt, H. J., Scully, M., Courtney, W., Rachakonda, S., Scott, A., Caprihan, A., Fries, J., Kalyanam, R., Segall, J., De la Garza, R., Lane, S., and Calhoun, V. D. (2010). Mining the mind research network: a novel framework for exploring large scale, heterogeneous translational neuroscience research data sources. *Front. Neuroinformatics* 3:36. doi:10.3389/neuro.11.036.2009

Broyd, S. J., Demanuele, C., Debener, S., Helps, S. K., James, C. J., and Sonuga-Barke, E. J. (2009). Default-mode brain dysfunction in mental disorders: a systematic review. *Neurosci. Biobehav. Rev.* 33, 279–296.

Buckner, R. L., Andrews-Hanna, J. R., and Schacter, D. L. (2008). The brain's default network: anatomy, function, and relevance to disease. *Ann. N. Y. Acad. Sci.* 1124, 1–38.

Bush, G., Luu, P., and Posner, M. I. (2000). Cognitive and emotional influences in anterior cingulate cortex. *Trends Cogn. Sci. (Regul. Ed.)* 4, 215–222.

Calhoun, V. D., and Adali, T. (2009). Feature-based fusion of medical imaging data. *IEEE Trans. Inf. Technol. Biomed.* 13, 1–10.

Calhoun, V. D., Adali, T., Giuliani, N., Pekar, J. J., Pearlson, G. D., and Kiehl, K. A. (2006). A method for multimodal analysis of independent source differences in schizophrenia: combining gray matter structural and auditory oddball functional data. *Hum. Brain Mapp.* 27, 47–62.

Calhoun, V. D., Adali, T., Pearlson, G. D., and Pekar, J. J. (2001). A method for making group inferences from functional MRI data using independent component analysis. *Hum. Brain Mapp.* 14, 140–151.

Calhoun, V. D., Eichele, T., and Pearlson, G. (2009a). Functional brain networks in schizophrenia: a review. *Front. Neurosci.* 3:17. doi:10.3389/neuro.09.017.2009

Calhoun, V. D., Liu, J., and Adali, T. (2009b). A review of group ICA for fMRI data and ICA for joint inference of imaging, genetic, and ERP data. *Neuroimage* 45, 163–172.

Calhoun, V. D., Kiehl, K. A., Liddle, P. F., and Pearlson, G. D. (2004). aberrant localization of synchronous hemodynamic activity in auditory cortex reliably characterizes schizophrenia. *Biol. Psychiatry* 55, 842–849.

Calhoun, V. D., Kiehl, K. A., and Pearlson, G. D. (2008a). Modulation of temporally coherent brain networks estimated using ICA at rest and during cognitive tasks. *Hum. Brain Mapp.* 29, 828–838.

Calhoun, V. D., Pearlson, G. D., Maciejewski, P., and Kiehl, K. A. (2008b). Temporal lobe and "default" hemodynamic brain modes discriminate between schizophrenia and bipolar disorder. *Hum. Brain Mapp.* 29, 1265–1275.

Calhoun, V. D., Wu, L., Kiehl, K. A., Eichele, T., and Pearlson, G. D. (2010). Aberrant processing of deviant stimuli in schizophrenia revealed by fusion of fMRI and EEG data. *Acta Neuropsychiatr.* 22, 127–138.

Chance, S. A., Casanova, M. F., Switala, A. E., and Crow, T. J. (2008). Auditory cortex asymmetry, altered minicolumn spacing and absence of ageing effects in schizophrenia. *Brain* 131(Pt 12), 3178–3192.

Cordes, D., Haughton, V. M., Arfanakis, K., Carew, J. D., Turski, P. A., Moritz, C. H., Quigley, M. A., and Meyerand, M. E. (2001). Frequencies contributing to functional connectivity in the cerebral cortex in "resting-state" data. *AJNR Am. J. Neuroradiol.* 22, 1326–1333.

Curtis, V. A., Dixon, T. A., Morris, R. G., Bullmore, E. T., Brammer, M. J., Williams, S. C., Sharma, T., Murray, R. M., and McGuire, P. K. (2001). Differential frontal activation in schizophrenia and bipolar illness during verbal fluency. *J. Affect. Disord.* 66, 111–121.

Eichele, T., Debener, S., Calhoun, V. D., Specht, K., Engel, A. K., Hugdahl, K., Cramon, D. Y., and Ullsperger, M. (2008). Prediction of human errors by maladaptive changes in event-related brain networks. *Proc. Natl. Acad. Sci. U.S.A.* 105, 6173–6178.

Erhardt, E., Rachakonda, S., Bedrick, E., Adali, T., and Calhoun, V. D. (in press). Comparison of multi-subject ICA methods for analysis of fMRI data. *Hum. Brain Mapp.*

First, M., Spitzer, R. L., Gibbon, M., and Williams, J. B. (1995). *Structured Clinical Interview for DSM-IV Axis I Disorders-Patient Edition (SCID-I/P, Version 2.0).* New York: New York State Psychiatric Institute.

Ford, J. M., White, P., Lim, K. O., and Pfefferbaum, A. (1994). Schizophrenics have fewer and smaller P300s: a single-trial analysis. *Biol. Psychiatry* 352, 96–103.

Friston, K., Ashburner, J., Frith, C. D., Poline, J. P., Heather, J. D., and Frackowiak, R. S. (1995). Spatial registration and normalization of images. *Hum. Brain Mapp.* 2, 165–189.

Fusar-Poli, P., Borgwardt, S., Crescini, A., Deste, G., Kempton, M. J., Lawrie, S., Mc Guire, P., and Sacchetti, E. (2011). Neuroanatomy of vulnerability to psychosis: a voxel-based meta-analysis. *Neurosci. Biobehav. Rev.* 35, 1175–1185.

Garrity, A., Pearlson, G. D., McKiernan, K., Lloyd, D., Kiehl, K. A., and Calhoun, V. D. (2007). Aberrant "default mode" functional connectivity in schizophrenia. *Am. J. Psychiatry* 164, 450–457.

Genovese, C. R., Lazar, N. A., and Nichols, T. (2002). Thresholding of statistical maps in functional neuroimaging using the false discovery rate. *Neuroimage* 15, 870–878.

Glahn, D. C., Bearden, C. E., Niendam, T. A., and Escamilla, M. A. (2004). The feasibility of neuropsychological endophenotypes in the search for genes associated with bipolar affective disorder. *Bipolar. Disord.* 6, 171–182.

Glahn, D. C., Robinson, J. L., Tordesillas-Gutierrez, D., Monkul, E. S., Holmes, M. K., Green, M. J., and Bearden, C. E. (2010). Fronto-temporal dysregulation in asymptomatic bipolar I patients: a paired associate functional MRI study. *Hum. Brain Mapp.* 31, 1041–1051.

Goes, F. S., Zandi, P. P., Miao, K., McMahon, F. J., Steele, J., Willour, V. L., Mackinnon, D. F., Mondimore, F. M., Schweizer, B., Nurnberger, J. I. Jr., Rice, J. P., Scheftner, W., Coryell, W., Berrettini, W. H., Kelsoe, J. R., Byerley, W., Murphy, D. L., Gershon, E. S., Bipolar Disorder Phenome, G., Depaulo, J. R. Jr., McInnis, M. G., and Potash, J. B. (2007). Mood-incongruent psychotic features in bipolar disorder: familial aggregation and suggestive linkage to 2p11-q14 and 13q21-33. *Am. J. Psychiatry* 164, 236–247.

Goodwin, F. K., and Jamison, K. R. (2007). *Manic-Depressive Illness.* New York, NY: Oxford University Press, 54–59.

Greicius, M. D., Srivastava, G., Reiss, A. L., and Menon, V. (2004). Default-mode network activity distinguishes Alzheimer's disease from healthy aging: evidence from functional MRI. *Proc. Natl. Acad. Sci. U.S.A.* 101, 4637–4642.

Guze, S. B., Woodruff, R. A. Jr., and Clayton, P. J. (1975). The significance of psychotic affective disorders. *Arch. Gen. Psychiatry* 32, 1147–1150.

Hahn, B., Ross, T. J., Yang, Y., Kim, I., Huestis, M. A., and Stein, E. A. (2007). Nicotine enhances visuospatial attention by deactivating areas of the resting brain default network. *J. Neurosci.* 27, 3477–3489.

Hamilton, L. S., Altshuler, L. L., Townsend, J., Bookheimer, S. Y., Phillips, O. R., Fischer, J., Woods, R. P., Mazziotta, J. C., Toga, A. W., Nuechterlein, K. H., and Narr, K. L. (2009). Alterations in functional activation in euthymic bipolar disorder and schizophrenia during a working memory task. *Hum. Brain Mapp.* 30, 3958–3969.

Jafri, M., Pearlson, G. D., Stevens, M., and Calhoun, V. D. (2008). A method for functional network connectivity among spatially independent resting-state components in schizophrenia. *Neuroimage* 39, 1666–1681.

Kay, S. R., Fiszbein, A., and Opler, L. A. (1987). The positive and negative syndrome scale (PANSS) for schizophrenia. *Schizophr. Bull.* 13, 261–276.

Kempton, M. J., Haldane, M., Jogia, J., Grasby, P. M., Collier, D., and Frangou, S. (2009). Dissociable brain structural changes associated with predisposition, resilience, and disease expression in bipolar disorder. *J. Neurosci.* 29, 10863–10868.

Keshavan, M., Morris, D. W., Sweeney, J. A., Pearlson, G. D., Thaker, G., Seidman, L. J., Eack, S. M., and Tamminga, C. A. (in press). A dimensional approach to the continuum between bipolar disorder with psychosis and schizophrenia: the Schizo-Bipolar Scale. *Schizophr. Res.*

Kiehl, K. A., and Liddle, P. F. (2001). An event-related functional magnetic resonance imaging study of an auditory oddball task in schizophrenia. *Schizophr. Res.* 48, 159–171.

Kiehl, K. A., Stevens, M. C., Celone, K., Kurtz, M., and Krystal, J. H. (2005). Abnormal hemodynamics in schizophrenia during an auditory oddball task. *Biol. Psychiatry* 57, 1029–1040.

Kim, D., Mathalon, D., Ford, J. M., Mannell, M., Turner, J., Brown, G., Belger, A., Gollub, R. L., Lauriello, J., Wible, C. G., O'Leary, D., Lim, K., Potkin, S., and Calhoun, V. D. (2009). Auditory oddball deficits in schizophrenia: an independent component analysis of the fMRI multisite function BIRN study. *Schizophr. Bull.* 35, 67–81.

Kiviniemi, V., Starck, T., Remes, J., Long, X., Nikkinen, J., Haapea, M., Veijola, J., Moilanen, I., Isohanni, M., and Zang, Y. F. (2009). Functional segmentation of the brain cortex using high model order group PICA. *Hum. Brain Mapp.* 30, 3865–3886.

Laird, A. R., Eickhoff, S. B., Li, K., Robin, D. A., Glahn, D. C., and Fox, P. T. (2009). Investigating the functional heterogeneity of the default mode network using coordinate-based meta-analytic modeling. *J. Neurosci.* 29, 14496–14505.

Lichtenstein, P., Yip, B. H., Bjork, C., Pawitan, Y., Cannon, T. D., Sullivan, P. F., and Hultman, C. M. (2009). Common genetic determinants of schizophrenia and bipolar disorder in Swedish families: a population-based study. *Lancet* 373, 234–239.

Lynall, M. E., Bassett, D. S., Kerwin, R., McKenna, P. J., Kitzbichler, M., Muller, U., and Bullmore, E. (2010). Functional connectivity and brain networks in schizophrenia. *J. Neurosci.* 30, 9477–9487.

Ma, S., Correa, N., Li, X., Eichele, T., Calhoun, V. D., Adali, T. (in press). Automatic identification of functional clusters in fMRI data using spatial information. *IEEE Trans. Biomed. Eng.*

McIntosh, A. M., Whalley, H. C., McKirdy, J., Hall, J., Sussmann, J. E., Shankar, P., Johnstone, E. C., and Lawrie, S. M. (2008). Prefrontal function and activation in bipolar disorder and schizophrenia. *Am. J. Psychiatry* 165, 378–384.

Michael, A., Baum, S., White, T., Demirci, O., Andreasen, N. C., Segall, J. M., Jung, R. E., Pearlson, G. D., Clark, V. P., Gollub, R. L., Schulz, S. C., Roffmann, J., Lim, K. O., Ho, B. C., Bockholt, H. J., and Calhoun, V. D. (2010). Does function follow form? Methods to fuse structural and functional brain images show decreased linkage in schizophrenia. *Hum. Brain Mapp.* 49, 2626–2637.

Muller, T. J., Kalus, P., and Strik, W. K. (2001). The neurophysiological meaning of auditory P300 in subtypes of schizophrenia. *World J. Biol. Psychiatry* 2, 9–17.

Ongur, D., Lundy, M., Greenhouse, I., Shinn, A. K., Menon, V., Cohen, B. M., and Renshaw, P. F. (2010). Default mode network abnormalities in bipolar disorder and schizophrenia. *Psychiatry Res.* 183, 59–68.

Pearlson, G. D. (1997). Superior temporal gyrus and planum temporale in schizophrenia: a selective review. *Prog. Neuropsychopharmacol. Biol. Psychiatry* 21, 1203–1229.

Raichle, M. E., MacLeod, A. M., Snyder, A. Z., Powers, W. J., Gusnard, D. A., and Shulman, G. L. (2001). A default mode of brain function. *Proc. Natl. Acad. Sci. U.S.A.* 98, 676–682.

Schulze, K. K., Hall, M. H., McDonald, C., Marshall, N., Walshe, M., Murray, R. M., and Bramon, E. (2008). Auditory P300 in patients with bipolar disorder and their unaffected relatives. *Bipolar. Disord.* 10, 377–386.

Segall, J., and Calhoun, V. D. (2011). *Structural and Functional Networks in the Human Brain Proc.* Quebec City: HBM.

Skudlarski, P., Jagannathan, K. A., Anderson, K., Stevens, M. C., Calhoun, V. D., and Pearlson, G. D. (2010). Brain connectivity is not only lower but also different in schizophrenia: a combined anatomical and functional approach. *Biol. Psychiatry* 68, 61–69.

Spitzer, R. L., Williams, J. B., and Gibbon, M. (1996). *Structured Clinical Interview for DSM-IV: Non-Patient Edition (SCID-NP).* New York, NY: New York State Psychiatric Institute.

Sporns, O. (2011). The human connectome: a complex network. *Ann. N. Y. Acad. Sci.* 1224, 109–125.

Strakowski, S. M., DelBello, M. P., and Adler, C. M. (2005). The functional neuroanatomy of bipolar disorder: a review of neuroimaging findings. *Mol. Psychiatry* 10, 105–116.

Strasser, H. C., Lilyestrom, J., Ashby, E. R., Honeycutt, N. A., Schretlen, D. J., Pulver, A. E., Hopkins, R. O., Depaulo, J. R., Potash, J. B., Schweizer, B., Yates, K. O., Kurian, E., Barta, P. E., and Pearlson, G. D. (2005). Hippocampal and ventricular volumes in psychotic and nonpsychotic bipolar patients compared with schizophrenia patients and community control subjects: a pilot study. *Biol. Psychiatry* 57, 633–639.

Sui, J., and Calhoun, V. D. (2011). *Discriminating Schizophrenia and Bipolar Disorder by Unique Patterns of Brain Function and Structure Proc.* Montreal: ISMRM.

Sui, J., Pearlson, G. D., Adali, T., Kiehl, K. A., Caprihan, A., Liu, J., Yamamoto, J., and Calhoun, V. D. (in press). Discriminating schizophrenia and bipolar disorder by fusing fMRI and DTI in a multimodal CCA+ joint ICA based model. *Neuroimage.*

Swerdlow, N. R. (2010). Integrative circuit models and their implications for the pathophysiologies and treatments of the schizophrenias. *Curr. Top. Behav. Neurosci.* 4, 555–583.

Turner, J., Chen, H., Mathalon, D., Allen, E., Mayer, A., Abbott, C., Calhoun, V. D., and Bustillo, J. (in press). Reliability of the amplitude of low-frequency fluctuations in resting state in chronic schizophrenia. *Psychol. Res. Neuroimaging.*

Uddin, L. Q., Kelly, A. M., Biswal, B. B., Xavier Castellanos, F., and Milham, M. P. (2009). Functional connectivity of default mode network components: correlation, anticorrelation, and causality. *Hum. Brain Mapp.* 30, 625–637.

van den Heuvel, M. P., Mandl, R. C., Kahn, R. S., and Hulshoff Pol, H. E. (2009). Functionally linked resting-state networks reflect the underlying structural connectivity architecture of the human brain. *Hum. Brain Mapp.* 30, 3127–3141.

Wang, Q., Su, T. P., Zhou, Y., Chou, K. H., Chen, I. Y., Jiang, T., and Lin, C. P. (2011). Anatomical insights into disrupted small-world networks in schizophrenia. *Neuroimage* 59, 1085–1093.

Williamson, P. (2007). Are anticorrelated networks in the brain relevant to schizophrenia? *Schizophr. Bull.* 33, 994.

Williamson, P., and Allman, J. (2011). *The Human Illnesses: Neuropsychiatri Disorders and the Nature of the Human Brain*. New York, NY: Oxford University Press.

Yu, Q., Sui, J., Rachakonda, S., He, H., Gruner, W., Pearlson, G. D., Kiehl, K. A., and Calhoun, V. D. (2011). Altered topological properties of functional network connectivity in schizophrenia during resting state: a small-world brain network study. *PLoS ONE* 6, e25423. doi:10.1371/journal.pone.0025423

Zalesky, A., Fornito, A., Egan, G. F., Pantelis, C., and Bullmore, E. T. (2011). The relationship between regional and inter-regional functional connectivity deficits in schizophrenia. *Hum. Brain Mapp.* doi: 10.1002/hbm.21379. [Epub ahead of print].

Conflict of Interest Statement: The authors declare that the research was conducted in the absence of any commercial or financial relationships that could be construed as a potential conflict of interest.

Received: 18 October 2011; accepted: 12 December 2011; published online: 10 January 2012.

Citation: Calhoun VD, Sui J, Kiehl K, Turner J, Allen E and Pearlson G (2012) Exploring the psychosis functional connectome: aberrant intrinsic networks in schizophrenia and bipolar disorder. Front. Psychiatry ***2****:75. doi: 10.3389/fpsyt.2011.00075*

This article was submitted to Frontiers in Neuropsychiatric Imaging and Stimulation, a specialty of Frontiers in Psychiatry.

frontiers in
PSYCHIATRY

ORIGINAL RESEARCH ARTICLE
published: 16 December 2011
doi: 10.3389/fpsyt.2011.00073

Impaired cerebellar functional connectivity in schizophrenia patients and their healthy siblings

Guusje Collin[1,2]*, Hilleke E. Hulshoff Pol[1,2], Sander V. Haijma[1,2], Wiepke Cahn[1,2], René S. Kahn[1,2] and Martijn P. van den Heuvel[1,2]

[1] *Rudolf Magnus Institute of Neuroscience, Utrecht, Netherlands*
[2] *University Medical Center Utrecht, Utrecht, Netherlands*

Edited by:
Alex Fornito, University of Melbourne, Australia

Reviewed by:
John Hart, University of Texas at Dallas, USA
Heather C. Whalley, University of Edinburgh, UK
Alex Fornito, University of Melbourne, Australia

***Correspondence:**
Guusje Collin, Department of Psychiatry, University Medical Center Utrecht, A.00.1.12, Heidelberglaan 100, 3584 CX Utrecht, Netherlands.
e-mail: g.collin@umcutrecht.nl

The long-standing notion of schizophrenia as a disorder of connectivity is supported by emerging evidence from recent neuroimaging studies, suggesting impairments of both structural and functional connectivity in schizophrenia. However, investigations are generally restricted to supratentorial brain regions, thereby excluding the cerebellum. As increasing evidence suggests that the cerebellum contributes to cognitive and affective processing, aberrant connectivity in schizophrenia may include cerebellar dysconnectivity. Moreover, as schizophrenia is highly heritable, unaffected family members of schizophrenia patients may exhibit similar connectivity profiles. The present study applies resting-state functional magnetic resonance imaging to determine cerebellar functional connectivity profiles, and the familial component of cerebellar connectivity profiles, in 62 schizophrenia patients and 67 siblings of schizophrenia patients. Compared to healthy control subjects, schizophrenia patients showed impaired functional connectivity between the cerebellum and several left-sided cerebral regions, including the hippocampus, thalamus, middle cingulate gyrus, triangular part of the inferior frontal gyrus, supplementary motor area, and lingual gyrus (all $p < 0.0025$, whole-brain significant). Importantly, siblings of schizophrenia patients showed several similarities to patients in cerebellar functional connectivity, suggesting that cerebellar dysconnectivity in schizophrenia might be related to familial factors. In conclusion, our findings suggest that dysconnectivity in schizophrenia involves the cerebellum and that this defect may be related to the risk to develop the illness.

Keywords: cerebellum, schizophrenia, siblings, functional connectivity, resting-state fMRI, dysconnectivity

INTRODUCTION

The cerebellum has long been regarded as a brain structure that is exclusively involved in motor systems, but an increasing body of evidence suggests that is also involved in cognition and emotion (Schmahmann and Caplan, 2006). The cerebellum is thought to influence motor systems by evaluating disparities between intention and action and by adjusting the operation of motor cortices accordingly, through feed-back and -forward loops via the thalamus and pons (Kandel et al., 2000). The cerebellum may be integrated in the neural circuits governing higher cognitive functions in a similar fashion. Cerebellar modulation of cognitive processes was shown in error-related learning and timing, but a more general involvement has also been suggested (Schmahmann, 2000; Andreasen and Pierson, 2008). According to the "cognitive dysmetria" and "dysmetria of thought" models of schizophrenia – a severe psychiatric disorder characterized by hallucinations, delusions, and disintegration of thinking – aberrant cerebellar modulation of information from and to the cerebral cortex may be a part of the pathophysiology of schizophrenia (Andreasen et al., 1998; Schmahmann, 1998).

The notion that schizophrenia involves the aberrant integration of information between anatomically separated brain regions is long-standing (Wernicke, 1906; Bleuler, 1911; Kraepelin, 1919; Friston, 1998; Stephan et al., 2009a) and is supported by recent neuroimaging studies showing aberrant structural (Assaf and Pasternak, 2008; Bassett et al., 2008; Bassett and Bullmore, 2009; Van den Heuvel et al., 2010; Zalesky et al., 2011) and functional (Lynall et al., 2010; Fornito et al., 2011) connectivity in schizophrenia (Petterson-Yeo et al., 2011; Rubinov and Bassett, 2011). However, the cerebellum is typically excluded from these "whole-brain" analyses of brain connectivity in schizophrenia. Interestingly, some studies using diffusion tensor imaging (DTI) to target specific white matter tracts have shown impaired structural connectivity of the cerebellum (Kanaan et al., 2009; Kyriakopoulos and Frangou, 2009). Furthermore, a few functional connectivity studies in schizophrenia have reported impaired functional integration of the cerebellum (Honey et al., 2005; Kim et al., 2008; Becerril et al., 2011; Repovs et al., 2011). However, it remains unclear whether functional connectivity between the cerebellum and the rest of the brain is affected in schizophrenia, and if so, to what extent. Functional connectivity between anatomically separated brain regions is defined as the temporal dependency of their neural activation patterns and is thought to be reflected, to some extent, by their coherence in spontaneous (resting-state) fluctuations in functional magnetic resonance imaging (fMRI) signal (Friston et al., 1993; Biswal et al., 1995, 1997; Van den Heuvel and Hulshoff Pol,

2010). Allowing for the investigation of all functional connections of the cerebellum, the present study employs resting-state fMRI to determine the functional connectivity profile of the cerebellum in schizophrenia. Furthermore, as schizophrenia is highly heritable (Sullivan et al., 2003), aberrant connectivity in schizophrenia may also be present in unaffected family members of schizophrenia patients. To determine the familial component of any changes in cerebellar connectivity profiles, these profiles are also investigated in siblings of schizophrenia patients, who share the genetic predisposition for psychosis, but are not (yet) ill. This way, the present study seeks to determine whether impaired cerebellar connectivity might be related to the risk to develop schizophrenia.

MATERIALS AND METHODS

PARTICIPANTS

A total of 62 schizophrenia patients, 67 siblings of schizophrenia patients, and 41 healthy comparison subjects were included in this study. Study participants were recruited at the University Medical Center Utrecht, during a large ongoing cohort in the Netherlands (Genetic Risk and Outcome of Psychosis; GROUP). The study was approved by the affiliated ethical committee. Study participants were between 18 and 60 years of age. All subjects provided written informed consent prior to participation. Subjects with a history of head trauma or major medical or neurological illness were excluded.

Presence or absence of current and lifetime psychopathology was established for all participants, using the Comprehensive Assessment of Symptoms and History (CASH) interview (Andreasen et al., 1992). Schizophrenia patients were eligible for the present study if they met Diagnostic and Statistical Manual of Mental Disorders fourth edition (DSM IV; American Psychiatric Association, 1994) criteria of schizophrenia or related spectrum disorders. Both siblings of schizophrenia patients and healthy comparison subjects could have no history of any psychiatric illness, including substance dependence of abuse; and healthy comparison subjects had no first- or second-degree family members with a lifetime psychotic disorder.

Study participants originated from a total number of 132 families. Within the healthy comparison group, there were two sibling pairs (both healthy control subjects, i.e., without a first- or second-degree relative with a lifetime psychotic disorder), and within the 67 siblings of patients, there were seven pairs of siblings of a schizophrenia patient and one set of three siblings of a schizophrenia patient. There were no family relationships within the patient group. Between the sibling and patient groups, there were a total number of 27 family-ties [i.e., a schizophrenia patient and (one of) their sibling(s) participated in the study].

For schizophrenia patients, symptom severity was assessed using the positive and negative syndrome scale (PANSS; Kay et al., 1987); Furthermore, the type and daily dose of antipsychotic medication at the time of scanning was recorded, and a haloperidol equivalent dose was calculated using conversion rates (risperidone 0.5:1; olanzapine 1.66:1; quetiapine 25:1; clozapine 33.33:1; aripiprazole 2.5:1; flupenthixol 0.66:1; perphenazine 2.66:1; Kroken et al., 2009). In healthy comparison subjects and siblings of patients, a shortened version of the structured interview of schizotypy-revised (SIS-R; Kendler et al., 1989; Vollema and Ormel, 2000) was employed [excluding four items: social isolation (last 3 years); antisocial behavior; dysfunction (obligatory activities); and dysfunction (personal caretaking)], to measure the overall severity of schizotypal signs and symptoms on a four-point scale (0 = absent, 1 = mild, 2 = moderate, 3 = severe). For all participants, global cognitive functioning, as measured by total IQ, was estimated using four subtests (i.e., Information, Arithmetic, Block design, and Digit symbol coding) of the Dutch version of the Wechsler adult intelligence scale (WAIS; Stinissen et al., 1970).

Finally, statistical testing of group-differences in demographic characteristics was performed using analysis of variance (ANOVA) for continuous and Chi-Square tests for categorical variables. All demographic and clinical characteristics are provided in **Table 1**.

IMAGE ACQUISITION AND PREPROCESSING

Resting-state fMRI data were acquired on two 1.5 T Magnetic Resonance Imaging scanners (Philips Medical Systems, Best, The Netherlands) at the University Medical Center Utrecht, The Netherlands. BOLD time-series were recorded during 9 minutes using a 3D-PRESTO sequence (Van Gelderen et al., 1995; Ramsey et al., 1996; acquisition parameters: TR/TE 21.1/31.1 ms; voxel size 4 mm × 4 mm × 4 mm). Subsequently, a T1 weighted image was acquired for anatomical reference (3D FFE pulse sequence, TR/TE = 30/4.6 ms, flip-angle 30°, FOV 256 mm × 256 mm, voxel size 1 mm × 1 mm × 1.2 mm, 160–180 contiguous slices; Ramsey et al., 2006). Preprocessing was performed using SPM5 software. In short, all resting-state functional images were registered to the last functional scan to correct for head movements and co-registered with the T1 scan to ensure overlap between the anatomical reference scan and resting-state time-series. The registered functional images were spatially smoothed, using an 8-mm full width half–max smoothing kernel. Next, the T1 scan and resting-state time-series were normalized to standard space, matching the MNI-152 template. To create individual anatomical label maps, the spatially normalized T1 image was overlaid with the automated anatomical labeling (AAL) template (Tzourio-Mazoyer et al., 2002), distinguishing 116 anatomical brain regions. Time-series were corrected for white matter, ventricle, and motion parameters (using regression) and band pass filtered (bandwidth 0.01–0.1 Hz) to eliminate low frequency noise and influences of frequencies reflecting possible cardiac or respiratory oscillations.

CEREBELLAR REGION OF INTEREST DEFINITION

The cerebellum has three anterior–posterior divisions (Kandel et al., 2000). The primary fissure separates the anterior lobe from the posterior lobe and the posterolateral fissure separates the posterior and flocculo-nodular lobe. Three mediolateral regions that are important functionally are distinguished by two longitudinal grooves that define an elevated ridge in the midline known as the vermis and the cerebellar hemispheres on either side of the vermis. Each of the 26 cerebellar regions distinguished by the AAL template was assigned to one of seven cerebellar anatomical regions of interest (ROI; **Table 2**), including the anterior and posterior vermis, the bilateral anterior and posterior cerebellar hemispheres and the flocculo-nodular lobe (see **Figure 1**, no. 3; 6; 1 and 2; 4 and 5; 7 respectively).

Table 1 | Demographic and clinical characteristics.

	Healthy control subjects ($N = 41$)	Siblings of patients ($N = 67$)	Schizophrenia patients ($N = 62$)
Age, mean (SD)	30.4 (8.8)	29.8 (8.0)	31.2 (5.8)
Gender, M/F	19/22	34/33	52/10*
Handedness[a], R/L	34/7	60/7	54/5
Highest degree of education[b] (SD)	5.5 (1.4)	5.2 (2.1)	4.1 (2.1)*
IQ[c] (SD)	110.1 (15.4)*	102.7 (14.9)*	93.7 (13.5)*
Duration of illness, years (SD)			7.5 (4.3)
Diagnosis			
Schizophrenia, *N* (%)			44 (71.0)
Schizophreniform disorder, *N* (%)			3 (4.8)
Schizoaffective disorder, *N* (%)			8 (12.9)
Other[d], *N* (%)			7 (11.3)
Schizotypal features, mean (SD) [range]	0.19 (0.18) [0–0.8]	0.17 (0.15) [0–0.5]	
PANSS symptoms[e]			
Positive, mean (SD) [range]			10.8 (4.0) [7–24]
Negative, mean (SD) [range]			11.8 (3.8) [7–23]
Total, mean (SD) [range]			61.8 (16.3) [41–108]
Antipsychotic medication[f]			
Atypical, *N*			43
Risperidone, *N*; HEQ dose (SD)			11; 5.8 (2.5)
Olanzapine, *N*; HEQ dose (SD)			17; 7.8 (4.2)
Quetiapine, *N*; HEQ dose (SD)			5; 19.2 (16.6)
Clozapine, *N*; HEQ dose (SD)			8; 13.7 (6.1)
Aripiprazole, *N*; HEQ dose (SD)			2; 9.0 (4.2)
Typical, *N*			5
Haloperidol, *N*; HEQ dose (SD)			2; 3.5 (0.7)
Other typical[g], *N*; HEQ dose (SD)			3; 4.7 (4.0)
No current antipsychotic therapy, *N*			8

*[a]Data missing for three patients; [b]Ranging from no education (0) to university (8). [c]Estimated intelligence quotient (IQ). [d]Other diagnoses include delusional disorder (N = 2), brief psychotic disorder (N = 2), and psychosis not otherwise specified (N = 3). [e]Positive and negative syndrome scale (PANSS), data missing for three patients; [f]Average haloperidol equivalent (HEQ) dose (mg); [g]other typical medication includes flupentixol (N = 1), perfenazine (N = 1), and penfluridol (N = 1), data missing for five patients; * indicates a statistically significant difference (at $p < 0.05$).*

Table 2 | Automated anatomical labeling regions per cerebellar ROI.

L anterior hemisphere	R anterior hemisphere	Anterior vermis	L posterior hemisphere	R posterior hemisphere	Posterior vermis	Flocculo-nodular lobe
L lobule III of cerebellar hemisphere	R lobule III of cerebellar hemisphere	Lobule I, II of vermis	L lobule VI of cerebellar hemisphere	R lobule VI of cerebellar hemisphere	Lobule VI of vermis	L lobule X of cerebellar hemisphere (flocculus)
L lobule IV, V of cerebellar hemisphere	R lobule IV, V of cerebellar hemisphere	Lobule III of vermis	L crus I of cerebellar hemisphere	R crus I of cerebellar hemisphere	Lobule VII of vermis	R lobule X of cerebellar hemisphere (flocculus)
		Lobule IV, V of vermis	L crus II of cerebellar hemisphere	R crus II of cerebellar hemisphere	Lobule VIII of vermis	Lobule X of vermis (nodulus)
			L lobule VIIB of cerebellar hemisphere	R lobule VIIB of cerebellar hemisphere	Lobule IX of vermis	
			L lobule VIII of cerebellar hemisphere	R lobule VIII of cerebellar hemisphere		
			L lobule IX of cerebellar hemisphere	R lobule IX of cerebellar hemisphere		

The 26 cerebellar regions distinguished by the automated anatomical labeling (AAL) atlas were assigned to one of seven cerebellar regions of interest; L, left; R, right.

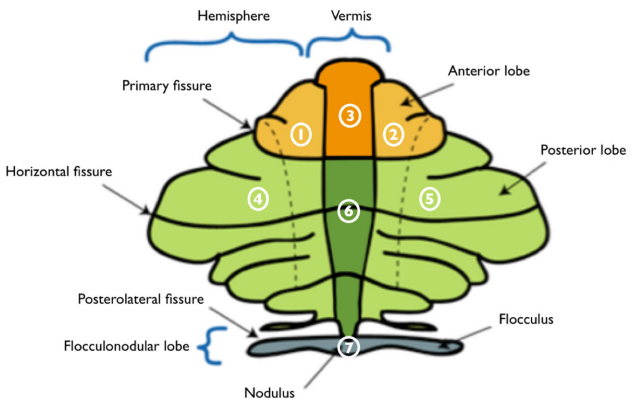

FIGURE 1 | Schematic illustration of the flattened cerebellar cortex and regions of interest. Major anatomical landmarks are depicted, as well as the cerebellar regions of interest, including the left (1) and right (2) anterior hemispheres, anterior vermis (3), left (4) and right (5) posterior hemispheres, posterior vermis (6), and flocculo-nodular lobe (7). Adjusted to the image "Schematic representation of the major anatomical divisions of the cerebellum," source: en.wikipedia, released under the GNU Free Documentation License, version 1.3, 2008, published by the Free Software Foundation.

FUNCTIONAL CONNECTIVITY ANALYSES

Figure 2 illustrates the consecutive steps of the performed functional connectivity analysis. For each subject, 116 regional mean time-series were computed by averaging the voxel-based time-series within each of the anatomically defined regions. Next, interregional correlation in resting-state time-series between each possible pair of the 26 cerebellar regions and the 90 cerebral regions in the AAL template was computed (**Figure 2A**). For each subject, functional connectivity per cerebellar ROI was then calculated by averaging the correlation coefficients of the AAL regions within each of the seven cerebellar regions (**Figure 2B**), rendering weighted correlation coefficients $r_{i,j}$ for the connections $\{i, j\}$ of each cerebellar ROI i ($N = 7$) with each cerebral region j ($N = 90$). Interregional correlations were first computed and subsequently averaged for each ROI (rather than averaging at the level of regional time-series) as the ROIs may comprise more than one functional region and averaging distinct regional time-series may lead signals to phase out when averaged. Fisher r-Z transforms were not applied as the correlations were normally distributed. Next, weighted correlation maps per subject group were computed for each cerebellar ROI (**Figure 2C**), rendering three matrices (for control, sibling, and patient groups) per ROI, with all 90 connections $\{i, j\}$ of the particular ROI i on the x-axis and the number of subjects in the group ($N = 41$; 67; 62 respectively) on the y-axis.

HEALTHY CEREBELLAR FUNCTIONAL CONNECTIVITY

In order to interpret possible differences in cerebellar functional connectivity between subject groups, the general pattern of functional connections per cerebellar ROI was investigated in the healthy control subjects. As functionally connected regions have been shown to exhibit a high degree of temporal coherence (Biswal et al., 1995; Van den Heuvel et al., 2008), higher interregional correlation in time-series was interpreted as a higher degree of functional connectivity between two regions.

CEREBELLAR FUNCTIONAL CONNECTIVITY IN SCHIZOPHRENIA PATIENTS AND SIBLINGS

Differences between subject groups in cerebellar functional connectivity patterns were examined using two functional connectivity measures. First, overall connectivity strength per cerebellar ROI was computed, providing information on the global level of communication between each cerebellar ROI and the rest of the brain.

Analysis 1 overall connectivity strength S per cerebellar ROI

Connectivity strength S_i of each cerebellar ROI i was computed as the average of all correlations between region i and all extra-cerebellar regions j, providing information on the total level of connectivity of each cerebellar ROI (**Figure 2D**). Formally:

$$S_i = \frac{\sum Fc_{i,j}}{N_j}$$

Overall connectivity strength is a global measure of the extent to which the ROI is integrated in the brain network. However, it is not specific as to whether any particular connections are affected. Therefore, a pairwise approach was used next, to "zoom in" on discrete connections.

Analysis 2 functional connectivity Fc of discrete connections

Computed as the (averaged) correlation of each cerebellar region i with each extra-cerebellar region j of the brain network, each functional connection $Fc_{i,j}$ is an element of the set Fc_i of all functional connections ($N = 90$) of the cerebellar ROI (**Figure 2E**):

$$Fc_{i,j} \in Fc_i$$

In both analyses, the actual values (i.e., both positive and negative correlations) were used when averaging across correlation coefficients. As a consequence, negative correlations – which were both scarce and small in amplitude (all mean correlation coefficients > -0.1) – were interpreted as lower levels of functional connectivity.

To exclude potential bias (in variance estimates) of family relationships within and between subject groups, the analyses were repeated with only unrelated individuals ($N = 132$), i.e., 46 schizophrenia patients, 47 siblings of patients, and 39 healthy control subjects.

CLINICAL CORRELATES OF CEREBELLAR CONNECTIVITY

Using linear regression analyses, the association between any possible changes in cerebellar connectivity measures and clinical variables (i.e., duration of illness; severity of PANSS symptoms and IQ) was investigated, and the dose of antipsychotic medication (in haloperidol equivalent) at the time of scanning was examined as a potential confounder.

STATISTICAL ANALYSIS OF GROUP-DIFFERENCES

Connectivity strength S of each cerebellar ROI and functional connectivity Fc of each individual connection of schizophrenia

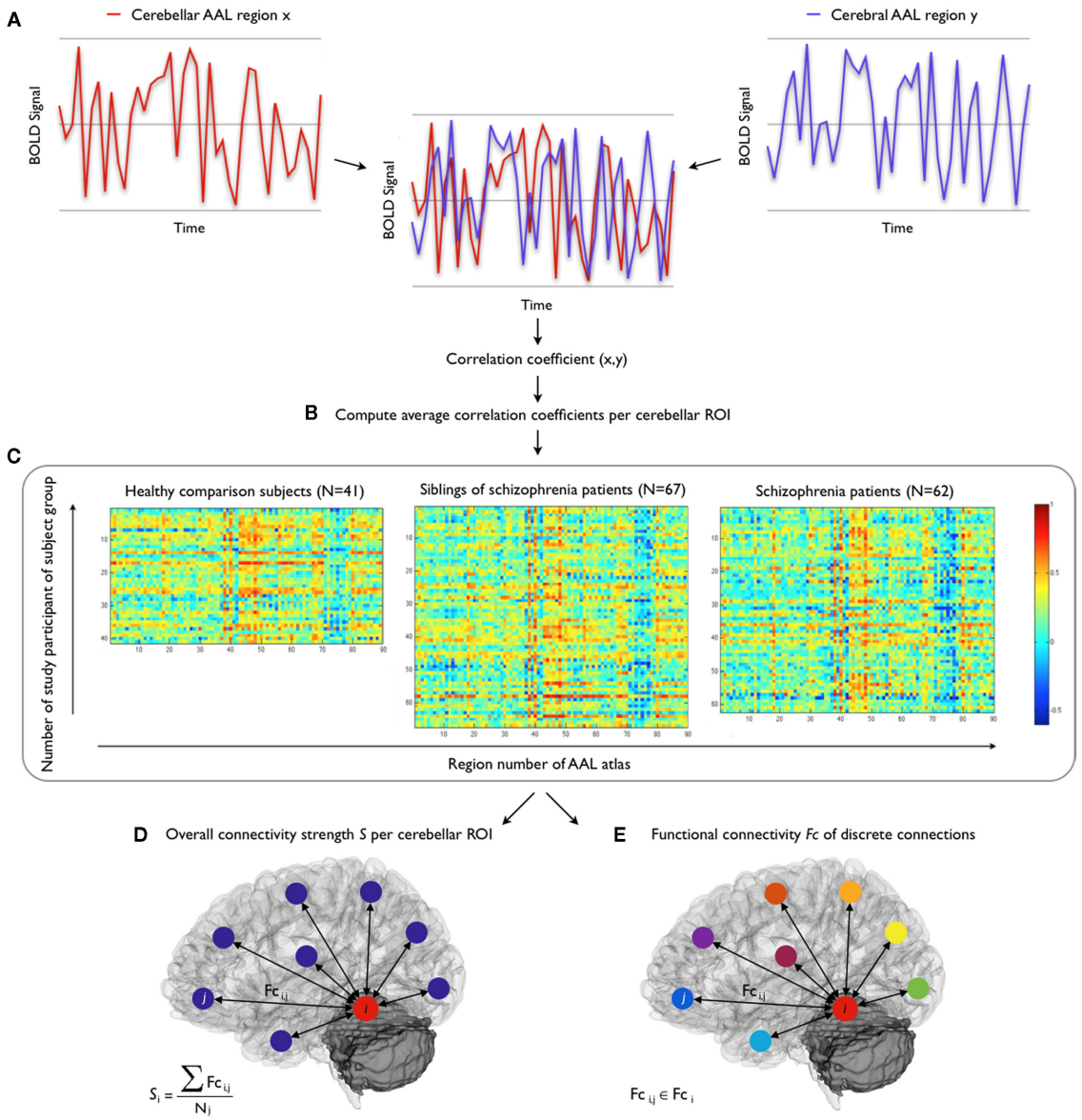

FIGURE 2 | Functional connectivity analysis. Consecutive steps of the functional connectivity analysis. **(A)** Computation of correlation between cerebellar and cerebral resting-state fMRI time-series, **(B)** calculation of correlation coefficients of cerebellar ROIs, **(C)** computation of weighted correlation maps per subject group and per cerebellar ROI. Next, computation of **(D)** overall connectivity strength per cerebellar ROI, and **(E)** functional connectivity of discrete connections.

patients and siblings of schizophrenia patients were compared to those of the healthy comparison subjects. To examine the statistical significance of group-differences, permutation testing was used (5000 permutations; Bassett et al., 2008; Lynall et al., 2010; Van den Heuvel et al., 2010). To this end, random permutation of group assignment was performed, maintaining the original number of subjects per group, rendering three groups of 41, 62, and 67 randomly assigned subjects. Consequently, weighted correlation maps per randomly assigned subject group were computed for each cerebellar ROI. Using the resulting correlation maps, the connectivity measures were recalculated. This process was repeated 5000 times, resulting in a between-group difference null distribution of the connectivity measures. Finally, the observed differences between the original subject groups were compared to the normal distribution of differences after random permutation, to explore the null hypothesis that the observed differences were not determined by subject group membership. Finally, *p*-values were assigned to the group effects by computing (after random permutation) the percentage of findings that was more extreme than the observed difference between the original subject groups. In view of the number of tests performed in the connectivity strength analysis (Analysis 1, **Figure 2D**), a *p*-value of <0.01 was considered to

indicate statistical significance, and a p-value of >0.01 and <0.05 to indicate a statistical trend. To account for the multiple comparisons of the second analysis (Analysis 2, **Figure 2E**), the effects on functional connectivity of discrete connections were subjected to a false discovery rate (FDR) threshold of $q = 0.05$ (Benjami and Hochberg, 1995; Storey, 2002) over all functional connections ($N = 90$) of each cerebellar ROI, providing control over false positive findings.

RESULTS

HEALTHY CEREBELLAR FUNCTIONAL CONNECTIVITY

In the healthy comparison subjects, mean functional connectivity of the posterior hemispheres [mean Fc (SD) = 0.27 (0.07)] > anterior hemispheres [mean Fc (SD) = 0.21 (0.06)] and the right cerebellum [mean Fc (SD) = 0.27 (0.08)] > left cerebellum [mean Fc (SD) = 0.22 (0.06)] (both $p < 0.0001$). Furthermore, mean functional connectivity of the lateral cerebellum (i.e., hemispheres) [mean Fc (SD) = 0.24 (0.06)] was significantly higher than that of midline structures (i.e., vermis and flocculo-nodular lobe) [mean Fc (SD) = 0.14 (0.05)] ($p < 0.0001$).

The highest levels of functional connectivity were found between the right anterior cerebellar hemisphere and right lingual gyrus (mean Fc = 0.54, SD 0.14), hippocampus [mean Fc (SD) = 0.50 (0.18)] and parahippocampal gyrus [mean Fc (SD) = 0.50 (0.15)]. Overall, cerebellar connections to posterior medial regions of the cerebral cortex [i.e., (pre)cuneus, calcarine sulcus, lingual gyrus] showed high levels of functional connectivity, irrespective of cerebellar ROI [mean Fc (SD) of all ROIs 0.26 (0.08), 0.26 (0.10); 0.34 (0.08), 0.32 (0.08); 0.32 (0.09), 0.29 (0.10); 0.29 (0.09), 0.33 (0.12); for the left and right cuneus; precuneus; calcarine sulcus; and lingual gyrus respectively]. The lowest levels of functional connectivity were observed for connections with the bilateral lentiform nucleus [mean Fc (SD) = 0.11 (0.15)], in particular the globus pallidus [left; right mean Fc (SD) = 0.05 (0.15); 0.09 (0.15)], and with the gyrus rectus [left; right mean FC (SD) = 0.11 (0.17); 0.09 (0.17)] (**Figure 3**).

ANALYSIS 1 OVERALL CONNECTIVITY STRENGTH S OF CEREBELLAR ROIs

Overall connectivity strength of the posterior and flocculo-nodular lobes of the cerebellum with the rest of the brain did not differ between groups, suggesting intact functional connectivity of posterior and flocculo-nodular cerebellar regions in schizophrenia. Connectivity strength of the right anterior hemisphere of the cerebellum however, was found to be 23% less ($p = 0.01$) in schizophrenia patients compared to healthy comparison subjects. Furthermore, on trend level, connectivity strength of the anterior vermis was less in both schizophrenia patients (−27%, $p = 0.04$) and siblings (−22%, $p = 0.05$), compared to healthy comparison subjects (**Figure 4**).

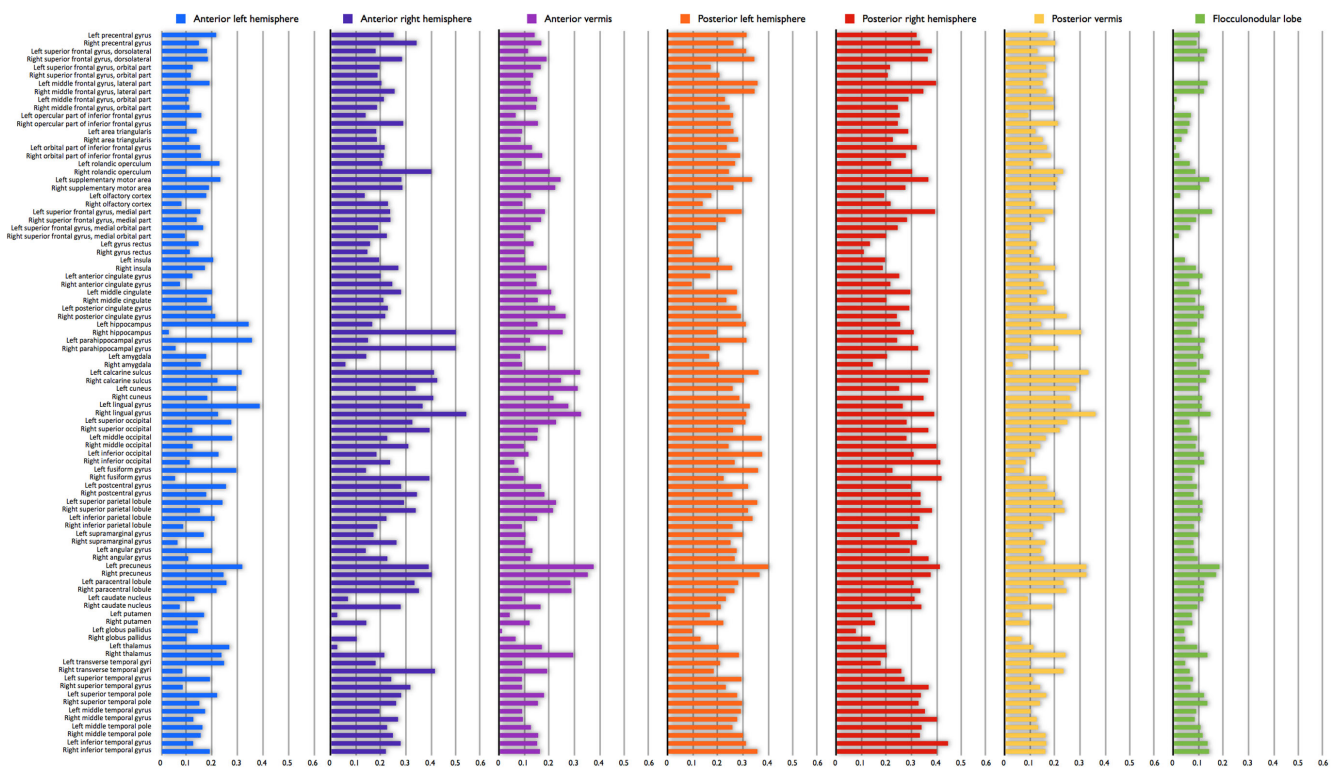

FIGURE 3 | Healthy cerebellar functional connectivity profile. Mean functional connectivity of all possible connections per cerebellar region of interest (ROI) in the healthy comparison sample. High correlations indicate high interregional functional connectivity; low correlations indicate low interregional functional connectivity. Negative correlations ($N = 4$; mean (SD) [range] = −0.05 (0.18) [−0.07 to −0.02]) are depicted as zero.

ANALYSIS 2 FUNCTIONAL CONNECTIVITY OF DISCRETE CONNECTIONS: PATIENTS VERSUS CONTROLS

Impaired functional connectivity was most pronounced in the connections between the right anterior cerebellar hemisphere and vermis, and left-cerebral regions. Particularly between the right anterior vermis and the left-sided triangular part of the inferior frontal gyrus (Fc = −0.13, $p = 0.0024$), supplementary motor area (Fc = −0.12, $p = 0.0014$), middle cingulate gyrus (Fc = −12, $p = 0.0004$), hippocampus (Fc = −0.17, $p = 0.0004$), and thalamus (Fc = −0.16, $p < 0.0001$). Functional connectivity between the latter two regions (i.e., left hippocampus and thalamus) and the anterior cerebellar vermis was also decreased in patients (Fc = −0.14, $p = < 0.0001$; Fc = −0.13, $p = 0.0008$ respectively). The only significant increase in functional connectivity in schizophrenia patients relative to controls was found between the posterior vermis and left lingual gyrus (Fc = 0.15, $p < 0.0001$). All these findings survived FDR-correction (**Figure 5**).

ANALYSIS 2 FUNCTIONAL CONNECTIVITY OF DISCRETE CONNECTIONS: SIBLINGS VERSUS CONTROLS

Compared to schizophrenia patients, the siblings demonstrated both similarities and disparities in functional connectivity of the

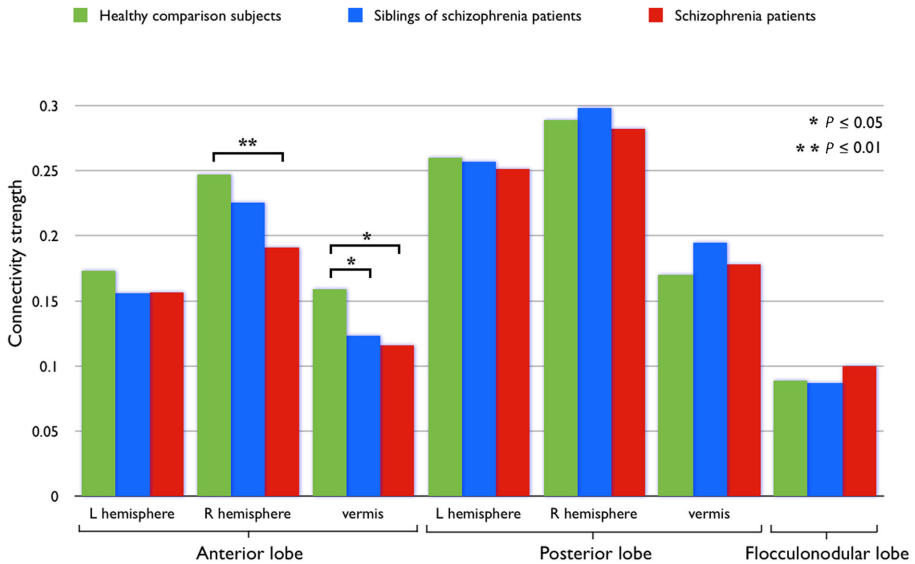

FIGURE 4 | Connectivity strength per cerebellar ROI. Connectivity strength S, as the average of all correlations (unthresholded) between the cerebellar ROI and all extra-cerebellar regions in the brain, per subject group.

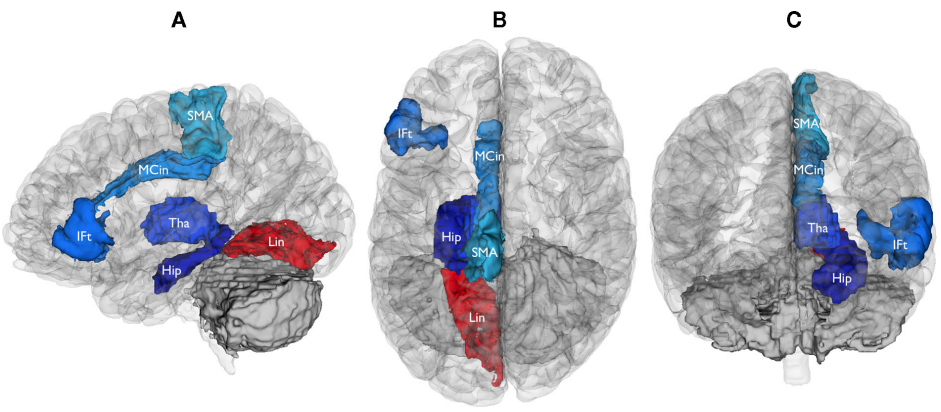

FIGURE 5 | Brain regions functionally dysconnected from the cerebellum in schizophrenia. Left lateral **(A)**, superior **(B)**, and anterior **(C)** views of the brain, showing the cerebral regions that were found to be functionally dysconnected (whole-brain significant) from the cerebellum. Blue signifies decreased functional connectivity with the cerebellum in schizophrenia patients compared to healthy comparison subjects (all $p < 0.0025$, FDR-corrected), red indicates increased functional connectivity ($p < 0.0001$, FDR-corrected). Reduced functional connectivity involved the right anterior cerebellar hemisphere (IFt, inferior frontal gyrus, triangular part; SMA, supplementary motor area; MCin, Middle Cingulate gyrus; Hip, Hippocampus; Tha, Thalamus) and anterior vermis of the cerebellum (Hip, Hippocampus; Tha, Thalamus). Increased functional connectivity involved the posterior cerebellar vermis (Lin, Lingual gyrus).

cerebellum. Siblings showed decreased functional connectivity (compared to control subjects) between the anterior cerebellar vermis and the triangular part of the left inferior frontal gyrus (Fc = −0.08, $p = 0.009$), left insula (Fc = −0.08, $p = 0.007$), and left hippocampus (Fc = −0.11, $p = 0.002$), as well as between the right anterior cerebellar hemisphere and left hippocampus (Fc = −0.12, $p = 0.003$), resembling the findings in patients. However, these findings were not as strong as in patients, as they failed to reach whole-brain significance (note that impaired functional connectivity between the anterior cerebellar vermis and left insula did not reach whole-brain significance in both siblings and patients), and should be considered exploratory. Conversely, functional connectivity to other brain regions that were found to be dysconnected from the cerebellum in schizophrenia patients (e.g., left thalamus, middle cingulate gyrus, and supplementary motor area) was not decreased in siblings of schizophrenia patients, compared to the healthy control subjects. **Table 3** depicts all findings at $p < 0.01$ in schizophrenia patients and siblings of patients.

Importantly, as siblings were psychiatrically healthy (see inclusion criteria and SIS-R scores, **Table 1**) and, on average, around 30 years of age, it is unlikely that any would still convert to illness. Lastly, repeating the functional connectivity analyses in a reduced

Table 3 | Absolute differences in functional connectivity between subject groups.

	Cerebellar regions													
	L anterior hemisphere		R anterior hemisphere		Anterior vermis		L posterior hemisphere		R posterior hemisphere		Posterior vermis		Flocculo-nodular lobe	
	Sz	Sib	Sz	Sib	Sz	Sib	Sz	Sib	Sz	Sib	Sz	Sib	Sz	Sib
CEREBRAL REGIONS														
R superior frontal gyrus, dorsolateral			0.10											
L superior frontal gyrus, orbital			0.11			0.07								
L middle frontal gyrus, orbital			0.10											
L inferior frontal gyrus, triangular			0.13*		0.09	0.08								
L supplementary motor area			0.12*		0.09									
R supplementary motor area			0.10											
R superior frontal gyrus, medial			0.09											
L superior frontal gyrus, medialorbital	0.08													
L gyrus rectus	0.09													
R gyrus rectus						0.07								
L insula					0.10	0.08								
L anterior cingulate gyrus												0.07		
L middle cingulate gyrus			0.12*		0.10									
L hippocampus			0.17*	0.12	0.14*	0.11					0.11			
L lingual gyrus											0.15*		0.08	
R lingual gyrus											0.10			
R inferior occipital gyrus			0.11											
L inferior parietal lobule						0.08								
L paracentral lobule			0.10											
L caudate nucleus												0.08		
R caudate nucleus					0.09									
R globus pallidus			0.10											
L thalamus			0.16*		0.13*						0.11			
L superior temporal gyrus													0.06	
R superior temporal pole			0.11											

*Absolute difference in interregional correlation coefficients between schizophrenia patients and healthy comparison subjects; and siblings of patients and healthy comparison subjects. Decreased functional connectivity relative to healthy comparison subjects is displayed in blue, increased functional connectivity in red. Findings at p < 0.01 are depicted; * indicates whole-brain significance after FDR-correction. Sz, schizophrenia patients; Sib, siblings of schizophrenia patients, L, left-sided, R, right-sided.*

number of study participants that were completely unrelated did not alter the findings.

CLINICAL CORRELATES OF CEREBELLAR CONNECTIVITY

Cerebellar functional connectivity measures that were significantly different in schizophrenia patients, compared to healthy comparison subjects, were investigated for associations with medication dose, duration of illness, symptom severity, and global cognitive performance, using linear regression analysis. No association between the dose of antipsychotic medication at the time of scanning and cerebellar functional connectivity was found (all $p > 0.420$). After multiple comparison correction, there were no significant associations between aberrant cerebellar functional connectivity measures and clinical variables. On trend level, a counter-intuitive association between more negative symptoms and increased Fc between the cerebellar right anterior hemisphere and left hippocampus was observed (**Table 4**).

DISCUSSION

The main finding of our study is the presence of an aberrant level of functional connectivity of the cerebellum in schizophrenia patients and their healthy siblings. Our findings suggest that in schizophrenia, the cerebellum, specifically the vermis, and right anterior hemisphere, is functionally dysconnected from a range of left-cerebral cortical and subcortical regions, including frontal, cingulate, and occipital regions, as well as the thalamus and hippocampus. Importantly, unaffected siblings of schizophrenia patients demonstrated several similarities in cerebellar functional dysconnectivity compared to patients, in particular reduced functional connectivity of the cerebellum to the left hippocampus. This overlap suggests that cerebellar dysconnectivity may be related, at least in part, to familial (and possibly genetic) factors.

Disparities in cerebellar connectivity between schizophrenia patients and their siblings were also found. Of these, the dissimilarity in cerebellar–thalamic dysconnectivity may be the most meaningful, as the thalamus is the obligatory relay for all efferent cerebellar projections to the cortex. In this context, our findings may imply that cerebellar–thalamic dysconnectivity might be related more to the manifestation of the illness, than to familial (or genetic) factors.

Although the term "dysconnectivity" emphasizes the notion of abnormal, rather than necessarily decreased, functional integration between brain regions (Stephan et al., 2009a), structural and functional connectivity studies in schizophrenia have mostly reported reduced (rather than increased) connectivity in schizophrenia (Petterson-Yeo et al., 2011). In line with these findings, our study shows that in schizophrenia, functional connectivity of the cerebellum is mostly decreased. Furthermore, studies have reported changing patterns of reduced connectivity across the different stages of disease, from chronic schizophrenia to individuals at high (genetic) risk for psychosis (including healthy first-degree relatives of schizophrenia patients; Petterson-Yeo et al., 2011). These findings support the presently reported overlap in cerebellar dysconnectivity between patients and siblings. Additional support for this finding comes from a recent study examining functional connectivity within and between four predefined functional networks: the default mode network and three cognitive control (frontal–parietal, cingulo-opercular, and cerebellar) networks (Repovs et al., 2011). Compared to controls, reduced connectivity between cerebellar, frontal–parietal, and cingulo-opercular networks was shown in both schizophrenia patients and siblings of patients. Intriguingly, greater reductions in connectivity between the frontal–parietal and cerebellar regions were found to be robustly predictive of worse cognitive performance across groups and predictive of more disorganization symptoms among patients. The association between cognitive performance and cerebellar functional connectivity is not replicated by the present study. However, as modest cognitive deficits are reported in adult patients with (especially right-sided) cerebellar lesions, while similar lesions in children lead to pervasive impairments (suggesting a critical role for the cerebellum in development; Alexander et al., 2011), the relationship between cerebellar abnormalities and cognition may not be straightforward and may depend on factors such as age of illness onset. Regarding the relationship with clinical symptoms, the meaning of the counter-intuitive trend between greater severity of PANSS

Table 4 | Clinical correlates of aberrant functional connectivity measures.

	Aberrant functional connectivity measures									
	S Cer2	**S Cer3**	**Fc Cer2-IFt**	**Fc Cer2-SMA**	**Fc Cer2-MCin**	**Fc Cer2- Hip**	**Fc Cer2-Tha**	**Fc Cer3-Hip**	**Fc Cer3-Tha**	**Fc Cer6-Lin**
Duration of illness	−0.21	−0.07	−0.29	−0.26	−0.15	−0.05	−0.10	0.10	0.12	−0.22
PANSS										
Total score	0.24	0.12	0.09	0.02	0.29	0.33	0.31	0.26	0.10	−0.10
Positive symptoms	0.16	0.15	−0.01	0.01	0.23	0.17	0.26	0.16	0.03	−0.01
Negative symptoms	0.17	0.07	0.05	−0.01	0.22	0.37*	0.27	0.25	0.18	−0.07
IQ	−0.02	−0.04	−0.15	−0.02	−0.03	−0.29	−0.16	−0.11	−0.07	−0.12

Standardized correlation coefficients (ß) describing the correlation between clinical variables and cerebellar functional connectivity metrics that were found to be aberrant in schizophrenia patients compared to healthy comparison subjects ($p < 0.01$, uncorrected). S = connectivity strength; Fc = functional connectivity; Cerebellar ROI 2 (Cer2) = right anterior cerebellar hemisphere; Cerebellar ROI 3 (Cer3) = Anterior vermis; IFt, inferior frontal gyrus, triangular part; SMA, supplementary motor area, MCin, middle cingulate gyrus, Hip, hippocampus, Tha, thalamus, Lin, lingual gyrus.*

negative symptoms and increased functional connectivity between the cerebellar anterior right hemisphere and left hippocampus is unclear, but may be an indication of discrete symptom dimensions in schizophrenia with distinct underlying neurobiology (Ke et al., 2010).

Our findings suggest that functional dysconnectivity of the cerebellum to the cerebrum involves mainly anterior and vermal areas of the cerebellum. The vermis has previously been labeled the "limbic cerebellum," as the (anterior) vermis is the principal cerebellar target of limbic projections (Schmahmann, 2000). Furthermore, behavioral studies support a relationship between cerebellar midline structures and the modulation of emotion (Heath and Harper, 1974; Stoodley and Schmahmann, 2010), and lesions of the vermis have been shown to produce affective symptoms, ranging from emotional blunting and depression to disinhibition and psychotic features (Schmahmann and Sherman, 1998). The observed reduction in functional integration between this cerebellar region and limbic regions such as the hippocampus, cingulate cortex and (anterior nuclei of) the thalamus, could perhaps be interpreted in this context. Notably, the present study found no evidence for impaired functional connectivity of the posterior cerebellar hemispheres, while these cerebellar regions have been preferentially linked to cognitive processing (Habas et al., 2009; Krienen and Buckner, 2009). Cerebellar involvement in schizophrenia may be either limited to the vermis and anterior lobe, or involvement of the posterior cerebellar hemispheres in (cognitive deficits in) schizophrenia may be more subtle, attenuating in our whole-brain approach with corresponding stringent correction for multiple comparisons. Alternatively, as a distinct topographic organization of the cerebellum has been proposed in which certain areas of the cerebellar cortex interact specifically with certain areas of the cerebral cortex (Stoodley and Schmahmann, 2010; Buckner et al., 2011), the relatively large posterior hemispheres (compared to the other cerebellar ROIs) may have such distributed functional connections, that "picking up" on dysconnectivity of any particular connection(s) was precluded by our definition of ROIs.

The neuronal basis for dysconnectivity remains to be established. It could result from either aberrant wiring of connections during development or from impaired synaptic plasticity (or both; Stephan et al., 2009a). As studies have suggested a link between functional and structural brain connectivity (Hagmann et al., 2008; Honey et al., 2009; Van den Heuvel et al., 2009), our findings may reflect impaired structural connections (i.e., white matter tracts) between affected brain regions. Indeed, reduced fractional anisotropy (FA), commonly interpreted as reduced integrity, of cerebellar white matter tracts has been shown in schizophrenia (Kanaan et al., 2009; Kyriakopoulos and Frangou, 2009). Accompanied by normal mean diffusivity, this FA reduction is most likely due to disordered microstructural architecture, rather than disordered myelination (Kanaan et al., 2009). Accordingly, one study using magnetic resonance spectroscopic imaging reported decreased levels of a putative neuronal/axonal marker in the anterior cerebellar vermis, suggesting dysfunction or loss of neurons in that region (Deicken et al., 2001). Cerebellar dysconnectivity may thus result from decreased neurons or disordered neuronal architecture in the cerebellum.

Some issues have to be taken into account when interpreting the results of our study. First, medicated patients were studied and antipsychotic mediation has been shown to affect cerebellar functional connectivity (Stephan et al., 2009b). However, the haloperidol equivalent dose of antipsychotic medication at the time of scanning was not associated with functional connectivity measures and the unmedicated siblings of schizophrenia patients showed similar abnormalities in cerebellar functional connectivity, suggesting that cerebellar dysconnectivity is unlikely to be due to antipsychotic medication alone. Second, there was a preponderance of men in the schizophrenia patients, which was not paralleled in the healthy control and sibling groups. Nonetheless, as we applied permutation testing, it is very unlikely that our findings were driven by any other factor than group membership (i.e., patient, sibling, or control), as group-differences determined by other factors – such as gender – would not have been among the most extreme findings after random permutation of group assignment and thus not be deemed significant. Furthermore, our subdivision of the cerebellum may not be the optimal division of the cerebellum in terms of its functional connections. As the connectional properties of the cerebellum (i.e., connected to the cerebral cortex only by ways of polysynaptic connections) are relatively unamenable to traditional anatomical methods, the connectional topography of the cerebellum remains largely unmapped (O'Reilly et al., 2010). Recent studies using transneuronal tracing techniques and functional neuroimaging have provided some insight into the functional organization of the cerebellar cortex, but both distinct and overlapping functional zones of the cerebellar cortex have been reported and findings diverge between studies (O'Reilly et al., 2010; Stoodley and Schmahmann, 2010; Buckner et al., 2011). It was therefore decided to adhere to a broad division of the cerebellum, based on gross anatomy. Moreover, although various preprocessing steps were used to deal with potential confounds associated with resting-state fMRI (e.g., cardiorespiratory oscillations, head movement, scanner noise), influences of these factors cannot be ruled out. There is also an inherent risk of potential bias associated with cortical parcellation methods such as the AAL template, as the spatial scale of nodal parcellation has been shown to influence brain network properties (Wang et al., 2009; Fornito et al., 2010). New approaches are being developed to perform whole-brain connectivity mapping using individual pairs of voxels, without the need of arbitrary parcellation of the cortex (Zalesky et al., 2010), but interpreting voxels as distinct information processing units has its own limitations and inevitably, investigations of *in vivo* whole-brain functional connectivity have a resolution limit (Wig et al., 2011). Finally, although we interpret our findings of cerebellar dysconnectivity in schizophrenia in terms of underlying neurobiology and psychopathology, it should be noted that cause and effect cannot be derived from our cross-sectional data.

In conclusion, our study indicates that the cerebellum, in particular the vermis and right anterior hemisphere, is functionally dysconnected in schizophrenia. Furthermore, the observed overlap in cerebellar dysconnectivity between schizophrenia patients and their healthy siblings suggest that cerebellar dysconnectivity is related, at least in part, to familial risk for psychosis. Whether, and if so to what extent, cerebellar dysconnectivity is mediated by genetic factors needs to be established in genetic studies.

REFERENCES

Alexander, M. P., Gillingham, S., Schweizer, T., and Stuss, D. T. (2011). Cognitive impairments due to focal cerebellar injuries in adults. *Cortex*. doi:10.1016/j.cortex.2011.03.012. [Epub ahead of print].

American Psychiatric Association. (1994). *Diagnostic and Statistical Manual of Mental Disorders*, 4th Edn. Washington: American Psychiatric Association.

Andreasen, N. C., Flaum, M., and Arndt, S. (1992). The comprehensive assessment of symptoms and history (CASH): an instrument for assessing diagnosis and psychopathology. *Arch. Gen. Psychiatry* 49, 615–623.

Andreasen, N. C., Paradiso, S., and O'Leary, D. S. (1998). "Cognitive dysmetria" as an integrative theory of schizophrenia: a dysfunction in cortical-subcortical-cerebellar circuitry? *Schizophr. Bull.* 24, 203–218.

Andreasen, N. C., and Pierson, R. (2008). The role of the cerebellum in schizophrenia. *Biol. Psychiatry* 64, 81–88.

Assaf, Y., and Pasternak, O. (2008). Diffusion tensor imaging (DTI)-based white matter mapping in brain research: a review. *J. Mol. Neurosci.* 34, 51–61.

Bassett, D. S., and Bullmore, E. T. (2009). Human brain networks in health and disease. *Curr. Opin. Neurol.* 22, 340–347.

Bassett, D. S., Bullmore, E. T., Verchinski, B. A., Mattay, V. S., Weinberger, D. R., and Meyer-Linderberg, A. (2008). Hierarchical organization of human cortical networks in health and schizophrenia. *J. Neurosci.* 28, 9239–9248.

Becerril, K. E., Repovs, G., and Barch, D. M. (2011). Error processing network dynamics in schizophrenia. *Neuroimage* 54, 1495–1505.

Benjami, Y., and Hochberg, Y. (1995). Controlling for the false discovery rate: a practical and powerful approach to multiple testing. *J. R. Stat. Soc. Series B Stat. Methodol.* 57, 289–300.

Biswal, B., Van Kylen, J., and Hyde, J. S. (1997). Simultaneous assessment of flow and BOLD signals in resting state functional connectivity maps. *NMR. Biomed.* 10, 165–170.

Biswal, B., Yetkin, F. Z., Haughton, V. M., and Hyde, J. S. (1995). Functional connectivity in the motor cortex of resting human brain using echo-planar MRI. *Magn. Reson. Med.* 34, 537–541.

Bleuler, E. (1911). *Dementia Praecox or the Group of Schizophrenias (In German)*. New York, NY: International Universities Press.

Buckner, R. L., Krienen, F. M., Castellanos, A., Diaz, J. C., and Yeo, B. T. (2011). The organization of the human cerebellum estimated by intrinsic functional connectivity. *J. Neurophysiol.* 106, 2322–2345.

Deicken, R. F., Feiwell, R., Schuff, N., and Soher, B. (2001). Evidence for altered cerebellar vermis neuronal integrity in schizophrenia. *Psychiatry Res.* 107, 125–134.

Fornito, A., Yoon, J., Zalesky, A., Bullmore, E. T., and Carter, C. S. (2011). General and specific functional connectivity disturbances in first-episode schizophrenia during cognitive control performance. *Biol. Psychiatry* 70, 64–72.

Fornito, A., Zalesky, A., and Bullmore, E. T. (2010). Network scaling effects in graph analytic studies of human resting-state FMRI data. *Front. Syst. Neurosci.* 4:22. doi:10.3389/fnsys.2010.00022

Friston, K. J. (1998). The disconnection hypothesis. *Schizophr. Res.* 30, 115–125.

Friston, K. J., Frith, C. D., Liddle, P. F., and Frackowiak, S. J. (1993). Functional connectivity: the principal-component analysis of large (PET) data sets. *J. Cereb. Blood Flow Metab.* 13, 5–14.

Habas, C., Kamdar, N., Nguyen, D., Prater, K., Beckmann, C. F., Menon, V., and Greicus, M. D. (2009). Distinct cerebellar contributions to intrinsic connectivity networks. *J. Neurosci.* 29, 8586–8594.

Hagmann, P., Cammoun, L., Gigandet, X., Meuli, R., Honey, C. J., Wedeen, V. J., and Sporns, O. (2008). Mapping the structural core of human cerebral cortex. *PLoS Biol.* 6, e159. doi:10.1371/journal.pbio.0060159

Heath, R. G., and Harper, J. W. (1974). Ascending projections of the cerebellar fastigial nucleus to the hippocampus, amygdala, and other temporal lobe sites: evoked potential and histological studies in monkeys and cats. *Exp. Neurol.* 45, 2682–2687.

Honey, C. J., Sporns, O., Cammoun, L., Gigandet, X., Thiran, J. P., Meuli, R., and Hagmann, P. (2009). Predicting human resting-state functional connectivity from structural connectivity. *Proc. Natl. Acad. Sci. U.S.A.* 106, 2035–2040.

Honey, G. D., Pomarol-Clotet, E., Corlett, P. R., Honey, R. A. E., McKenna, P. J., Bullmore, E. T., and Flechter, P. C. (2005). Functional dysconnectivity in schizophrenia associated with attentional modulation of motor function. *Brain* 128, 2597–2611.

Kanaan, R. A. A., Borgwardt, S., McGuire, P. K., Craig, M. C., Murphy, D. G. M., Picchioni, M., Shergill, S. S., Jones, D. K., and Catani, M. (2009). Microstructural organization of cerebellar tracts in schizophrenia. *Biol. Psychiatry* 66, 1067–1069.

Kandel, E. R., Schwartz, J. H., and Jessell, T. M. (2000). "The cerebellum," in *Principles of Neural Science*, 4th Edn, eds J. Butler, and H. Lebowitz (New York, NY: McGraw-Hill Companies), 833–835.

Kay, S. R., Fiszbein, A., and Opler, L. A. (1987). The positive and negative syndrome scale (PANSS) for schizophrenia. *Schizophr. Bull.* 13, 261–276.

Ke, M., Zou, R., Shen, H., Huang, X., Zhou, Z., Liu, Z., Xue, Z., and Hu, D. (2010). Bilateral functional asymmetry disparity in positive and negative schizophrenia revealed by resting-state fMRI. *Psychiatry Res.* 182, 30–39.

Kendler, K. S., Lieberman, J. A., and Walsh, D. (1989). The Structured Interview for Schizotypy (SIS): a preliminary report. *Schizophr. Bull.* 15, 559–571.

Kim, D., Burge, J., Lane, T., Pearlson, G. D., Kiehl, K. A., and Calhoun, V. D. (2008). Hybrid ICA-Bayesian network approach reveals distinct effective connectivity differences in schizophrenia. *Neuroimage* 42, 1560–1568.

Kraepelin, E. (1919). *Dementia Praecox and Paraphrenia*. Edinburgh: Livingstone.

Krienen, F. M., and Buckner, R. L. (2009). Segregated fronto-cerebellar circuits revealed by intrinsic functional connectivity. *Cereb. Cortex* 19, 2485–2497.

Kroken, R. A., Johnsen, E., Ruud, T., Wentzel-Larsen, T., and Jørgensen, H. A. (2009). Treatment of schizophrenia with antipsychotics in Norwegian emergency wards, a cross-sectional national study. *BMC Psychiatry* 9, 24. doi:10.1186/1471-244X-9-24

Kyriakopoulos, M., and Frangou, S. (2009). Recent diffusion tensor imaging findings in early stages of schizophrenia. *Curr. Opin. Psychiatry* 22, 168–176.

Lynall, M. E., Bassett, D. S., Kerwin, R., McKenna, P. J., Kitzbichler, M., Muller, U., and Bullmore, E. T. (2010). Functional connectivity and brain networks in schizophrenia. *J. Neurosci.* 30, 9477–9487.

O'Reilly, J. X., Beckmann, C. F., Tomassini, V., Ramnane, N., and Johansen-Berg, H. (2010). Distinct and overlapping functional zones in the cerebellum defined by resting-state functional connectivity. *Cereb. Cortex* 20, 953–965.

Petterson-Yeo, W., Allen, P., Benetti, S., McGuire, P., and Mechelli, A. (2011). Dysconnectivity in schizophrenia: where are we now? *Neurosci. Biobehav. Rev.* 35, 1110–1124.

Ramsey, N. F., Kirkby, B. S., Van Gelderen, P., Berman, K. F., Duyn, J. H., Frank, J. A., Mattay, V. S., Van Horn, J. D., Esposito, G., Moonen, C. T., and Weinberger, D. R. (1996). Functional mapping of human sensorimotor cortex with 3D BOLD fMRI correlates highly with H2(15)O PET rCBF. *J. Cereb. Blood Flow Metab.* 16, 755–764.

Ramsey, N. F., Van den Heuvel, M. P., Kho, K. H., and Leijten, F. S. (2006). Towards human BCI applications based on cognitive brain systems: an investigation of neural signals recorded from the dorsolateral prefrontal cortex. *IEEE Trans. Neural Syst. Rehabil. Eng.* 14, 214–217.

Repovs, G., Csernansky, J. G., and Barch, D. M. (2011). Brain network connectivity in individuals with schizophrenia and their siblings. *Biol. Psychiatry* 69, 967–973.

Rubinov, M., and Bassett, D. S. (2011). Emerging evidence of connectomic abnormalities in schizophrenia. *J. Neurosci.* 31, 6263–6265.

Schmahmann, J. D. (1998). Dysmetria of thought: clinical consequences of cerebellar dysfunction on cognition and affect. *Trends Cogn. Sci. (Regul. Ed.)* 2, 362–371.

Schmahmann, J. D. (2000). The role of the cerebellum in affect and psychosis. *J. Neurolinguistics* 13, 189–214.

Schmahmann, J. D., and Caplan, D. (2006). Cognition, emotion and the cerebellum. *Brain* 129, 290–292.

Schmahmann, J. D., and Sherman, J. C. (1998). The cerebellar cognitive affective syndrome. *Brain* 121, 561–579.

Stephan, K. E., Friston, K. J., and Frith, C. D. (2009a). Dysconnection in schizophrenia: from abnormal synaptic plasticity to failures of self-monitoring. *Schizophr. Bull.* 35, 509–527.

Stephan, K. E., Magnotta, V. A., White, T., Arndt, S., Flaum, M., O'Leary, D. S., and Andreasen, N. C. (2009b). Effects of olanzapine on cerebellar functional connectivity in schizophrenia measured by fMRI during a simple motor task. *Psychol. Med.* 31, 1065–1078.

Stinissen, J., Willems, P. J., Coetsier, P., and Hulsman, W. L. L. (1970). *Manual of the Dutch Translation of the Wechsler Adult Intelligence Scale*. Amsterdam: Swets.

Stoodley, C. S., and Schmahmann, J. D. (2010). Evidence for topographic organization in the cerebellum of motor control versus cognitive and affective processing. *Cortex* 46, 831–844.

Storey, J. D. (2002). A direct approach to false discovery rates. *J. R. Stat. Soc. Series B Stat. Methodol.* 64, 479–498.

Sullivan, P. F., Kendler, K. S., and Neale, M. C. (2003). Schizophrenia as a complex trait: evidence from a meta-analysis of twin studies. *Arch. Gen. Psychiatry* 60, 1187–1192.

Tzourio-Mazoyer, N., Landeau, B., Papathanassiou, D., Crivello, F., Etard, O., Delcroix, N., Mazoyer, B., and Joliot, M. (2002). Automated anatomical labeling of activations in SPM using macroscopic anatomical parcellation of the MN MRI single-subject brain. *Neuroimage* 15, 273–289.

Van den Heuvel, M. P., and Hulshoff Pol, H. E. (2010). Exploring the brain network: a review on resting state fMRI functional connectivity. *Eur. Neuropsychopharmacol.* 20, 519–534.

Van den Heuvel, M. P., Mandl, R. C., and Hulshoff Pol, H. E. (2008). Normalized group clustering of resting-state fMRI data. *PLoS ONE* 3, e2001. doi:10.1371/journal.pone.0002001

Van den Heuvel, M. P., Mandl, R. C., Kahn, R. S., and Hulshoff Pol, H. E. (2009). Functionally linked resting-state networks reflect the underlying structural connectivity architecture of the human brain. *Hum. Brain Mapp.* 30, 3127–3141.

Van den Heuvel, M. P., Mandl, R. C., Stam, C. J., Kahn, R. S., and Hulshoff Pol, H. E. (2010). Aberrant frontal and temporal complex network structure in schizophrenia: a graph theoretical analysis. *J. Neurosci.* 30, 15915–15926.

Van Gelderen, P., Ramsey, N. F., Liu, G., Duyn, J. H., Frank, J. A., Weinberger, D. R., and Moonen, C. T. W. (1995). Three dimensional functional MRI of human brain on a clinical 1.5 T scanner. *Proc. Natl. Acad. Sci. U.S.A.* 92, 6906–6910.

Vollema, M. G., and Ormel, J. (2000). The reliability of the structured interview for schizotypy-revised. *Schizophr. Bull.* 26, 619–629.

Wang, J., Wang, L., Zang, Y., Yang, H., Tang, H., Gong, Q., Chen, Z., Zhu, C., and He, Y. (2009). Parcellation-dependent small-world brain functional networks: a resting-state fMRI study. *Hum. Brain Mapp.* 30, 1511–1523.

Wernicke, C. (1906). *Grundrisse der Psychiatrie.* Leipzig: Thieme.

Wig, G. S., Schlaggar, B. L., and Petersen, S. E. (2011). Concepts and principles in the analysis of brain networks. *Ann. N. Y. Acad. Sci.* 1224, 126–146.

Zalesky, A., Fornito, A., and Bullmore, E. T. (2010). Network-based statistic: identifying differences in brain networks. *Neuroimage* 53, 1197–1207.

Zalesky, A., Fornito, A., Seal, M. L., Cocchi, L., Westin, C. L., Bullmore, E. T., Egan, G. F., and Pantelis, C. (2011). Disrupted axonal fiber connectivity in schizophrenia. *Biol. Psychiatry* 69, 80–89.

Conflict of Interest Statement: The authors declare that the research was conducted in the absence of any commercial or financial relationships that could be construed as a potential conflict of interest.

Received: 14 September 2011; accepted: 28 November 2011; published online: 16 December 2011.

Citation: Collin G, Hulshoff Pol HE, Haijma SV, Cahn W, Kahn RS and van den Heuvel MP (2011) Impaired cerebellar functional connectivity in schizophrenia patients and their healthy siblings. Front. Psychiatry ***2****:73. doi: 10.3389/fpsyt.2011.00073*

This article was submitted to Frontiers in Neuropsychiatric Imaging and Stimulation, a specialty of Frontiers in Psychiatry.

frontiers in
PSYCHIATRY

ORIGINAL RESEARCH ARTICLE
published: 03 February 2012
doi: 10.3389/fpsyt.2012.00001

Agenesis of corpus callosum and emotional information processing in schizophrenia

***Ovidiu Lungu*[1,2] *and Emmanuel Stip*[1,3] ***

[1] *Departement de Psychiatrie, Université de Montréal, Montréal, QC, Canada*
[2] *Centre de Recherche de l'Institut Universitaire de Gériatrie de Montréal, Montréal, QC, Canada*
[3] *Centre de Recherche Fernand Seguin, Affilié à l'Université de Montréal, Montréal, QC, Canada*

Edited by:
Alex Fornito, University of Melbourne, Australia

Reviewed by:
Aristotle Voineskos, Centre for Addiction and Mental Health, Canada
Tarek Rajji, Centre for Addiction and Mental Health, Canada
Mark Walterfang, Royal Melbourne Hospital, Australia

***Correspondence:**
Emmanuel Stip, Centre de Recherche Centre Hospitalier de l'Université de Montréal, 1560, Sherbrooke East, Montreal, QC, Canada H2L 4M1.
e-mail: emmanuel.stip@umontreal.ca

Corpus callosum (CC) is essential in providing the integration of information related to perception and action within a subcortico-cortical network, thus supporting the generation of a unified experience about and reaction to changes in the environment. Its role in schizophrenia is yet to be fully elucidated, but there is accumulating evidence that there could be differences between patients and healthy controls regarding the morphology and function of CC, especially when individuals face emotionally laden information. Here, we report a case study of a patient with partial agenesis of corpus callosum (agCC patient with agenesis of the anterior aspect, above the genu) and we provide a direct comparison with a group of patients with no apparent callosal damage (CC group) regarding the brain activity during the processing of emotionally laden information. We found that although the visual cortex activation in response to visual stimuli regardless of their emotional content was comparable in agCC patient and CC group both in terms of localization and intensity of activation, we observed a very large, non-specific and non-lateralized cerebral activation in the agCC patient, in contrast with the CC group, which showed a more lateralized and spatially localized activation, when the emotional content of the stimuli was considered. Further analysis of brain activity in the regions obtained in the CC group revealed that the agCC patient actually had an opposite activation pattern relative to most participants with no CC agenesis, indicating a dysfunctional response to these kind of stimuli, consistent with the clinical presentation of this particular patient. Our results seem to give support to the disconnection hypothesis which posits that the core symptoms of schizophrenia are related to aberrant connectivity between distinct brain areas, especially when faced with emotional stimuli, a fact consistent with the clinical tableau of this particular patient.

Keywords: schizophrenia, agenesis, corpus callosum, fMRI

INTRODUCTION

The corpus callosum (CC), with its central position in the cerebrum, has an essential role in relaying sensory, motor, and cognitive information from homologous brain regions across cerebral hemispheres (de Lacoste et al., 1985; Buklina, 2005). A review of studies on patients with varying degrees of callosal damage (from complete agenesis, partial atrophies to subtle degradations), with and without interhemispheric disconnection, revealed that callosal functions are distributed and dissociated along an antero-posterior direction, with anterior callosal regions involved in interhemispheric inhibition in cognitive and perceptual (visuospatial) tasks requiring the management of resource competition (e.g., Stroop, hierarchical letters), and with posterior callosal areas implicated in interhemispheric facilitation processes at visuomotor and cognitive levels (Schulte and Muller-Oehring, 2011). Taken together, these findings argue for an important role of CC in the integration of information related to perception and action within a subcortico-cortical network, most likely supporting the generation of a unified experience about and reaction to changes in the environment.

The agenesis of corpus callosum (agCC) is defined as the absence, at birth, of parts or of the entire structure (National Institute of Neurological Disorders and Stroke, NIH). Studies comparing healthy individuals with those presenting the agCC found that highly functioning agCC patients have trouble processing emotional information (e.g., interpreting correctly the arousal generated by emotional stimuli; Paul et al., 2006) or a marked deficit in processing social information (Brown and Paul, 2000; Symington et al., 2011). In addition, a review of studies with agCC and autism spectrum disorder (ASD) subjects suggests that the theory-of-mind and emotion-processing deficits in agCC are similar to those observed in ASD (Booth et al., 2011). These findings suggest that CC plays an important role in processing of emotional information, especially in the social contexts, where the fast recognition of emotions seems to require interhemispheric cooperation, rather than hemispheric lateralization (Tamietto et al., 2007). While it is true that at the moment there are few studies comparing agCC individuals with healthy individuals (probably due to the low prevalence of this condition in the general population), recent techniques such as diffusion tension imaging could

lead in the future to more studies with healthy individuals which would correlate social and emotional information processing with the structural integrity of this part of the brain.

Understanding the role of CC in schizophrenia has long been of interest since post-mortem anatomical morphology investigations suggested decreased thickness, cross-sectional area, and fiber density in these patients (Rosenthal and Bigelow, 1972; Bigelow et al., 1983; Highley et al., 1999). More recently, *in vivo* magnetic resonance imaging studies revealed that callosal area is reduced relative to healthy controls, more so in first-episode than in chronic patients (Arnone et al., 2008, for a review). However, despite these advances, the functional consequences stemming from these morphological differences in CC have not been systematically explored. Given the evidence that agCC was found to be associated with deficits in emotion recognition, labeling of emotional arousal, and decoding visual social cues even in highly functioning and otherwise healthy individuals (Paul et al., 2006; Symington et al., 2011), it is conceivable that callosal dysgenesis in schizophrenia may also be associated with dysfunction in the treatment of emotionally laden information. Two case studies of patients with schizophrenia and agCC provided such evidence (Hallak et al., 2007; Micoulaud-Franchi et al., 2011), but a direct comparison between these kind of individuals and schizophrenia patients with no evidence of callosal abnormality has not been attempted.

Here, we report a case study of a patient with partial agCC and we also provide a direct comparison with a group of patients with no evident callosal abnormality regarding the brain activity during processing of emotionally laden information.

MATERIALS AND METHODS

PARTICIPANTS AND CLINICAL ASSESSMENT

Schizophrenia patient with agenesis of corpus callosum patient

The patient of interest was a young female (23 years of age) diagnosed with schizophrenia 1 year before hospitalization (age 22) and discovered at the time as having agCC. Specifically, the dorsal CC aspect, above the genu, and surrounding the midline was dysgenic or atrophied, including the istmus and anterior half of the spelnium; the Probst bundles were also atrophied. The lateral ventricles were large, especially in the posterior side, extending into the occipital lobe (up to −82 mm posterior from the anterior commissure, in the Talairach space). For a comparison, we present in **Figure 1** this patients' anatomical image normalized to Talairach template (Talairach and Tournoux, 1988), in the three planes (transversal, coronal, sagittal) side-by-side with the averaged anatomical image of the 13 schizophrenic patients with no CC agenesis, also normalized to Talairach template.

Personal history. The 23-year-old agCC patient was a single woman living with her brother and father. Her parents were separated; she was unemployed, living on social support. She was brought to the emergency department because she had bitten her father; in fact, for weeks she could not bear to be approached, or allowed anyone to enter into her personal space. She avoided contact with people for several months after the biting incident.

Clinical tableau. The patient had rituals of washing often her hands and clothes because of a fear of germs. She also collected objects, in particular issues from the magazine "People," predominantly for the performances of the American singer Mariah Carey. In addition to this, her environment was completely disordered. In fact she manifested a megalomaniacal delusion in regards to Maria Carey, the American singer, with whom she believed she had a very privileged relationship – a mental puerilism. In the emergency phase, we observed that the patient was obsessed with several ritual events and feelings of persecution and that she was capable of extreme anger, lacked judgment about her condition and did not understand that she can get medical help. Patient's persecution belief revolved around the idea that every person around her was conspiring against her, wishing her ill. Her solution to this situation was to move out and leave the city, to flee her persecutors and,

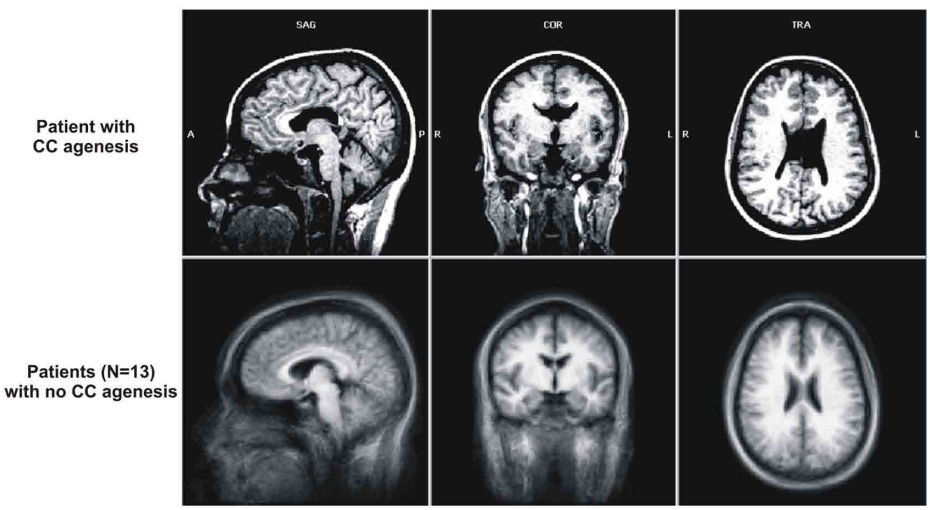

FIGURE 1 | The anatomical images for the schizophrenia patient with corpus callosum (CC) agenesis (top) and the average anatomical images for the 13 schizophrenia patients with no apparent CC agenesis. All images are normalized to Talairach space and the coordinates are Talairach coordinates.

at last, to end up with Maria Carey, who – she believed – was waiting for her. In her mind, Maria Carey represented a confidante, a friend. She also experienced irritability, and there were recurrent refusals to take her antipsychotics or anxiolytics. From time to time, her mood became labile and she believed that her father wanted to destroy or even rape her. She had social difficulties and strained relationship with both her parents and, at the age of 15, she thought that she was possessed by the devil. At times, she refused to wash her body, believing that this could endanger the life of the singer Maria Carey; in contrast she washed her hands obsessively. She manifested visual distortions as well as visual hallucinations.

Neuropsychological evaluation. The patient was right-handed, was able to write her name, and other phrases. Her drawings were accurate – a clock, a bicycle, a person. She was able to copy the position of her right arm or leg with the left, whilst her eyes were closed. She was able to draw a spiral with each hand separately and both together. Her head circumference was 56.7 cm (75th percentile). The patient presented no facial *dimorphisms* nor of the limbs, although the patient would not allow an inspection of her feet for reasons that she would not divulge. At the level of language, there was no dysphasia or lack of words. Overall intellectual performance was however at the lower end of average (IQ = 87). She completed the Wechsler Adult Intelligence Scale (Wechsler, 2008), the revised Wechsler test for memory and the Boston diagnostic aphasia examination. She performed the reading tests and tracking of letters and symbols, written numerical problems; drawings from Wechsler's memory scale, complex figures of Rey, logic of stories, California verbal learning test, left-right distinction, trail making A and B, generation of words and proverbs. She presented no visual-perceptive or visuo-constructive difficulties and she appeared to have adequate visual coding, with no memory difficulties. However, encoding a list of 16 words in 5 tried revealed difficulties. We noted perseverations and retrospective interference and a notable delayed recall. Encoding of short stories is deficient. There were no attentional disorders in either selective or sustained attention. At the level of frontal functions, we noted a form of apathy in the generation of words, and a tendency to give up. Abstract thought measured by the interpretation of proverbs was clearly defective; there were many errors when performing the Stroop test. Examination of left–right distinction revealed difficulties in designating the right and left sides of another person when standing opposite her and we observed that the patient had to turn to be on the same side as the other person to arrive at the correct answer. Then there were also difficulties in double instructions. Examination of praxis revealed that the execution of symbolic gestures was adequate but the imitation of simple gestures was difficult to evaluate. We observed a tendency to laugh a lot during the testing and we noted that the gestures were still rough and performed incorrectly, which seems to suggest an ideomotor dyspraxia. Many bilateral mistakes were made in the examination of graph esthesia, but the patient did not present adiadochokinesia.

Psychiatric evaluation. Based on DSM-IV, the patient was diagnosed with a schizophreniform syndrome, with impulsivity and difficulty in anticipating the consequences of her behavior and planning difficulty. The Calgary depressions scale did not show a score of depression and her Positive and Negative Syndrome Scale (PANSS; Kay et al., 1987) total score was 83 (positive scale score: 23; negative scale score: 18). She had an air of listlessness and cognitive rigidity, which distinguished the obsessional component of this patient's symptoms and classic OCD, namely the *egosyntonic* aspect of her rituals which borders on delusion. As well as these atypical obsessional manifestations the patient seemed to show a deficiency in theory-of-mind, notably the incapacity to interpret the intentions and actions of others face to face with her. The proposed pharmacological treatment was risperidone, 1 mg a day.

Schizophrenia patients with no agenesis of corpus callosum (CC group)

Thirteen young (mean age 24.84 ± 6.35 years) patients with schizophrenia (three females), fulfilling the DSM-IV criteria, and with no evident damage or agCC were recruited for this study. The patients were all under antipsychotic medication and were assessed using the PANSS (Kay et al., 1987). They were all treated by the same antipsychotic medication since 15 weeks, quetiapine (mean dosage: 425 mg/day). The mean PANSS total score of the CC group was 88.2 (SD = 19.97), with 21.11 (SD = 6.12), and 24.73 (SD = 9.45) on the Positive and Negative scales, respectively. All participants signed an informed detailed consent form approved by the ethics committee prior to participation in the study.

TASK DESCRIPTION AND EXPERIMENTAL DESIGN

All subjects participated in a passive viewing task during a functional magnetic resonance imaging (fMRI) session in two experimental conditions: *Negative* and *Neutral*. During the Negative condition, a series of 44 emotionally laden negative pictures (e.g., plane crash, snake, spider, shark, angry face, sad face, mutilation, accident, burn victim, dead body, etc.) were presented to the participants, whereas in the Neutral condition, they saw a series of 44 emotionally neutral pictures (e.g., tourist, rocks, boat, leaves, outlet, towel, spoon, mug, etc.). The two categories of pictures were selected from the international affective picture system (IAPS; Lang et al., 1988). They were matched as much as possible in terms of visual complexity. The mean valence was 2.66 ± 1.58 for the negative pictures and 5.74 ± 1.47 for the neutral pictures. The mean arousal level was 6.11 ± 2.14 for the negative pictures and 2.97 ± 2.08 for the neutral pictures. These mean valence and arousal scores are based on the valence and arousal ratings from Lang's normative groups.

During the functional scan, four blocks of negative and four blocks of neutral images were presented to the subjects in an alternating manner either starting with negative or neutral block, in a counterbalanced manner across subjects. Each image was presented for a period of 2.88 s and each block-which lasted 31 s (11 images per block). The blocks were separated by rest periods of 14.4 s, during which subjects viewed a cyan screen. Subjects were instructed to look carefully at each of the 88 pictures presented to them during the run.

IMAGING PARAMETERS

A 1.5-T whole Body MR System (Magnetom Vision, Siemens, Erlangen, Germany) used normally for clinical purposes at Centre Hospitalier de l'Université de Montréal (CHUM) was

employed for image acquisition. Prior to the functional run, 165 structural images were acquired in sagittal plane by using an MPRAGE imaging sequence (TR = 9.7 ms; TE = 4.0 ms; FA = 12°; FoV = 250 mm^2; matrix size = 256 × 256; slice thickness = 0.975 mm, voxel size = 0.975 mm^3; 164 slices). Then, whole brain fMRI was performed using an echo-planar imaging (EPI) sequence measuring blood oxygenation level dependent (BOLD) signal (TR = 3000 ms; TE = 44 ms; FA = 90°; FoV = 215 mm^2; matrix size = 64 × 64; slice thickness = 5.00 mm, voxel size = 3.36 mm × 3.36 mm × 5 mm; 28 slices). Functional slices covered the whole brain, were oriented in transverse plane and were angled to be parallel to the AC-PC line. A total of 132 functional volumes were recorded during the functional run.

DATA ANALYSIS

Brain Voyager QX (Brain Innovation B.V., Maastricht, the Netherlands) software was used for fMRI data preprocessing and analysis. The first two volumes of the functional run, we discarded from the analyses to allow for T1 equilibration effects. The remaining functional bi-dimensional images of every subject were preprocessed to correct for the difference in time slice acquisition (slice scan time correction). In addition to linear detrending, a high-pass filter of three cycles per time course (frequency domain) was applied to the corrected 2D slices. Then, the functional series was preprocessed to correct for possible motion artifacts in any plane of the tridimensional space and to ensure that the movements in any plane did not exceed 3 mm. These motion corrected functional images were subsequently used to reconstruct the 3D functional volume for every subject and every run. The 3D functional volume was aligned with the corresponding 3D anatomical volume, and both were normalized to standard Talairach space (Talairach and Tournoux, 1988). Spatial smoothing using a Gaussian kernel at 8 mm full width at half maximum (FWHM) was applied to the 3D functional data.

A blocked-design approach was employed for data analysis. Two predictors were defined for the functional run (Negative and Neutral), corresponding to the blocks of presentation of negative, and respective neutral items images. For the group analysis, these predictors were entered as fixed factors in single subject general linear model (GLM), then the parameters of this GLM model were subsequently entered into a second level of analysis corresponding to a random-effect GLM model that was used for group analysis (Penny and Holmes, 2003). The statistical parameters of this latter model were estimated voxelwise for the entire brain and activation maps were computed for the contrast between the two predictors. The criteria used to display the activation maps: a cluster size of 180 adjacent significant voxels (1 mm × 1 mm × 1 mm) and a statistical threshold for each voxel in the cluster $p < 0.005$ (uncorr.). For the analysis of functional data coming from the patient with agCC we performed only difference analysis, using a GLM model with two predictors (Negative and Neutral). To display the activation maps for this individual we use the following criteria: minimal t-value $t(127) = 4.02$; $p < 0.0001$; minimum cluster size 180 voxels.

In the subsequent stage of the analysis, the clusters obtained as a result of various contrasts at the group level were defined as regions of interest (ROIs) and further GLM analyses were performed separately for each of them in order to compare the percentage of signal change at the group level with that in the patient with agCC. These latter analyses were performed taking into account the time-course of the signal averaged over all voxels in each ROI. The data extracted from Brain Voyager were analyzed with SPSS software (SPSS Inc., Chicago, IL, USA).

RESULTS

PROCESSING VISUAL INFORMATION

Contrasting the brain activity during visual blocks of either type (sad or neutral images) with the activity during rest periods (just a fixation cross) revealed a strong activation in left and right occipital poles in both the agCC patient (**Figure 2**, upper row) as well as in the CC group (**Figure 2**, lower row). The detailed analysis of the activation clusters revealed that the average individual activation in the CC group was similar to the level of activation of agCC patient in both left [average $t(127) = 3.18$, $p < 0.002$, for CC group and $t(127) = 3.22$, $p < 0.002$ for agCC patient] and right occipital regions [$t(127) = 3.58$, $p < 0.001$, for CC group and $t(127) = 4.11$, $p < 0.001$ for agCC patient]. Furthermore, the analysis of cerebral activity locked to the onset of visual stimuli (**Figure 2**, graphs on the right) indicated that the changes in activation were similar in magnitude for both the agCC patient, as well as the for CC patients (about 1%, on average); however, the signal was more variable during the block duration (yellow rectangle) for agCC patient than for the CC group. Finally, the total volume of activation in the whole brain induced by the general processing of visual information was more than 20 times as large in CC group as compared to agCC patient (191.96 vs. 9.15 cm^3). In conclusion, visual cortex activation in response to visual stimuli regardless of their emotional content was comparable in agCC patient and CC group both in terms of localization and intensity of activation; the only difference was that in the CC group a larger area was recruited, which included, among others, subcortical and prefrontal regions.

PROCESSING EMOTIONAL INFORMATION

When comparing the emotional valence of the visual information (SAD > NEUTRAL) we observed significant activation in three prefrontal regions, one in temporal and two in cingulate cortex for the CC group (**Figure 3**, orange clusters) and in a much wider network including cortical and subcortical regions from almost all cerebral lobes for the agCC patient (**Figure 3**, blue clusters). The laterality index computed separately for each subject for the regions obtained from the same contrast (SAD > NEUTRAL) at the individual level revealed that in the CC group the average laterality was 0.4470 (SD = 0.34), corresponding to about 44.7% more voxels activated in one cerebral hemisphere than in the other. In contrast, for the agCC patient, the laterality index was 0.084, corresponding to only 8% of lateralization, a value which is more than 1 SD farther away from the CC group average. Regarding the volume of activation for the contrast (SAD > NEUTRAL) measured at the individual level, we obtained an average of 18.56 cm^3 (SD = 27.83 cm^3) for the CC group and a value 10 times as large for the agCC patient (189.54 cm^3).

In summary, when we assessed the emotional nature of visual information processing we observed a very large, non-specific and non-lateralized cerebral activation in the agCC patient, in contrast with the CC group, which showed a more lateralized and

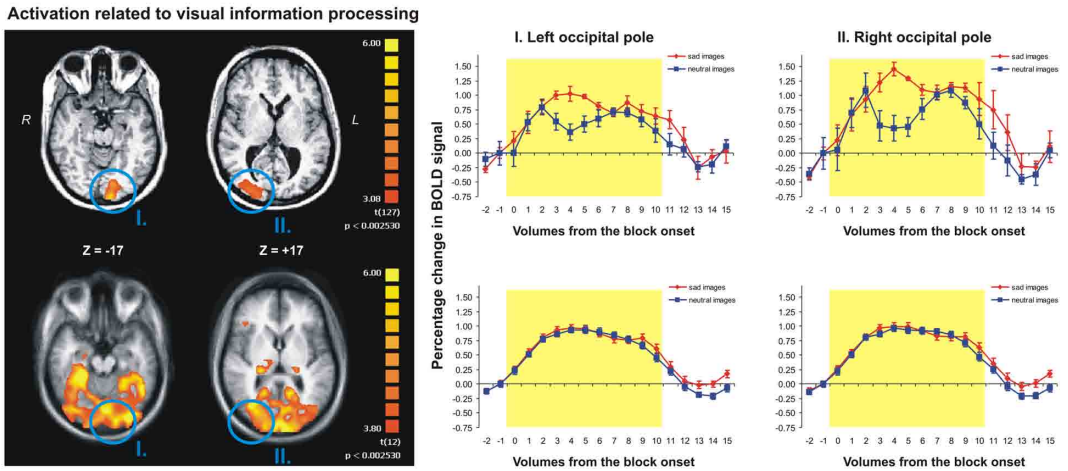

FIGURE 2 | The images to the left present the statistical maps reflecting the activation related to processing of visual information, regardless of the emotional content of the stimuli presented to the participants. The graphs on the left indicate the changes in BOLD signal (percentages) in the occipital poles relative to the onset of the visual stimulation for emotionally charged (red lines) and neutral (blue lines) stimuli. The upper images and the upper graphs pertain to the schizophrenia patient with CC agenesis, whereas the lower images and graphs reflect the group average (13 schizophrenia patients with no apparent CC agenesis).

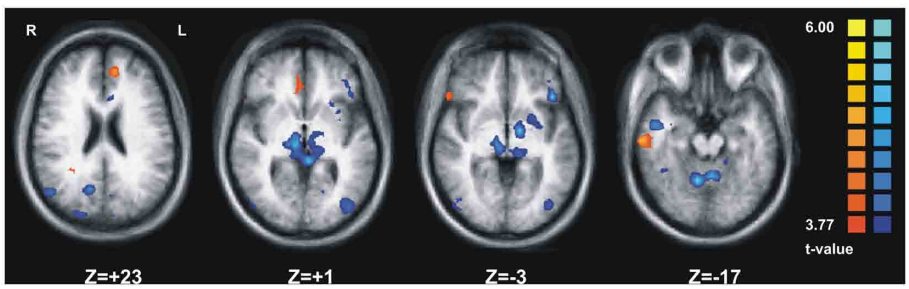

FIGURE 3 | The statistical maps reflecting the brain activation in response to emotional stimuli (contrast: SAD > NEUTRAL). The orange clusters indicate brain activations pertaining to the schizophrenia patient with CC agenesis, whereas the blue clusters correspond to the activation at the group level for the 13 schizophrenia patients with no apparent CC agenesis (CC group).

spatially localized activation. Furthermore, the detailed analysis of the BOLD signal change in each of the six clusters obtained in the CC group revealed that the agCC patient had an opposite activation pattern (**Figure 4**, red line) relative to most participants with no CC agenesis (**Figure 4**, green lines).

DISCUSSION

We assessed here the brain activity in response to emotionally laden visual stimuli in one schizophrenia patient with agCC and in a group of schizophrenia patients of similar age, but with no evident damage to the brain (CC group). The results showed that the visual cortex activation in response to visual stimuli, regardless of their emotional content, was comparable in agCC patient and CC group both in terms of localization and intensity of activation. The only difference in this respect was that in the CC group a larger area was recruited, which included, among others, subcortical and prefrontal regions. In contrast, when comparing the brain activation in response to the emotional charge of the visual stimulation we observed a very large, non-specific and non-lateralized cerebral activation in the agCC patient, in contrast with the CC group, which showed a more lateralized and spatially localized activation. The analysis of the BOLD signal change in each of the activated regions obtained in the CC group revealed that the agCC patient actually had an opposite activation pattern relative to most participants with no CC agenesis, indicating a dysfunctional response to these kind of stimuli, consistent with the clinical presentation of this particular patient.

The congenital absence of CC, agenesis, is the main "natural" pathology of this brain structure and it has recently been estimated to have a prevalence of 1:4000 (Paul et al., 2007). While its etiology is yet unclear, there are studies linking this condition to genetic and environmental factors occurring prenatally, typically between the 3rd and 12th week of pregnancy when this structure develops. For instance, both in animal models, as well as in humans, the pioneer axons from cingulate cortex are the first to cross the midline during embryonic development, providing guidance, and support for the

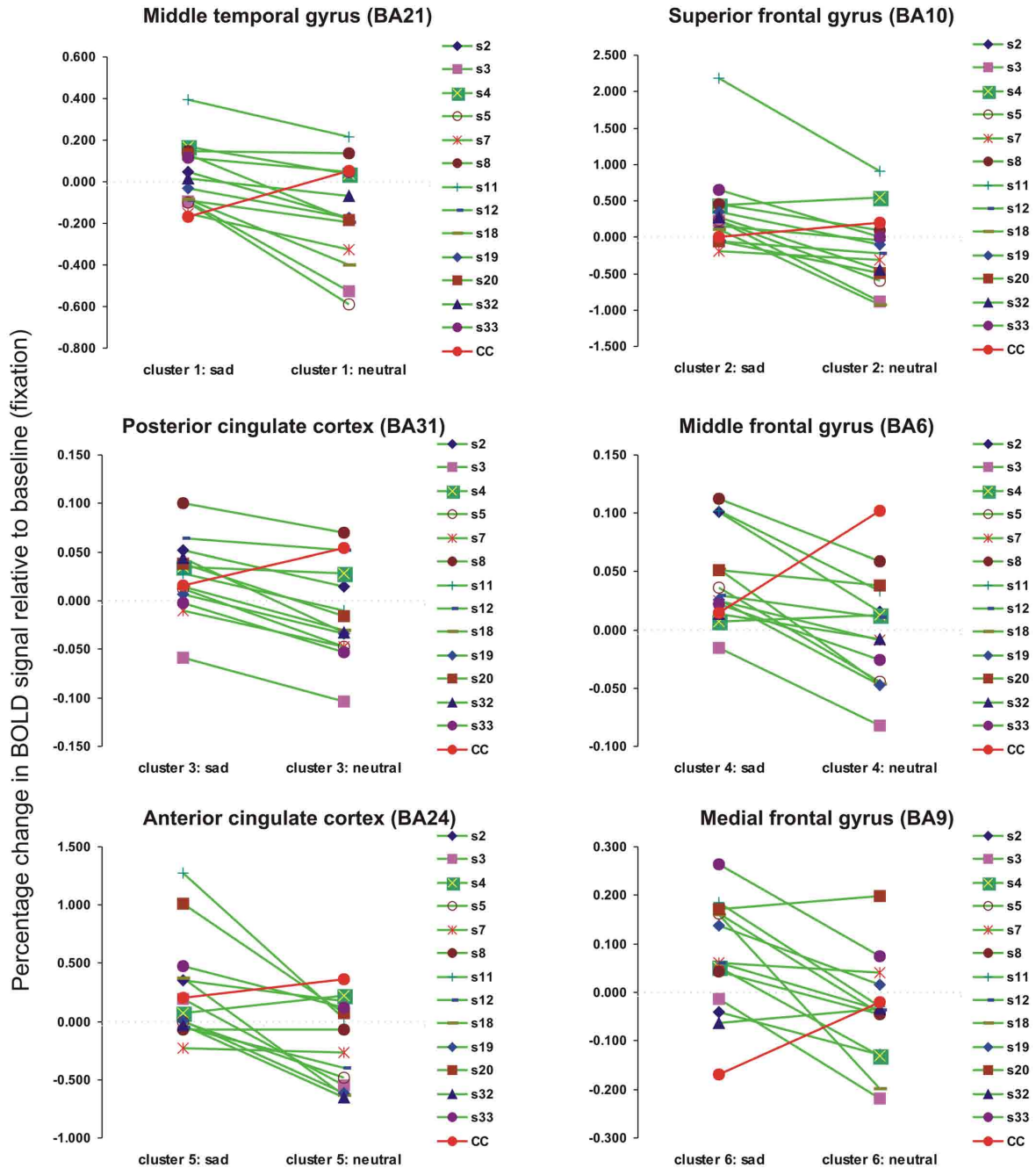

FIGURE 4 | The changes in BOLD signal (percentage) relative to the baseline for individual subjects and for each type of visual stimulus (sad or neutral) in six regions of interest obtained in the contrast SAD > NEUTRAL at the group level (CC group). The detailed analysis of the BOLD signal change in each of the six clusters obtained in the CC group (green lines) revealed that the agCC patient had an opposite activation pattern (the red line).

callosal axons which cross the midline later (Rash and Richards, 2001; Ren et al., 2006). It is interesting to note that the gene disrupted in schizophrenia 1 (DISC1) was found to be inactivated in all 129 strain mice (an animal model in which 70% present agCC) and was causally linked to the agCC (Clapcote and Roder, 2006). This finding not only shows that a genetic mutation may cause the agCC, but that there may be a *common* genetic mutation that is seen in both agCC and schizophrenia. In addition to the genetic

factors, infectious, vascular, and toxic causes of agCC were also identified (Paul et al., 2007).

Based on the topography of the agenesis in our case study, which encompassed the dorsal CC aspect, above the genu, and surrounding the midline, as well as the istmus and anterior half of the spelnium, there are a number of cortical areas that may be disconnected from their contralateral homotopic parts. Parts of dorsolateral prefrontal cortex (BA9/BA44/BA45), including Broca's area, as well as the superior temporal cortex, including Wernicke's area, are usually connected to parts of CC that are absent in our patient. Even though the patient did not show marked language problems, she had nevertheless difficulty in encoding and interpreting verbal material. Other cortical regions that could be disconnected in our clinical case are: anterior cingulate cortex (BA32), posterior parietal cortex (BA7), supplementary motor, and premotor areas (BA6). Taken together, these regions are part of mirror neuron system (Iacoboni and Mazziotta, 2007) and the clinical evidence that they could be affected by the agCC in our patient is given by her difficulty in imitating the other's gestures.

Our imaging results illustrate two main points. On the one hand, we showed that in both our agCC patient and in the group of patients with no apparent damage to the CC, there was similar brain activity during basic visual information processing. Corroborated with the neurological evaluation showing that the patient did not have difficulty integrating visual information from the two visual fields, this indicates that, contrary to cases of corpus callosotomy (Schulte and Muller-Oehring, 2011), the developmental dysgenesis of this structure does not affect the visual pathways and the integration of information from both visual fields. This may be due to the fact that the posterior part of the splenium, which connects the occipital and inferior temporal cortices, was intact in our agCC patient. On the other hand, the CC group and agCC patient showed different patterns of brain activity when the emotional nature of visual information was taken into account. Corroborated with the presence of visual distortions and hallucinations, as well as with the increased suspicion and persecution beliefs in agCC patient, our findings suggest that the CC agenesis may be a compounding factor in exacerbating some of the positive symptoms in schizophrenia. Of course, further research is necessary to actually link the severity of the positive symptoms to structural damage of the CC, but in the future it may be an important indicator for clinicians to suspect callosal damage when positive symptoms are very prominent in the early onset of the disease.

LIMITATIONS

There are two main limitations in our study. First, is that we have only one case with CC agenesis and schizophrenia; it would have been better to compare two groups instead of a case with a group. However, given the rarity of the agenesis (1:4000) in the general population, finding enough cases is very difficult. Another limitation in our study is the lack of a clinical case that presents CC agenesis, but does not have schizophrenia. Such a case would have been useful in illustrating the impact of the structural damage on the emotional information processing in the absence of schizophrenia. However, we believe that despite these limitation, our data can be useful in showing the compounding effect of a structural damage in schizophrenia on the brain functioning.

CONCLUSION

Our case study shows a patient who has a dual diagnosis: schizophrenia and corpus callosum agenesis. We know that the disconnection hypothesis suggests that the core symptoms of schizophrenia are related to aberrant connectivity between distinct brain areas. Both functional and structural neuroimaging studies have been conducted to investigate this hypothesis, across the full course of the disorder; from people at ultra-high-risk of developing psychosis to patients with established schizophrenia. Our case study is a first-episode psychosis leading to a schizophrenia and it was compared to a group a young schizophrenia patients. The role of the CC in the emotional information processing confirms the needed connectivity in the two hemispheres since the observation of a very large, non-specific and non-lateralized cerebral activation in the agCC patient, in contrast with the CC group, which showed a more lateralized and spatially localized activation.

ACKNOWLEDGMENTS

Dr. Emmanuel Stip is the Eli Lilly Canadian Chair in Schizophrenia. This study was conducted by Emmanuel Stip as a clinical scientist Junior2, funded by the FRSQ and as part of investigator initiated trials funded by Astra Zeneca Canada.

REFERENCES

Arnone, D., McIntosh, A. M., Tan, G. M., and Ebmeier, K. P. (2008). Meta-analysis of magnetic resonance imaging studies of the corpus callosum in schizophrenia. *Schizophr. Res.* 101, 124–132.

Bigelow, L. B., Nasrallah, H. A., and Rauscher, F. P. (1983). Corpus callosum thickness in chronic schizophrenia. *Br. J. Psychiatry* 142, 284–287.

Booth, R., Wallace, G. L., and Happe, F. (2011). Connectivity and the corpus callosum in autism spectrum conditions Insights from comparison of autism and callosal agenesis. *Prog. Brain Res.* 189, 303–317.

Brown, W. S., and Paul, L. K. (2000). Cognitive and psychosocial deficits in agenesis of the corpus callosum with normal intelligence. *Cogn. Neuropsychiatry* 5, 135–157.

Buklina, S. B. (2005). The corpus callosum, interhemisphere interactions, and the function of the right hemisphere of the brain. *Neurosci. Behav. Physiol.* 35, 473–480.

Clapcote, S. J., and Roder, J. C. (2006). Deletion polymorphism of Disc1 is common to all 129 mouse substrains: implications for gene-targeting studies of brain function. *Genetics* 173, 2407–2410.

de Lacoste, M. C., Kirkpatrick, J. B., and Ross, E. D. (1985). Topography of the human corpus callosum. *J. Neuropathol. Exp. Neurol.* 44, 578–591.

Hallak, J. E., Crippa, J. A., Pinto, J. P., Machado de Sousa, J. P., Trzesniak, C., Dursun, S. M., McGuire, P., Deakin, J. F., and Zuardi, A. W. (2007). Total agenesis of the corpus callosum in a patient with childhood-onset schizophrenia. *Arq. Neuropsiquiatr.* 65, 1216–1219.

Highley, J. R., Esiri, M. M., McDonald, B., Cortina-Borja, M., Herron, B. M., and Crow, T. J. (1999). The size and fibre composition of the corpus callosum with respect to gender and schizophrenia: a post-mortem study. *Brain* 122(Pt 1), 99–110.

Iacoboni, M., and Mazziotta, J. C. (2007). Mirror neuron system: basic findings and clinical applications. *Ann. Neurol.* 62, 213–218.

Kay, S. R., Fiszbein, A., and Opler, L. A. (1987). The positive and negative syndrome scale (PANSS) for schizophrenia. *Schizophr. Bull.* 13, 261–276.

Lang, P. J., Öhman, A., and Vaitl, D. (1988). *The International Affective Picture System (Photographic Slides).* Gainesville: Center for Research in Psychophysiology, University of Florida.

Micoulaud-Franchi, J. A., Bat-Pitault, F., Da Fonseca, D., and Rufo, M. (2011). Early onset schizophrenia and partial agenesis of corpus callosum. *Arch. Pediatr.* 18, 189–192.

Paul, L. K., Brown, W. S., Adolphs, R., Tyszka, J. M., Richards, L. J., Mukherjee, P., and Sherr, E. H. (2007). Agenesis of the corpus callosum: genetic, developmental and functional aspects of connectivity. *Nat. Rev. Neurosci.* 8, 287–299.

Paul, L. K., Lautzenhiser, A., Brown, W. S., Hart, A., Neumann, D., Spezio, M., and Adolphs, R. (2006). Emotional arousal in agenesis of the corpus callosum. *Int. J. Psychophysiol.* 61, 47–56.

Penny, W. D., and Holmes, A. J. (2003). "Random-effects analysis," in *Human Brain Function*, eds R. S. Frackowiak, K. J. Friston, C. Frith, R. Dolan, C. J. Price, S. Zeki, J. Ashburner, and W. D. Penny (London: Academic Press), 843–850.

Rash, B. G., and Richards, L. J. (2001). A role for cingulate pioneering axons in the development of the corpus callosum. *J. Comp. Neurol.* 434, 147–157.

Ren, T., Anderson, A., Shen, W. B., Huang, H., Plachez, C., Zhang, J., Mori, S., Kinsman, S. L., and Richards, L. J. (2006). Imaging, anatomical, and molecular analysis of callosal formation in the developing human fetal brain. *Anat. Rec. A Discov. Mol. Cell. Evol. Biol.* 288, 191–204.

Rosenthal, R., and Bigelow, L. B. (1972). Quantitative brain measurements in chronic schizophrenia. *Br. J. Psychiatry* 121, 259–264.

Schulte, T., and Muller-Oehring, E. M. (2011). Contribution of callosal connections to the interhemispheric integration of visuomotor and cognitive processes. *Neuropsychol. Rev.* 20, 174–190.

Symington, S. H., Paul, L. K., Symington, M. F., Ono, M., and Brown, W. S. (2011). Social cognition in individuals with agenesis of the corpus callosum. *Soc. Neurosci.* 5, 296–308.

Talairach, J., and Tournoux, P. (1988). *Co-planar Stereotaxic Atlas of the Human Brain.* New York: Thieme Medical Publishers.

Tamietto, M., Adenzato, M., Geminiani, G., and de Gelder, B. (2007). Fast recognition of social emotions takes the whole brain: interhemispheric cooperation in the absence of cerebral asymmetry. *Neuropsychologia* 45, 836–843.

Wechsler, D. (2008). *WAIS-IV Manual.* New York: NY: The Psychological Corporation.

Conflict of Interest Statement: The authors declare that the research was conducted in the absence of any commercial or financial relationships that could be construed as a potential conflict of interest.

Received: 31 August 2011; accepted: 04 January 2012; published online: 03 February 2012.

*Citation: Lungu O and Stip E (2012) Agenesis of corpus callosum and emotional information processing in schizophrenia. Front. Psychiatry **3**:1. doi: 10.3389/fpsyt.2012.00001*

This article was submitted to Frontiers in Neuropsychiatric Imaging and Stimulation, a specialty of Frontiers in Psychiatry.

frontiers in
PSYCHIATRY

ORIGINAL RESEARCH ARTICLE
published: 08 December 2011
doi: 10.3389/fpsyt.2011.00069

Abnormal left-sided orbitomedial prefrontal cortical–amygdala connectivity during happy and fear face processing: a potential neural mechanism of female MDD

Jorge Renner Cardoso de Almeida[1], Dina Michaela Kronhaus[2], Etienne L. Sibille[1], Scott A. Langenecker[3], Amelia Versace[1], Edmund James LaBarbara[1] and Mary Louise Phillips[1,4]*

[1] *Department of Psychiatry, University of Pittsburgh School of Medicine, Pittsburgh, PA, USA*
[2] *St. Catharine's College and Computer Laboratory, University of Cambridge, Cambridge, UK*
[3] *University of Michigan Medical Center, Ann Arbor, MI, USA*
[4] *Department of Psychological Medicine, Cardiff University, Cardiff, UK*

Edited by:
Alex Fornito, University of Melbourne, Australia

Reviewed by:
Christopher G. Davey, The University of Melbourne, Australia
Udo Dannlowski, University of Münster, Germany

****Correspondence:***
Mary Louise Phillips, Director of Functional Neuroimaging Program, Western Psychiatric Institute and Clinic, 3811 O'Hara Street, Pittsburgh, PA 15213-2593, USA.
e-mail: phillipsml@upmc.edu

Background: Pathophysiologic processes supporting abnormal emotion regulation in major depressive disorder (MDD) are poorly understood. We previously found abnormal inverse left-sided ventromedial prefrontal cortical–amygdala effective connectivity to happy faces in females with MDD. We aimed to replicate and expand this previous finding in an independent participant sample, using a more inclusive neural model, and a novel emotion processing paradigm. **Methods:** Nineteen individuals with MDD in depressed episode (12 females), and 19 healthy individuals, age, and gender matched, performed an implicit emotion processing and automatic attentional control paradigm to examine abnormalities in prefrontal cortical–amygdala neural circuitry during happy, angry, fearful, and sad face processing measured with functional magnetic resonance imaging in a 3-T scanner. Effective connectivity was estimated with dynamic causal modeling in a trinodal neural model including two anatomically defined prefrontal cortical regions, ventromedial prefrontal cortex, and subgenual cingulate cortex (sgACC), and the amygdala. **Results:** We replicated our previous finding of abnormal inverse left-sided top-down ventromedial prefrontal cortical–amygdala connectivity to happy faces in females with MDD ($p = 0.04$), and also showed a similar pattern of abnormal inverse left-sided sgACC–amygdala connectivity to these stimuli ($p = 0.03$). These findings were paralleled by abnormally reduced positive left-sided ventromedial prefrontal cortical–sgACC connectivity to happy faces in females with MDD ($p = 0.008$), and abnormally increased positive left-sided sgACC–amygdala connectivity to fearful faces in females, and all individuals, with MDD ($p = 0.008$; $p = 0.003$). **Conclusion:** Different patterns of abnormal prefrontal cortical–amygdala connectivity to happy and fearful stimuli might represent neural mechanisms for the excessive self-reproach and comorbid anxiety that characterize female MDD.

Keywords: major depressive disorder, effective connectivity, emotion regulation, dynamic causal modeling, amygdala, prefrontal cortex

INTRODUCTION

Major depressive disorder (MDD) is one of the most prevalent of all illnesses (Goodwin and Jamison, 2007). Elucidating neural system abnormalities reflecting pathophysiologic processes in MDD can help identify biological markers of the illness. The majority of neuroimaging studies in MDD focused on examination of activity within key neural regions supporting emotion processing and emotion regulation, including the amygdala and orbitomedial prefrontal cortex (OMPFC; Siegle et al., 2002, 2007; Anand et al., 2005; Dannlowski et al., 2007, 2009; Fales et al., 2008; Phillips et al., 2008a). Findings from these studies indicate abnormally increased amygdala activity to fear, happy, and neutral facial expressions (Sheline et al., 2001; Abler et al., 2007; Dannlowski et al., 2007; Fales et al., 2008), although others, no abnormalities in amygdala activity to emotional stimuli in individuals with MDD (Lawrence et al., 2004; Surguladze et al., 2005; Fu et al., 2007; Dannlowski et al., 2008; Almeida et al., 2010b). Recent studies point to a valence specificity of amygdala hyperresponsiveness in MDD: while depressed patients were found to show stronger responsiveness to negative stimuli, less amygdala responsiveness to positive stimuli has been described (Suslow et al., 2010; Victor et al., 2010). The subgenual anterior cingulate cortex (sgACC, Brodmann Area, BA25) is one region of the OMPFC implicated in mood regulation and processing of negative self-referential information (Ongur et al., 2003; Phillips et al., 2008a; Price and Drevets, 2010), that has been the focus of an increasing number of neuroimaging studies in MDD. In MDD, volume in this region is reduced (Drevets, 2001; Bremner et al., 2002; Wagner et al., 2008), and resting blood flow in this region is increased (Mayberg et al., 1999; Jaracz and Rybakowski, 2002; Kito et al., 2008; Brockmann

et al., 2009; Price and Drevets, 2010). Individuals with MDD who respond to antidepressant treatment have greater baseline activity and metabolism in sgACC (Saxena et al., 2003; Langenecker et al., 2007; Mulert et al., 2007; Korb et al., 2009; Keedwell et al., 2010), and the region has more recently been used as a biological target for deep brain stimulation for MDD (Gutman et al., 2009). Together, these studies highlight the roles of abnormal activity in amygdala and OMPFC in the pathophysiology of MDD.

Effective connectivity estimates are measures of the influence that different neural regions exert over others in a given neural system (Friston et al., 2003). These measures of function within a neural systems are potentially more consistent over time and sensitive than conventional neuroimaging measures of activity in different neural regions (Schuyler et al., 2010). Dynamic causal modeling (DCM) is an established method to estimate effective connectivity that has been validated with concomitant functional neuroimaging and electroencephalography (EEG), and intracerebral EEG in an animal model (David et al., 2008). The employment of effective connectivity in neuroimaging studies of psychiatric illness therefore has the potential to identify robust biological markers of MDD. Yet, few neuroimaging studies examined effective connectivity using DCM between neural regions of interest (ROI) in MDD (Schlösser et al., 2008; Almeida et al., 2009c). Some studies employed functional connectivity to examine correlation over time between regions in MDD. These studies reported decreased functional connectivity between subcortical regions (amygdala and ventral striatum) and prefrontal regions, including anterior cingulate gyrus (Anand et al., 2005; Chen et al., 2008; Matthews et al., 2008; Dannlowski et al., 2009; Heller et al., 2009; Frodl et al., 2010), consistent with the hypothesis of decreased prefrontal cortical regulation of subcortical limbic regions in MDD (Mayberg, 2003; Phillips et al., 2003; Anand et al., 2005; Price and Drevets, 2010). However, other studies showed increased connectivity within prefrontal areas (Hamilton et al., 2011), between prefrontal areas and thalamus (Greicius et al., 2007), and between prefrontal areas and affective, cognitive control and default mode networks in MDD (Sheline et al., 2010). Other studies showed normalization of abnormal anterior cingulate gyral–subcortical functional connectivity after pharmacological treatment in MDD (Anand et al., 2007; Chen et al., 2008). Replication of key neuroimaging findings is clearly essential to identify biological markers of MDD.

Using DCM, we recently demonstrated in individuals with MDD abnormal inverse left-sided effective connectivity to positive emotional stimuli (happy faces) between OMPFC and amygdala (Almeida et al., 2009c). Our finding was particularly evident in females with MDD (Cohen d' effect size of 0.97). There were two main limitations to this previous study, however. First, we did not directly compare females with males with MDD because the majority of our sample was female. The prevalence of MDD in females is almost double that in males (Goodwin and Jamison, 2007); yet, relationships between gender and neural system abnormalities in MDD remain poorly understood. Second, we included only one sub-region of the OMPFC, ventromedial prefrontal cortex (vmPFC, BA11).

In the present study, we therefore first aimed to examine the extent to which we could replicate our previous findings showing abnormal inverse left-sided vmPFC–amygdala connectivity to happy faces, especially in females with MDD. Secondly, we wished to extend our dynamic causal model to include sgACC as a third node to enhance our understanding of abnormal pathophysiologic mechanisms involved in MDD. We recruited a new group of male and female individuals with MDD, and employed a novel implicit emotion processing and automatic attention control of emotion paradigm. This paradigm allowed us to examine effective connectivity to positive and negative emotional faces (happy, anger, fear, and sad) in MDD and healthy individuals.

MATERIALS AND METHODS

PARTICIPANTS

Nineteen healthy individuals (12 females and 7 males) and 19 individuals (12 females and 7 males) with SCID-verified (First et al., 1995) current MDD in depressed episode (no current or past psychosis) were recruited (**Table 1** includes demographic and clinical data). These groups did not differ in age [$t(36) = 0.7$, $p = 0.5$], or estimated premorbid intellectual ability [NART (Grober and Sliwinski, 1991), $t(36) = 1.2$, $p = 0.2$]. The Hamilton Rating Scale for Depression (Hamilton, 1960) score in individuals with MDD (HDRS-25-item, mean = 28.1, SD = 6.3) was significantly greater than healthy individuals [mean = 1.4, SD = 2.2; $t(22.5) = 17.5$, $p = 0.0001$]. Most individuals with MDD were medicated (78.9%, see descriptive list in **Table A1** in Appendix), most had lifetime history of comorbid anxiety disorder (63.2%), while a proportion had lifetime history of comorbid substance disorder (26.3%).

Exclusion criteria included history of head injury (from medical records and participant report), systemic medical illness, cognitive impairment (score <24 in the Mini-Mental State Examination, premorbid IQ estimate <85 using the National Adult Reading Test), Axis-II borderline personality disorder, and general exclusion criteria for MRI (presence/questionable history of metallic objects in the body, positive pregnancy test/self-reporting of pregnancy, and proneness to panicking in enclosed spaces). For healthy individuals, current alcohol and illicit substance abuse (determined by SCID-I, saliva, and urine screen) were further exclusion criteria.

The University of Pittsburgh Institutional Review Board approved the study protocol. All participants were right-handed. All participants were aware of the purpose of the study and gave written informed consent after explanation of the purpose of the research before participation in the study.

The participant population reflected the demographics of Pittsburgh and the surrounding area and/or the patient population of the University of Pittsburgh Medical Center (UPMC). Depressed participants were recruited from outpatient populations of the University of Pittsburgh Medical Center (UPMC), and through local advertising.

MEDICATION LOAD

A problem for all neuroimaging studies of psychiatric disorders is the potential confounding effect of psychotropic medication. We wished to examine the potential impact of psychotropic medication upon effective connectivity in MDD patients using an index of "medication load." This index reflects the number and dose of different medications for each individual: the greater the number and dose of the medication, the greater the medication load. This strategy has been employed in our previous neuroimaging studies (Hassel et al., 2008; Versace et al., 2008; Almeida et al., 2009a,c).

Table 1 | Demographic, clinical variables, and behavior performance.

Group	MDD ($n = 19$)		HI ($n = 19$)		Stat.	p
Age at scan (mean/SD)	30.3	7	31.8	6.8	$t(36) = 0.67$	0.51
Gender (Number/Percent)						
Male	7	37	7	37%	$x^2(1) = 0$	>0.99
Female	12	63	12	63%		
Age of illness onset (mean/SD)	19.4	8.2	–		–	–
Illness duration (mean/SD)	11	6.1	–		–	–
Medication load (mean/SD)	2.6	2.2	–		–	–
HRSD-25 (mean/SD)	28.1	6.25	1.4	2.2	$U = 0$	<0.001
NART (mean/SD)	114.5	9	111.2	7.3	$t(36) = 1.2$	0.23
Level of education (mean/SD)	6.2	1.4	6.1	1.3	$U = 172.5$	0.81
Lifetime presence of anxiety disorders (yes/no–percent yes)	12/7	63%		–	–	
Lifetime presence of alcohol/drug abuse or dependence (yes/no–percent yes)	5/14	26%		–	–	–

Task performance					Whole group		Female		Male	
					Stat.	p	Stat.	p	Stat.	p
Color labeling accuracy for anger faces (mean/SD)	91%	9.8%	97%	3.3%	$U = 137$	0.2	$U = 47$	0.1	$U = 20$	0.5
Reaction time during color labeling for anger faces (ms–mean/SD)	951.4	146.9	935.9	108.7	$U = 172$	0.8	$U = 68$	0.8	$U = 18$	0.4
Color labeling accuracy for fear faces (mean/SD)	94%	9.0%	96%	4.0%	$U = 166$	0.6	$U = 60$	0.5	$U = 24$	0.9
Reaction time during color labeling for fear faces (ms–mean/SD)	985.3	169.1	935.2	104.3	$U = 156$	0.5	$U = 71$	1.0	$U = 15$	0.2
Color labeling accuracy for sad faces (mean/SD)	94%	7.5%	97%	3.8%	$U = 151$	0.4	$U = 47$	0.1	$U = 24$	0.9
Reaction time during color labeling for sad faces (ms–mean/SD)	956.5	168.6	950	118.5	$U = 174$	0.9	$U = 62$	0.6	$U = 22$	0.7
Color labeling accuracy for happy faces (mean/SD)	92%	7.6%	95%	4.4%	$U = 145$	0.3	$U = 57$	0.4	$U = 20$	0.5
Reaction time during color labeling for happy faces (ms–mean/SD)	964.5	146.9	952.5	131.4	$U = 161$	0.6	$U = 68$	0.8	$U = 17$	0.3

HI, healthy individuals; MDD, individuals with major depression disorder in depressed episode; SD, standard deviation; HRSD-25, 25-item Hamilton rating scale for depression; Stat.: statistical test value; p: p value; U = Mann–Whitney U non-parametric test; ms, milliseconds; NART, national adult reading test.

To compute an index of medication load for each MDD participant, we first coded the dose of each antidepressant, mood-stabilizer, antipsychotic, and anxiolytic medication as absent (0), low (1), or high (2). For antidepressants and mood-stabilizers, we converted each medication into low- or high-dose groupings using a previously employed approach (Sackeim, 2001). Individuals on levels 1 and 2 of these criteria were coded as low-dose, those with levels 3 and 4 as high-dose. We added a no-dose subtype for those not taking these medications. We converted antipsychotic doses into chlorpromazine dose equivalents, and coded as 0, 1, or 2, for no medication, chlorpromazine equivalents dose equal or below, or above, the mean effective daily dose (ED_{50}) of chlorpromazine as defined by Davis and Chen (2004). Lorazepam dose was similarly coded as, 0, 1, or 2, with reference to the midpoint of the Physician's Desk Reference-recommended daily dose range. We generated a composite measure of total medication load, reflecting dose, and variety of different medications taken, by summing all individual medication codes for each medication category for each individual MDD participant.

DYNAMIC FACES TASK

Participants completed a 12.5-min emotional dynamic face processing task during the neuroimaging procedure. Participants were asked to use one of three fingers to press a button indicating the color of a semi-transparent foreground color flash (orange, turquoise, or yellow) that appeared during the mid 200–650 ms of a 1-s presentation of a dynamically changing background face (neutral to emotional; **Figure 1**). These emotional faces were considered task-irrelevant, as accurate task performance required participants to direct attention away from these faces and toward the color flash. The task therefore essentially measures implicit emotion processing and automatic attentional control of emotion. Faces from the NimStim stimulus set (Tottenham et al., 2009) were morphed in 5% increments, from neutral (0% emotion) to 100% emotion for four emotions: happy, sad, angry, and fearful. Morphed faces were made into 1 s movies progressing from 0 to 100% emotion. In control trials, movies comprised a simple shape (dark oval) superimposed on a light-gray oval, with similar structural characteristics to each face stimulus, which was subsequently morphed into a larger shape, approximating the movement shown by the morphed faces. There were three blocks for each of the above four types of emotion trial, with 12 stimuli per block, and six control (shape) blocks, with six stimuli per block. Emotional and control blocks were presented in a pseudorandomized order so that no two blocks of any condition were presented sequentially. Therefore, 36 stimuli per condition were presented in the task.

fMRI DATA ANALYSES

Neuroimaging data were collected using a 3-T Siemens Trio MRI scanner at the Magnetic Resonance Research Center in the University of Pittsburgh Medical Center (MRRC). Structural 3D axial MPRAGE images were acquired in the same session (TE: 3.29 ms,

TR: 2200 ms, Flip angle 9°, FOV = 256 mm × 192 mm, Slice thickness: 1 mm, Matrix: 256 × 256, 192 continuous slices). Blood-oxygen-level dependent (BOLD) images were then acquired with a gradient echo EPI sequence during 13 min covering 39 axial slices (3.1 mm thick, TR/TE = 2000/28 ms, FOV = 205 cm × 205 cm, matrix = 64 × 64; Flip angle 90°).

Analyses were conducted in (SPM5; http://www.fil.ion.ucl.ac.uk/spm) with slice time correction, realignment, co-registration, normalized to MNI template, resampled to 2 mm × 2 mm × 2 mm voxels, and smoothed with a 8-mm FWHM Gaussian kernel.

FUNCTIONAL SPECIALIZATION

A first-level fixed-effect model was constructed with four emotions (anger, fear, sad, and happy) and the control condition entered as separate regressors in the design matrix, including movement parameters as nuisance variables and the canonical HRF model. The four emotion versus control contrasts were then entered into a second-level random-effects group analysis, that was conducted on the *t*-contrast images generated in the previous single-subject analyses in a two (group) by four (condition) repeated-measures analyses of variance (ANOVA). Bilateral ventromedial prefrontal cortex (BA11), bilateral subgenual anterior cingulate cortex (BA25), and bilateral amygdala ROIs included in our analyses were defined using the Wake Forest PickAtlas Talairach Daemon Brodmann Areas (Maldjian et al., 2003). To control for multiple statistical testing in the second-level random-effect analysis, we maintained a cluster-level false positive detection rate at $p < 0.05$ by using a voxel threshold of $p < 0.05$ with a cluster (k) extent empirically determined by Monte Carlo simulations implemented in AlphaSim, which accounted for spatial correlations between BOLD signal changes in neighboring voxels.

FUNCTIONAL INTEGRATION: DYNAMIC CAUSAL MODELING ANALYSES

Effective connectivity (termed "connectivity" from now on) was estimated using DCM (Friston et al., 2003; Mechelli et al., 2003) implemented in SPM8 software, as previously employed (Almeida et al., 2009b,c). The main goal was to replicate and extend our previous finding regarding abnormal inverse left-sided OMPFC (specifically the vmPFC and sgACC)–amygdala connectivity to happy faces. We therefore included these three anatomically defined regions in our dynamic causal model. DCM uses a neuronal model of distributed regional responses, and a validated biophysical model of hemodynamic signals, to model observed fMRI responses. The fitting or inversion of this model entails optimizing both the connection strength that couple different regions and the estimates of noise in each region. This optimization takes place in E and M-steps respectively. Here the parameters correspond to both the region-specific hemodynamic parameters generating observed BOLD responses and the connectivity or coupling strengths among regions (Friston et al., 2003). In this study, we were primarily interested in endogenous connectivity among amygdala, vmPFC, and sgACC to emotional stimuli, and between-group differences in these connectivity measures. We therefore focused on examination of between-group differences in connectivity among the three regions to the four different emotion conditions. We generated a separate dynamic causal model for each emotion condition (see below). This individualized strategy allowed us, in effect, to examine the modulatory effect of emotion upon all endogenous connections in the model. We did not therefore use bilinear or modulatory terms in our dynamic causal model (to model changes in connectivity associated with change in condition).

The dynamic causal model for each emotion condition comprised bilateral amygdala, sgACC (BA25), and vmPFC (BA11), with reciprocal forward and backward ipsilateral connections among these three regions (**Figure 2**). The structure of this model was informed by understanding of the anatomical connections between these three regions from the large animal literature (Ongur et al., 2003; for review: Price and Drevets, 2010), that indicates bidirectional amygdala–vmPFC, amygdala–sgACC, and vmPFC–sgACC connections, with each region receiving sensory input from primary sensory processing cortices (Ongur et al., 2003; for review: Price and Drevets, 2010). Each emotion condition (happy, sad, angry, and fearful faces) was a separate input to each node in the model. This model therefore included in total 48 connectivity estimates per participants (three pairs of bidirectional connections in each hemisphere for each condition).

To account for individual differences, we extracted principal eigenvariates to summarize regional responses in anatomical

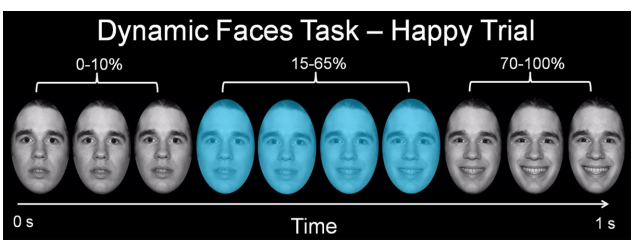

FIGURE 1 | Graphic representation of a single happy trial of our emotional dynamic faces task. Over a 1-s duration, the face changed from neutral (0% emotion) to a happy, sad, angry, or fearful face (100% emotion). Participants were asked to identify the color flash presented in mid dynamic change.

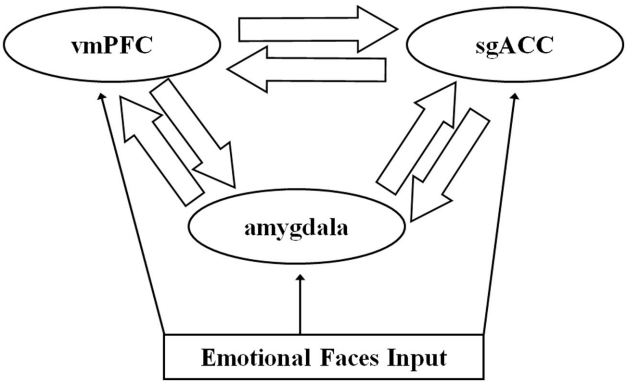

FIGURE 2 | The trinodal model including subgenual anterior cingulate cortex (sgACC), ventromedial prefrontal cortex (vmPFC), and amygdala and bidirectional connections among regions. Facial stimuli entered the model at each node.

templates centered on the three regions above created with the Wake Forest University Pick Atlas (Maldjian et al., 2003). In DCM, the units of connections are per unit time and therefore correspond to rates: a strong connection means an influence that is expressed quickly or with a large rate-constant. A positive connection indicates that "high" activity in the "source" region is associated with an increase in activity in the "target" region, while a negative, or inverse, connection indicates that "high" activity in the "source" region is associated with a decrease in activity in the "target" region. The underlying model links rates of change in the target to the level of activity in the source (Friston et al., 2003).

BETWEEN-GROUP DIFFERENCES IN CONNECTIVITY

To assess between-group differences in connectivity we used a conventional summary statistic approach, where the within-subject estimates of coupling were passed to a second (between-subject) level for classical inference. Individual-specific estimates of connectivity were first entered into Predictive Analytics SoftWare (PASW, SPSS Inc.). We then used Mann–Whitney *U*-tests to compare groups on connectivity measures because data were not normally distributed.

Our primary analyses focused on our *a priori* connectivity measures: left sgACC–amygdala, and left vmPFC–amygdala to happy faces (statistical threshold set at $p < 0.05$). We first compared all individuals with MDD versus healthy individuals, and then compared females with MDD versus healthy females, because we had specific *a priori* hypotheses about these connections in females with MDD based on our previous study (Almeida et al., 2009c). We also compared males with MDD relative to healthy males, although the smaller number of males made this comparison preliminary only.

In parallel analyses, we performed between-group comparisons on the remaining connectivity measures to all four emotion conditions (happy anger, fear, and sad). Here, we used the sequential goodness of fit (SGoF) metatest to correct for multiple test of between-group differences in the remaining 46 connectivity measures (6 pairs × 2 hemispheres × 4 emotional conditions, minus the above two *a priori* measures). The SGoF is an especially good method to correct for multiple tests in data sets where the sample size is not large, when the hypothesis to be tested may be weakly to moderately deviated from the null hypothesis, when there may be widespread effects through the family of tests, and when the number of tests is large (Carvajal-Rodriguez et al., 2009). The method is based on a comparison of the expected likely false positive error rate over all tests (computed from the per test significance level and the total number of tests performed), and the observed number of tests that meet the per test significance level. Contrary to other methods, the SGoF increases its statistical power with the number of tests, resolving in this way the trade-off between false positive finding (type I error) and statistical power (Carvajal-Rodriguez et al., 2009), and can show a statistical power up to two orders of magnitude higher than the Bonferroni method without increasing the false discovery rate (FDR). The SGoF is therefore an appropriate analytic strategy for multitest correction when working with high-dimensional biological data.

EXPLORATORY ANALYSES

In exploratory analyses, we compared healthy males with females, and males with females with MDD on connectivity measures that showed significant between-group differences. Connectivity measures showing significant abnormalities were also explored for possible relationships, using Spearman rank correlation tests and Mann–Whitney *U*-tests as appropriate, with: age, age of illness onset, illness duration, depression severity (measured using the HRSD-25), medication load (see Appendix), taking versus not taking individual psychotropic medication classes, and lifetime history of comorbid anxiety and/or substance disorder. Here, in individuals with MDD, we used a statistical threshold of $p = 0.05/10 = 0.005$, to control for the 10 separate tests for each connectivity measure. For healthy individuals, relationships between connectivity measures and age and subthreshold depression symptom severity using the HRSD-25 were examined using Spearman rank correlation tests and a statistical threshold of $p = 0.05/2 = 0.025$, to control for the two tests for each connectivity measure.

RESULTS

TASK PERFORMANCE

Task performance accuracy was high: 91% face color labeling accuracy for individuals with MDD, and 94% face color labeling accuracy for healthy individuals. There were no significant between-group differences in all individuals, females, or males in accuracy or reaction time, for any emotion condition (**Table 1**).

FUNCTIONAL SPECIALIZATION ON vmPFC, sgACC, AND AMYGDALA ROIs

We found no significant main effect of group or interaction; however, we found a significant positive effect of condition in all ROI bilaterally. Thus, revealing that the individuals recruited these regions to perform the task (**Table 2**).

DYNAMIC CAUSAL MODELING

Primary analyses: between-group differences in left vmPFC–amygdala and sgACC–amygdala connectivity to happy faces

Comparison of all individuals with MDD and healthy individuals did not reveal any significant differences in left vmPFC–amygdala or sgACC–amygdala connectivity to happy faces. Comparison of females with MDD relative to healthy females replicated our previous finding of significantly greater inverse left-sided vmPFC–amygdala connectivity to happy faces, and extended this to also show significantly greater inverse left-sided sgACC–amygdala connectivity in females with MDD relative to healthy females ($p = 0.04$ and $p = 0.02$, respectively). Males with MDD did not differ significantly from healthy males in either of these connectivity measures (**Table 3**; **Figure 3**).

Parallel analysis: remaining connectivity measures

For all individuals with MDD versus all healthy individuals, five pairwise between-group comparisons met the per test significance threshold of $p = 0.05$ (**Table 4**). One of these comparisons survived SGoF correction: all individuals with MDD relative to healthy individuals showed significantly greater positive left-sided sgACC–amygdala connectivity ($p = 0.003$) to fearful faces (**Table 3**; **Figure 4**).

Table 2 | Effective connectivity estimates in *a priori* and parallel analysis to happy, angry, sad, and fearful faces.

A priori analysis	MDD ($n = 19$)		HI ($n = 19$)		Whole group		Females only		Males only	
	Mean	SD	Mean	SD	MW	*p*	MW	*p*	MW	*p*
LEFT TOP-DOWN CONNECTIVITY TO HAPPY FACES										
vmPFC–Amy	−0.0004	0.003	0.0012	0.005	130	0.14	37	**0.04**$^{\#}$	22	0.75
sgACC–Amy	−0.0006	0.002	0.0008	0.003	118	0.07	32	**0.02**$^{\#}$	22	0.75
Parallel analysis										
HAPPY FACES										
vmPFC–sgACC left	0.0002	0.001	0.0008	0.003	139	0.23	26	**0.008****	14	0.18
vmPFC–sgACC right	−0.0003	0.002	−0.0001	0.004	135	0.18	38	0.05*	21	0.65
FEARFUL FACES										
sgACC–amygdala left	0.0024	0.003	−0.0002	0.002	77	**0.003****	26	**0.008****	15	0.22
vmPFC–sgACC right	0.0006	0.002	−0.0003	0.003	157	0.49	38	0.05*	10	0.06
vmPFC–sgACC left	0.0004	0.002	−0.0011	0.005	143	0.27	32	0.02*	14	0.18
vmPFC–amygdala left	0.0003	0.002	−0.0011	0.007	147	0.33	34	0.03*	13	0.14
ANGRY FACES										
Amygdala–vmPFC left	0.0003	0.003	−0.0018	0.004	108	0.03*	42	0.08	15	0.22
SAD FACES										
Amygdala–sgACC right	−0.0003	0.002	0.0016	0.003	106	0.03*	45	0.12	12	0.11
sgACC–amygdala right	−0.0007	0.003	0.0008	0.002	122	0.09	69	0.86	8	0.04*
vmPFC–sgACC right	−0.0007	0.002	0.0013	0.005	114	0.05*	60	0.49	4	0.009*
sgACC–vmPFC right	−0.0008	0.003	0.0020	0.004	103	0.02*	42	0.08	12	0.11
sgACC–vmPFC left	0.0003	0.002	0.0025	0.003	122	0.09	64	0.64	8	0.04*

HI, healthy individuals; MDD, individuals with major depression disorder in depressed episode; vmPFC, ventromedial prefrontal cortex; sgACC, subgenual prefrontal cortex; *p value survives alpha < 0.05 but does not survive SGoF correction for multiple tests; **p value survives SGoF correction for multiple tests; $^{\#}$p value survive a priori alpha threshold of p < 0.05; SD, standard deviation; MW, Mann–Whitney U non-parametric test; SGoF, sequential goodness of fit.

Table 3 | Amygdala, vmPFC, and sgACC activity during the dynamic faces task.

Region	Side	Mini coordinators			*K*	*T*	*Z*	*P*
		X	*Y*	*Z*				
POSITIVE EFFECT OF CONDITION								
vmPFC (BA11)	R	4	52	−14	28	2.61	2.57	0.05**
	L	−4	54	−12	11	2.23	2.21	0.013*
sgACC (BA25)	R	2	8	−14	7	2.18	2.14	0.016*
	L	−2	6	−12	4	1.74	1.73	0.041*
Amygdala	R	20	−4	−16	114	3.72	3.63	0.024**
	L	−20	−6	−16	113	2.89	2.84	0.049**

vmPFC, ventromedial prefrontal cortex; sgACC, subgenual anterior cingulate cortex; R, right; L, left; BA, Brodmann area; coordinates correspond to the stereotaxic array of Montreal Neurologic Institute; k: cluster size; *alphasim correction; **false discovery rate correction.

For females with MDD versus healthy females, six pairwise between-group comparisons met the per test significance threshold of $p = 0.05$ (**Table 4**). Two of these comparisons survived SGoF correction. 1. to happy faces: significantly reduced positive left-sided vmPFC–sgACC connectivity ($p = 0.008$) in females with MDD relative to healthy females. 2. to fearful faces: significantly greater positive left-sided sgACC–amygdala connectivity ($p = 0.008$), where females with MDD showed a positive connectivity, healthy females showed an inverse connectivity (**Table 3**; **Figure 4**).

For males with MDD relative to healthy males, three pairwise between-group comparisons met the threshold of $p = 0.05$, but none survived SGoF correction (**Tables 3** and **4**).

Within-group gender comparison

In healthy individuals, the left-sided vmPFC–sgACC connectivity to happy faces that survived the SGoF correction for between-group differences in connectivity in female participants showed a significant effect of gender. Here, healthy females had positive, and healthy males, inverse connectivity between these regions

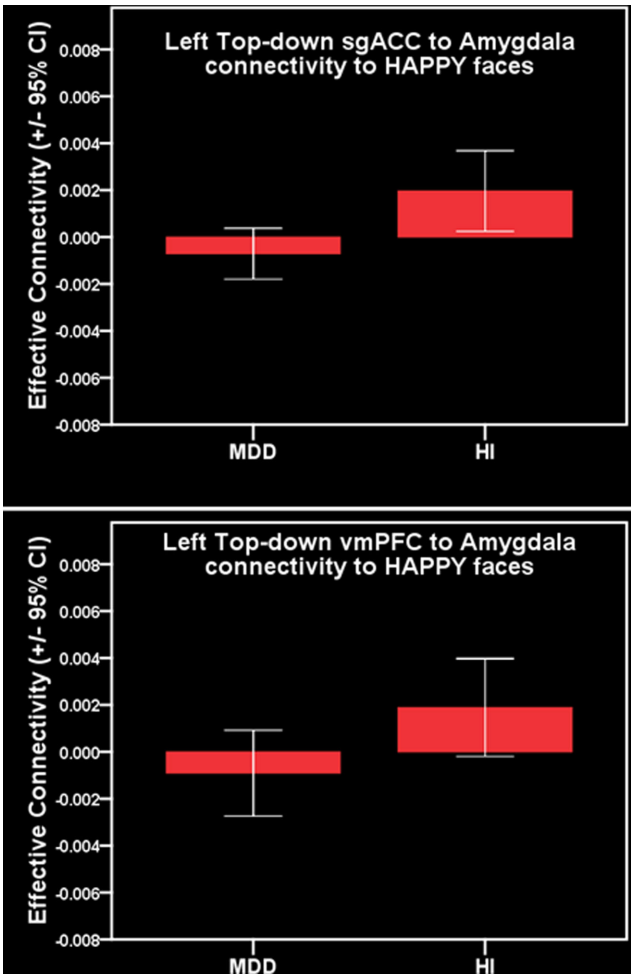

FIGURE 3 | Primary *a priori* analysis. Top: inverse left-sided vmPFC–amygdala connectivity to happy faces in females with MDD. Bottom: inverse left-sided sgACC–amygdala connectivity to happy faces in females with MDD.

($p = 0.022$). In individuals with MDD, there were no significant effects of gender on any of the connectivity measures that survived the SGoF correction for examination of between-group differences in connectivity.

Exploratory relationships between abnormal connectivity and age, task performance, and illness history

In individuals with MDD, there were no significant relationships between any clinical, demographic, or task performance measure and connectivity measures showing between-group differences in connectivity using the Bonferroni-corrected threshold of $p \leq 0.005$ (**Table 5**). In healthy individuals, however, there was a significant negative correlation between sub-syndromal depressive symptoms, and left sgACC–amygdala connectivity to happy faces ($p = 0.01$). Here, greater sub-syndromal depressive symptom severity was associated with reduced left-sided sgACC–amygdala connectivity to happy faces (**Table 6**).

DISCUSSION

The goal of the present study was to identify neuroimaging measures of recurrent MDD in females by examining the extent to which we could replicate in an independent sample, of females with MDD, and extend to a trinodal model, our previous finding of abnormal inverse left-sided OMPFC–amygdala connectivity to positive emotional stimuli (happy faces). In *a priori* hypothesis testing, we replicated our previous finding of abnormal inverse left-sided vmPFC–amygdala connectivity, and also showed abnormal inverse left-sided sgACC–amygdala connectivity, to happy faces in females (but not males) with MDD. Parallel analyses across all other remaining connectivity measures in our trinodal dynamic causal model revealed abnormally reduced positive left-sided vmPFC–sgACC connectivity, to happy faces, and abnormal *positive* left-sided sgACC–amygdala connectivity to fearful faces in females with MDD. Our present and previous findings highlight the fact that gender is an important factor to be considered in neuroimaging studies of MDD, and that abnormal left-sided OMPFC–amygdala connectivity during processing of both happy and fearful stimuli may be specific to female MDD.

Females experience depression at a rate twice that of males (Kendler et al., 2002; McGrath et al., 2009). Females are also more likely than males to have atypical depression, characterized by transient mood reactivity to actual or potential positive events, increase in appetite, hypersomnia, interpersonal rejection sensitivity and/or comorbid anxiety (APA, 2000), and are more likely to describe interpersonal stress and excessive self-reproach (Hammen, 2003; Smith et al., 2008). Interpretation of the abnormal patterns of connectivity between vmPFC, sgACC, and amygdala to happy and fearful faces in females with MDD in the context of these clinical features of female MDD can be guided by previous studies that elucidated the roles of the vmPFC and sgACC in emotion regulation. Both vmPFC and sgACC are part of the medial network within OMPFC implicated in emotion and visceromotor regulation (Ongur et al., 2003; Price and Drevets, 2010) and have strong reciprocal connections with the amygdala (Ongur et al., 2003; Price and Drevets, 2010). Human neuroimaging studies implicate both bilateral sgACC (Williams et al., 2006) and vmPFC (Van Veen and Carter, 2002; Luks et al., 2007) in fear extinction, an example of automatic behavioral control of emotion (Phillips et al., 2008b). The left vmPFC is also implicated in aversive conditioning (Gottfried and Dolan, 2004), while left/bilateral sgACC are implicated in the generation of sad mood (Mayberg, 1999), depression (Mayberg, 2005), and elevated monitoring of internal states in individuals with attachment avoidant personality styles (Gillath et al., 2005). The pattern of abnormal inverse or reduced positive connectivity between sgACC, vmPFC, and amygdala to happy faces may therefore reflect abnormal inhibition, or reduced functional integration, in this circuitry during positive emotion processing, that may lead to abnormally increased regulation of emotional response to, and reduced representation of the positive emotional value of, positive emotional stimuli in female MDD. This in turn may be associated with only transient positive mood reactivity to positive events and excessive self-reproach observed in female MDD. By contrast, the abnormally elevated left-sided positive sgACC–amygdala connectivity to fearful faces in females

Table 4 | Effective connectivity estimates to happy, fearful, sad, and angry faces.

	MDD ($n = 19$)		HI ($n = 19$)		Whole group		Females only		males only	
	Mean	SD	Mean	SD	MW	*p*	MW	*p*	MW	*p*
HAPPY FACES										
Amygdala–sgACC left	0.0010	0.002	0.0000	0.003	153	0.42	66	0.73	19	0.48
Amygdala–sgACC right	0.0013	0.003	−0.0002	0.003	141	0.25	58	0.42	19	0.48
Amygdala–vmPFC left	0.0021	0.006	−0.0003	0.003	148	0.34	51	0.23	22	0.75
Amygdala–vmPFC right	0.0015	0.005	0.0001	0.003	163	0.61	55	0.33	21	0.65
sgACC–Amy left	−0.0006	0.002	0.0008	0.003	118	0.07	32	**0.02***	22	0.75
sgACC–amygdala right	0.0003	0.002	−0.0004	0.003	172	0.80	60	0.49	23	0.85
sgACC–vmPFC left	0.0001	0.002	0.0020	0.005	147	0.33	51	0.23	22	0.75
sgACC–vmPFC right	0.0000	0.002	0.0010	0.003	144	0.29	50	0.20	24	0.95
vmPFC–Amy left	−0.0004	0.003	0.0012	0.005	130	0.14	37	**0.04**$^{\#}$	22	0.75
vmPFC–amygdala right	−0.0005	0.003	−0.0004	0.005	158	0.51	66	0.73	19	0.48
vmPFC–sgACC left	0.0002	0.001	0.0008	0.003	139	0.23	26	**0.008****	14	0.18
vmPFC–sgACC right	−0.0003	0.002	−0.0001	0.004	135	0.18	38	0.05*	21	0.65
ANGRY FACES										
Amygdala–sgACC left	0.0003	0.002	−0.0005	0.003	120	0.08	46	0.13	23	0.85
Amygdala–sgACC right	−0.0002	0.003	0.0000	0.004	148	0.34	39	0.06	14	0.18
Amygdala–vmPFC left	0.0003	0.003	−0.0018	0.004	108	0.03*	42	0.08	15	0.22
Amygdala–vmPFC right	−0.0001	0.002	−0.0002	0.004	140	0.24	65	0.69	12	0.11
sgACC–amygdala left	−0.0003	0.003	0.0012	0.005	158	0.51	51	0.23	22	0.75
sgACC–amygdala right	−0.0011	0.006	−0.0001	0.004	167	0.69	65	0.69	16	0.28
sgACC–vmPFC left	−0.0006	0.003	−0.0013	0.007	175	0.87	71	0.95	24	0.95
sgACC–vmPFC right	−0.0003	0.002	−0.0010	0.006	158	0.51	48	0.17	18	0.41
vmPFC–amygdala left	−0.0005	0.002	0.0009	0.005	162	0.59	71	0.95	17	0.34
vmPFC–amygdala right	−0.0015	0.004	−0.0001	0.005	180	0.99	55	0.33	15	0.22
vmPFC–sgACC left	0.0011	0.003	0.0011	0.005	167	0.69	67	0.77	18	0.41
vmPFC–sgACC right	0.0008	0.003	0.0001	0.004	158	0.51	55	0.33	23	0.85
FEARFUL FACES										
Amygdala–sgACC left	0.0002	0.004	0.0007	0.004	167	0.69	69	0.86	18	0.41
Amygdala–sgACC right	−0.0001	0.003	−0.0003	0.004	171	0.78	71	0.95	19	0.48
Amygdala–vmPFC left	0.0002	0.003	0.0007	0.006	159	0.53	62	0.56	21	0.65
Amygdala–vmPFC right	−0.0003	0.004	−0.0003	0.006	180	0.99	64	0.64	18	0.41
sgACC–amygdala left	0.0024	0.003	−0.0002	0.002	77	**0.003****	26	**0.008****	15	0.22
sgACC–amygdala right	0.0004	0.003	−0.0003	0.003	152	0.41	44	0.11	20	0.57
sgACC–vmPFC left	0.0002	0.005	−0.0011	0.004	140	0.24	56	0.36	19	0.48
sgACC–vmPFC right	0.0004	0.005	−0.0007	0.004	158	0.51	63	0.60	22	0.75
vmPFC–amygdala left	0.0003	0.002	−0.0011	0.007	147	0.33	34	0.03*	13	0.14
vmPFC–amygdala right	0.0003	0.002	−0.0012	0.005	134	0.17	40	0.06	21	0.65
vmPFC–sgACC left	0.0004	0.002	−0.0011	0.005	143	0.27	32	0.02*	14	0.18
vmPFC–sgACC right	0.0006	0.002	−0.0003	0.003	157	0.49	38	0.05*	10	0.06
SAD FACES										
Amygdala–sgACC left	−0.0008	0.004	0.0012	0.004	158	0.51	66	0.73	12	0.11
Amygdala–sgACC right	−0.0003	0.002	0.0016	0.003	106	0.03*	45	0.12	12	0.11
Amygdala–vmPFC left	0.0006	0.003	0.0018	0.004	179	0.97	66	0.73	22	0.75
Amygdala–vmPFC right	0.0006	0.003	0.0013	0.003	167	0.69	66	0.73	21	0.65
sgACC–amygdala left	−0.0008	0.002	0.0013	0.003	129	0.13	57	0.39	13	0.14
sgACC–amygdala right	−0.0007	0.003	0.0008	0.002	122	0.09	69	0.86	8	0.04*
sgACC–vmPFC left	0.0003	0.002	0.0025	0.003	122	0.09	64	0.64	8	0.04*
sgACC–vmPFC right	−0.0008	0.003	0.0020	0.004	103	0.02*	42	0.08	12	0.11
vmPFC–amygdala left	−0.0002	0.004	0.0010	0.004	139	0.23	58	0.42	16	0.28
vmPFC–amygdala right	−0.0005	0.003	0.0013	0.005	144	0.29	60	0.49	17	0.34

(Continued)

Table 4 | Continued

	MDD ($n = 19$)		HI ($n = 19$)		Whole group		Females only		males only	
	Mean	SD	Mean	SD	MW	*p*	MW	*p*	MW	*p*
vmPFC–sgACC left	−0.0007	0.002	0.0012	0.006	129	0.13	62	0.56	13	0.14
vmPFC–sgACC right	−0.0007	0.002	0.0013	0.005	114	0.05*	60	0.49	4	0.009*

*HI, healthy individuals; MDD, individuals with major depression disorder in depressed episode; vmPFC, ventromedial prefrontal cortex; sgACC, subgenual prefrontal cortex; *p value survives alpha < 0.05 but does not survive SGoF correction for multiple tests; **p value survives SGoF correction for multiple tests; #p value survive a priori alpha threshold of p < 0.05; SD, standard deviation; MW, Mann–Whitney U non-parametric test; SGoF, sequential goodness of fit.*

with MDD may represent a neural mechanism for the abnormally increased representation of threat depicted by fearful faces, which in turn may be related to the comorbid anxiety and interpersonal stress associated with female MDD.

Interpretation of the abnormal patterns of sgACC–amygdala connectivity to happy and fearful faces in females with MDD can also be guided by previous neuroimaging studies that focused on the sgACC in MDD. Previous studies provide increasing evidence that differential patterns of sgACC activity to negative versus positive emotional stimuli may moderate and mediate response to different antidepressant treatments in MDD. Previous findings indicate, for example, that greater levels of activity in individuals with MDD in the sgACC to negative emotional stimuli may predict subsequent successful response to antidepressant treatment (Saxena et al., 2003; Langenecker et al., 2007; Mulert et al., 2007; Korb et al., 2009; Keedwell et al., 2010). Other findings show that successful response to antidepressant treatments is paralleled by decreased activity in sgACC to negative emotional stimuli (Anand et al., 2007; Fu et al., 2007; Chen et al., 2008; Keedwell et al., 2010), but by greater activity in this region to positive emotional stimuli (Fu et al., 2007; Keedwell et al., 2010). These findings therefore suggest that differential patterns of sgACC activity to negative versus positive emotional stimuli may reflect pathophysiologic processes of MDD. Little is yet known, however, regarding the extent to which differential patterns of abnormal *connectivity* between the sgACC and amygdala to positive versus negative emotional stimuli may reflect different pathophysiologic processes associated with female versus male MDD, or may moderate and mediate treatment response in the illness in females and males.

No previous neuroimaging studies directly compared females and males with MDD during emotion processing tasks. Previous studies that focused only on females with MDD indicate abnormal OMPFC and amygdala activity to emotional stimuli in females with MDD versus healthy females. For example, these previous studies showed abnormally increased bilateral amygdala activity to negative emotional stimuli, and abnormally increased left sgACC activity to positive emotional stimuli (Abler et al., 2007), although no difference in amygdala or OMPFC activity during a cognitive control of emotion task between females with high severity depression symptoms compared to females with low depression symptoms (Beevers et al., 2010). Females with MDD recovered from depression were reported to show greater right amygdala and reduced left ACC activity to parental criticism stimuli, and reduced right ACC activity to parental praise and neutral stimuli compared to healthy females (Hooley et al., 2009). Previous studies

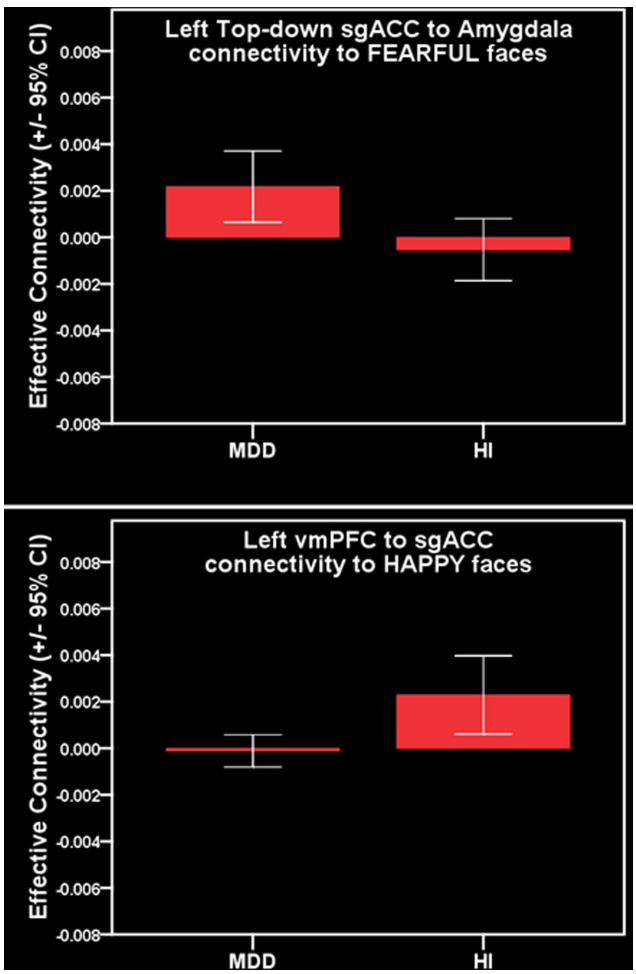

FIGURE 4 | Parallel analysis. Top: greater positive left-sided sgACC–amygdala connectivity to fearful faces in females with MDD. Bottom: reduced positive left-sided vmPFC–sgACC connectivity to happy faces in females with MDD.

also indicate greater activity in left ACC and right lateral prefrontal cortex to positive emotional stimuli in females with MDD versus healthy females (Mitterschiffthaler et al., 2003). Another study showed greater left ACC and left dorsolateral prefrontal cortical activity (Wagner et al., 2006) and greater effective connectivity between left dorsal and rostral ACC during performance of the

Table 5 | Relation between effective connectivity, clinical, demographic, and experiment performance variables in individuals with MDD.

	Happy faces						Fearful faces			
	Left-sided sgACC–Amy EC		Left-sided vmPFC–Amy EC		Left-sided vmPFC–sgACC EC		Left-sided sgACC–Amy EC			
	Females only; MDD ($n = 12$)		Females only; MDD ($n = 12$)		Females only; MDD ($n = 12$)		Whole group; MDD ($n = 19$)		Females only; MDD ($n = 12$)	
	Rho	*p* Value	Rho	*p* Value	Rho	*p* Value	Rho	*p* Value	Rho	*p* Value
Age at scan	0.08	0.80	0.24	0.46	0.13	0.68	−0.12	0.63	0.13	0.70
Age of illness onset	−0.18	0.58	0.35	0.26	0.41	0.18	0.00	0.99	−0.05	0.87
Illness duration	0.15	0.65	−0.24	0.46	−0.37	0.24	0.06	0.81	0.17	0.59
Medication load	0.23	0.47	0.06	0.86	−0.21	0.51	−0.49	0.03*	−0.22	0.50
HRSD-25	0.30	0.34	0.13	0.69	−0.04	0.91	−0.17	0.48	−0.36	0.24
Accuracy emotional face	−0.23	0.47	0.13	0.69	−0.25	0.43	−0.24	0.32	−0.09	0.79
Reaction time emotional face	0.14	0.66	−0.04	0.90	0.57	0.06	−0.08	0.75	0.13	0.68
	MW	*p* Value	MW	*p* Value	MW	*p* Value	MW	*p* Value	MW	*p* Value
Mood stabilizators (on/off)	0	0.11	1	0.19	4	0.66	12	0.18	2	0.31
Anti psychotic medications (on/off)	6	0.39	4	0.20	10	1.00	19	0.58	5	0.28
Anti depressants (on/off)	12	0.78	10	0.52	8	0.30	13	0.09	9	0.41
Benzodiazepines (on/off)	4	0.08	12	0.78	12	0.78	28	0.24	12	0.78
Lifetime presence of alcohol/drugs Abuse or dependence (yes/no)	13	0.93	11	0.64	12	0.78	13	0.04*	6	0.17
Lifetime presence of anxiety disorder (yes/no)	16	0.81	8	0.12	13	0.46	16	0.03*	5	0.04*

*MDD, individuals with major depression disorder in depressed episode; MW, Mann–Whitney U; Rho: Spearman rank correlation; HRSD-25: 25-item Hamilton rating scale for depression; vmPFC, ventromedial prefrontal cortex; sgACC, subgenual prefrontal cortex; *p does not survive multiple correction; EC, effective connectivity.*

Table 6 | Relation between effective connectivity, clinical, demographic, and experiment performance variables in HI.

	Happy faces						Fearful faces			
	Left-sided sgACC–Amy EC		Left-sided vmPFC–Amy EC		Left-sided vmPFC–sgACC EC		Left-sided sgACC–Amy EC			
	Females only HI ($n = 12$)		Females only HI ($n = 12$)		Females only HI ($n = 12$)		Whole group HI ($n = 19$)		Females only HI ($n = 12$)	
	Rho	*p* Value	Rho	*p* Value	Rho	*p* Value	Rho	*p* Value	Rho	*p* Value
Age at scan	−0.59	0.04*	−0.40	0.20	−0.43	0.16	−0.35	0.15	−0.59	0.04*
HRSD-25	**−0.69**	**0.01****	−0.48	0.11	−0.26	0.42	−0.06	0.82	−0.32	0.32
Accuracy emotional face	−0.19	0.55	−0.27	0.40	0.00	1.00	−0.45	0.05*	−0.34	0.28
Reaction time Emotional face	−0.50	0.10	−0.37	0.24	−0.31	0.32	0.24	0.33	0.31	0.33

*HI, healthy individuals; Rho, Spearman rank correlation; HRSD-25, 25-item Hamilton rating scale for depression; vmPFC, ventromedial prefrontal cortex; sgACC, subgenual prefrontal cortex; *p does not survive multiple correction; **p value survives multiple correction; EC, effective connectivity.*

incongruent condition of the Stroop task in females with MDD relative to healthy females (Schlösser et al., 2008). Together with our present findings, these findings therefore suggest abnormal functional integration between, predominantly, left-sided OMPFC and bilateral amygdala to positive and negative emotional stimuli, and also during attentional tasks, in females with MDD. Further studies are clearly needed to elucidate pathophysiologic processes that may differ between male and female MDD.

A popular theory emphasizes the role of the left hemisphere in processing approach-related emotional stimuli (Davidson et al., 1990; Sutton and Davidson, 1997). Cognitive neuroscience accounts of face processing, however, highlight the role of the left hemisphere as critical in "detail-oriented" processing, whereas the right hemisphere may support "gestalt" processing (Sergent and Bindra, 1981; Rossion et al., 2000). Our findings therefore suggest that the left-lateralized pattern of abnormal

connectivity in females with MDD may reflect not only abnormal processing of approach-related emotional stimuli, but also the employment of detail-oriented left-hemisphere-centered strategies during implicit processing of the emotional faces, and automatic regulation of response to these stimuli, to a greater extent than other groups. This should be the focus of future studies.

Examination of gender differences in connectivity measures that were abnormal in individuals with MDD revealed significantly greater inverse left-sided vmPFC–sgACC connectivity to happy faces in healthy males relative to healthy females, such that healthy males showed a pattern of connectivity between these regions that was more similar to that shown by females with MDD than that shown by healthy females. These findings suggest that one pathophysiologic process in female MDD is to render the functional integrity within left-sided vmPFC–sgACC circuitry during positive emotion processing similar to that shown by healthy males, but this requires further study. Interestingly, in healthy individuals, more severe sub-syndromal depression was associated with significantly reduced left-sided sgACC–amygdala connectivity to happy faces, a connectivity pattern that resembled females with MDD.

While a limitation of our study was the small number of males with MDD, our main focus was to examine OMPFC–amygdala connectivity to positive and negative emotional stimuli in females with MDD. Another limitation was the recruitment of medicated individuals with MDD, although our findings indicate normalizing rather than confounding effects of such medication upon one of our connectivity measures, providing a valuable insight into putative neural mechanisms that may mediate antidepressant treatment response in MDD. Further replications of our current and previous findings are clearly needed in future studies. Future studies can determine whether the observed group differences represent state or trait markers of depression by including individuals who have recovered from depression in analyses. Future studies can also aim to examine the extent to which adolescents and adults at potential future risk of mood disorders show these patterns of abnormal connectivity between vmPFC and amygdala during emotion processing paradigms. Furthermore, given promising findings from activation studies in MDD, showing that baseline activity in frontocingulate areas may predict future treatment response in MDD (Almeida et al., 2010a; Pizzagalli, 2011), future studies can also aim to examine the extent to which measures of abnormal connectivity may also predict treatment response in MDD.

In conclusion, we replicated our previous finding of abnormal inverse left-sided OMPFC–amygdala connectivity to positive emotional stimuli in an independent group of females with MDD using a novel implicit emotion processing paradigm. Our present findings show a more extensive pattern of abnormal left-sided connectivity among sgACC, vmPFC, and amygdala to happy and fearful faces in females, but not males, with MDD. The differential pattern of abnormal left-sided OMPFC–amygdala connectivity to happy and fearful faces may therefore represent a neural mechanism for female MDD, which is characterized by comorbid anxiety and high levels of interpersonal stress. Our findings highlight the utility of effective connectivity studies in identifying gender-specific markers of MDD that may help identify potential biological targets for novel, personalized treatments for individuals with MDD.

ACKNOWLEDGMENTS

All work was carried out within the Department of Psychiatry, University of Pittsburgh, neuroimaging data was collected at the Magnetic Resonance Research Center (MRRC), University of Pittsburgh. We thank Dr. Fernando Boada and his staff for their help acquiring neuroimaging data. Dr. Phillips reports having support from R01 MH076971-01. Dr.Versace reports support from a NARSAD young investigator award, Dr. Almeida, Dr. Kronhaus, Mr. LaBarbara, reported no biomedical financial interests or potential conflicts of interest.

REFERENCES

Abler, B., Erk, S., Herwig, U., and Walter, H. (2007). Anticipation of aversive stimuli activates extended amygdala in unipolar depression. *J. Psychiatr. Res.* 41, 511–522.

Almeida, J. R., Akkal, D., Hassel, S., Travis, M. J., Banihashemi, L., Kerr, N., Kupfer, D. J., and Phillips, M. L. (2009a). Reduced gray matter volume in ventral prefrontal cortex but not amygdala in bipolar disorder: significant effects of gender and trait anxiety. *Psychiatry Res.* 171, 54–68.

Almeida, J. R., Mechelli, A., Hassel, S., Versace, A., Kupfer, D. J., and Phillips, M. L. (2009b). Abnormally increased effective connectivity between parahippocampal gyrus and ventromedial prefrontal regions during emotion labeling in bipolar disorder. *Psychiatry Res.* 174, 195–201.

Almeida, J. R., Versace, A., Mechelli, A., Hassel, S., Quevedo, K., Kupfer, D. J., and Phillips, M. L. (2009c). Abnormal amygdala-prefrontal effective connectivity to happy faces differentiates bipolar from major depression. *Biol. Psychiatry* 66, 451–459.

Almeida, J. R. C., Phillips, M. L., Cerqueira, C. T., Zilberman, M., Lobo, D., Henna, E., Tavares, H., Amaro, E., Gorenstein, C., Gentil, V., and Busatto, G. F. (2010a). Neural activity changes to emotional stimuli in healthy individuals under chronic use of clomipramine. *J. Psychopharmacol. (Oxford)* 24, 1165–1174.

Almeida, J. R. C., Versace, A., Hassel, S., Kupfer, D. J., and Phillips, M. L. (2010b). Elevated amygdala activity to sad facial expressions: a state marker of bipolar but not unipolar depression. *Biol. Psychiatry* 67, 414–421.

Anand, A., Li, Y., Wang, Y., Gardner, K., and Lowe, M. J. (2007). Reciprocal effects of antidepressant treatment on activity and connectivity of the mood regulating circuit: an FMRI study. *J. Neuropsychiatry Clin. Neurosci.* 19, 274–282.

Anand, A., Li, Y., Wang, Y., Wu, J., Gao, S., Bukhari, L., Mathews, V. P., Kalnin, A., and Lowe, M. J. (2005). Activity and connectivity of brain mood regulating circuit in depression: a functional magnetic resonance study. *Biol. Psychiatry* 57, 1079–1088.

APA. (2000). *Diagnostic and Statistical Manual of Mental Disorders: DSM-IV-TR.* Washington, DC: American Psychiatric Association.

Beevers, C. G., Clasen, P., Stice, E., and Schnyer, D. (2010). Depression symptoms and cognitive control of emotion cues: a functional magnetic resonance imaging study. *Neuroscience* 167, 97–103.

Bremner, J. D., Vythilingam, M., Vermetten, E., Nazeer, A., Adil, J., Khan, S., Staib, L. H., and Charney, D. S. (2002). Reduced volume of orbitofrontal cortex in major depression. *Biol. Psychiatry* 51, 273–279.

Brockmann, H., Zobel, A., Joe, A., Biermann, K., Scheef, L., Schuhmacher, A., Von Widdern, O., Metten, M., Biersack, H. J., Maier, W., and Boecker, H. (2009). The value of HMPAO SPECT in predicting treatment response to citalopram in patients with major depression. *Psychiatry Res.* 173, 107–112.

Carvajal-Rodriguez, A., De Una-Alvarez, J., and Rolan-Alvarez, E. (2009). A new multitest correction (SGoF) that increases its statistical power when increasing the number of tests. *BMC Bioinformatics* 10, 209. doi:10.1186/1471-2105-10-209

Chen, C. H., Suckling, J., Ooi, C., Fu, C. H., Williams, S. C., Walsh, N. D., Mitterschiffthaler, M. T., Pich, E. M., and Bullmore, E. (2008). Functional coupling of the amygdala in depressed patients treated with antidepressant medication. *Neuropsychopharmacology* 33, 1909–1918.

Dannlowski, U., Ohrmann, P., Bauer, J., Deckert, J., Hohoff, C., Kugel, H., Arolt, V., Heindel, W., Kersting, A., Baune, B. T., and Suslow, T. (2008). 5-HTTLPR biases amygdala activity in response to masked facial expressions in major depression. *Neuropsychopharmacology* 33, 418–424.

Dannlowski, U., Ohrmann, P., Bauer, J., Kugel, H., Arolt, V., Heindel, W., and Suslow, T. (2007). Amygdala reactivity predicts automatic negative evaluations for facial emotions. *Psychiatry Res.* 154, 13–20.

Dannlowski, U., Ohrmann, P., Konrad, C., Domschke, K., Bauer, J., Kugel, H., Hohoff, C., Schoning, S., Kersting, A., Baune, B. T., Mortensen, L. S., Arolt, V., Zwitserlood, P., Deckert, J., Heindel, W., and Suslow, T. (2009). Reduced amygdala-prefrontal coupling in major depression: association with MAOA genotype and illness severity. *Int. J. Neuropsychopharmacol.* 12, 11–22.

David, O., Guillemain, I., Saillet, S., Reyt, S., Deransart, C., Segebarth, C., and Depaulis, A. (2008). Identifying neural drivers with functional MRI: an electrophysiological validation. *PLoS Biol.* 6, e315. doi:10.1371/journal.pbio.0060315

Davidson, R. J., Ekman, P., Saron, C. D., Senulis, J. A., and Friesen, W. V. (1990). Approach-withdrawal and cerebral asymmetry: emotional expression and brain physiology. I. *J. Pers. Soc. Psychol.* 58, 330–341.

Davis, J. M., and Chen, N. (2004). Dose response and dose equivalence of antipsychotics. *J. Clin. Psychopharmacol.* 24, 192–208.

Drevets, W. C. (2001). Neuroimaging and neuropathological studies of depression: implications for the cognitive-emotional features of mood disorders. *Curr. Opin. Neurobiol.* 11, 240–249.

Fales, C. L., Barch, D. M., Rundle, M. M., Mintun, M. A., Snyder, A. Z., Cohen, J. D., Mathews, J., and Sheline, Y. I. (2008). Altered emotional interference processing in affective and cognitive-control brain circuitry in major depression. *Biol. Psychiatry* 63, 377–384.

First, M. B., Spitzer, R. L., Gibbon, M., and Willians, J. B. W. (1995). *Structured Clinical Interview for DSM-IV Axis I Disorders (SCID-, version 2.0)*. New York: Biometric research Department, New York State Psychiatric Institute.

Friston, K. J., Harrison, L., and Penny, W. (2003). Dynamic causal modelling. *Neuroimage* 19, 1273–1302.

Frodl, T., Bokde, A. L. W., Scheuerecker, J., Lisiecka, D., Schoepf, V., Hampel, H., Möller, H.-J., Brückmann, H., Wiesmann, M., and Meisenzahl, E. (2010). Functional connectivity bias of the orbitofrontal cortex in drug-free patients with major depression. *Biol. Psychiatry* 67, 161–167.

Fu, C. H., Williams, S. C., Brammer, M. J., Suckling, J., Kim, J., Cleare, A. J., Walsh, N. D., Mitterschiffthaler, M. T., Andrew, C. M., Pich, E. M., and Bullmore, E. T. (2007). Neural responses to happy facial expressions in major depression following antidepressant treatment. *Am. J. Psychiatry* 164, 599–607.

Gillath, O., Bunge, S. A., Shaver, P. R., Wendelken, C., and Mikulincer, M. (2005). Attachment-style differences in the ability to suppress negative thoughts: exploring the neural correlates. *Neuroimage* 28, 835–847.

Goodwin, F. K., and Jamison, K. R. (2007). *Manic-Depressive Illness: Bipolar Disorders and Recurrent Depression.* New York, NY: Oxford University Press.

Gottfried, J. A., and Dolan, R. J. (2004). Human orbitofrontal cortex mediates extinction learning while accessing conditioned representations of value. *Nat. Neurosci.* 7, 1144–1152.

Greicius, M. D., Flores, B. H., Menon, V., Glover, G. H., Solvason, H. B., Kenna, H., Reiss, A. L., and Schatzberg, A. F. (2007). Resting-state functional connectivity in major depression: abnormally increased contributions from subgenual cingulate cortex and thalamus. *Biol. Psychiatry* 62, 429–437.

Grober, E., and Sliwinski, M. (1991). Development and validation of a model for estimating premorbid verbal intelligence in the elderly. *J. Clin. Exp. Neuropsychol.* 13, 933–949.

Gutman, D. A., Holtzheimer, P. E., Behrens, T. E. J., Johansen-Berg, H., and Mayberg, H. S. (2009). A tractography analysis of two deep brain stimulation white matter targets for depression. *Biol. Psychiatry* 65, 276–282.

Hamilton, J. P., Chen, G., Thomason, M. E., Schwartz, M. E., and Gotlib, I. H. (2011). Investigating neural primacy in major depressive disorder: multivariate Granger causality analysis of resting-state fMRI time-series data. *Mol. Psychiatry* 16, 763–772.

Hamilton, M. (1960). A rating scale for depression. *J. Neurol. Neurosurg. Psychiatry* 23, 56–62.

Hammen, C. (2003). Interpersonal stress and depression in women. *J. Affect. Disord.* 74, 49–57.

Hassel, S., Almeida, J. R. C., Kerr, N., Nau, S., Ladouceur, C. D., Fissell, K., Kupfer, D. J., and Phillips, M. L. (2008). Elevated striatal and decreased dorsolateral prefrontal cortical activity in response to emotional stimuli in euthymic bipolar disorder: no associations with psychotropic medication load. *Bipolar Disord.* 10, 916–927.

Heller, A. S., Johnstone, T., Shackman, A. J., Light, S. N., Peterson, M. J., Kolden, G. G., Kalin, N. H., and Davidson, R. J. (2009). Reduced capacity to sustain positive emotion in major depression reflects diminished maintenance of fronto-striatal brain activation. *Proc. Natl. Acad. Sci. U.S.A.* 106, 22445–22450.

Hooley, J. M., Gruber, S. A., Parker, H. A., Guillaumot, J., Rogowska, J., and Yurgelun-Todd, D. A. (2009). Cortico-limbic response to personally challenging emotional stimuli after complete recovery from depression. *Psychiatry Res.* 172, 83–91.

Jaracz, J., and Rybakowski, J. (2002). Studies of cerebral blood flow in metabolism in depression using positron emission tomography (PET). *Psychiatr. Pol.* 36, 617–628.

Keedwell, P. A., Drapier, D., Surguladze, S., Giampietro, V., Brammer, M., and Phillips, M. (2010). Subgenual cingulate and visual cortex responses to sad faces predict clinical outcome during antidepressant treatment for depression. *J. Affect. Disord.* 120, 120–125.

Kendler, K. S., Gardner, C. O., and Prescott, C. A. (2002). Toward a comprehensive developmental model for major depression in women. *Am. J. Psychiatry* 159, 1133–1145.

Kito, S., Fujita, K., and Koga, Y. (2008). Changes in regional cerebral blood flow after repetitive transcranial magnetic stimulation of the left dorsolateral prefrontal cortex in treatment-resistant depression. *J. Neuropsychiatry Clin. Neurosci.* 20, 74–80.

Korb, A. S., Hunter, A. M., Cook, I. A., and Leuchter, A. F. (2009). Rostral anterior cingulate cortex theta current density and response to antidepressants and placebo in major depression. *Clin. Neurophysiol.* 120, 1313–1319.

Langenecker, S. A., Kennedy, S. E., Guidotti, L. M., Briceno, E. M., Own, L. S., Hooven, T., Young, E. A., Akil, H., Noll, D. C., and Zubieta, J.-K. (2007). Frontal and limbic activation during inhibitory control predicts treatment response in major depressive disorder. *Biol. Psychiatry* 62, 1272–1280.

Lawrence, N. S., Williams, A. M., Surguladze, S., Giampietro, V., Brammer, M. J., Andrew, C., Frangou, S., Ecker, C., and Phillips, M. L. (2004). Subcortical and ventral prefrontal cortical neural responses to facial expressions distinguish patients with bipolar disorder and major depression. *Biol. Psychiatry* 55, 578–587.

Luks, T. L., Simpson, G. V., Dale, C. L., and Hough, M. G. (2007). Preparatory allocation of attention and adjustments in conflict processing. *Neuroimage* 35, 949–958.

Maldjian, J. A., Laurienti, P. J., Kraft, R. A., and Burdette, J. H. (2003). An automated method for neuroanatomic and cytoarchitectonic atlas-based interrogation of fMRI data sets. *Neuroimage* 19, 1233–1239.

Matthews, S. C., Strigo, I. A., Simmons, A. N., Yang, T. T., and Paulus, M. P. (2008). Decreased functional coupling of the amygdala and supragenual cingulate is related to increased depression in unmedicated individuals with current major depressive disorder. *J. Affect. Disord.* 111, 13–20.

Mayberg, H. S. (1999). Reciprocal limbic-cortical function and negative mood: converging PET findings in depression and normal sadness. *Am. J. Psychiatry* 156, 675–682.

Mayberg, H. S. (2003). Modulating dysfunctional limbic-cortical circuits in depression: towards development of brain-based algorithms for diagnosis and optimised treatment. *Br. Med. Bull.* 65, 193–207.

Mayberg, H. S. (2005). Deep brain stimulation for treatment-resistant depression. *Neuron* 45, 651–660.

Mayberg, H. S., Liotti, M., Brannan, S. K., Mcginnis, S., Mahurin, R. K., Jerabek, P. A., Silva, J. A., Tekell, J. L., Martin, C. C., Lancaster, J. L., and Fox, P. T. (1999). Reciprocal limbic-cortical function and negative mood: converging PET findings in depression and normal sadness. *Am. J. Psychiatry* 156, 675–682.

McGrath, E., Keita, G. P., Strickland, B. R., and Russo, N. F. (2009). *Women and Depression: Risk Factors and Treatment Issues: Final Report of the American Psychological Association's National Task Force on Women and Depression.* Washington, DC: American Psychological Association.

Mechelli, A., Price, C. J., Noppeney, U., and Friston, K. J. (2003). A dynamic causal modeling study on category effects: bottom-up or top-down mediation? *J. Cogn. Neurosci.* 15, 925–934.

Mitterschiffthaler, M. T., Kumari, V., Malhi, G. S., Brown, R. G., Giampietro, V. P., Brammer, M. J., Suckling, J., Poon, L., Simmons, A., Andrew, C., and Sharma, T. (2003). Neural response to pleasant stimuli in anhedonia: an fMRI study. *Neuroreport* 14, 177–182.

Mulert, C., Juckel, G., Brunnmeier, M., Karch, S., Leicht, G., Mergl, R., Moller, H. J., Hegerl, U., and Pogarell, O. (2007). Rostral anterior cingulate cortex activity in the theta band predicts response to antidepressive medication. *Clin. EEG Neurosci.* 38, 78–81.

Ongur, D., Ferry, A. T., and Price, J. L. (2003). Architectonic subdivision of the human orbital and medial prefrontal cortex. *J. Comp. Neurol.* 460, 425–449.

Phillips, M. L., Drevets, W. C., Rauch, S. L., and Lane, R. (2003). Neurobiology of emotion perception II: implications for major psychiatric disorders. *Biol. Psychiatry* 54, 515–528.

Phillips, M. L., Ladouceur, C. D., and Drevets, W. C. (2008a). A neural model of voluntary and automatic emotion regulation: implications for understanding the pathophysiology and neurodevelopment of bipolar disorder. *Mol. Psychiatry* 13, 829, 833–857.

Phillips, M. L., Ladouceur, C. D., and Drevets, W. C. (2008b). A neural model of voluntary and automatic emotion regulation: implications for understanding the pathophysiology and neurodevelopment of bipolar disorder. *Mol. Psychiatry* 13, 833–857.

Pizzagalli, D. A. (2011). Frontocingulate dysfunction in depression: toward biomarkers of treatment response. *Neuropsychopharmacology* 36, 183–206.

Price, J. L., and Drevets, W. C. (2010). Neurocircuitry of mood disorders. *Neuropsychopharmacology* 35, 192–216.

Rossion, B., Dricot, L., Devolder, A., Bodart, J.-M., Crommelinck, M., Gelder, B. D., and Zoontjes, R. (2000). Hemispheric asymmetries for whole-based and part-based face processing in the human fusiform gyrus. *J. Cogn. Neurosci.* 12, 793–802.

Sackeim, H. A. (2001). The definition and meaning of treatment-resistant depression. *J. Clin. Psychiatry* 62(Suppl. 16), 10–17.

Saxena, S., Brody, A. L., Ho, M. L., Zohrabi, N., Maidment, K. M., and Baxter, L. R. Jr. (2003). Differential brain metabolic predictors of response to paroxetine in obsessive-compulsive disorder versus major depression. *Am. J. Psychiatry* 160, 522–532.

Schlösser, R. G. M., Wagner, G., Koch, K., Dahnke, R., Reichenbach, J. R., and Sauer, H. (2008). Fronto-cingulate effective connectivity in major depression: a study with fMRI and dynamic causal modeling. *Neuroimage* 43, 645–655.

Schuyler, B., Ollinger, J. M., Oakes, T. R., Johnstone, T., and Davidson, R. J. (2010). Dynamic causal modeling applied to fMRI data shows high reliability. *Neuroimage* 49, 603–611.

Sergent, J., and Bindra, D. (1981). Differential hemispheric processing of faces: methodological considerations and reinterpretation. *Psychol. Bull.* 89, 541–554.

Sheline, Y. I., Barch, D. M., Donnelly, J. M., Ollinger, J. M., Snyder, A. Z., and Mintun, M. A. (2001). Increased amygdala response to masked emotional faces in depressed subjects resolves with antidepressant treatment: an fMRI study. *Biol. Psychiatry* 50, 651–658.

Sheline, Y. I., Price, J. L., Yan, Z., and Mintun, M. A. (2010). Resting-state functional MRI in depression unmasks increased connectivity between networks via the dorsal nexus. *Proc. Natl. Acad. Sci. U.S.A.* 107, 11020–11025.

Siegle, G. J., Steinhauer, S. R., Thase, M. E., Stenger, V. A., and Carter, C. S. (2002). Can't shake that feeling: event-related fMRI assessment of sustained amygdala activity in response to emotional information in depressed individuals. *Biol. Psychiatry* 51, 693–707.

Siegle, G. J., Thompson, W., Carter, C. S., Steinhauer, S. R., and Thase, M. E. (2007). Increased amygdala and decreased dorsolateral prefrontal BOLD responses in unipolar depression: related and independent features. *Biol. Psychiatry* 61, 198–209.

Smith, D. J., Kyle, S., Forty, L., Cooper, C., Walters, J., Russell, E., Caesar, S., Farmer, A., Mcguffin, P., Jones, I., Jones, L., and Craddock, N. (2008). Differences in depressive symptom profile between males and females. *J. Affect. Disord.* 108, 279–284.

Surguladze, S., Brammer, M. J., Keedwell, P., Giampietro, V., Young, A. W., Travis, M. J., Williams, S. C. R., and Phillips, M. L. (2005). A differential pattern of neural response toward sad versus happy facial expressions in major depressive disorder. *Biol. Psychiatry* 57, 201.

Suslow, T., Konrad, C., Kugel, H., Rumstadt, D., Zwitserlood, P., Schöning, S., Ohrmann, P., Bauer, J., Pyka, M., Kersting, A., Arolt, V., Heindel, W., and Dannlowski, U. (2010). Automatic mood-congruent amygdala responses to masked facial expressions in major depression. *Biol. Psychiatry* 67, 155–160.

Sutton, S. K., and Davidson, R. J. (1997). Prefrontal brain asymmetry: a biological substrate of the behavioral approach and inhibition systems. *Psychol. Sci.* 8, 204–210.

Tottenham, N., Tanaka, J. W., Leon, A. C., Mccarry, T., Nurse, M., Hare, T. A., Marcus, D. J., Westerlund, A., Casey, B. J., and Nelson, C. (2009). The NimStim set of facial expressions: judgments from untrained research participants. *Psychiatry Res.* 168, 242–249.

Van Veen, V., and Carter, C. S. (2002). The timing of action-monitoring processes in the anterior cingulate cortex. *J. Cogn. Neurosci.* 14, 593–602.

Versace, A., Almeida, J. R., Hassel, S., Walsh, N. D., Novelli, M., Klein, C. R., Kupfer, D. J., and Phillips, M. L. (2008). Elevated left and reduced right orbitomedial prefrontal fractional anisotropy in adults with bipolar disorder revealed by tract-based spatial statistics. *Arch. Gen. Psychiatry* 65, 1041–1052.

Victor, T. A., Furey, M. L., Fromm, S. J., Ohman, A., and Drevets, W. C. (2010). Relationship between amygdala responses to masked faces and mood state and treatment in major depressive disorder. *Arch. Gen. Psychiatry* 67, 1128–1138.

Wagner, G., Koch, K., Schachtzabel, C., Reichenbach, J. R., Sauer, H., and Schlosser Md, R. G. (2008). Enhanced rostral anterior cingulate cortex activation during cognitive control is related to orbitofrontal volume reduction in unipolar depression. *J. Psychiatry Neurosci.* 33, 199–208.

Wagner, G., Sinsel, E., Sobanski, T., Kohler, S., Marinou, V., Mentzel, H. J., Sauer, H., and Schlosser, R. G. (2006). Cortical inefficiency in patients with unipolar depression: an event-related FMRI study with the Stroop task. *Biol. Psychiatry* 59, 958–965.

Williams, L. M., Das, P., Liddell, B. J., Kemp, A. H., Rennie, C. J., and Gordon, E. (2006). Mode of functional connectivity in amygdala pathways dissociates level of awareness for signals of fear. *J. Neurosci.* 26, 9264–9271.

Conflict of Interest Statement: The authors declare that the research was conducted in the absence of any commercial or financial relationships that could be construed as a potential conflict of interest.

Received: 30 August 2011; accepted: 18 November 2011; published online: 08 December 2011.

Citation: Almeida JRC, Kronhaus DM, Sibille EL, Langenecker SA, Versace A, LaBarbara EJ and Phillips ML (2011) Abnormal left-sided orbitomedial prefrontal cortical–amygdala connectivity during happy and fear face processing: a potential neural mechanism of female MDD. Front. Psychiatry ***2****:69. doi: 10.3389/fpsyt.2011.00069*

This article was submitted to Frontiers in Neuropsychiatric Imaging and Stimulation, a specialty of Frontiers in Psychiatry.

APPENDIX

Table A1 | Descriptive list of medication for each individual with major depressive disorder.

Subject	Drug name				
1	Bupropion				
2	N/A				
3	Bupropion				
4	Fluvoxamine	Clonazepam	Risperidona		
5	Fluoxetine	Clonazepam			
6	Fluoxetine				
7	Venlafaxine	Bupropion			
8	N/A				
9	Lithium	Trazodone	Clonazepam		
10	Paroxetine	Temazepam	Chlorpromazine	Gabapentin	Lorazepam
11	Venlafaxine	Trazodone			
12	Lorazepam	Desipramine	Lamotrigine	Mirtazapine	
13	N/A				
14	Duloxetine				
15	Duloxetine				
16	Citalopram	Bupropion			
17	Alprazolam	Citalopram			
18	N/A				
19	Aripiprazole	Zolpidem	Venlafaxine		

frontiers in PSYCHIATRY

ORIGINAL RESEARCH ARTICLE
published: 28 February 2012
doi: 10.3389/fpsyt.2012.00014

Task-related deactivation and functional connectivity of the subgenual cingulate cortex in major depressive disorder

***Christopher G. Davey*[1,2]*, *Murat Yücel*[2], *Nicholas B. Allen*[1,3] *and Ben J. Harrison*[2]**

[1] *Orygen Youth Health Research Centre, The University of Melbourne, Melbourne, VIC, Australia*
[2] *Melbourne Neuropsychiatry Centre, Department of Psychiatry and Melbourne Health, The University of Melbourne, Melbourne, VIC, Australia*
[3] *Department of Psychological Sciences, The University of Melbourne, Melbourne, VIC, Australia*

Edited by:
Alex Fornito, The University of Melbourne, Australia

Reviewed by:
Amit Anand, Indiana University, USA
Jorge Almeida, University of Pittsburgh, USA

****Correspondence:***
Christopher G. Davey, Orygen Youth Health Research Centre, The University of Melbourne, Parkville, VIC 3052, Australia.
e-mail: c.davey@unimelb.edu.au

Background: Major depressive disorder is associated with functional alterations in activity and resting-state connectivity of the extended medial frontal network. In this study we aimed to examine how task-related medial network activity and connectivity were affected in depression. **Methods:** 18 patients with major depressive disorder, aged 15- to 24-years-old, were matched with 19 healthy control participants. We characterized task-related activations and deactivations while participants engaged with an executive-control task (the multi-source interference task, MSIT). We used a psycho-physiological interactions approach to examine functional connectivity changes with subgenual anterior cingulate cortex. Voxel-wise statistical maps for each analysis were compared between the patient and control groups. **Results:** There were no differences between groups in their behavioral performances on the MSIT task, and nor in patterns of activation and deactivation. Assessment of functional connectivity with the subgenual cingulate showed that depressed patients did not demonstrate the same reduction in functional connectivity with the ventral striatum during task performance, but that they showed greater reduction in functional connectivity with adjacent ventromedial frontal cortex. The magnitude of this latter connectivity change predicted the relative activation of task-relevant executive-control regions in depressed patients. **Conclusion:** The study reinforces the importance of the subgenual cingulate cortex for depression, and demonstrates how dysfunctional connectivity with ventral brain regions might influence executive–attentional processes.

Keywords: major depressive disorder, cognition, anterior cingulate cortex, striatum, default mode network, connectivity, fMRI, adolescence

INTRODUCTION

Major depressive disorder is characterized by symptoms in affective, somatic, and cognitive domains. The diversity of symptoms provides an indication that the illness arises from systemic alterations in brain function, and not from specific regional dysfunction. The brain system that has been most consistently implicated in the pathophysiology of depression is the extended medial prefrontal network (or "medial network") – a set of ventrally located brain regions that includes ventromedial frontal cortex, anterior and posterior cingulate cortex, striatum, amygdala, and thalamus (Price and Drevets, 2010). The abnormal function of these regions has been linked to key symptoms of depression such as low mood, anhedonia, and self-related disturbances (Keedwell et al., 2005; Grimm et al., 2009; Sheline et al., 2009). In addition to these disturbances, impairments of goal-directed cognitive processes are common in patients with depression, who frequently report problems with sustained attention and concentration (Gotlib and Joormann, 2010). By and large such processes are thought to reflect disturbances in the activity of dorsal frontoparietal brain regions, including the so-called "executive-control network" (Seeley et al., 2007). While both networks interact dynamically in the service of goal-directed behavior (Sridharan et al., 2008; Spreng et al., 2010), disturbances of the executive-control network are hypothesized to be secondary to medial network alterations in depressed patients (Price and Drevets, 2010). However, the putative mechanisms by which medial network activity may influence the engagement of executive-control processes in depression have not been well characterized.

The medial network, an essentially anatomical concept, shows considerable overlap with the hypothesized "default mode network," with both networks including as core components the ventromedial prefrontal cortex and ventral and posterior regions of the cingulate cortex. The default mode network was first described when it was observed that these regions, together with temporoparietal regions, showed greater metabolic activity when a person was at rest compared to when they were engaged in demanding cognitive tasks (Ghatan et al., 1995; Shulman et al., 1997; Raichle et al., 2001). This observed rest–task difference was termed "deactivation" because early imaging studies were primarily focused on "activation" to cognitive–attentional stimuli (Buckner et al., 2008), and we use the term in that sense here: to refer to brain activity that is reduced during task engagement compared to rest. It was subsequently noted that the default mode network showed functionally correlated activity during extended periods of continuous rest – while a person was engaged in "stimulus independent thought" (Greicius et al., 2003; Fox et al., 2005). More

recently, examination of functional connectivity during these two types of rest – blocks of rest interleaved within cognitive tasks, and extended continuous rest – has shown that, while minor differences are evident, they are qualitatively and quantitatively very similar (Fair et al., 2007b).

The extent to which resting-state activity becomes less prominent, or "deactivates," during the performance of cognitive tasks has been related to their specific levels of demand (McKiernan et al., 2003; Mayer et al., 2010; Harrison et al., 2011), and has been shown to correlate with individual differences in task reaction times and accuracy (Harrison et al., 2007; Anticevic et al., 2010; Sala-Llonch et al., 2011). In healthy people cognitive tasks have been shown to affect default mode network connectivity in two ways: firstly, connectivity between different regions of the default mode network remains relatively consistent during task performance (Hampson et al., 2006; Fransson and Marrelec, 2008; Harrison et al., 2008; Bluhm et al., 2011); and secondly, there is reduced functional connectivity between default and non-default mode network regions (Bluhm et al., 2011).

The above observations may be relevant to depression, in which resting-state alterations in activity and connectivity of ventral regions of the anterior cingulate cortex (ACC) have been a frequent finding. The subgenual ACC, in particular, has been reported to show increased resting-state activity in nuclear imaging studies of depressed patients (Drevets, 1999; Dunn et al., 2002), and stronger functional connectivity between the subgenual ACC and other regions of the medial network have been shown using functional magnetic resonance imaging (Greicius et al., 2007; Hamilton et al., 2011; Davey et al., 2012). A recent study reported increased functional connectivity of dorsomedial frontal cortex (in a region the authors labeled the "dorsal nexus") with subgenual ACC, dorsolateral frontal cortex, and precuneus (Sheline et al., 2010). Alterations in connectivity with the dorsal ACC – an important region for cognitive control processes – have also been reported, with demonstration of reduced connectivity with striatum, amygdala, and medial thalamus (Anand et al., 2005). During performance of cognitive tasks depressed patients have shown broadly reduced deactivation of the ventral ACC and extended medial frontal cortex (Harvey et al., 2005; Wagner et al., 2006). Connectivity changes in medial network regions during cognitive task performance, however, have not previously been reported for depressed patients, despite evidence that such changes may underlie task-related cognitive impairment in other psychiatric disorders (Whitfield-Gabrieli et al., 2009).

The goal of the current study was therefore to examine whether depressed patients showed differences in deactivation, and in functional connectivity of the subgenual ACC, during cognitive task performance. We selected the subgenual ACC as a region-of-interest because of its frequent implication in depression (Hamani et al., 2011) – including being the site for the placement of electrical leads in deep-brain-stimulation (DBS) treatment of the illness (Lozano et al., 2008). The subgenual ACC has previously been shown to be more strongly connected with the default mode network in depressed compared to control participants (Greicius et al., 2007), suggesting the possibility of altered changes in connectivity during engagement with cognitive tasks that could be expected to deactivate the network. Our predictions were that depressed participants would show less deactivation of default mode regions during cognitive task performance, in keeping with other studies. Secondly, we expected that functional connectivity with the subgenual ACC would be distinctly modulated in depressed patients when comparing rest and task performance periods. To assess this, participants were examined with functional MRI while they performed the multi-source interference task (MSIT; Bush and Shin, 2006). The MSIT is a well-validated executive-control paradigm that evokes robust activation of dorsal frontoparietal regions, and corresponding deactivation of the default mode network (Bush and Shin, 2006; Harrison et al., 2007; Yucel et al., 2007). In order to reliably assess changes in deactivation and subgenual ACC functional connectivity from a resting baseline, we developed a modified version of the MSIT that interleaved specific rest-fixation periods between each task block. We employed an analysis based on psycho-physiological interactions (PPI; Friston et al., 1997) in order to identify changes in functional connectivity of the subgenual ACC between the resting and task performance states.

MATERIALS AND METHODS

PARTICIPANTS

Depressed participants were recruited for the study from Orygen Youth Health, a public mental health service for young people in Melbourne, Australia. Patients were between 15 and 24 years of age, and had major depressive disorder determined by Structured Clinical Interview for DSM-IV (SCID; First et al., 1997). Patients were included from an age range that extended from the middle teenage years to early adulthood, which accords with a clinical focus on youth mental health (McGorry, 1998), and is consistent with our current understanding of the continuities in brain and social development through this period (Davey et al., 2008). Patients did not meet the criteria for psychotic disorder, substance dependence disorder, pervasive developmental disorder, or intellectual disability; and were not excluded if they were taking antidepressant medication. The depressed participants were successfully matched with a group of control participants on age, gender, and full-scale IQ (**Table 1**). The control participants were recruited via advertisement placed in a daily metropolitan newspaper, and had no history of mental illness, as determined by SCID. The participants (and their parents if they were younger than 18 years of age) provided their informed consent to participate in the study, which was approved by the local research and ethics committees. Imaging data from one control participant and one depressed participant were excluded due to excessive head movements during scanning (see further), resulting in a control group of 19 participants and a depressed group of 18 participants.

The illness characteristics of the depressed participants reflected their relatively young age, and their recruitment via a public mental health service, which treats young people with relatively severe illness. The mean Beck Depression Inventory (BDI-II) score for the depressed participants of 34.4 indicates that their illnesses were at the severe end of the illness spectrum (Beck et al., 1996). Nine of the depressed participants were being treated with antidepressant medication: fluoxetine ($n = 4$), citalopram ($n = 2$), and venlafaxine ($n = 3$).

Table 1 | Characteristics of the control and depressed participants.

Participant variable	Mean (SD), median or % (number)	Mean (SD), median or % (number)
Age	19.9 (2.7)	18.9 (2.2)
Female	58% (11)	61% (11)
Full-scale IQ	109.8 (11.0)	107.9 (9.3)
BDI score	3.1 (3.6)	34.4 (12.6)
First episode of depression	–	50.0% (9)
Median length of episode	–	10.5 months
Comorbid anxiety disorder	–	33.3% (6)
Antidepressant medication	–	50.0% (9)
Median length of treatment	–	4 months

TASK DESCRIPTION

Each participant performed a modified block-design version of the MSIT, which involved responding to eight 30-s task blocks of congruent (i.e., lower cognitive demand) and incongruent (i.e., higher cognitive demand) stimulus trials. During both task conditions, participants were instructed to indicate the identity (not the position) of a visually presented target number in a three-digit sequence corresponding to learned button box associations using the index (1), middle (2), and ring (3) fingers. During congruent trials the target number always matched its appropriate button box position and was flanked by zeros (e.g., "0 2 0"). During incongruent trials, the target never matched its appropriate position and was flanked by incongruent numbers (e.g., "3 1 1"). Each block consisted of 12 trials of either the congruent or incongruent stimulus conditions, with the stimulus presented for 2000 ms and an inter-stimulus interval of 500 ms. As implemented by Harrison et al. (2011), each task block was interleaved with 15 s periods of rest-fixation. The main focus of our analysis was on comparison of the rest blocks with the cognitively demanding incongruent task blocks.

IMAGE ACQUISITION AND PREPROCESSING

A 3-T Siemens Magnetom Trio magnetic resonance scanner (Erlangen, Germany) was used to acquire whole-brain functional T2∗-weighted echo-planar images (EPIs). Functional sequences consisted of gradient-recalled acquisition in the steady state [time of repetition (TR), 2400 ms; time of echo (TE), 40 ms; pulse angle, 90°) within a field of view of 210 mm, with a 64 × 64-pixel matrix, and with a slice thickness of 3 mm (no inter-slice gap). Thirty-six interleaved slices were acquired parallel to the anterior–posterior commissure line, with particular attention paid to ensuring good coverage of ventral brain areas. Field maps were also acquired to correct for distortion caused by magnetic field inhomogeneities (TR, 400 ms; short TE, 5.19 ms; long TE, 7.65 ms; pixel matrix, 64 × 64; slice thickness, 3 mm). While completing the MSIT task 157 whole-brain EPIs were acquired for each participant. In addition, prior to performing the MSIT, each participant underwent a single 12.3-min resting-state sequence (they were instructed to relax, stay awake, and lie still with their eyes closed) with the acquisition of 307 EPIs. A high-resolution T1-weighted anatomical image was also acquired to aid co-registration of the functional sequences to standard neuroanatomical space. During scanning participants were provided with earphones to reduce scanner noise, and foam-rubber inserts were used to aid head stability.

Imaging data were transferred and processed on an Apple OSX platform running MATLAB version 7 (MathWorks, Natick, MA, USA), and using Statistical Parametric Mapping 8 (SPM8)[1]. Motion correction was performed by aligning each participant's time series to the first image using least-squares minimization and a six-parameter (rigid body) spatial transformation, and the field maps were used to unwarp the images. Participants' data were excluded from analysis if translation and rotation estimates were greater than 2 mm or 2°, respectively. Excessive movement resulted in the exclusion of data from one control participant and one depressed participant. The realigned and unwarped functional sequences were then coregistered to each participant's respective anatomical scan. Anatomical scans were segmented and spatially normalized to the International Consortium for Brain Mapping template using the unified segmentation approach, and the normalization parameters were applied to the coregistered functional images, which were resliced to 2 mm isotropic resolution. Functional images were smoothed with a 6-mm (full-width half-maximum) Gaussian filter. All image sequences were routinely inspected for potential normalization artifacts.

STATISTICAL ANALYSIS

For each participant primary task regressors were created by specifying the onset and duration of each task block, followed by convolution with a canonical hemodynamic response function and its temporal derivative, and use of a high-pass filter set at 128 s to remove low-frequency drifts. Parameter estimates were calculated at each voxel using the general linear model and local autocorrelation correction. Second-level analysis identified voxels that showed greater activation in the incongruent compared to congruent task, and in the rest block compared to the incongruent task (i.e., that were deactivated during the task). To characterize any between-group differences we thresholded the statistical maps at $P < 0.005$, and determined whether any clusters survived whole-brain cluster-wise correction ($P_{FDR} < 0.05$) within broad global masks of relevant activated or deactivated brain regions (formed by global conjunction of the control and depressed participants, thresholded at $P < 0.05$, uncorrected).

Psycho-physiological interactions were examined using seed regions of interest in the subgenual ACC. PPI analysis allows an examination of whether connectivity between brain regions differs in different psychological context. It assesses whether there is an interaction between correlated brain activations and the psychological task; in other words whether there is an influence of one brain region on another that is over-and-above correlated activations and deactivations produced by the task (Friston et al., 1997). In this study our focus was on how connectivity with the subgenual ACC changed between resting-state periods and performance of the incongruent MSIT condition. The location of the seeds was taken from Margulies et al.'s (2007) study of cingulate connectivity: spheres of 3.5 mm radius were created in left and right subgenual ACC ($x = \pm 5$, $y = 25$, $z = -10$). Time series

[1] http://www.fil.ion.ucl.ac.uk/spm/

were extracted for each seed; and the deconvolved time course, along with the task model (rest > incongruent task), and their interaction, were entered into a first-level GLM analysis for each participant. The voxel-wise statistical maps calculated for each PPI were then included in group (second-level) random-effects analyses, adopting a 2 × 2 factorial model [group (control, patient) by hemisphere (right seed, left seed)]. Age and medication status were included as covariates.

Our primary interest was in characterizing how resting functional connectivity of the subgenual ACC changed in response to task performance in the two groups. We therefore limited our analysis to only those regions that showed significant functional connectivity with the subgenual ACC during resting-state conditions by masking our second-level PPI analyses with an independently derived resting-state functional connectivity map (i.e., from the 12-min resting-state scans from the same participants; reported in Davey et al., 2012). The map was created by including the resting-state time-courses for the subgenual ACC seeds and nuisance signals (white matter, cerebrospinal fluid, and global brain signal fluctuations) as predictors of interest and no interest, respectively, in whole-brain, linear regression analyses. Contrast images were generated for each participant by estimating the regression coefficient between all brain voxels and each seed's time series, separately for each hemisphere. These images were then included in group random-effects analyses, using a similar 2 × 2 factorial as above (detailed results of the analyses are to be presented elsewhere). The resting-state mask was created for the subgenual ACC by thresholding a conjunction map for control and depressed participants at voxel-wise $P_{FDR} < 0.05$, ensuring that the second-level PPI analyses were restricted to only those brain regions that showed significant resting-state correlations with the subgenual ACC in both the depressed and control groups. The mask consisted of the core components of the medial network, including ventral cingulate cortex, ventromedial frontal cortex, posterior cingulate cortex, striatum, and anterior thalamus. Analyses of within- and between-group PPI effects were thresholded at a voxel-wise $P < 0.005$, and cluster-level probabilities were calculated using Monte Carlo simulation, as implemented by AlphaSim[2]

To investigate potential associations between subgenual ACC connectivity and other task-related brain and behavioral indices, we performed second-level GLM covariance analyses in each group that examined whether changes in connectivity predicted: (i) the relative magnitude of task-related activation of executive-control regions during the MSIT; and (ii) individual differences in task performance with regards to participants' reaction-time and accuracy scores. In the first analysis, the strengths of connectivity between the subgenual ACC and implicated regions of interest (see Results) were estimated by extracting the first eigenvariate of the voxels within each region-of-interest using SPM8. These values were then entered into the second-level model of task activation effects (incongruent task > rest). In the next analysis, participants' performance scores were entered as covariates of interest into the second-level model of task-related subgenual ACC connectivity changes (rest > incongruent task). For the patient group only, we additionally examined direct associations between connectivity changes and clinical severity, as measured with the BDI. All analysis were thresholded at $P < 0.005$ with whole-brain cluster-wise correction ($P < 0.05$).

RESULTS

The control and depressed groups performed the MSIT task similarly. They showed similar high rates of accuracy (controls: congruent 99.8%, incongruent 97.5%; depressed: congruent 99.6%, incongruent 96.1%; main effect of task: $F_{1,35} = 22.6$, $P = < 0.001$; main effect of group: $F_{1,35} = 0.86$, $P = 0.36$; interaction: $F_{1,35} = 0.38$, $P = 0.54$); and similar reaction times (controls: congruent 657 ms, incongruent 1032 ms; depressed: congruent 628 ms, incongruent 1035 ms; main effect of task: $F_{1,35} = 372.8$, $P = < 0.001$; main effect of group: $F_{1,35} = 0.22$, $P = 0.65$; interaction: $F_{1,35} = 0.64$, $P = 0.43$).

The MSIT paradigm led to robust activation (incongruent task > congruent task) of the bilateral dorsal frontoparietal cortex, dorsal anterior ACC, supplementary motor cortex, and other executive-control areas. Prominent task-related deactivations (rest > incongruent task) were observed in the ventral and dorsal posterior cingulate cortex, precuneus and the ventromedial frontal cortex (**Figure 1**). When comparing the two groups directly, no significant differences in task-related activation or deactivation were observed, even at a lenient uncorrected minimum cluster size of 20 voxels. Further region-of-interest analysis of deactivations within the subgenual ACC seeds confirmed no differences between groups (main effect of group: $F_{1,35} = 1.53$, $P = 0.23$).

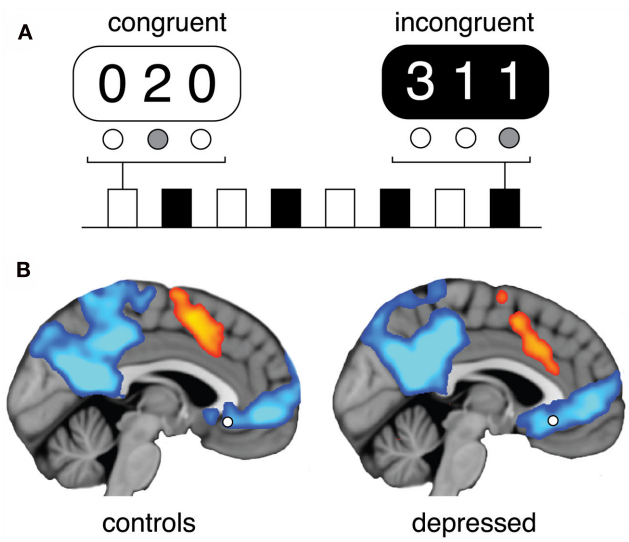

FIGURE 1 | The MSIT involved participants completing alternating blocks of the congruent and incongruent task, interleaved with blocks of rest (A). Task-induced activations (incongruent > congruent; in orange) and deactivations (rest > incongruent; in blue) were apparent in executive-control and default mode network regions, respectively **(B)**. There were no significant differences between groups. The approximate position of the subgenual ACC seeds used for the PPI analysis is shown.

[2]http://afni.nimh.nih.gov/afni/doc/manual/AlphaSim.

In our assessment of task-related functional connectivity, control participants demonstrated greater connectivity of the subgenual ACC with the right ventral caudate/nucleus accumbens during rest when compared to task performance; that is, task engagement was associated with a decreased in connectivity between the regions. Depressed participants, on the other hand, showed greater connectivity between the subgenual ACC and adjacent ventromedial frontal cortex regions at rest compared to task performance: task engagement was associated with a decrease in connectivity. Between-group comparisons confirmed that these task-related connectivity changes were significantly different between the healthy and depressed participants (**Table 2**; **Figure 2**).

No significant linear associations were observed between the aforementioned connectivity changes and participants' behavioral task performance (i.e., reaction-time and accuracy), nor with depression severity in the depressed participants. However, correlations were observed between the magnitude of task-induced reduction in connectivity with the ventromedial frontal cortex in MDD patients and task-related activation of the left superior parietal cortex [cluster size, 694 voxels; peak coordinate (x y z), −28 −32 40; peak Z-score, 5.3; cluster-level $P_{FDR} = 0.002$] and left dorsolateral frontal cortex [cluster size, 287 voxels; peak coordinate (x y z), −48 26 26; peak Z-score, 4.4; cluster-level $P_{FDR} = 0.11$; **Figure 2**]. That is, patients who demonstrated a more prominent decrease in connectivity between the subgenual ACC and ventromedial frontal cortex in the rest compared to task conditions also demonstrated more prominent task-related activations of left frontoparietal regions. No such significant associations were observed in control participants.

DISCUSSION

The aim of the study was to examine how medial network regions were affected by cognitive task performance in depression, both in terms of task-induced deactivations and functional connectivity changes. The results demonstrate that despite being similarly deactivated during the performance of the MSIT task, the subgenual ACC was distinctly modulated in its functional connectivity with other brain regions in depressed participants. Whereas a reduction in connectivity between this region and the ventral striatum was characteristic of the transition between rest and task performance in the control group, a reduction in connectivity with the ventromedial frontal cortex was characteristic of depression. Moreover, the magnitude of this latter connectivity change was found to predict the corresponding activation of task-related frontoparietal regions, suggesting a direct link between putative medial network alterations and executive-control processes in depression.

Medial network areas project prominently to ventral striatum (which is particularly a target of subgenual ACC) and to the medial edge of the caudate nucleus (Ferry et al., 2000; Beckmann et al., 2009). In healthy participants, cognitive task engagement was found to significantly decrease functional connectivity between the subgenual ACC and ventral striatum from its resting-baseline level, which is an observation that has not previously been reported (we are, in fact, not aware of any studies that have specifically investigated the effects of cognitive engagement on the functional connectivity of the subgenual ACC). Given that both regions are major components of the medial frontal network, which underlies mood and emotional states, it is possible that a decrease in their functional connectivity during task performance corresponds with reduced subjective awareness in these domains. This idea is consistent with a growing body of evidence that has associated the deactivation of default mode network regions during external task performance with reduced self-focused spontaneous cognition that is characteristic of wakeful resting conditions (Mason et al., 2007; Christoff et al., 2009; Andrews-Hanna et al., 2010; see also Harrison et al., 2011). Whether task-induced changes in subgenual ACC connectivity represent a reduction in awareness or experience of mood or emotional state requires further investigation.

Unlike healthy participants, depressed participants did not show any modulation of connectivity between the subgenual ACC and ventral striatum, suggesting that the functional coupling of these regions persisted between the resting and task conditions. The subgenual ACC and ventral striatum showed significant resting-state connectivity in both groups (as incorporated in our resting-state mask), and have not previously been reported to show resting-state connectivity alterations in depression. The finding is therefore most likely explained by connectivity differences during task performance. The striatum has previously been reported to show decreased activation to rewarding stimuli in both depressed patients (Pizzagalli et al., 2009) and those at risk of depression

Table 2 | Functional connectivity changes with subgenual ACC from rest to cognitive control task, thresholded at $P < 0.005$.

Brain region	Number of voxels in cluster	Peak Z-score	Peak voxel coordinates (x y z)	Cluster-level probability*
CONTROLS				
R. Ventral striatum	155	5.1	16 16 −6	<0.01
DEPRESSED				
L. Medial frontal gyrus (BA 10)	57	3.6	−12 34 −10	0.01
CONTROLS > DEPRESSED				
R. Ventral striatum	52	3.4	14 16 −6	0.01
DEPRESSED > CONTROL				
L. Medial frontal gyrus (BA 10)	61	4.4	−16 34 −8	<0.01
R. Medial frontal gyrus (BA 10)	19	3.5	12 38 −10	(0.06)

**Cluster-level probabilities were calculated using Monte Carlo simulation (as implemented in AlphaSim) within a mask consisting of the resting-state connectivity map for the subgenual ACC.*

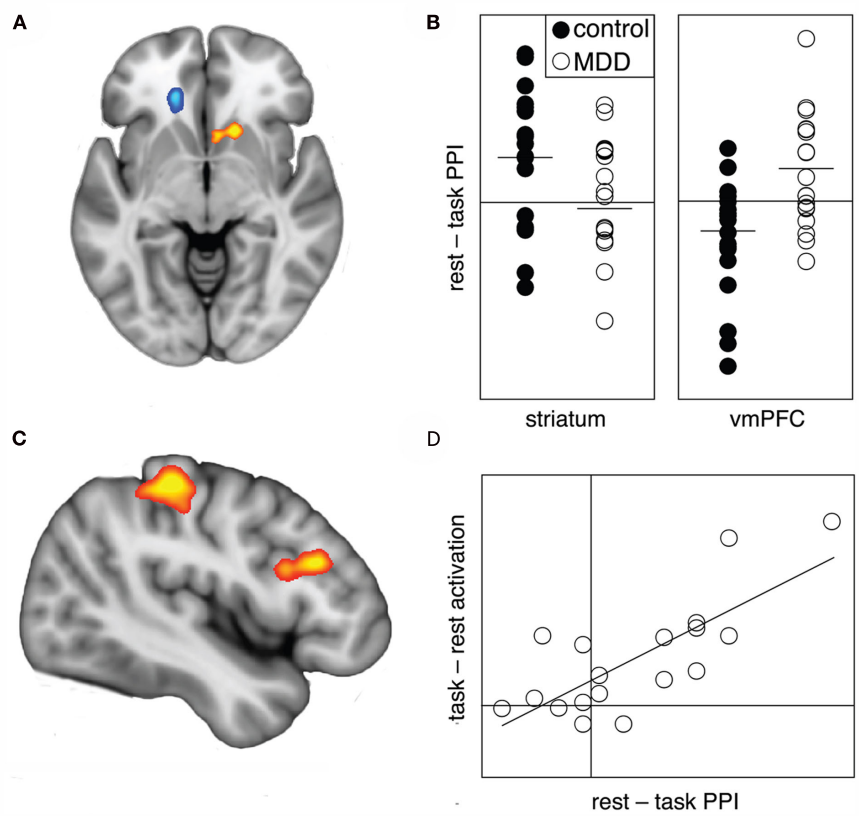

FIGURE 2 | Psycho-physiological interactions analysis demonstrated between-group differences in connectivity with the subgenual ACC between rest and task blocks (A). Control participants showed significantly greater changes in connectivity between rest and task conditions in ventral striatum (orange), while depressed participants showed greater connectivity changes in ventromedial frontal cortex (blue). The nature of the changes are illustrated in the adjacent charts **(B)**, with the parameter values extracted from a 3.5 mm sphere around the peak voxel: note that a positive parameter value indicates increased connectivity at rest compared to task (or reduced connectivity during task performance). For the depressed participants, the extent of the reduction in connectivity between the subgenual ACC and ventromedial frontal cortex predicted task-induced activations in left superior parietal cortex and left dorsolateral frontal cortex **(C)**. The adjacent chart **(D)** illustrates the correlation, with the parameter values extracted from 3.5 mm spheres around the peak voxels from the ventromedial frontal cortex and superior parietal cortex.

(Gotlib et al., 2010). The results of this study suggest that this might in part be explained by depression-related impairment of task-induced connectivity changes with the subgenual ACC, whereby the altered connectivity influences the responsiveness of the ventral striatum to certain types of external stimulation. An examination of such interactions may usefully extend previous studies on reward processing impairments in depression.

While depressed participants did not show connectivity changes between subgenual ACC and striatum, they did show connectivity changes with adjacent ventromedial frontal cortex. Default mode network functional connectivity has been demonstrated to be robust and relatively consistent across task conditions in healthy participants (Hampson et al., 2006; Fransson and Marrelec, 2008; Harrison et al., 2008; Bluhm et al., 2011), and no differences in connectivity between the subgenual ACC and default mode regions were observed in control participants in this study. Not only did depressed participants show reduced connectivity between the subgenual ACC and ventromedial frontal cortex during task performance compared to rest, but the extent of the reduction showed correlation with greater activation of task-relevant executive-control regions. The fact that there were no differences between the groups in either behavioral performance or task-induced activations suggests that the connectivity changes may be functionally adaptive: that is, the connectivity changes allowed the depressed participants to perform the task in a manner similar to the control participants.

The lack of task-induced deactivation changes is in contrast to previous studies that have reported reduced deactivations in depressed participants performing cognitive tasks (Harvey et al., 2005; Wagner et al., 2005) – who, similarly to the findings of our study, showed no differences in behavioral performances. It is not clear why our study did not show the same deactivation differences, though one explanation is that our study included younger patients in early phases of illness, when cognitive impairment is not such a significant component (Grant et al., 2001; Kyte et al., 2005). Despite not showing differences in task-induced deactivations, the depressed participants did show different patterns of connectivity changes, which may presage changes in medial network deactivation and cognitive task performances later in the course of their illnesses.

The study has its limitations. Our study sample included young people ranging in age from late adolescence to early adulthood; and while the age range is relatively narrow, it does encompass a developmental period over which significant brain maturational processes occur, including changes in brain connectivity These changes from childhood to adulthood include decreases in short-range connections and increases in longer-range connections (Fair et al., 2007a; Supekar et al., 2009; Dosenbach et al., 2010) – including with cingulate regions (Kelly et al., 2009) – with increasing coherence in connectivity of the default mode network (Fair et al., 2008). Age was included as a covariate in our analyses, however, and is therefore unlikely to have had significant influence on the results. We included participants who were taking medication, reflective of the nature of the clinical group recruited for the study. Again, this was added as a covariate to the analyses to mitigate its influence on the current results. A further limitation of the study is inherent in the PPI methodology used. While PPI provides a relatively simple and robust way of investigating functional connectivity changes during task performance, it cannot provide information on the causal influence that one brain region exerts on another (or "effective connectivity"). The results of study could be usefully validated and extended with the use of a technique such as dynamic causal modeling (DCM; Friston et al., 2003), which would be able to provide more information on what was driving the connectivity changes we have shown.

The study reinforces the importance of the extended medial prefrontal network for depression. It demonstrates how alterations in connectivity in the network, which mainly supports visceromotor function, might also influence cognitive–attentional processes. The reported dysfunction in cognitive and attentional processes that are often reported in depressed participants – and in the underlying frontoparietal brain regions that support them – might in fact be a secondary consequence of medial network dysfunction. The subgenual cingulate cortex is an important region for depression, and the results of the study provide further evidence for how dysfunction of subgenual ACC contributes to the illness.

ACKNOWLEDGMENTS

Dr. Davey is supported by a National Health and Medical Research Council (NHMRC) Early Career Fellowship (ID No. 628922), Dr. Harrison (ID No. 628509) is supported by an NHMRC Clinical Career Development Award, Dr. Yücel (ID No. 509345) is supported by an NHMRC Senior Research Fellowship (ID No. 1021973), and Dr. Allen is partially supported by a grant from the Colonial Foundation.

REFERENCES

Anand, A., Li, Y., Wang, Y., Wu, J., Gao, S., Bukhari, L., Mathews, V. P., Kalnin, A., and Lowe, M. J. (2005). Activity and connectivity of brain mood regulating circuit in depression: a functional magnetic resonance study. *Biol. Psychiatry* 57, 1079–1088.

Andrews-Hanna, J. R., Reidler, J. S., Huang, C., and Buckner, R. L. (2010). Evidence for the default network's role in spontaneous cognition. *J. Neurophysiol.* 104, 322–335.

Anticevic, A., Repovs, G., Shulman, G. L., and Barch, D. M. (2010). When less is more: TPJ and default network deactivation during encoding predicts working memory performance. *Neuroimage* 49, 2638–2648.

Beck, A. T., Steer, R. A., and Brown, G. K. (1996). *Manual for the Beck Depression Inventory-II.* San Antonio: Psychological Corporation.

Beckmann, M., Johansen-Berg, H., and Rushworth, M. F. (2009). Connectivity-based parcellation of human cingulate cortex and its relation to functional specialization. *J. Neurosci.* 29, 1175–1190.

Bluhm, R. L., Clark, C. R., McFarlane, A. C., Moores, K. A., Shaw, M. E., and Lanius, R. A. (2011). Default network connectivity during a working memory task. *Hum. Brain Mapp.* 32, 1029–1035.

Buckner, R. L., Andrews-Hanna, J. R., and Schacter, D. L. (2008). The brain's default network: anatomy, function, and relevance to disease. *Ann. N. Y. Acad. Sci.* 1124, 1–38.

Bush, G., and Shin, L. M. (2006). The multi-source interference task: an fMRI task that reliably activates the cingulo-frontal-parietal cognitive/attention network. *Nat. Protoc.* 1, 308–313.

Christoff, K., Gordon, A. M., Smallwood, J., Smith, R., and Schooler, J. W. (2009). Experience sampling during fMRI reveals default network and executive system contributions to mind wandering. *Proc. Natl. Acad. Sci. U.S.A.* 106, 8719–8724.

Davey, C. G., Harrison, B. J., Yücel, M., and Allen, N. B. (2012). Regionally specific alterations in functional connectivity of the anterior cingulate cortex in major depressive disorder. *Psychol. Med.*

Davey, C. G., Yucel, M., and Allen, N. B. (2008). The emergence of depression in adolescence: development of the prefrontal cortex and the representation of reward. *Neurosci. Biobehav. Rev.* 32, 1–19.

Dosenbach, N. U., Nardos, B., Cohen, A. L., Fair, D. A., Power, J. D., Church, J. A., Nelson, S. M., Wig, G. S., Vogel, A. C., Lessov-Schlaggar, C. N., Barnes, K. A., Dubis, J. W., Feczko, E., Coalson, R. S., Pruett, J. R. J., Barch, D. M., Petersen, S. E., and Schlaggar, B. L. (2010). Prediction of individual brain maturity using fMRI. *Science* 329, 1358–1361.

Drevets, W. C. (1999). Prefrontal cortical-amygdalar metabolism in major depression. *Ann. N. Y. Acad. Sci.* 877, 614–637.

Dunn, R. T., Kimbrell, T. A., Ketter, T. A., Frye, M. A., Willis, M. W., Luckenbaugh, D. A., and Post, R. M. (2002). Principal components of the Beck Depression Inventory and regional cerebral metabolism in unipolar and bipolar depression. *Biol. Psychiatry* 51, 387–399.

Fair, D. A., Cohen, A. L., Dosenbach, N. U., Church, J. A., Miezin, F. M., Barch, D. M., Raichle, M. E., Petersen, S. E., and Schlaggar, B. L. (2008). The maturing architecture of the brain's default network. *Proc. Natl. Acad. Sci. U.S.A.* 105, 4028–4032.

Fair, D. A., Dosenbach, N. U., Church, J. A., Cohen, A. L., Brahmbhatt, S., Miezin, F. M., Barch, D. M., Raichle, M. E., Petersen, S. E., and Schlaggar, B. L. (2007a). Development of distinct control networks through segregation and integration. *Proc. Natl. Acad. Sci. U.S.A.* 104, 13507–13512.

Fair, D. A., Schlaggar, B. L., Cohen, A. L., Miezin, F. M., Dosenbach, N. U., Wenger, K. K., Fox, M. D., Snyder, A. Z., Raichle, M. E., and Petersen, S. E. (2007b). A method for using blocked and event-related fMRI data to study "resting state" functional connectivity. *Neuroimage* 35, 396–405.

Ferry, A. T., Ongur, D., An, X., and Price, J. L. (2000). Prefrontal cortical projections to the striatum in macaque monkeys: evidence for an organization related to prefrontal networks. *J. Comp. Neurol.* 425, 447–470.

First, M. B., Spitzer, R. L., Gibbon, M., and Williams, J. B. W. (1997). *Structured Clinical Interview for DSM-IV Axis I Disorders (SCID-I).* Washington: American Psychiatric Publishing.

Fox, M. D., Snyder, A. Z., Vincent, J. L., Corbetta, M., Van Essen, D. C., and Raichle, M. E. (2005). The human brain is intrinsically organized into dynamic, anticorrelated functional networks. *Proc. Natl. Acad. Sci. U.S.A.* 102, 9673–9678.

Fransson, P., and Marrelec, G. (2008). The precuneus/posterior cingulate cortex plays a pivotal role in the default mode network: evidence from a partial correlation network analysis. *Neuroimage* 42, 1178–1184.

Friston, K. J., Buechel, C., Fink, G. R., Morris, J., Rolls, E., and Dolan, R. J. (1997). Psychophysiological and modulatory interactions in neuroimaging. *Neuroimage* 6, 218–229.

Friston, K. J., Harrison, L., and Penny, W. (2003). Dynamic causal modelling. *Neuroimage* 19, 1273–1302.

Ghatan, P. H., Hsieh, J. C., Wirsen-Meurling, A., Wredling, R., Eriksson, L., Stone-Elander, S., Levander, S., and Ingvar, M. (1995). Brain activation induced by the perceptual maze test: a PET study of cognitive performance. *Neuroimage* 2, 112–124.

Gotlib, I. H., Hamilton, J. P., Cooney, R. E., Singh, M. K., Henry, M. L., and Joormann, J. (2010). Neural processing of reward and loss in girls at risk for major depression. *Arch. Gen. Psychiatry* 67, 380–387.

Gotlib, I. H., and Joormann, J. (2010). Cognition and depression: current status and future directions. *Annu. Rev. Clin. Psychol.* 6, 285–312.

Grant, M. M., Thase, M. E., and Sweeney, J. A. (2001). Cognitive disturbance in outpatient depressed younger adults: evidence of modest impairment. *Biol. Psychiatry* 50, 35–43.

Greicius, M. D., Flores, B. H., Menon, V., Glover, G. H., Solvason, H. B., Kenna, H., Reiss, A. L., and Schatzberg, A. F. (2007). Resting-state functional connectivity in major depression: abnormally increased contributions from subgenual cingulate cortex and thalamus. *Biol. Psychiatry* 62, 429–437.

Greicius, M. D., Krasnow, B., Reiss, A. L., and Menon, V. (2003). Functional connectivity in the resting brain: a network analysis of the default mode hypothesis. *Proc. Natl. Acad. Sci. U.S.A.* 100, 253–258.

Grimm, S., Ernst, J., Boesiger, P., Schuepbach, D., Hell, D., Boeker, H., and Northoff, G. (2009). Increased self-focus in major depressive disorder is related to neural abnormalities in subcortical-cortical midline structures. *Hum. Brain Mapp.* 30, 2617–2627.

Hamani, C., Mayberg, H., Stone, S., Laxton, A., Haber, S., and Lozano, A. M. (2011). The subcallosal cingulate gyrus in the context of major depression. *Biol. Psychiatry* 69, 301–308.

Hamilton, J. P., Chen, G., Thomason, M. E., Schwartz, M. E., and Gotlib, I. H. (2011). Investigating neural primacy in major depressive disorder: multivariate Granger causality analysis of resting-state fMRI time-series data. *Mol. Psychiatry* 16, 763–772.

Hampson, M., Driesen, N. R., Skudlarski, P., Gore, J. C., and Constable, R. T. (2006). Brain connectivity related to working memory performance. *J. Neurosci.* 26, 13338–13343.

Harrison, B. J., Pujol, J., Contreras-Rodriguez, O., Soriano-Mas, C., Lopez-Sola, M., Deus, J., Ortiz, H., Blanco-Hinojo, L., Alonso, P., Hernandez-Ribas, R., Cardoner, N., and Menchon, J. M. (2011). Task-induced deactivation from rest extends beyond the default mode brain network. *PLoS ONE* 6, e22964. doi:10.1371/journal.pone.0022964

Harrison, B. J., Pujol, J., Lopez-Sola, M., Hernandez-Ribas, R., Deus, J., Ortiz, H., Soriano-Mas, C., Yucel, M., Pantelis, C., and Cardoner, N. (2008). Consistency and functional specialization in the default mode brain network. *Proc. Natl. Acad. Sci. U.S.A.* 105, 9781–9786.

Harrison, B. J., Yucel, M., Pujol, J., and Pantelis, C. (2007). Task-induced deactivation of midline cortical regions in schizophrenia assessed with fMRI. *Schizophr. Res.* 91, 82–86.

Harvey, P. O., Fossati, P., Pochon, J. B., Levy, R., Lebastard, G., Lehericy, S., Allilaire, J. F., and Dubois, B. (2005). Cognitive control and brain resources in major depression: an fMRI study using the n-back task. *Neuroimage* 26, 860–869.

Keedwell, P. A., Andrew, C., Williams, S. C., Brammer, M. J., and Phillips, M. L. (2005). The neural correlates of anhedonia in major depressive disorder. *Biol. Psychiatry* 58, 843–853.

Kelly, A. M., Di Martino, A., Uddin, L. Q., Shehzad, Z., Gee, D. G., Reiss, P. T., Margulies, D. S., Castellanos, F. X., and Milham, M. P. (2009). Development of anterior cingulate functional connectivity from late childhood to early adulthood. *Cereb. Cortex* 19, 640–657.

Kyte, Z. A., Goodyer, I. M., and Sahakian, B. J. (2005). Selected executive skills in adolescents with recent first episode major depression. *J. Child Psychol. Psychiatry* 46, 995–1005.

Lozano, A. M., Mayberg, H. S., Giacobbe, P., Hamani, C., Craddock, R. C., and Kennedy, S. H. (2008). Subcallosal cingulate gyrus deep brain stimulation for treatment-resistant depression. *Biol. Psychiatry* 64, 461–467.

Margulies, D. S., Kelly, A. M., Uddin, L. Q., Biswal, B. B., Castellanos, F. X., and Milham, M. P. (2007). Mapping the functional connectivity of anterior cingulate cortex. *Neuroimage* 37, 579–588.

Mason, M. F., Norton, M. I., Van Horn, J. D., Wegner, D. M., Grafton, S. T., and Macrae, C. N. (2007). Wandering minds: the default network and stimulus-independent thought. *Science* 315, 393–395.

Mayer, J. S., Roebroeck, A., Maurer, K., and Linden, D. E. (2010). Specialization in the default mode: task-induced brain deactivations dissociate between visual working memory and attention. *Hum. Brain Mapp.* 31, 126–139.

McGorry, P. (1998). Beyond adolescent psychiatry: the logic of a youth mental health model. *Aust. N. Z. J. Psychiatry* 32, 138–140.

McKiernan, K. A., Kaufman, J. N., Kucera-Thompson, J., and Binder, J. R. (2003). A parametric manipulation of factors affecting task-induced deactivation in functional neuroimaging. *J. Cogn. Neurosci.* 15, 394–408.

Pizzagalli, D. A., Holmes, A. J., Dillon, D. G., Goetz, E. L., Birk, J. L., Bogdan, R., Dougherty, D. D., Iosifescu, D. V., Rauch, S. L., and Fava, M. (2009). Reduced caudate and nucleus accumbens response to rewards in unmedicated individuals with major depressive disorder. *Am. J. Psychiatry* 166, 702–710.

Price, J. L., and Drevets, W. C. (2010). Neurocircuitry of mood disorders. *Neuropsychopharmacology* 35, 192–216.

Raichle, M. E., MacLeod, A. M., Snyder, A. Z., Powers, W. J., Gusnard, D. A., and Shulman, G. L. (2001). A default mode of brain function. *Proc. Natl. Acad. Sci. U.S.A.* 98, 676–682.

Sala-Llonch, R., Pena-Gomez, C., Arenaza-Urquijo, E. M., Vidal-Pineiro, D., Bargallo, N., Junque, C., and Bartres-Faz, D. (2011). Brain connectivity during resting state and subsequent working memory task predicts behavioural performance. *Cortex.* (in press).

Seeley, W. W., Menon, V., Schatzberg, A. F., Keller, J., Glover, G. H., Kenna, H., Reiss, A. L., and Greicius, M. D. (2007). Dissociable intrinsic connectivity networks for salience processing and executive control. *J. Neurosci.* 27, 2349–2356.

Sheline, Y. I., Barch, D. M., Price, J. L., Rundle, M. M., Vaishnavi, S. N., Snyder, A. Z., Mintun, M. A., Wang, S., Coalson, R. S., and Raichle, M. E. (2009). The default mode network and self-referential processes in depression. *Proc. Natl. Acad. Sci. U.S.A.* 106, 1942–1947.

Sheline, Y. I., Price, J. L., Yan, Z., and Mintun, M. A. (2010). Resting-state functional MRI in depression unmasks increased connectivity between networks via the dorsal nexus. *Proc. Natl. Acad. Sci. U.S.A.* 107, 11020–11025.

Shulman, G. L., Corbetta, M., Buckner, R. L., Fiez, J. A., Miezin, F. M., Raichle, M. E., and Petersen, S. E. (1997). Common blood flow changes across visual tasks: II. Decreases in cerebral cortex. *J. Cogn. Neurosci.* 9, 648–663.

Spreng, R. N., Stevens, W. D., Chamberlain, J. P., Gilmore, A. W., and Schacter, D. L. (2010). Default network activity, coupled with the frontoparietal control network, supports goal-directed cognition. *Neuroimage* 53, 303–317.

Sridharan, D., Levitin, D. J., and Menon, V. (2008). A critical role for the right fronto-insular cortex in switching between central-executive and default-mode networks. *Proc. Natl. Acad. Sci. U.S.A.* 105, 12569–12574.

Supekar, K., Musen, M., and Menon, V. (2009). Development of large-scale functional brain networks in children. *PLoS Biol.* 7, e1000157. doi:10.1371/journal.pbio.1000157

Wagner, A. D., Shannon, B. J., Kahn, I., and Buckner, R. L. (2005). Parietal lobe contributions to episodic memory retrieval. *Trends Cogn. Sci. (Regul. Ed.)* 9, 445–453.

Wagner, G., Sinsel, E., Sobanski, T., Kohler, S., Marinou, V., Mentzel, H. J., Sauer, H., and Schlosser, R. G. (2006). Cortical inefficiency in patients with unipolar depression: an event-related fMRI study with the Stroop task. *Biol. Psychiatry* 59, 958–965.

Whitfield-Gabrieli, S., Thermenos, H. W., Milanovic, S., Tsuang, M. T., Faraone, S. V., McCarley, R. W., Shenton, M. E., Green, A. I., Nieto-Castanon, A., LaViolette, P., Wojcik, J., Gabrieli, J. D., and Seidman, L. J. (2009). Hyperactivity and hyperconnectivity of the default network in schizophrenia and in first-degree relatives of persons with schizophrenia. *Proc. Natl. Acad. Sci. U.S.A.* 106, 1279–1284.

Yucel, M., Harrison, B. J., Wood, S. J., Fornito, A., Clarke, K., Wellard, R. M., Cotton, S., and Pantelis, C. (2007). State, trait and biochemical influences on human anterior cingulate function. *Neuroimage* 34, 1766–1773.

Conflict of Interest Statement: The authors declare that the research was conducted in the absence of any commercial or financial relationships that could be construed as a potential conflict of interest.

Received: 25 November 2011; accepted: 14 February 2012; published online: 28 February 2012.

*Citation: Davey CG, Yücel M, Allen NB and Harrison BJ (2012) Task-related deactivation and functional connectivity of the subgenual cingulate cortex in major depressive disorder. Front. Psychiatry **3**:14. doi: 10.3389/fpsyt.2012.00014*

This article was submitted to Frontiers in Neuropsychiatric Imaging and Stimulation, a specialty of Frontiers in Psychiatry.

frontiers in
PSYCHIATRY

ORIGINAL RESEARCH ARTICLE
published: 11 January 2012
doi: 10.3389/fpsyt.2011.00083

Resting state functional connectivity correlates of inhibitory control in children with attention-deficit/hyperactivity disorder

Maarten Mennes[1†], Natan Vega Potler[1†], Clare Kelly[1], Adriana Di Martino[1], F. Xavier Castellanos[1,2] and Michael P. Milham[2,3]*

[1] *Phyllis Green and Randolph Cowen Institute for Pediatric Neuroscience, NYU Langone School of Medicine, NYU Child Study Center, New York, NY, USA*
[2] *Nathan Kline Institute for Psychiatric Research, Orangeburg, NY, USA*
[3] *Center for the Developing Brain, Child Mind Institute, New York, NY, USA*

Edited by:
Alex Fornito, University of Melbourne, Australia

Reviewed by:
Damien Fair, Oregon Health and Science University, USA
Jessica A. Church, Washington University School of Medicine, USA

****Correspondence:***
Michael P. Milham, Child Mind Institute, 445 Park Avenue, New York, NY 10022, USA.
e-mail: michael.milham@childmind.org

†Maarten Mennes and Natan Vega Potler have contributed equally to this work.

Motor inhibition is among the most commonly studied executive functions in attention-deficit/hyperactivity disorder (ADHD). Imaging studies using probes of motor inhibition such as the stop signal task (SST) consistently demonstrate ADHD-related dysfunction within a right-hemisphere fronto-striatal network that includes inferior frontal gyrus and pre-supplementary motor area. Beyond findings of focal hypo- or hyper-function, emerging models of ADHD psychopathology highlight disease-related changes in functional interactions between network components. Resting state fMRI (R-fMRI) approaches have emerged as powerful tools for mapping such interactions (i.e., resting state functional connectivity, RSFC), and for relating behavioral and diagnostic variables to network properties. We used R-fMRI data collected from 17 typically developing controls (TDC) and 17 age-matched children with ADHD (aged 8–13 years) to identify neural correlates of SST performance measured outside the scanner. We examined two related inhibition indices: stop signal reaction time (SSRT), indexing inhibitory speed, and stop signal delay (SSD), indexing inhibitory success. Using 11 fronto-striatal seed regions-of-interest, we queried the brain for relationships between RSFC and each performance index, as well as for interactions with diagnostic status. Both SSRT and SSD exhibited connectivity–behavior relationships independent of diagnosis. At the same time, we found differential connectivity–behavior relationships in children with ADHD relative to TDC. Our results demonstrate the utility of RSFC approaches for assessing brain/behavior relationships, and for identifying pathology-related differences in the contributions of neural circuits to cognition and behavior.

Keywords: ADHD, connectivity, intrinsic architecture, transition zones, rest, fMRI, interaction

INTRODUCTION

Emerging models of attention-deficit/hyperactivity disorder (ADHD) pathophysiology highlight disease-related alterations in functional interactions among multiple brain regions, extending the traditional focus on frontal–striatal dysfunction (Dickstein et al., 2006). Using resting state functional connectivity (RSFC) as an index of functional interactions, studies have demonstrated ADHD-related abnormalities in the interactions among brain regions supporting the implementation and maintenance of attentional control [e.g., dorsal anterior cingulate cortex (dACC) and insula; Tian et al., 2006]. ADHD-related constraints in the segregation of processing between attentional control regions and those implicated in *internal mentation* (i.e., the default network) have been demonstrated (Castellanos et al., 2008), as well as ADHD-related differences in functional connectivity within the default network itself (Fair et al., 2010; Chabernaud et al., in press). Reminiscent of developmental immaturity (Fair et al., 2008), these findings have intrigued researchers and invigorated new avenues of inquiry. Yet, little has been done experimentally to bridge emerging dysconnectivity models with existent neuropsychological models of ADHD.

Here, we take a first step toward linking neuropsychological and dysconnectivity models of ADHD. In particular, we focus on impaired inhibitory control, commonly considered a hallmark of ADHD (Nigg, 2001). Previously, task-based imaging studies using common behavioral probes of inhibitory control such as the Go–No Go and stop signal task (SST) have implicated fronto-striatal circuitry in ADHD (Nigg, 1999; Konrad et al., 2000; Aron and Poldrack, 2005). Specifically, they revealed hypoactivation in a predominantly right-hemispheric network encompassing the inferior frontal gyrus/anterior insula, pre-supplementary motor area (pre-SMA), dACC, thalamus, and caudate nucleus (Rubia et al., 1999; Aron and Poldrack, 2005; for a review see Dickstein et al., 2006; Cubillo et al., 2010). In the present work, we related inter-individual differences in SST performance to differences in connectivity observed for fronto-striatal regions-of-interest (ROI). In addition, we assessed the modulatory effect of the presence or absence of an ADHD diagnosis on such relationships.

We focused on inhibitory measures obtained during SST performance. The SST is a common probe for inhibitory control, requiring inhibition of a prepotent Go response upon presentation of an auditory stop signal. Two performance measures related to inhibitory control can be derived from the SST. (1) The stop signal delay (SSD) is the average delay between stimulus presentation and presentation of the auditory stop signal. Across "stop trials," the SSD is titrated based on the participant's inhibitory success. (2) The stop signal reaction time (SSRT) is an index of inhibitory process speed, and is estimated by subtracting the mean SSD from the mean go reaction time. While increased SSRT in ADHD is commonly interpreted as less efficient inhibitory control, higher SSRT in ADHD may also reflect slower and more inconsistent motor responses and visual stimulus processing (Alderson et al., 2007, 2008). Finding that children with ADHD exhibited slower SSRT and Go reaction times, but not shorter SSD, Alderson and colleagues concluded that children with ADHD exhibited motor slowing or general inattention rather than a primary inhibition deficit (see also Castellanos et al., 2006). This prompted the recommendation that SSD be included as an additional measure of motor inhibition given its more direct link to inhibitory success (Alderson et al., 2007, 2008). Indeed, in tracking versions of the SST (such as the one we used), the SSD is adjusted on every stop trial depending on whether the participant successfully inhibited his/her response on the previous stop trial.

Both SST inhibition performance measures (SSD, SSRT), obtained outside the MRI scanner, were related to RSFC measured during functional MRI scans in which participants were simply directed to rest. In particular, we investigated patterns of functional connectivity related to 11 fronto-striatal brain ROI implicated in inhibitory control (Boehler et al., 2010).

MATERIALS AND METHODS

PARTICIPANTS

Sixty-three children, including typically developing children (TDC) and children with ADHD, completed the SST task and a resting state scan session. Eighteen participants were excluded from further analyses due to SST Go trial accuracy < 75% (Nigg, 1999), and five more because of excessive motion during the resting state scan (see fMRI Image Preprocessing). In addition, six participants were excluded because their performance was >2 SD beyond the mean on a behavioral performance variable (SSRT, SSD, mean reaction time, or reaction time coefficient of variation). Our intent was to include only those children who could be confidently regarded as having followed task instructions.

Consequently, data from 34 children (aged 8–13 years) were analyzed in the current study (**Table 1** shows participant characteristics). Seventeen children were TDC (mean age 10.8 years) and 17 were diagnosed with ADHD (mean age 11 years). Within TDC 47% were female, in contrast with 18% females in the ADHD group ($\chi^2_{(1)} = 5.4$, $p = 0.015$). Children with ADHD and TDC exhibited similar estimates of full IQ indexed by the Wechsler Abbreviated Scale of Intelligence (WASI).

Typically developing children had no past or present DSM-IV-TR axis-I diagnosis or neurological illness nor history of treatment with psychotropic medications, as confirmed by parent administration of the Schedule of Affective Disorders and Schizophrenia for Children – Present and Lifetime Version (Kaufman et al., 1997; KSADS-PL). Children with Combined type ADHD ($n = 11$) and predominantly Inattentive type ADHD ($n = 6$) were included. Clinicians' DSM-IV-TR ADHD diagnoses were based on KSADS-PL interview. Four children with ADHD had comorbid oppositional defiant disorder, and one had comorbid adjustment disorder with depressive mood. Children with ADHD were excluded if they had a diagnosis of pervasive developmental disorders, psychosis or major depression or if they were treated with any non-stimulant psychotropic medications within the month prior to participation (3 months for neuroleptics). Only children with an estimated full IQ above 80 were included. Twelve children with ADHD (66%) were medication-naïve. Three children with ADHD currently treated with stimulant were asked to discontinue their medication 72 h prior to the scan session. Two remaining children were not treated with stimulants at the time of the study, but were treated at earlier points in their life. Finally, we obtained Conners Parent Rating Scale-Revised:Long Version (CPRS-R:L; Conners et al., 1998) scores for all participants. The CPRS-R:L is a widely used, normed parent questionnaire that assesses problems related to conduct, hyperactivity–impulsivity, and inattention as well as a range of other psychopathology.

As part of a 1-h scan session, all participants completed at least one 6.5 min resting state scan as well as a high-resolution anatomical scan (MPRAGE). After the scan session each participant completed a SST (Nigg, 1999) outside the scanner.

Table 1 | Participant characteristics and behavioral performance scores obtained from the stop signal task (SST).

	ADHD	TDC	*p*-Value
N	17; 3 female/14 male	17; 8 female/9 male	<**0.02**
Age	11.0 ± 1.26	10.8 ± 1.92	0.87
IQ	111.8 ± 14.26	112.1 ± 14.11	0.95
Mean go RT	629.9 ± 54.25	637.5 ± 62.97	0.35
Go RT CV	0.24 ± 0.02	0.23 ± 0.03	0.37
SSRT	299.1 ± 46.25	263.2 ± 63.94	<**0.03**
SSD	330.8 ± 73.26	374.3 ± 108.56	0.09
Go accuracy	0.89 ± 0.04	0.91 ± 0.05	0.23
Stop accuracy	0.52 ± 0.03	0.54 ± 0.05	0.21
CPRS-R			
DSM-IV total	71.24 ± 9.16	44.24 ± 4.58	<**0.01**
DSM-IV inattentive	71.00 ± 9.37	43.47 ± 3.76	<**0.01**
DSM-IV hyperactive/impulsive	67.53 ± 12.43	46.18 ± 5.33	<**0.01**
Cognitive problems/inattention	69.59 ± 8.69	43.76 ± 3.25	<**0.01**
Hyperactivity	65.29 ± 14.25	45.00 ± 2.78	<**0.01**
ADHD Index	72.59 ± 8.02	44.24 ± 3.73	<**0.01**

Go, Go trials; RT, reaction time; CV, coefficient of variation; SSRT, stop signal reaction time; SSD, stop signal delay; Stop, stop trials. p-Values for the SST behavioral measures and the Conners Parent Rating Scale-Revised (CPRS-R) measures are based on one-tailed t-tests. A significance level of $p < 0.05$ was used for all comparisons.

fMRI DATA ACQUISITION

Data were collected on a Siemens Allegra 3.0 Tesla scanner. All participants completed at least one 6.5 min long resting state fMRI (R-fMRI) scan (180 EPI volumes, TR = 2000 ms, TE = 25 ms, flip angle = 90°, 33 slices, voxels = 3 mm × 3 mm × 4 mm). All participants were instructed to rest with their eyes open during the scan. For spatial normalization and localization purposes we also acquired a high-resolution T1-weighted anatomical image (MPRAGE, TR = 2530 ms; TE = 3.25 ms; TI = 1100 ms; flip angle = 7°; 128 slices; FOV = 256 mm; voxel-size = 1 mm × 1.3 mm × 1.3 mm). Finally, a field map and short-TE EPI scan were also acquired to improve functional-to-anatomical co-registration.

STOP SIGNAL TASK

The SST is a computerized visual choice reaction time task aimed at examining inhibitory control (Logan et al., 1997; Nigg, 1999). On each trial an "X" or "O" was visually presented. Participants were required to respond as quickly and accurately as possible to the "X" or "O" by pressing "Enter" or "O," respectively. Each visual stimulus was displayed on the screen for 1000 ms. Trials were separated by a 500-ms display of a fixation cross and a 1000-ms blank screen. The SST comprised 80% Go trials and 20% Stop trials. On Go trials, participants were required to respond to the visual stimulus. In contrast, on Stop trials, an auditory stop stimulus was presented after the visual stimulus, indicating that participants had to inhibit their response. The delay between the visual stimulus and auditory stop stimulus (SSD) started at 250 ms. If participants successfully inhibited the prepotent Go response, the SSD on the next stop trial was increased by 50 ms, making inhibition more difficult on the next stop trial. If the participant failed to inhibit, the SSD on the next stop trial was decreased by 50 ms, i.e., the auditory tone was presented sooner, making inhibition easier. This procedure was implemented to attain a SSD at which participants were able to successfully inhibit 50% of the Stop trials. Based on the horse-race model (Logan et al., 1984), which posits a race between the go and inhibition processes, the process that finishes first gets executed. In successful stop trials the inhibition process is able to catch up and override the go process, while in unsuccessful stop trials the go response is executed before the inhibition process finishes. Based on this theory, titrating the SSD to obtain a 50% inhibition success rate makes it possible to obtain an estimate of the length of the inhibition process (SSRT) by subtracting the mean SSD from the mean Go reaction time. A smaller SSRT indicates a faster inhibition process. A smaller SSD indicates less successful inhibition, as participants require a shorter delay between the go stimulus and the stop signal to achieve successful inhibition. The SSRT and SSD thus form two related inhibitory indices of interest. After two practice blocks, all participants completed six task blocks. Each block comprised 32 trials: 24 go trials and 8 stop trials.

fMRI IMAGE PREPROCESSING

Data processing was performed using Analysis of Functional NeuroImaging[1] (AFNI) and FMRIB Software Library[2] (FSL). Image preprocessing consisted of discarding the first 4 EPI volumes from each resting state scan to allow for signal equilibration; slice time correction for interleaved acquisitions; 3-D motion correction with Fourier interpolation; despiking (detection and removal of extreme time series outliers); spatial smoothing using a 6-mm FWHM Gaussian kernel; mean-based intensity normalization of all volumes by the same factor; temporal bandpass filtering (0.009–0.1 Hz); and linear and quadratic detrending. FSL FLIRT was used for linear registration of the high-resolution structural images to the MNI152 template (Jenkinson and Smith, 2001; Jenkinson et al., 2002). This transformation was then refined using FNIRT non-linear registration (Andersson et al., 2007). Linear registration of each participant's functional time series to the high-resolution structural image was performed using FLIRT. This functional-to-anatomical co-registration was improved by intermediate registration to a low-resolution image and b0 unwarping.

We did not analyze participants who exhibited >4 mm maximum displacement between consecutive timepoints in their resting state scans as movement artifacts may affect resting state analyses (Van Dijk et al., 2012; Power et al., in press). When possible we analyzed the first resting state scan of the scan session. The first resting state scan was analyzed for all but one participant, whose first scan contained excessive motion. The second resting state scan was used for that participant. As indicated by the data shown in **Table 2**, our final sample contained limited motion artifacts, and children with ADHD did not differ from TDC in motion parameters. To remove between-participant variance related to differences in motion, we included the root mean square (RMS) of the maximum displacement between consecutive timepoints in the resting state scan as a covariate in all group-level analyses. Finally, in an effort to minimize the impact of motion artifacts, Power et al. (in press) propose removing timepoints containing movement artifacts from each

Table 2 | Mean ± SD for movement parameters calculated for the resting state scans.

	TDC	ADHD	*p*-Value
RMS mean relative displacement[v]	0.03 (±0.03)	0.03 (±0.02)	0.39
RMS maximum relative displacement[v]	0.23 (±0.30)	0.35 (±0.45)	0.18
N relative displacements >0.1 mm[v#]	8.65 (±12.7)	7.88 (±9.34)	0.42
Framewise displacement[p]	0.13 (±0.10)	0.12 (±0.07)	0.42
N framewise displacements >0.5 mm[p#]	4.53 (±8.99)	5.06 (±6.61)	0.85

Movement was calculated as the displacement between two consecutive timepoints (i.e., relative or framewise displacement). p-Values are indicated for one-sided unpaired t-tests between TDC and ADHD. RMS: Root Mean Square. [v]Measures derived from Van Dijk et al. (2012). [p]Measures derived from Power et al. (in press). [#]There were 180 available timepoints for every participant. As such, 10 displacements correspond to 5.5% of all timepoints and 5 displacements correspond to 3% of all timepoints.

[1] http://afni.nimh.nih.gov/afni
[2] www.fmrib.ox.ac.uk

participant's time series. Accordingly, we also repeated our analyses removing timepoints that exhibited micromovements exceeding 0.5 mm. As described in the supplementary material accompanying this paper, removing these timepoints did not alter our results.

NUISANCE SIGNAL REGRESSION

To control for the effects of motion and physiological processes (i.e., cardiac and respiratory fluctuations) at each timepoint, each participant's 4-D preprocessed volume was regressed with nine predictors that modeled white matter, cerebrospinal fluid, the global signal, and six motion parameters. The resultant 4-D residuals volumes were used in all subsequent analyses.

SEED SELECTION

We selected 11 seed ROIs from a recent study that attempted to improve the two most commonly used contrasts in SST-based fMRI investigations, namely comparing successful to unsuccessful stop trials and comparing successful stop to successful go trials (Boehler et al., 2010). As those authors note, the former approach is overly conservative, as it is not sensitive enough to measure the influence of inhibitory control in unsuccessful stop trials, while the latter approach does not account for the differential sensory requirements of the two trial types. Instead, Boehler and colleagues examined regions implicated in inhibitory control during successful as well as unsuccessful inhibitory trials, taking into account potential differences in sensory requirements. To this end they modeled a second-level conjunction contrast that included a comparison of successful and unsuccessful stop trials versus go trials, as well as a comparison of successful and unsuccessful stop trials versus stimulus-irrelevant stop trials. The stimulus-irrelevant stop trials shared the same sensory stimuli as the normal stop trials, but consisted of a passive viewing block.

We created spherical seeds (radius = 4 mm) centered on 11 different regions of the functional network implicated in response inhibition, as defined by the second-level conjunction analysis from Boehler et al. (see Table 5 in Boehler et al., 2010). Three coordinates of peak activity in the left insula that were less than 8 mm apart were averaged to avoid inclusion of redundant seed regions in our analysis. In addition, the left thalamus coordinates were adjusted to avoid partial voluming effects because the seed placed at the original coordinates included CSF voxels. Seed names and their coordinates are shown in **Table 3**. **Figure 1** displays the seeds on brain surface renderings.

PARTICIPANT-LEVEL ANALYSES

After extracting the mean time series for each seed in MNI152 2 mm standard space, we calculated whole-brain functional connectivity maps in native space by correlating the mean seed time series with the time series of every other voxel in the brain using AFNI 3dfim+. This produced participant-level correlation maps of voxels in the brain that positively or negatively correlated with the mean times series of each seed. The correlation maps were Fisher-z transformed to improve normal distribution and transformed into MNI152 2 mm × 2 mm × 2 mm standard space for further group-level analyses.

Table 3 | MNI152 standard space coordinates for seed regions used in the functional connectivity analyses.

Seed ROI	Hemisphere	MNI coordinates (*x, y, z*)		
Frontal operculum	R	50	18	0
Insula	R	42	10	−6
Insula[a]	L	−34	18	2
Pre-SMA	R	2	14	50
ACC	L/R	0	26	22
Supramarginal gyrus	R	58	−44	30
Mid-occipital gyrus	L	−32	−88	−2
Caudate	L	−8	16	6
Caudate	R	8	12	2
Thalamus	R	2	−20	2
Thalamus[b]	L	−4 (−2)	−16 (−12)	0 (0)

Seeds were selected from Boehler et al. (2010). [a]To avoid inclusion of redundant seed ROIs we averaged the coordinates of three insula seeds located near each other. [b]To avoid effects of partial voluming due to the fact that a seed placed at the original coordinates included CSF voxels, we adjusted the coordinates of the left thalamus seed. Original coordinates are shown between parentheses.

GROUP-LEVEL ANALYSES

Group-level mixed-effects analyses for each seed ROI were performed using FSL FEAT[3]. We assessed the relationship between RSFC and inhibition performance on the SST, as well as a possible interaction of this relationship with diagnosis. To this end we modeled diagnosis, SSRT, SSD, and a diagnosis-by-behavior interaction (obtained by multiplying diagnosis with the behavioral variables) for each SSRT and SSD in a two-sample t-test. Age, sex, maximum RMS displacement, and FIQ were included as covariates. While SSRT and SSD were highly correlated ($r = -0.81$), tolerance $[(1-r^2) = 0.32]$, and a variance inflation factor of 3.1 support the validity of including both measures in the same model.

We also investigated the effect of diagnosis in a two-sample t-test. Age, sex, maximum RMS displacement, and FIQ were again included as covariates. For all analyses, correction for multiple comparisons was carried out at the cluster level using Gaussian random field theory (voxel-wise: minimum Z-score > 2.3; $p < 0.05$ corrected).

RESULTS

BEHAVIORAL RESULTS

Replicating previous findings, children with ADHD exhibited significantly higher SSRT relative to TDC (one-tailed unpaired t-test $p = 0.03$; **Figure 2**; **Table 1**). Although not significant, we observed marginally lower SSD in ADHD relative to TDC ($p = 0.09$, one-tailed; **Figure 2**). No significant differences were observed for mean Go reaction time ($p = 0.35$), Go reaction time coefficient of variation ($p = 0.37$), Go trial accuracy ($p = 0.23$), or stop trial accuracy ($p = 0.21$; see **Table 1**).

CONNECTIVITY–BEHAVIOR RELATIONSHIPS ACROSS PARTICIPANTS

Regression analysis revealed a significant relationship between differences in SSRT among participants and inter-individual

[3]http://fsl.fmrib.ox.ac.uk/fsl/feat5

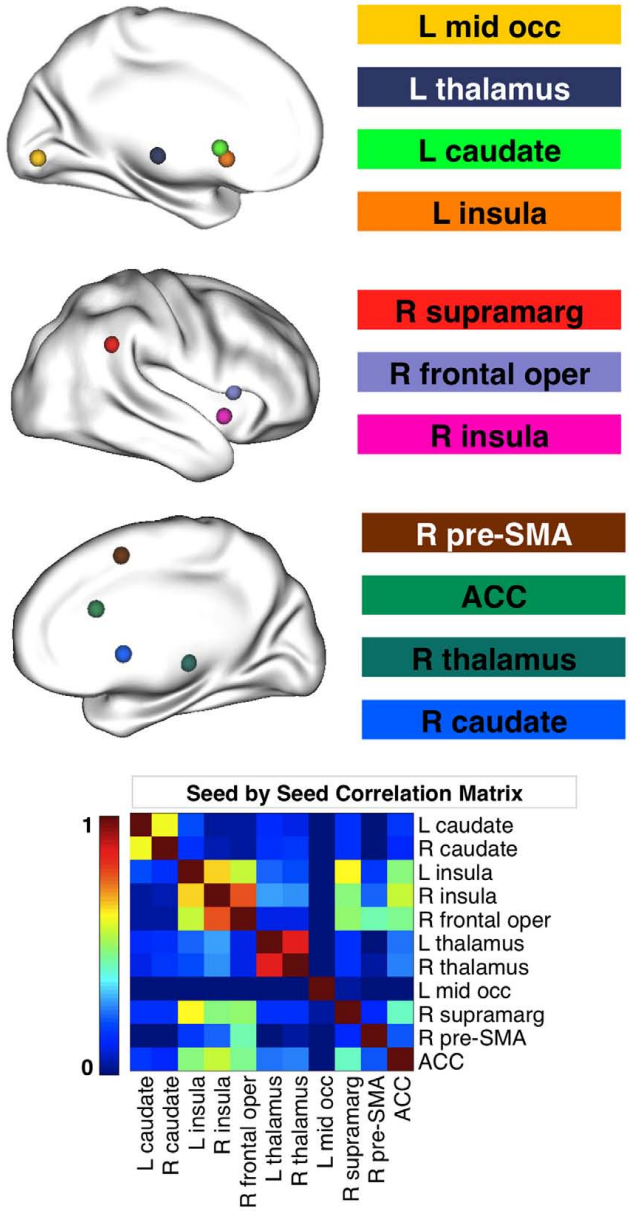

FIGURE 1 | Seed ROI used for functional connectivity analyses. The 11 seed regions were derived from Boehler et al. (2010) and are based on a conjunction analysis that assessed inhibitory control in the stop signal task (SST). The matrix at the bottom of the figure illustrates the seed by seed correlations for the typically developing children in our study. There was no effect of diagnosis on the seed by seed correlations, nor were the correlations related to the SST performance measures. R, right; L, left; mid occ, middle occipital gyrus; supramarg, supramarginal gyrus; pre-SMA, pre-supplementary motor area; ACC, anterior cingulate cortex.

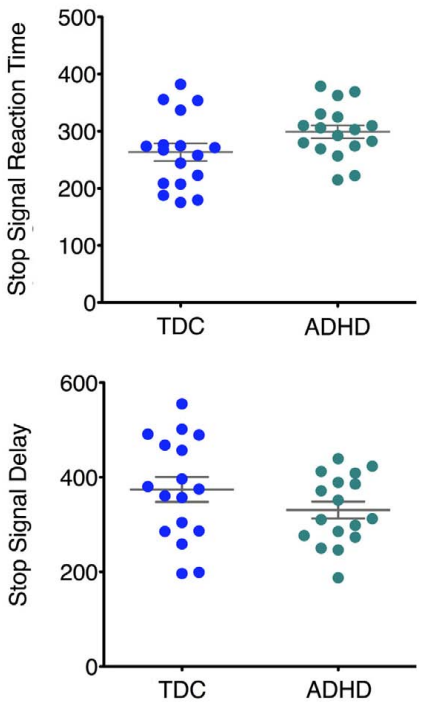

FIGURE 2 | Main effect of ADHD on SSRT ($p < 0.03$) and SSD ($p = 0.09$). Gray lines indicate mean ± SE.

variation in the functional connectivity networks of the anterior cingulate cortex, right pre-SMA, and right thalamus seeds (see **Figure 3**; **Table 4** lists the peak coordinates for each significant cluster). Specifically, higher SSRT (slower inhibition process) was associated with increased positive connectivity between right thalamus and anterior cingulate cortex. A similar effect was observed for the ACC and pre-SMA seeds ($Z > 2.3$; $p < 0.05$, corrected). The significant cluster observed for the pre-SMA seed further extended into left superior frontal gyrus. Finally, we also observed a significant positive SSRT-connectivity relationship between the right thalamus seed and left putamen.

Differences in SSD among participants were related to inter-individual variation in the functional connectivity networks of right caudate and pre-SMA (**Figure 3**). Longer SSD were associated with increased *positive* connectivity between pre-SMA and anterior cingulate cortex/left superior frontal gyrus. In contrast, increased *positive* connectivity between pre-SMA and right middle frontal gyrus was associated with shorter SSD. Shorter SSD were also associated with increased *negative* functional connectivity between the right caudate seed and left intracalcarine cortex.

As shown in **Figure 4**, the clusters exhibiting a significant positive connectivity–behavior relationship for pre-SMA were highly similar whether based on SSRT or SSD. In addition, **Figure 4** shows that the clusters that exhibited a significant RSFC–behavior relationship for the pre-SMA seed were located in so-called "transition zones" located between overall positive and negative RSFC of the pre-SMA seed.

CONNECTIVITY–BEHAVIOR RELATIONSHIPS MODULATED BY DIAGNOSIS

We further assessed whether connectivity–behavior relationships were modulated by the presence or absence of ADHD. This was achieved by including a diagnosis-by-behavior interaction for

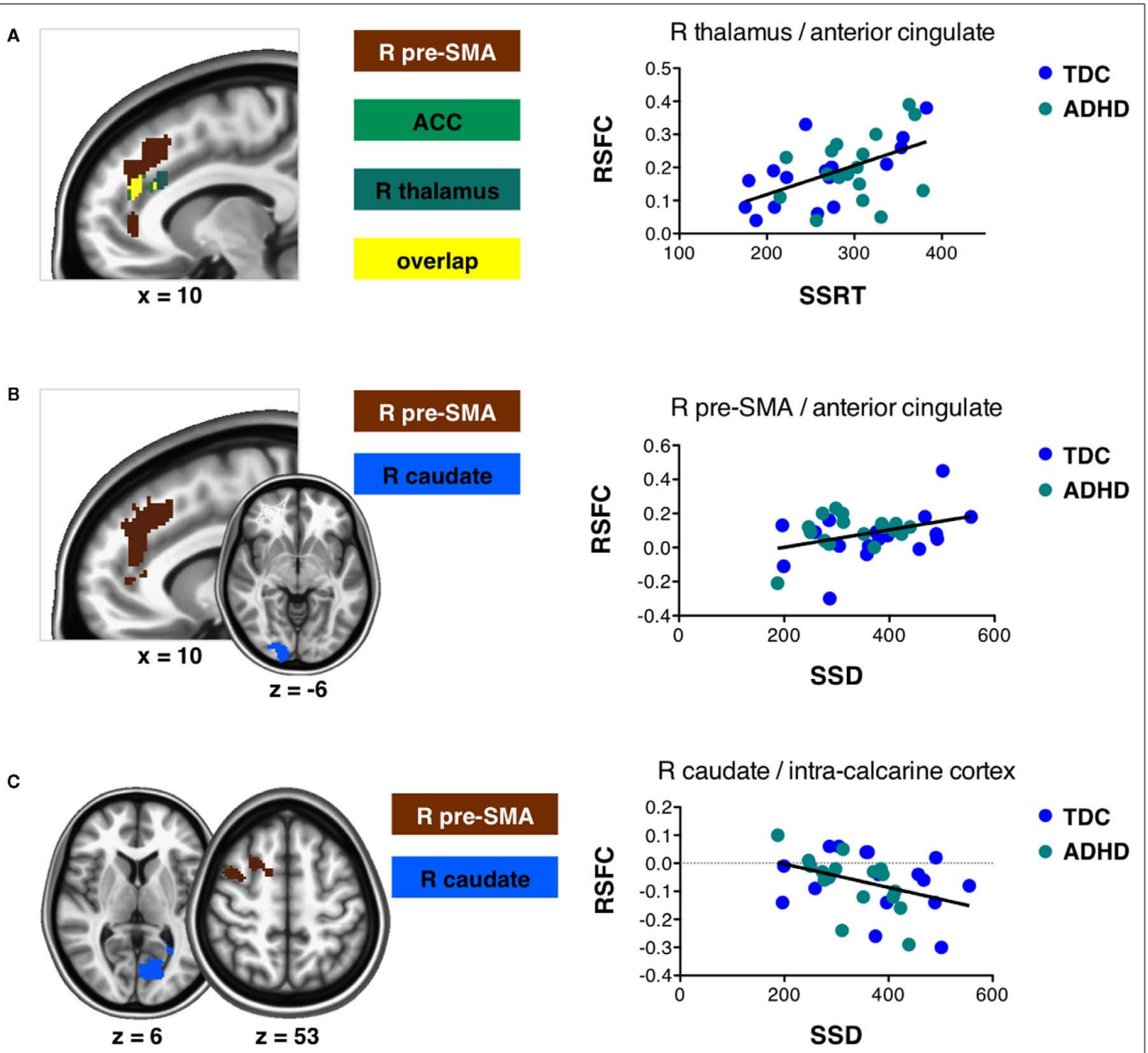

FIGURE 3 | Connectivity–behavior relationships across participants for SSRT and SSD. Slices display regions exhibiting a significantly positive or negative relationship across participants between resting state functional connectivity (RSFC) and the SSRT **(A)** or SSD **(B,C)** measures obtained from the stop signal task ($Z > 2.3$; $p < 0.05$, corrected for multiple comparisons). **(A)** Regions exhibiting a significantly positive relationship between RSFC and SSRT. **(B)** Regions exhibiting a significantly positive relationship between RSFC and SSD. **(C)** Regions exhibiting a significantly negative relationship between RSFC and SSD. Graphs illustrate example relationships. Data points are shown for typically developing children (TDC) and children with ADHD. R, right; pre-SMA, pre-supplementary motor area; ACC, anterior cingulate cortex.

each behavioral measure in the group-level analysis. For both SSRT and SSD, diagnosis-by-behavior interactions revealed several dissociations.

For SSRT, diagnosis-by-behavior interactions were found for the left insula, left thalamus, and right pre-SMA seeds (**Figure 5**). In children with ADHD, functional connectivity between right pre-SMA and right SMA, right supramarginal gyrus and parietal operculum cortex was increased in children exhibiting slower SSRTs. In contrast, TDC showed no effect. Similar interactions were obtained for functional connectivity between left insula and left putamen and right caudate. The reverse interaction, i.e., decreasing connectivity with decreased SSRT in TDC compared to decreasing connectivity with increased SSRT in ADHD, was found for functional connectivity between left thalamus and the right cerebellum.

Diagnosis-by-behavior interactions involving SSD were found for the right pre-SMA, left insula, right supramarginal gyrus, and ACC seeds (**Figures 5C,D**). Functional connectivity with right

Table 4 | MNI152 coordinates and Harvard–Oxford Atlas regions associated with all effects of interest.

Effect of interest	Seed ROI	Cluster size	*Z*-value	MNI coordinates			Region
				x	*y*	*z*	
SSRT POSITIVE							
	ACC	663	3.48	−10	42	22	Paracingulate gyrus
	R pre-SMA	983	3.93	−12	30	42	Superior frontal gyrus
	R thalamus	723	3.68	−22	8	−2	Putamen
SSD POSITIVE							
	R caudate	573	3.59	24	−92	−14	Occipital pole
	R pre-SMA	1798	4.05	−10	42	26	Paracingulate gyrus
SSD NEGATIVE							
	R caudate	794	3.75	−8	−76	6	Intracalcarine cortex
	R pre-SMA	779	4.11	34	2	40	Middle frontal gyrus
SSRT × DIAG							
	L insula	990	3.71	−28	0	−6	Putamen
	R pre-SMA						
	1	1498	3.75	46	−30	38	Supramarginal gyrus
	2	935	3.41	2	4	40	Cingulate gyrus
	L thalamus	850	3.69	20	−70	−24	Cerebellum
SSD × DIAG							
	ACC	668	3.49	22	32	36	Superior frontal gyrus
	L insula	770	3.47	−22	−8	16	Putamen
	R pre-SMA						
	1	1108	3.69	52	−34	36	Supramarginal gyrus
	2	1016	3.76	30	−64	−14	Occipital fusiform gyrus
	R supramarginal gyrus	1234	3.8	22	−66	−2	Lingual gyrus
ADHD > TDC							
	R caudate						
	1	3408	4.29	48	18	−4	Frontal operculum
	2	1304	4.05	−60	−26	8	Planum temporale
	3	1177	4.01	−32	50	36	Frontal pole
	4	916	4.36	−38	10	4	Frontal operculum
	5	805	3.95	6	26	26	Cingulate gyrus
	R frontal operculum	1274	4.32	8	10	4	Caudate
	R supramarginal gyrus						
	1	1783	4.31	10	12	6	Caudate
	2	769	3.8	12	32	24	Cingulate gyrus
	L thalamus						
	1	1853	4.87	−56	−44	10	Supramarginal gyrus
	2	973	4.57	−30	8	26	Middle frontal gyrus
	R thalamus						
	1	1009	3.75	−22	40	26	Frontal pole
	2	978	3.74	−54	−42	−4	Middle temporal gyrus
ADHD < TDC							
	L caudate	1092	3.86	2	10	−12	Subcallosal cortex
	R frontal operculum	1028	3.74	2	−48	62	Precuneus
	L thalamus	1338	3.97	2	−72	−12	Cerebellum

Coordinates are indicated for the location of the peak Z-value in each significant cluster. Correction for multiple comparisons was done using Gaussian random field theory with $Z > 2.3$ and $p < 0.05$ corrected.

pre-SMA showed the most extensive interactions including clusters in lateral occipital cortex and supramarginal gyrus. Increased negative connectivity with lateral occipital cortex was associated with longer SSD in children with ADHD, but not in TDC. Pre-SMA connectivity with supramarginal gyrus was lower in TDC exhibiting longer SSD relative to TDC exhibiting shorter SSD. The opposite was true for children with ADHD. Functional connectivity between ACC and right superior frontal gyrus decreased in

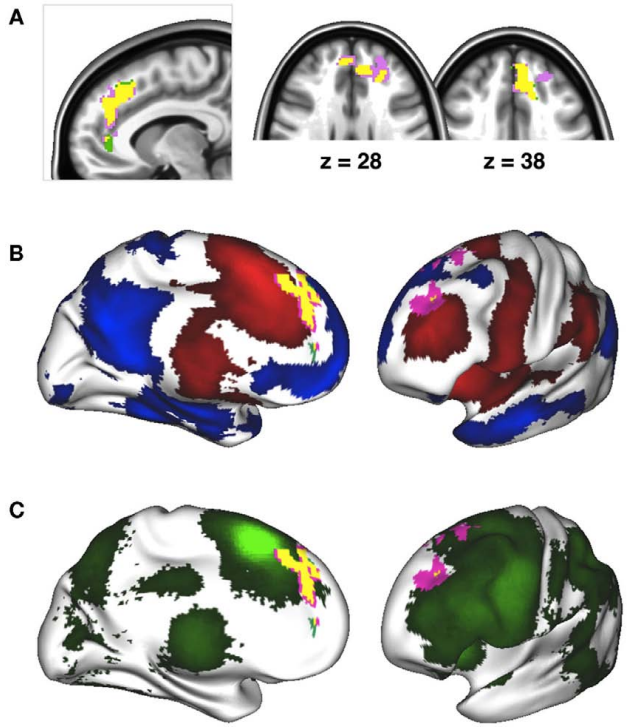

FIGURE 4 | (A) Inter-individual differences in SSRT and SSD both modulated resting state functional connectivity between right pre-supplementary motor area (pre-SMA) and a similar cluster in anterior cingulate cortex/superior frontal gyrus. Yellow indicates overlap between the cluster exhibiting a significant connectivity–behavior relationship for SSRT (grass green) and the cluster exhibiting a significant connectivity–behavior relationship for SSD (pink). **(B)** Overlap between the connectivity–behavior clusters shown in **(A)** and the overall positive (red) and negative (blue) functional connectivity network maps obtained for the pre-SMA seed. The connectivity–behavior cluster was located in transition zones between areas of overall positive or negative connectivity. **(C)** Overlap between connectivity–behavior clusters shown in **(A)** and a pre-SMA task-based co-activation map obtained from www.neurosynth.org. The co-activation map is based on a meta-analysis of activation coordinates reported together with the coordinates of the pre-SMA seed region (Yarkoni et al., 2011).

children with ADHD exhibiting longer SSD, while there was no RSFC–SSD relationship for TDC. Finally, connectivity between left insula and bilateral putamen decreased with increased SSD in TDC, while no RSFC–SSD relationship was observed for children with ADHD.

MAIN EFFECTS OF DIAGNOSIS

Figure 6 shows regions whose functional connectivity was modulated by diagnosis. We observed regions where connectivity was increased in children with ADHD relative to TDC (**Figure 6A**) as well as regions where connectivity was increased for TDC relative to children with ADHD (**Figure 6B**).

Several seeds exhibited increased connectivity strength in ADHD relative to no or weak connectivity in TDC. The right supramarginal gyrus and right caudate exhibited increased connectivity with a similar cluster in anterior cingulate cortex in children with ADHD relative to TDC. The supramarginal gyrus showed the same effect for a cluster in posterior cingulate cortex. In addition, the right frontal operculum exhibited increased connectivity with bilateral caudate in ADHD relative to TDC. A similar observation was made for the right caudate seed, whose local connectivity as well as connectivity strength with the left caudate was increased in ADHD relative to TDC. Finally, connectivity between left thalamus and left middle frontal gyrus as well as left superior temporal gyrus was increased in children with ADHD relative to no connectivity in TDC.

In contrast to these results, connectivity between the left caudate seed and ventromedial prefrontal cortex was absent in children with ADHD whereas it was significantly positive in TDC. The same effect was observed for connectivity between left thalamus and lingual gyrus. We observed no significant connectivity between frontal operculum and the right sensory–motor subdivision of the precuneus in TDC, but increased negative connectivity in ADHD.

For each cluster that showed a significant effect of diagnosis, we assessed the relationship between RSFC and ADHD-related measures obtained with the CPRS-R:L. In particular, within the children with ADHD we correlated the DSM-IV Total Score, DSM-IV Inattentive Score, DSM-IV Hyperactive–Impulsive Score, Cognitive Problems/Inattention Score, Hyperactivity Score, and the ADHD Index Score with mean RSFC obtained for each cluster. No correlation survived FDR correction for multiple comparisons ($p < 0.05$).

DISCUSSION

Recent models of ADHD highlight the contributions of aberrant functional connectivity to the pathophysiology of the disorder (Liston et al., 2011). The interpretation of such disconnection models would benefit from integration with leading neuropsychological models of ADHD, though little work has yet been done in this regard. Here, we took steps toward this goal by investigating the functional connectivity correlates of inhibitory performance during a SST and by assessing the effect of ADHD on those connections. Our findings highlight several novel brain–behavior relationships that warrant further investigation for their role in the inhibitory deficits associated with ADHD.

Previous studies have suggested that several characteristics of the brain's resting state functional architecture are relevant for understanding relationships between brain functional organization and behavior. We can apply two recently documented characteristics to the current findings. First, we recently highlighted the importance of so-called "transition zones" between an ROI's positive and negative functional connectivity networks (Mennes et al., 2010). Those transition zones are characterized by increased between-participant variability in connectivity strength and valence – regions at the boundaries of the networks might be positively connected to the ROI in some individuals, but negatively connected in others, resulting in overall non-significant connectivity. We previously found that this variability in network boundaries was predictive of the magnitude of task-induced BOLD activity (Mennes et al., 2010). In the current work regions exhibiting a significant connectivity–SSRT relationship for the pre-SMA seed

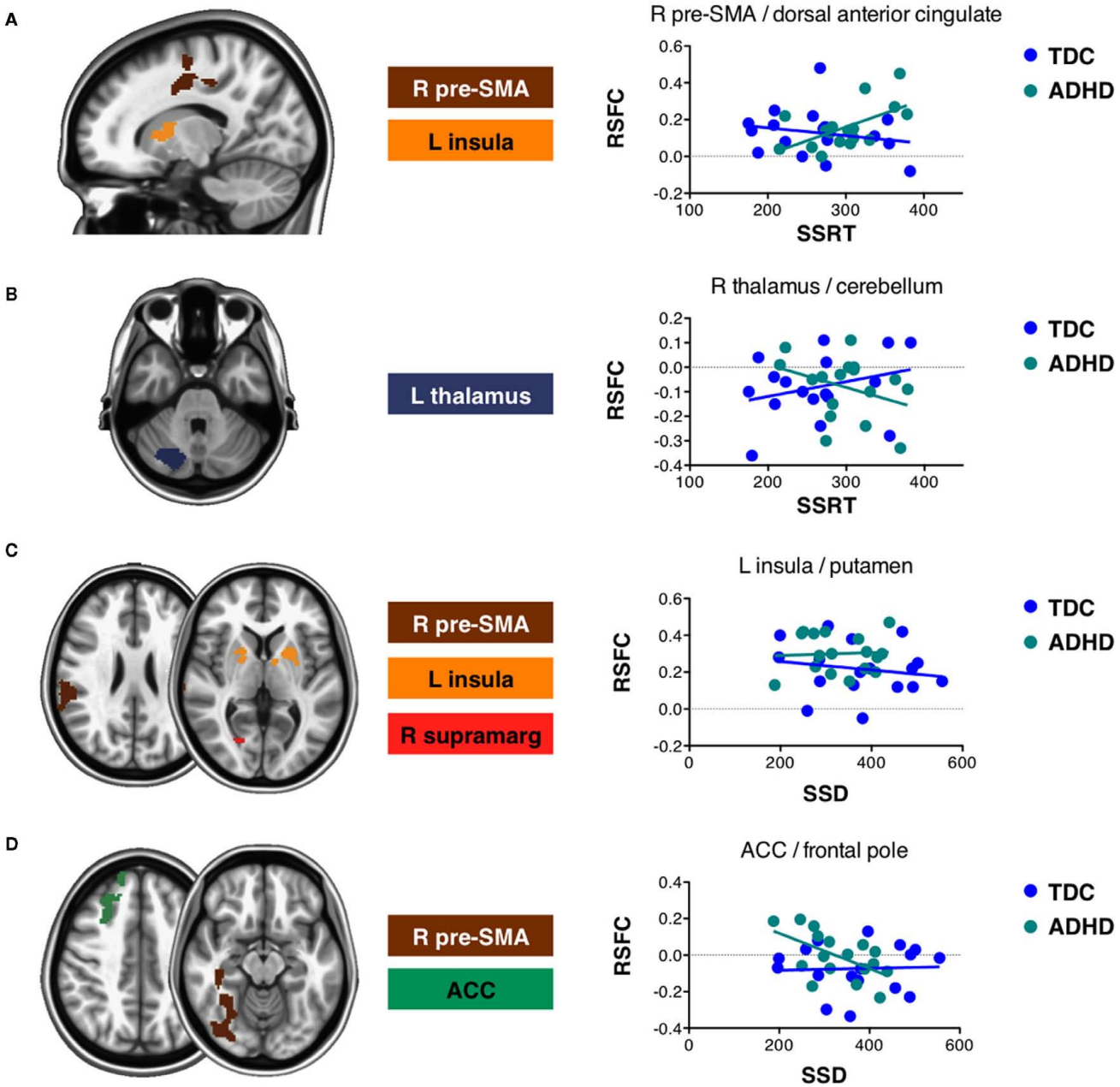

FIGURE 5 | Attention-deficit/hyperactivity disorder diagnosis modulated connectivity–behavior relationships for SSRT and SSD. Slices display regions exhibiting a significant effect of diagnosis on their connectivity–behavior relationship ($Z > 2.3$; $p < 0.05$, corrected for multiple comparisons). Interactions were observed for both SSRT and SSD obtained during the stop signal task. Graphs illustrate example interactions. **(A)** Significantly positive interactions between diagnosis and SSRT. **(B)** Significantly negative interactions between diagnosis and SSRT. **(C)** Significantly positive interactions between diagnosis and SSD. **(D)** Significantly negative interactions between diagnosis and SSD. Data points are shown for typically developing children (TDC) and children with ADHD. R, right; L, Left; pre-SMA, pre-supplementary motor area; ACC, anterior cingulate cortex; supramarg: supramarginal gyrus.

ROI were located in transition zones between regions of positive and negative connectivity (**Figure 4**). As indicated above, these transition zones exhibited slightly positive connectivity in some participants and negative connectivity in others. This observation explains why the mean of several of the observed brain–behavior relationships hovered around 0. Similar to the transition zones observed in RSFC networks, overlaying the pre-SMA clusters on a task co-activation map created by meta-analytic mining of task-based fMRI coordinates[4] (Yarkoni et al., 2011) indicated that

[4]www.neurosynth.org

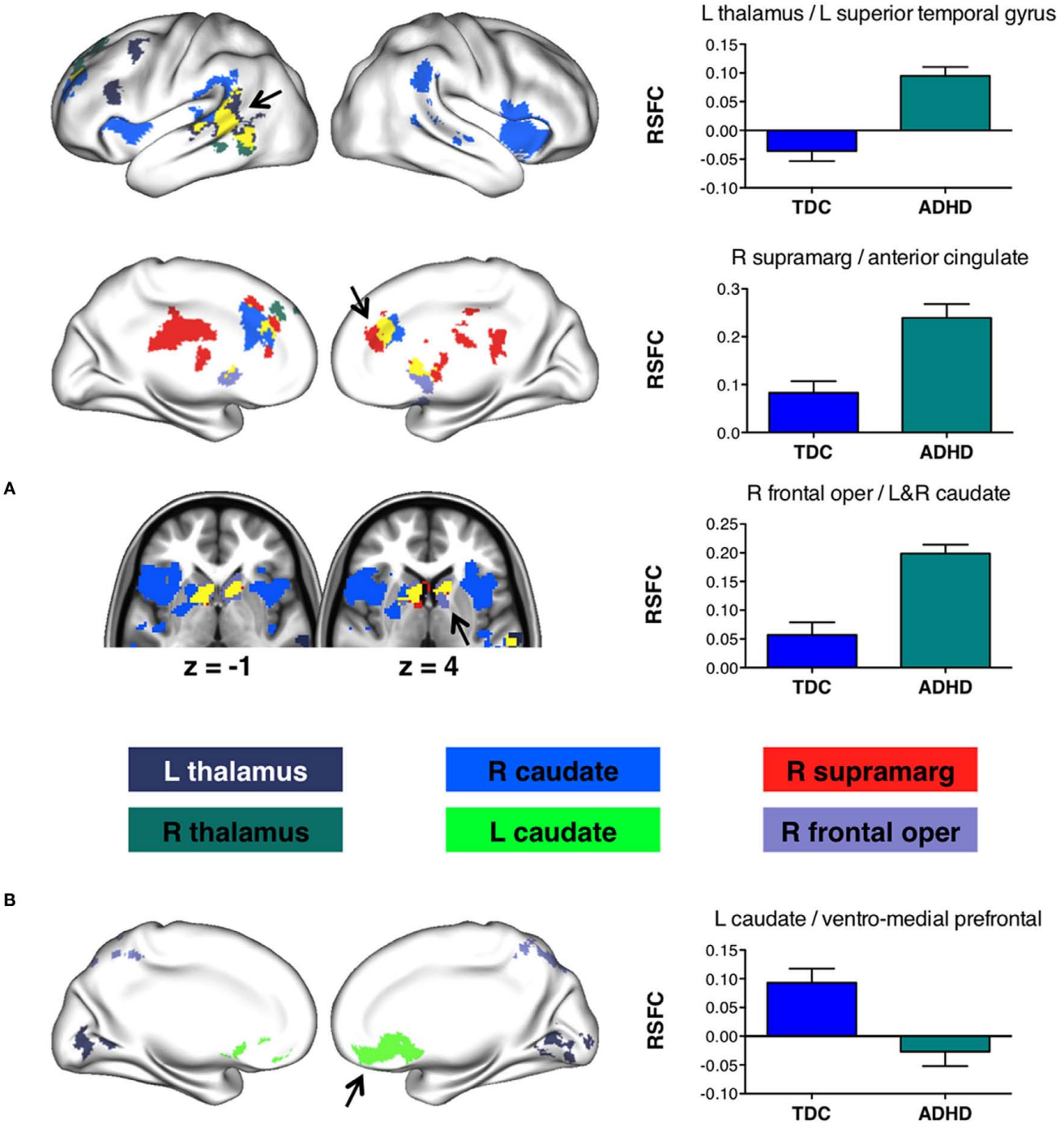

FIGURE 6 | Main effect of ADHD on resting state functional connectivity (RSFC) associated with 11 fronto-striatal seeds (Boehler et al., 2010). Surface renderings display regions exhibiting a significant main effect of diagnosis on RSFC ($Z > 2.3$; $p < 0.05$; corrected for multiple comparisons). Graphs illustrate example effects for the regions indicated by arrows on the surface renderings. **(A)** Regions exhibiting a significant ADHD > TDC effect on RSFC. **(B)** Regions exhibiting a significant ADHD < TDC effect on RSFC. R, right; L, Left; supramarg, supramarginal gyrus; frontal oper, frontal operculum.

these clusters were located on the borders of their respective task-based co-activation networks (see **Figure 4C**). Together, these findings suggest that between-subject variation in performance is linked to variation in functional network boundaries, rather than to variation in the connectivity strength of core network regions.

A second characteristic that may represent an important feature of relationships between behavior and functional brain architecture is network differentiation (Fox et al., 2005). Networks or regions are thought to be functionally differentiated if there are no correlations between them or if they are negatively correlated. This is based on the hypothesis that functional brain networks (at times) benefit from preventing cross talk between each other. For instance, participants whose brains exhibited stronger functional differentiation performed more optimally compared to participants exhibiting weaker or aberrant functional differentiation (Kelly et al., 2008; Chabernaud et al., in press). Accordingly, we observed that better differentiation between right caudate and left intracalcarine sulcus (i.e., increased negative connectivity) was associated with better inhibitory success (i.e., longer SSD; **Figure 3**). In addition, children with ADHD exhibited functional connections not observed for TDC (**Figure 6**) suggesting a less differentiated and less efficient connectivity profile (Di Martino et al., 2011).

The notion that SSRT provides the most specific index of inhibitory function has been central to most prior analyses of the SST. However, SSRT is not directly measured, but derived by subtracting SSD from the mean Go reaction time. As Alderson et al. (2007) point out, SSD should be considered when interpreting group differences in SSRT as SSD is more tightly related to inhibitory success. In the present work, we included both SSD and SSRT in the same regression model to partial out common variance associated with these two highly correlated measures. As described above, we found evidence for neural circuitry that was specifically related to either SSRT or SSD. In addition, we found neural circuitry related to SSD as well as SSRT. In particular, inter-individual differences in SSRT as well as SSD were associated with inter-individual differences in functional connectivity strength between pre-SMA and anterior cingulate cortex/superior frontal gyrus (**Figure 4**). Although SSRT and SSD are inversely related ($r = -0.81$), both RSFC/behavior relationships were positive. Therefore, rather than capturing specific aspects of the inhibition process, these results are in accordance with the observation that anterior cingulate cortex and superior frontal gyrus are activated by a variety of cognitive tasks that measure aspects of more general endogenous cognitive control (see meta-analysis Figure 1 in Mennes et al., 2006), while pre-SMA is sensitive to aspects of task difficulty and motor preparation (Milham and Banich, 2005; Stiers et al., 2010). In addition, increased pre-SMA activation has been reported in ADHD participants exhibiting higher intra-individual response speed variability, while increased superior frontal gyrus activity was observed for ADHD participants exhibiting lower intra-individual response speed variability (Suskauer et al., 2008). Further research including larger sample sizes is needed to disentangle the precise interaction between SSRT and SSD, and their relationship with RSFC. For example, short SSRT but long SSD indicate optimal inhibitory performance, yet the overlapping connectivity-behavior relationships observed for pre-SMA were positive for both SSRT and SSD.

The presence or absence of ADHD modulated connectivity–behavior relationships for both SSRT and SSD in several regions including putamen, post-central gyrus, posterior cingulate, and intracalcarine cortex. Similarly, the presence of ADHD modulated connectivity–behavior relationships for internalizing and externalizing scores obtained from the Child Behavior Checklist questionnaire (Chabernaud et al., in press). Further research is needed to unravel mechanisms underlying such differential relationships. As ADHD effects on connectivity are often interpreted in light of dysmaturational processes (Fair et al., 2010), future work should investigate age-related modulations of connectivity–behavior relationships. In the meantime, the current results suggest that ADHD should not be considered a simple extreme of brain function, since various aspects of brain function show qualitative differences depending on the presence or absence of psychopathology (Rubia et al., 2007; Chabernaud et al., in press).

Behavioral studies using the SST commonly report slower mean Go reaction times and increased reaction time variability in ADHD (see Alderson et al., 2007 and Lijffijt et al., 2005 for meta-analyses). In particular, reaction time variability has recently been put forward as an alternative phenotype for ADHD as behavioral studies have consistently demonstrated significantly higher intra-individual variability in ADHD versus neurotypical populations (Kuntsi et al., 2001; Castellanos et al., 2005; Alderson et al., 2007; Rubia et al., 2007). We did not observe a significant effect of ADHD on mean Go reaction time or reaction time variability (neither for the coefficient of variation or SD). The factors contributing to this lack of replication remain unclear and further studies are warranted. One possible reason for the absence of such effects might be the strict performance criteria used here. Yet, Nigg (1999) used the same criteria and observed an ADHD effect on reaction time variability. A second reason for the absence of such effects might be that our sample of ADHD children represents a specific neuropsychological ADHD phenotype. Accordingly, comparing our behavioral data to those reported in Nigg (1999) suggests that the ADHD children included here outperformed the ADHD children included in Nigg (1999), with faster reaction times (629 versus 713 ms) and SSRT (299 versus 405 ms). These observations are consistent with the notion that several ADHD phenotypes exist, each with their own behavioral and cognitive profile (Nigg et al., 2005).

With regard to the effects of diagnosis on functional connectivity, we replicated previous findings of ADHD-related differences in functional connectivity in ventromedial prefrontal cortex (Fair et al., 2010), and frontal operculum (Tian et al., 2006). Such findings of aberrant functional connectivity can be interpreted in terms of disrupted maturational processes (Fair et al., 2010), an interpretation that was also made in the context of functional connectivity differences in children with autism (Di Martino et al., 2011) or Tourette syndrome (Church et al., 2009). The developmental interpretation is based on observations that with maturation local connectivity (i.e., close to the seed region) decreases while long-range connectivity increases (Fair et al., 2008, 2009; Kelly et al., 2009). Similarly, we observed increased local frontal operculum connectivity and decreased long-range connectivity (e.g., left thalamus – lingual gyrus connectivity was absent in children with ADHD relative to TDC). In addition, as shown in **Figure 6**, we also observed significant effects of diagnosis in inferior frontal gyrus, anterior cingulate cortex, left dorsolateral prefrontal cortex, and insula. These

regions are known to be actively involved in higher order cognitive control operations (Koechlin et al., 2003; Brass et al., 2005; Badre and D'Esposito, 2007) and have been suggested to show differential activity in the context of ADHD (Burgess et al., 2010; Shaw et al., 2011; Spinelli et al., 2011). Interestingly, we observed these regions while assessing functional connectivity of seed ROI that were found to be related to inhibitory processing, which is in turn deemed an important aspect of cognitive control.

LIMITATIONS

Our results need to be considered in light of several limitations. Although 63 children initially participated in the study, only 34 were included in our analyses, indicating 46% data-loss. Of the omitted participants, 65% were excluded because they had a Go trial accuracy below the 75% criterion proposed by Nigg (1999). For instance, six excluded participants performed below chance level, indicating clear failure to comply with the task. One possible reason for such sub-criterion performance may be fatigue, as all children performed the SST after a 1-h long MRI scan session. In addition, the TDC were not matched to reflect the typical overrepresentation of boys among children with ADHD. However, as illustrated by **Figure 7**, our results were not driven by sex differences between both groups. Third, because of the substantial loss of analyzable data, the sample sizes were relatively small. While such sample sizes are common in neuroimaging studies of ADHD, our results warrant replication in larger sex-matched samples. Additionally, our smaller sample size might have limited our ability to detect significant behavior–connectivity relationships, especially for the clusters exhibiting a significant effect of diagnosis. Finally, we selected 11 *a priori* seed ROI for functional connectivity analyses. These were based on a prior study of the stop task and used to constrain our hypotheses, as is necessary in seed-based functional connectivity analyses (Fox and Greicius, 2010). Despite this limitation, our analyses included the whole brain, and were corrected accordingly. In the meantime, approaches for connectome wide association studies are emerging, such as graph-theory based centrality metrics (Lohmann et al., 2010; Rubinov and Sporns, 2010; Zuo et al., in press) and multivariate distance regression (Shezhad et al., oral presentation at Annual Meeting of the Organization for Human Brain Mapping, Quebec City). While the present work was motivated directly from prior findings (e.g., seed selection), future work may take advantage of these more exploratory approaches to generate novel hypotheses.

CONCLUSION

We found that two inhibitory measures derived from the SST are differentially related to functional connectivity of selected fronto-striatal seed regions. While SSRT is the traditional measure of choice, our results suggest that a different set of functional connections is related to SSD. Moreover, we showed that these functional relationships are modulated by the presence or absence of ADHD. While preliminary, our results warrant further work relating behavioral inhibition metrics to functional brain networks. Integrating neuropsychological data with emerging brain

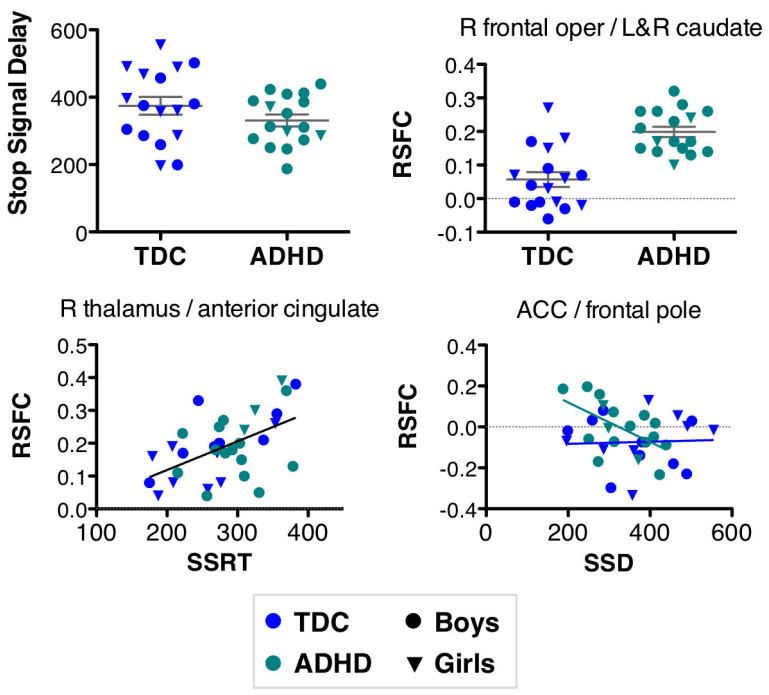

FIGURE 7 | Our results were not driven by a difference in male/female ratio between typically developing children (TDC) and children with ADHD. TDC included 8 females/9 males, while ADHD included 3 females/14 males. Graphs illustrate effects that are also shown in **Figures 2**, **6**, **3**, **5** (from left to right, top to bottom).

dysconnectivity models of ADHD will ultimately advance our understanding of the pathophysiology of this complex disorder.

ACKNOWLEDGMENTS

The authors thank all children and their parents for participating in this study. We also thank Joel Nigg for providing the stop signal task and Camille Chabernaud and Samuele Cortese for helpful comments on earlier versions of this manuscript. This research was partially supported by Grants from National Institute of Mental Health (R01MH083246 and K23MH087770), Autism Speaks, the Stavros Niarchos Foundation, the Leon Levy Foundation, and the endowment provided by Phyllis Green and Randolph Cowen. The funders had no role in study design, data collection and analysis, decision to publish, or preparation of the manuscript. Dr. Castellanos serves on the DSM-5 Workgroup on Attention-Deficit Hyperactivity and Disruptive Behavior Disorders; the views expressed in this paper are his own and do not represent those of the Workgroup or of the DSM-5 Task Force.

REFERENCES

Alderson, R. M., Rapport, M. D., and Kofler, M. J. (2007). Attention-deficit/hyperactivity disorder and behavioral inhibition: a meta-analytic review of the stop-signal paradigm. *J. Abnorm. Child. Psychol.* 35, 745–758.

Alderson, R. M., Rapport, M. D., Sarver, D. E., and Kofler, M. J. (2008). ADHD and behavioral inhibition: a re-examination of the stop-signal task. *J. Abnorm. Child. Psychol.* 36, 989–998.

Andersson, J. L. R., Jenkinson, M., and Smith, S. M. (2007). *TR07JA2: Non-linear Registration, AKA Spatial Normalisation.* FMRIB Analysis Group Technical Reports. Available at: http://www.fmrib.ox.ac.uk/analysis/techrep/

Aron, A. R., and Poldrack, R. A. (2005). The cognitive neuroscience of response inhibition: relevance for genetic research in attention-deficit/hyperactivity disorder. *Biol. Psychiatry* 57, 1285–1292.

Badre, D., and D'Esposito, M. (2007). Functional magnetic resonance imaging evidence for a hierarchical organization of the prefrontal cortex. *J. Cogn. Neurosci.* 19, 2082–2099.

Boehler, C. N., Appelbaum, L. G., Krebs, R. M., Hopf, J. M., and Woldorff, M. G. (2010). Pinning down response inhibition in the brain – conjunction analyses of the stop-signal task. *Neuroimage* 52, 1621–1632.

Brass, M., Derrfuss, J., Forstmann, B., and Von Cramon, D. Y. (2005). The role of the inferior frontal junction area in cognitive control. *Trends Cogn. Sci. (Regul. Ed.)* 9, 314–316.

Burgess, G. C., Depue, B. E., Ruzic, L., Willcutt, E. G., Du, Y. P., and Banich, M. T. (2010). Attentional control activation relates to working memory in attention-deficit/hyperactivity disorder. *Biol. Psychiatry* 67, 632–640.

Castellanos, F. X., Margulies, D. S., Kelly, C., Uddin, L. Q., Ghaffari, M., Kirsch, A., Shaw, D., Shehzad, Z., Di Martino, A., Biswal, B., Sonuga-Barke, E. J., Rotrosen, J., Adler, L. A., and Milham, M. P. (2008). Cingulate-precuneus interactions: a new locus of dysfunction in adult attention-deficit/hyperactivity disorder. *Biol. Psychiatry* 63, 332–337.

Castellanos, F. X., Sonuga-Barke, E. J., Scheres, A., Di Martino, A., Hyde, C., and Walters, J. R. (2005). Varieties of attention-deficit/hyperactivity disorder-related intra-individual variability. *Biol. Psychiatry* 57, 1416–1423.

Castellanos, F. X., Sonuga-Barke, E. J. S., Milham, M. P., and Tannock, R. (2006). Characterizing cognition in ADHD: beyond executive dysfunction. *Trends Cogn. Sci.* 10, 117–123.

Chabernaud, C., Mennes, M., Kelly, C., Nooner, K., Di Martino, A., Castellanos, F. X., and Milham, M. P. (in press). Integration of dimensional and categorical analyses of brain-behavior relationships in children with attention-deficit/hyperactivity disorder and healthy controls. *Biol. Psychiatry.* doi: 10.1016/j.biopsych.2011.08.013

Church, J. A., Fair, D. A., Dosenbach, N. U., Cohen, A. L., Miezin, F. M., Petersen, S. E., and Schlaggar, B. L. (2009). Control networks in paediatric Tourette syndrome show immature and anomalous patterns of functional connectivity. *Brain* 132, 225–238.

Conners, C. K., Sitarenios, G., Parker, J. D., and Epstein, J. N. (1998). The revised Conners' Parent Rating Scale (CPRS-R): factor structure, reliability, and criterion validity. *J. Abnorm. Child. Psychol.* 26, 257–268.

Cubillo, A., Halari, R., Ecker, C., Giampietro, V., Taylor, E., and Rubia, K. (2010). Reduced activation and inter-regional functional connectivity of fronto-striatal networks in adults with childhood attention-deficit hyperactivity disorder (ADHD) and persisting symptoms during tasks of motor inhibition and cognitive switching. *J. Psychiatr. Res.* 44, 629–639.

Di Martino, A., Kelly, C., Grzadzinski, R., Zuo, X. N., Mennes, M., Mairena, M. A., Lord, C., Castellanos, F. X., and Milham, M. P. (2011). Aberrant striatal functional connectivity in children with autism. *Biol. Psychiatry* 69, 847–856.

Dickstein, S. G., Bannon, K., Castellanos, F. X., and Milham, M. P. (2006). The neural correlates of attention deficit hyperactivity disorder: an ALE meta-analysis. *J. Child. Psychol. Psychiatry* 47, 1051–1062.

Fair, D. A., Cohen, A. L., Dosenbach, N. U., Church, J. A., Miezin, F. M., Barch, D. M., Raichle, M. E., Petersen, S. E., and Schlaggar, B. L. (2008). The maturing architecture of the brain's default network. *Proc. Natl. Acad. Sci. U.S.A.* 105, 4028–4032.

Fair, D. A., Cohen, A. L., Power, J. D., Dosenbach, N. U., Church, J. A., Miezin, F. M., Schlaggar, B. L., and Petersen, S. E. (2009). Functional brain networks develop from a "local to distributed" organization. *PLoS Comput. Biol.* 5, e1000381. doi:10.1371/journal.pcbi.1000381

Fair, D. A., Posner, J., Nagel, B. J., Bathula, D., Dias, T. G., Mills, K. L., Blythe, M. S., Giwa, A., Schmitt, C. F., and Nigg, J. T. (2010). Atypical default network connectivity in youth with attention-deficit/hyperactivity disorder. *Biol. Psychiatry* 68, 1084–1091.

Fox, M. D., and Greicius, M. (2010). Clinical applications of resting state functional connectivity. *Front. Syst. Neurosci.* 4:19. doi:10.3389/fnsys.2010.00019

Fox, M. D., Snyder, A. Z., Vincent, J. L., Corbetta, M., Van Essen, D. C., and Raichle, M. E. (2005). The human brain is intrinsically organized into dynamic, anticorrelated functional networks. *Proc. Natl. Acad. Sci. U.S.A.* 102, 9673–9678.

Jenkinson, M., Bannister, P. R., Brady, J. M., and Smith, S. M. (2002). Improved optimisation for the robust and accurate linear registration and motion correction of brain images. *Neuroimage* 17, 825–841.

Jenkinson, M., and Smith, S. M. (2001). A global optimisation method for robust affine registration of brain images. *Med. Image Anal.* 5, 143–156.

Kaufman, J., Birmaher, B., Brent, D., Rao, U., Flynn, C., Moreci, P., Williamson, D., and Ryan, N. (1997). Schedule for affective disorders and schizophrenia for school-age children present and lifetime version (K-SADS-PL): initial reliability and validity data. *J. Am. Acad. Child Adolesc. Psychiatry* 36, 980–988.

Kelly, A. M., Di Martino, A., Uddin, L. Q., Shehzad, Z., Gee, D. G., Reiss, P. T., Margulies, D. S., Castellanos, F. X., and Milham, M. P. (2009). Development of anterior cingulate functional connectivity from late childhood to early adulthood. *Cereb. Cortex* 19, 640–657.

Kelly, A. M., Uddin, L. Q., Biswal, B. B., Castellanos, F. X., and Milham, M. P. (2008). Competition between functional brain networks mediates behavioral variability. *Neuroimage* 39, 527–537.

Koechlin, E., Ody, C., and Kouneiher, F. (2003). The architecture of cognitive control in the human prefrontal cortex. *Science* 302, 1181–1185.

Konrad, K., Gauggel, S., Manz, A., and Scholl, M. (2000). Inhibitory control in children with traumatic brain injury (TBI) and children with attention deficit/hyperactivity disorder (ADHD). *Brain Inj.* 14, 859–875.

Kuntsi, J., Oosterlaan, J., and Stevenson, J. (2001). Psychological mechanisms in hyperactivity: I. Response inhibition deficit, working memory impairment, delay aversion, or something else? *J. Child. Psychol. Psychiatry* 42, 199–210.

Lijffijt, M., Kenemans, J. L., Verbaten, M. N., and Van Engeland, H. (2005). A meta-analytic review of stopping performance in attention-deficit/hyperactivity disorder: deficient inhibitory motor control? *J. Abnorm. Psychol.* 114, 216–222.

Liston, C., Cohen, M. M., Teslovich, T., Levenson, D., and Casey, B. J. (2011). Atypical prefrontal connectivity in attention-deficit/hyperactivity disorder: pathway to disease or pathological end point? *Biol. Psychiatry* 69, 1168–1177.

Logan, G. D., Cowan, W. B., and Davis, K. A. (1984). On the ability to inhibit simple and choice reaction time responses: a model and a method. *J. Exp. Psychol. Hum. Percept. Perform.* 10, 276–291.

Logan, G. D., Schachar, R. J., and Tannock, R. (1997). Impulsivity and inhibitory control. *Psychol. Sci.* 8, 60–64.

Lohmann, G., Margulies, D. S., Horstmann, A., Pleger, B., Lepsien, J., Goldhahn, D., Schloegl, H., Stumvoll, M., Villringer, A., and Turner, R. (2010). Eigenvector centrality mapping for analyzing connectivity patterns in fMRI data of the human brain. *PLoS ONE* 5, e10232. doi:10.1371/journal.pone.0010232

Mennes, M., Kelly, C., Zuo, X. N., Di Martino, A., Biswal, B., Xavier Castellanos, F., and Milham, M. P. (2010). Inter-individual differences in resting state functional connectivity predict task-induced BOLD activity. *Neuroimage* 50, 1690–1701.

Mennes, M., Stiers, P., Lagae, L., and Van Den Bergh, B. (2006). Long-term cognitive sequelae of antenatal maternal anxiety: involvement of the orbitofrontal cortex. *Neurosci. Biobehav. Rev.* 30, 1078–1086.

Milham, M. P., and Banich, M. T. (2005). Anterior cingulate cortex: an fMRI analysis of conflict specificity and functional differentiation. *Hum. Brain Mapp.* 25, 328–335.

Nigg, J. T. (1999). The ADHD response-inhibition deficit as measured by the stop task: replication with DSM-IV combined type, extension, and qualification. *J. Abnorm. Child. Psychol.* 27, 393–402.

Nigg, J. T. (2001). Is ADHD a disinhibitory disorder? *Psychol. Bull.* 127, 571–598.

Nigg, J. T., Willcutt, E. G., Doyle, A. E., and Sonuga-Barke, E. J. (2005). Causal heterogeneity in attention-deficit/hyperactivity disorder: do we need neuropsychologically impaired subtypes? *Biol. Psychiatry* 57, 1224–1230.

Power, J. D., Barnes, K. A., Snyder, A. Z., Schlaggar, B. L., and Petersen, S. E. (in press). Spurious but systematic correlations in functional connectivity MRI networks arise from subject motion. *Neuroimage*. http://dx.doi.org/10.1016/j.neuroimage.2011.10.018

Rubia, K., Overmeyer, S., Taylor, E., Brammer, M., Williams, S. C., Simmons, A., and Bullmore, E. T. (1999). Hypofrontality in attention deficit hyperactivity disorder during higher-order motor control: a study with functional MRI. *Am. J. Psychiatry* 156, 891–896.

Rubia, K., Smith, A. B., Brammer, M. J., and Taylor, E. (2007). Temporal lobe dysfunction in medication-naive boys with attention-deficit/hyperactivity disorder during attention allocation and its relation to response variability. *Biol. Psychiatry* 62, 999–1006.

Rubinov, M., and Sporns, O. (2010). Complex network measures of brain connectivity: uses and interpretations. *Neuroimage* 52, 1059–1069.

Shaw, P., Gilliam, M., Liverpool, M., Weddle, C., Malek, M., Sharp, W., Greenstein, D., Evans, A., Rapoport, J., and Giedd, J. (2011). Cortical development in typically developing children with symptoms of hyperactivity and impulsivity: support for a dimensional view of attention deficit hyperactivity disorder. *Am. J. Psychiatry* 168, 143–151.

Spinelli, S., Joel, S., Nelson, T. E., Vasa, R. A., Pekar, J. J., and Mostofsky, S. H. (2011). Different neural patterns are associated with trials preceding inhibitory errors in children with and without attention-deficit/hyperactivity disorder. *J. Am. Acad. Child Adolesc. Psychiatry* 50, 705.e3–715.e3.

Stiers, P., Mennes, M., and Sunaert, S. (2010). Distributed task coding throughout the multiple demand network of the human frontal-insular cortex. *Neuroimage* 52, 252–262.

Suskauer, S. J., Simmonds, D. J., Fotedar, S., Blankner, J. G., Pekar, J. J., Denckla, M. B., and Mostofsky, S. H. (2008). Functional magnetic resonance imaging evidence for abnormalities in response selection in attention deficit hyperactivity disorder: differences in activation associated with response inhibition but not habitual motor response. *J. Cogn. Neurosci.* 20, 478–493.

Tian, L., Jiang, T., Wang, Y., Zang, Y., He, Y., Liang, M., Sui, M., Cao, Q., Hu, S., Peng, M., and Zhuo, Y. (2006). Altered resting-state functional connectivity patterns of anterior cingulate cortex in adolescents with attention deficit hyperactivity disorder. *Neurosci. Lett.* 400, 39–43.

Van Dijk, K. R., Sabuncu, M. R., and Buckner, R. L. (2012). The influence of head motion on intrinsic functional connectivity MRI. *Neuroimage* 59, 431–438.

Yarkoni, T., Poldrack, R. A., Nichols, T. E., Van Essen, D. C., and Wager, T. D. (2011). Large-scale automated synthesis of human functional neuroimaging data. *Nat. Methods* 8, 665–670.

Zuo, X., Ehmke, R., Mennes, M., Imperati, D., Castellanos, F. X., Sporns, O., and Milham, M. P. (in press). Network centrality and information flow in the human brain functional connectome. *Cereb. Cortex*. doi: 10.1093/cercor/bhr269

Conflict of Interest Statement: The authors declare that the research was conducted in the absence of any commercial or financial relationships that could be construed as a potential conflict of interest.

Received: 30 September 2011; accepted: 28 December 2011; published online: 11 January 2012.

*Citation: Mennes M, Vega Potler N, Kelly C, Di Martino A, Castellanos FX and Milham MP (2012) Resting state functional connectivity correlates of inhibitory control in children with attention-deficit/hyperactivity disorder. Front. Psychiatry **2**:83. doi: 10.3389/fpsyt.2011.00083*

This article was submitted to Frontiers in Neuropsychiatric Imaging and Stimulation, a specialty of Frontiers in Psychiatry.

APPENDIX

As described in Van Dijk et al. (2012) and Power et al. (in press), micromovements that occur during a resting state fMRI scan, can significantly influence measures and results derived from this scan. One suggestion to deal with such movements involves removing timepoints that exceed a threshold for excessive movement from the resting state time series before calculating any derived measures, this procedure is referred to as "scrubbing" (Power et al., in press). While easily adoptable for task-based fMRI scans, more research is needed to assess the effect of removing timepoints from analyses that investigate frequency measures or that focus on a certain frequency in the BOLD signal, as is the case for resting state functional connectivity.

The participants included in our manuscript exhibited limited movement during their resting state scan. Yet, here we present our main results while comparing analyses based on the original data versus analyses based on data after scrubbing timepoints contaminated with micromovements exceeding 0.5 mm framewise displacement (see Power et al., in press, for details).

Scrubbing our data according to the Power et al. (in press) method had very little impact on our results. Nineteen out of the 34 subjects needed scrubbing; of those only 4 needed more than 5% of frames (i.e., more than 10 frames) scrubbed (see **Figure A1**). The maximum number of frames scrubbed was: 18% (i.e., 33 frames). For each of the 11 seed ROI and effects of interest we observed very high correlations between the *Z*-statistic maps obtained with and without scrubbing. In fact, for each of the 55 *Z*-statistic maps we assessed (11 seed ROI, 5 contrasts), correlations exceeded 0.98. In addition, the maximum mean absolute difference in pre- and post-scrubbing *Z*-statistic values was 0.14, with a max SD of 0.12. The maximum absolute pre-/post-scrubbing difference in these 55 *Z*-statistic maps was 1.67. Together, these results suggests that, at the group level, scrubbing for micromovements had little impact on our statistical maps and did not alter the topography of our results (see **Figure A2**).

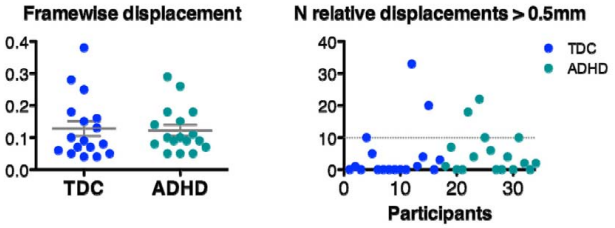

FIGURE A1 | Framewise displacement and *N* relative displacements calculated according to Power et al. (in press).

These results indicate limited variation in the pre/post-scrubbing *Z*-statistic maps. Although limited, such variations might cause some voxels to pass our statistical threshold after scrubbing while others, that passed pre-scrubbing, are now below that threshold. However, given the 0.98 correlation between pre/post-scrubbing *Z*-statistic values, it is clear that the topography of effects was not fundamentally altered after scrubbing. Across our effects of interest we observed 31 clusters in the data before scrubbing, and 33 in the scrubbed data. While six clusters disappeared by scrubbing, seven new clusters appeared. In the figures below we illustrate the observed effect for four ROI, two were significant before scrubbing, but not after scrubbing, while two were significant after scrubbing, but not present in the original, unscrubbed analyses. Yet, from **Figure A3** it is clear that for all clusters the effects of interest were highly similar pre/post-scrubbing, indicating that differences in cluster significance between the unscrubbed and scrubbed analyses were merely due to minor threshold changes at single voxels.

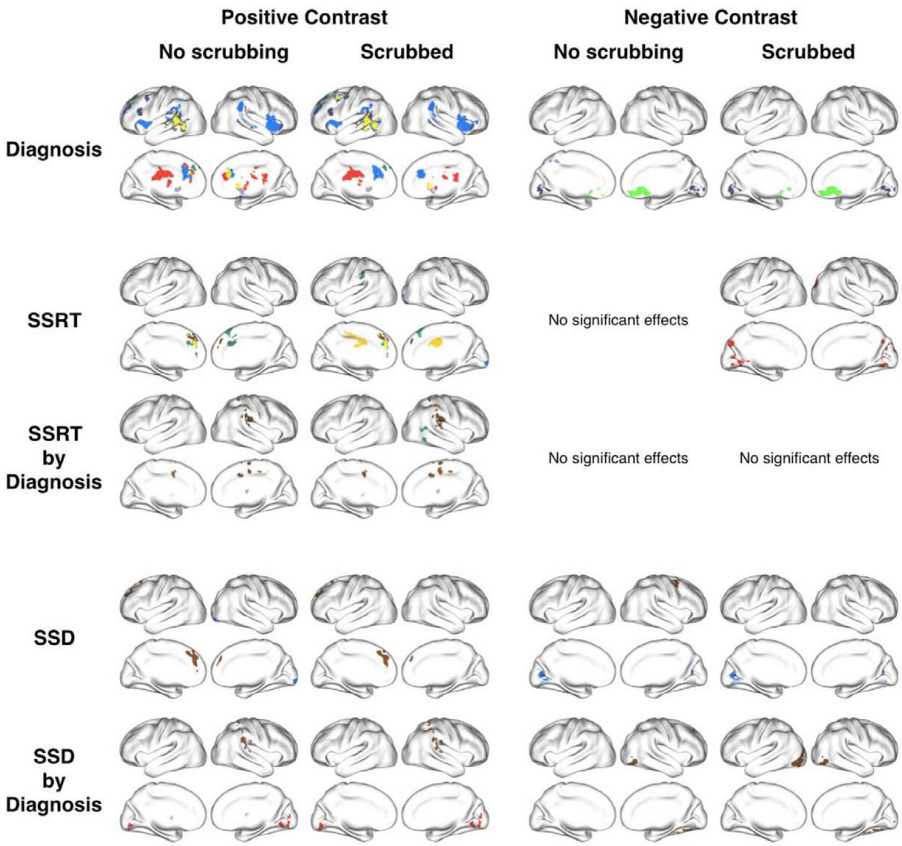

FIGURE A2 | Scrubbing timepoints containing micromovements from each participants' resting state timeseries had limited impact on our results. This figure shows the surface plots for each effect of interest for analyses using data without scrubbing (as reported in our manuscript) and analyses using scrubbed data.

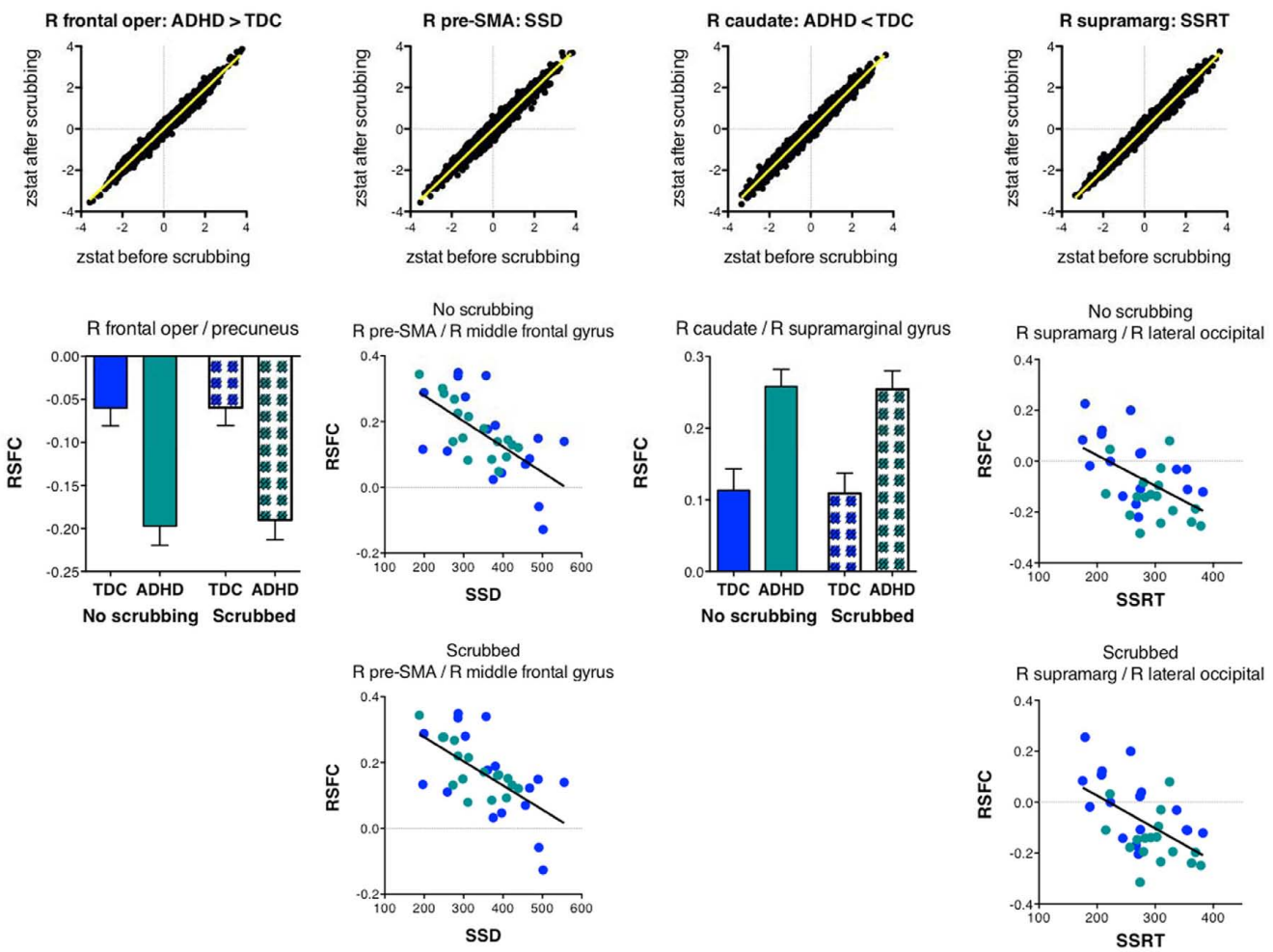

FIGURE A3 | Scrubbing the data for micromovements had limited impact on the *Z*-statistic values (*z*stat) and effects of interest obtained prior to scrubbing. This figure shows data for four clusters. The two clusters shown on the left reached significance in the analyses that used unscrubbed data, but were not significant at the whole-brain FWE corrected level in the analyses using the scrubbed data. In contrast, the two clusters on the right "appeared" in the analyses using the scrubbed data, but did not reach cluster significance in the analyses using unscrubbed data. For each cluster (column) the top row illustrates the similarity between the *Z*-statistic values of the effect of interest obtained for the analyses using unscrubbed and scrubbed data.

frontiers in
PSYCHIATRY

ORIGINAL RESEARCH ARTICLE
published: 25 January 2012
doi: 10.3389/fpsyt.2012.00002

Altered cortico-striatal–thalamic connectivity in relation to spatial working memory capacity in children with ADHD

Kathryn L. Mills[1,2]*, Deepti Bathula[3,4], Taciana G. Costa Dias[1,3], Swathi P. Iyer[1], Michelle C. Fenesy[3], Erica D. Musser[3], Corinne A. Stevens[1], Bria L. Thurlow[1], Samuel D. Carpenter[1], Bonnie J. Nagel[1,3], Joel T. Nigg[1,3] and Damien A. Fair[1,3,5]*

[1] *Department of Behavioral Neuroscience, Oregon Health and Science University, Portland, OR, USA*
[2] *Child Psychiatry Branch, National Institute of Mental Health, Bethesda, MD, USA*
[3] *Department of Psychiatry, Oregon Health and Science University, Portland, OR, USA*
[4] *Indian Institute of Technology, Ropar, India*
[5] *Advanced Imaging Research Center, Oregon Health and Science University, Portland, OR, USA*

Edited by:
Alex Fornito, University of Melbourne, Australia

Reviewed by:
Christopher A. Wall, Mayo Clinic, USA
Richard Bruce Bolster, University of Winnipeg, Canada

****Correspondence:***
Kathryn L. Mills, Child Psychiatry Branch, National Institute of Mental Health, 10 Center Drive, MSC 1367, Building 10, Room 4C432B, Bethesda, MD 20892, USA.
e-mail: millskl@mail.nih.gov;
Damien A. Fair, Psychiatry Department, Oregon Health and Science University, 3181 SW Sam Jackson Park Road UHN88, Portland, OR 97239, USA.
e-mail: faird@ohsu.edu

Introduction: Attention deficit hyperactivity disorder (ADHD) captures a heterogeneous group of children, who are characterized by a range of cognitive and behavioral symptoms. Previous resting-state functional connectivity MRI (rs-fcMRI) studies have sought to understand the neural correlates of ADHD by comparing connectivity measurements between those with and without the disorder, focusing primarily on cortical–striatal circuits mediated by the thalamus. To integrate the multiple phenotypic features associated with ADHD and help resolve its heterogeneity, it is helpful to determine how specific circuits relate to unique cognitive domains of the ADHD syndrome. Spatial working memory has been proposed as a key mechanism in the pathophysiology of ADHD. **Methods:** We correlated the rs-fcMRI of five thalamic regions of interest (ROIs) with spatial span working memory scores in a sample of 67 children aged 7–11 years [ADHD and typically developing children (TDC)]. In an independent dataset, we then examined group differences in thalamo-striatal functional connectivity between 70 ADHD and 89 TDC (7–11 years) from the ADHD-200 dataset. Thalamic ROIs were created based on previous methods that utilize known thalamo-cortical loops and rs-fcMRI to identify functional boundaries in the thalamus. **Results/Conclusion:** Using these thalamic regions, we found atypical rs-fcMRI between specific thalamic groupings with the basal ganglia. To identify the thalamic connections that relate to spatial working memory in ADHD, only connections identified in both the correlational and comparative analyses were considered. Multiple connections between the thalamus and basal ganglia, particularly between medial and anterior dorsal thalamus and the putamen, were related to spatial working memory and also altered in ADHD. These thalamo-striatal disruptions may be one of multiple atypical neural and cognitive mechanisms that relate to the ADHD clinical phenotype.

Keywords: ADHD, fMRI, connectivity, working memory, thalamus, striatum

INTRODUCTION

Brain imaging studies of attention deficit hyperactivity disorder (ADHD), including resting-state functional connectivity MRI (rs-fcMRI) studies, typically compare a group of children with the disorder to a typically developing control population (for a recent review, see Liston et al., 2011). In these studies, statistical differences between groups are used to inform current models of the disorder. However, with regard to resting connectivity in ADHD, the literature has generally not yet related group effects to specific behavioral symptoms or cognitive deficits, which are likely to vary across individuals with the disorder (Nigg, 2005). It is crucial to a comprehensive understanding of ADHD that the established cognitive correlates of the disorder are integrated with both clinical presentation and with contemporary, systemic analysis of brain function.

One approach to relating behavioral phenotypes to functional connectivity signatures of the disorder might be to first perform a traditional two-group analysis in a large sample to identify differences that are on average found in the test population. In conjunction, one would then apply a dimensional method in the same or, preferably, an independent sample to identify how atypical circuits relate to cognitive domains, even if they are not atypical in all participants with the disorder (Insel et al., 2010). This approach would extend our understanding of how differences in brain connectivity observed in children with ADHD relate to specific observed deficits in cognition and behavior, and potentially set the stage for refined diagnostics or refined phenotyping/subtyping based on brain physiology (Insel et al., 2010).

To this end, we begin our efforts examining the neurophysiology of ADHD and its relationship to spatial working memory. Deficits in spatial working memory have been proposed as a core mechanism in ADHD (Castellanos and Tannock, 2002; Westerberg et al., 2004; Nigg, 2005), are extensively studied, and appear to yield among the largest effect sizes of any cognitive measure

in ADHD (Nigg, 2005; Willcutt et al., 2005; Brown et al., 2011; Finke et al., 2011; Rhodes et al., 2012; Tillman et al., 2011). Typical measures of spatial span working memory ask the child to remember the sequence of a series of locations, and then to recall the sequence in order or in reverse. The latter task not only tests the child's ability to hold visual–spatial information in mind, but to also manipulate the information further in order to recall the sequence in the reverse order, presumably recruiting more central executive processes (Baddeley, 1996). Children with ADHD, as well as unaffected siblings of children with ADHD, successfully recall significantly shorter spatial span sequences than typically developing children (TDC) (Gau and Shang, 2010), making spatial working memory a viable candidate endophenotype for ADHD (Doyle et al., 2005).

Multiple neural pathways have been proposed as being involved in ADHD, many emphasizing subcortical–cortical circuits and dopaminergic projection pathways (Castellanos, 1997; Giedd et al., 2001; Nigg and Casey, 2005). While much attention has been given to the frontal–striatal aspect of these circuits, the role of the thalamus in ADHD has largely been unexplored. While a previous investigation of thalamic morphology in youths with ADHD revealed no overall difference in total thalamic volume, some region specific thalamic volumes were atypical in youths with ADHD, and were related to symptom dimensions of the disorder (Ivanov et al., 2010). Given the importance of the thalamus as a potential integration site of networks supporting the ability to modulate behavior (Haber and Calzavara, 2009), and its mediating role in cortico-striatal circuits, disrupted connections between the thalamus and other subcortical structures (i.e., basal ganglia) may correlate with certain behavioral components of ADHD. However, thalamic structures have traditionally been difficult to visualize *in vivo* in children, perhaps accounting for this gap in knowledge.

This problem may be overcome with resting state functional connectivity. Resting-state functional connectivity (rs-fcMRI) has been proposed as a method to study functional relationships between brain regions by examining spontaneous slow-wave (less than 0.1 Hz) oscillations in the blood–oxygen level dependent (BOLD) signal (Biswal et al., 1995). These functional connections are thought to reflect a history of co-activation between populations of neurons, and thus allow neuroimaging investigations the ability to examine the intrinsic functional architecture of the human brain (Bi and Poo, 1999; Dosenbach et al., 2007; Fair et al., 2007a). Previous studies have utilized rs-fcMRI to characterize atypical connections in ADHD (Zang et al., 2007; Castellanos et al., 2008; Uddin et al., 2008; Wang et al., 2009; Fair et al., 2010b), but tended to focus on cortical connections. To this date, rs-fcMRI investigations of subcortical–cortical interactions in children with ADHD remain scarce.

A recent technique that utilizes rs-fcMRI to examine functional relationships between the thalamus and cortex has created an opportunity for *in vivo* investigations of thalamo-cortical connectivity (Zhang et al., 2008, 2009). This technique has since been used to characterize thalamo-cortical connectivity across development (Fair et al., 2010a). Using this approach, it is possible to create functionally defined regions within the thalamus, and use these thalamic regions to examine interactions between the thalamus, basal ganglia, and cortex.

Drawing on subcortical–cortical models of ADHD (Nigg and Casey, 2005), we examined the functional connectivity between five thalamic regions of interest (ROI) and the basal ganglia. Taking advantage of recent techniques that allow functional parcellation of the thalamus (Zhang et al., 2008, 2009; Fair et al., 2010a), we correlated thalamic connection strength with spatial span backward scores in a sample of 67 children with and without ADHD. We then performed a comparative analysis of thalamic connection strength between children with and without ADHD-combined subtype (ADHD-C) in a matched independent sample comprising data collected across five institutions (see ADHD-200; http://fcon_1000.projects.nitrc.org/indi/adhd200). By examining connections that were both (a) related to spatial span working memory performance, and (b) associated with ADHD, we are able to distinguish how specific circuits relate to specific cognitive deficits that represent components of the ADHD syndrome.

MATERIALS AND METHODS

PARTICIPANTS

Data from Oregon Health and Science University, Brown University, Beijing Normal University, Kennedy Krieger Institute, and NYU Child Study Center were collected for youth aged 7–11 years ($N = 132$ TDC; $N = 94$ ADHD). Informed written consent or assent was obtained for all participants, and all procedures complied with the Human Investigation Review Board at respective universities. Due to differences in procedures across institutions, details on diagnostic criteria, data acquisition, and data processing are included in the Appendix.

This large dataset was divided into two subgroups for the analyses. The first subgroup comprised 67 children with and without ADHD (all subtypes included) from the Oregon Health and Science University site, for a correlational analysis (see **Table 1A**). The second subgroup comprised 89 TDC and 70 children with ADHD-C, matched for age, gender, and motion for a comparative analysis (see **Table 1B**).

BEHAVIORAL MEASURE

Spatial span working memory was assessed on the first subgroup of participants in this study (see **Table 1A**). These participants received the spatial span subtest of the Cambridge Neuropsychological Test Battery (CANTAB; CeNeS, 1998). The spatial span task is a computer-based task modeled on the Corsi Block Tapping Test (Milner, 1971). All children were presented a screen with indiscriminately placed boxes, and instructed to watch for the boxes that change. For this particular version of the task, boxes changed through the appearance of a green smiley-face within the box. After each sequence, children were asked to respond by clicking on the appropriate boxes after a 500 ms delay. Children were instructed to click on the boxes that changed in the same order for the spatial span forward task, or else they were instructed to click on the boxes that changed in reverse order for the spatial span backward task. The total span length and accuracy were recorded for each task. For the purposes of this study, we examined the spatial span backward total score for each child, which is the product of the total span length and mean accuracy across the spatial span backward task.

Table 1 | Participant characteristics.

Variable	TDC		ADHD		*p*
	Mean	**SD**	**Mean**	**SD**	
A. CORRELATION ANALYSIS					
Age	8.5	0.67	8.7	0.82	0.23
Full-scale IQ	118.35	13.82	106.66	13.54	<0.01**
Movement RMS	0.43	0.35	0.44	0.32	0.85
Volume-by-volume displacement	0.27	0.22	0.3	0.19	0.55
Spatial span backward total score	4.47	2.05	3.96	2.07	0.34
	%	***N***	**%**	***N***	
Gender					
Male	39.53	17	75	18	
Female	60.47	26	25	6	
ADHD subtype					
Combined	–	–	58.33	14	
Inattentive	–	–	37.5	9	
Hyperactive	–	–	4.17	1	
Variable	**TDC**		**ADHD-C**		***p***
	Mean	**SD**	**Mean**	**SD**	
B. COMPARISON ANALYSIS					
Age	9.94	1.23	9.85	1.28	0.65
Full-scale IQ	115.97	14.03	110.54	14.03	<0.02**
Volume-by-volume displacement	0.17	0.06	0.17	0.06	0.61
Movement RMS	0.46	0.21	0.47	0.25	0.64
	%	***N***	**%**	***N***	
Gender					
Male	73.03	65	80	56	
Female	26.97	24	20	14	

*Table (A) displays the age, gender, IQ, volume-by-volume displacement, movement RMS, and spatial span backward total scores for 67 children with and without ADHD from the OHSU sample. Table (B) displays the age, gender, IQ, volume-by-volume displacement, and movement RMS for 89 typically developing children (TDC) and 70 children with ADHD-combined (ADHD-C) subtype from the consortium sample. Movement is displayed as the average root mean square (RMS) across all included runs, before volumes were removed as indicated in the methods. **Indicates $p < 0.05$.*

DATA ACQUISITION AND PROCESSING

Participants were scanned on 3.0 Tesla scanners using standard resting-fMRI T2*-weighted echo-planar imaging. Due to the collaborative nature of this project (multiple sites of data collection), specific details regarding data acquisition, including scanning protocol and scanner details, are described in the Appendix to conserve space. All functional images were preprocessed to reduce artifacts (Miezin et al., 2000; see Appendix Text). Connectivity preprocessing followed prior methods (Fox et al., 2005; Fair et al., 2007a,b, 2008, 2009, 2010a) to reduce spurious variance unlikely to reflect neuronal activity (Fox and Raichle, 2007). These steps included: (i) a temporal band-pass filter ($0.009\ \text{Hz} < f < 0.08\ \text{Hz}$), (ii) regression of six parameters obtained by rigid body head motion correction, (iii) regression of the whole brain signal averaged over the whole brain, (iv) regression of ventricular signal averaged from ventricular region of interest (ROI), and (v) regression of white matter signal averaged from white matter ROI. Regression of first order derivative terms for the whole brain, ventricular, and white matter signals were also included in the correlation preprocessing. These preprocessing steps are, in part, intended to remove any developmental changes in connectivity driven by changes in respiration and heart rate over age. Motion was corrected and quantified using an analysis of head position based on rigid body translation and rotation. The data derived from these adjustments needed to realign head movement on a volume-by-volume basis were calculated as root mean square (RMS) values for translation and rotation in the *x*, *y*, and *z* planes in millimeters. Participant's BOLD runs with movement exceeding 1.5 mm RMS were removed. Overall movement was low across all participants (**Table 1**).

With that said, we were particularly sensitive to potential movement confounds. As such, we also evaluated the similarity between

each BOLD volume and the preceding volume to exclude volumes with excessive movement (Smyser et al., 2010; Shannon et al., 2011). Movement generally results in high variance in measured functional MRI signal. Thus, the algorithm used here excludes volumes whose signal change was >3 SD above the mean (Smyser et al., 2010; Shannon et al., 2011). Signal change is computed at each voxel by backward differences. The global measure of signal change then is

$$\sqrt{\left\langle [\Delta I_i(\vec{x})]^2 \right\rangle} = \sqrt{\left\langle [I_i(\vec{x}) - I_{i-1}(\vec{x})]^2 \right\rangle},$$

where $Ii(\vec{x})$ is image intensity at locus $\vec{x}$ on time point i and angle brackets denote the spatial average over the whole brain. For the remaining volumes we also limited our sample to ensure that mean volume-by-volume displacement was not related to our outcome measures (Power et al., 2012; Van Dijk et al., 2011). Volume-by-volume displacement (VD) – or frame-to-frame displacement (FD; Power et al., 2012) – was calculated as a scalar quantity using the formula, $\mathrm{VD}_i = |\boldsymbol{\Delta} d_{ix}| + |\boldsymbol{\Delta} d_{iy}| + |\boldsymbol{\Delta} d_{iz}| + |\boldsymbol{\Delta\alpha}_i| + |\boldsymbol{\Delta\beta}_i| + |\boldsymbol{\Delta\gamma}_i|$, where $\boldsymbol{\Delta} d_{ix} = d_{(i-1)x} - d_{ix}$, and similarly for the other five rigid body parameters (Power et al., 2012). This formula sums the absolute values of volume-by-volume changes in the six rigid body parameters. There was no relationship between mean volume-by-volume displacement (for the remaining volumes) and spatial span backward total scores ($p > 0.19$). We also matched our participants, such that there was no difference in mean volume-by-volume displacement (for remaining volumes) between children with ADHD and TDC in our sample ($p > 0.80$).

THALAMIC ROI DEFINITION USING "WINNER TAKE ALL" STRATEGY

Thalamic ROIs were defined using the "winner take all" strategy for all 226 participants in order limit group bias during ROI creation (Zhang et al., 2008, 2009; Fair et al., 2010a). The "winner take all" strategy assigns each voxel in the thalamus a value corresponding to the cortical subdivision to which it is most strongly correlated. Cortical subdivisions were defined as in Zhang et al. (2008). The anatomical image from a normal young adult volunteer was segmented along the gray/white boundary and deformed to the population-average, landmark, and surface-based (PALS)-B12 atlas (Van Essen, 2005) using SureFit and Caret software (Van Essen and Drury, 1997; Van Essen et al., 2001). Partition boundaries were manually drawn based on major sulcal landmarks, following work by Behrens et al. (2003). Five broad cortical ROIs were defined: (1) frontopolar and frontal cortex including the orbital surface and anterior cingulate; (2) motor and premotor cortex (Brodmann areas 6 and 4 – excluding adjacent portions of cingulate cortex); (3) somatosensory cortex (Brodmann areas 3, 1, 2, 5, and parts of 40); (4) parietal and occipital cortex including posterior cingulate and lingual gyrus; (5) temporal cortex including the lateral surface, temporal pole, and parahippocampal areas. These five surface partitions were assigned a thickness of 3 mm, 1.5 mm above and below the fiducial surface (corresponding to "layer IV"), and were then rendered into volume space.

For each of the cortical ROIs, volumetric correlation maps were generated for each subject (Fox et al., 2005). To calculate statistical significance, we converted correlation coefficients (r) to a normal distribution using Fisher's z transformation. z-transformed maps were then combined across participants using a random effects analysis. Results presented here are restricted to the thalamus, whose boundaries were created by manual tracing of the atlas template (Zhang et al., 2008). Finally, the "winner take all" strategy, as established in previous work (Zhang et al., 2008), was applied to subdivide the thalamus. For the five cortical subdivisions, an average resting-state time series was extracted and correlated with each voxel in the thalamus for each individual. These data were analyzed with a total correlation procedure, which included whole brain signal regression in the initial preprocessing steps. Shared variance among the five cortical subdivisions is accounted for in this instance with the initial whole brain signal regression, similar to the total correlation procedure used in Zhang et al. (2008).

This analysis allowed us to create functionally defined thalamic ROI. Five thalamic ROIs were created based on the correlations between the five cortical ROIs and each voxel in the thalamus. Given that functional connectivity between the thalamus and cortex changes across developmental periods (Fair et al., 2010a), we used this method to create functionally defined ROIs within the thalamus for our sample of 226 children aged 7–11 years, a relatively restricted development window. These five thalamic ROIs were then used to generate volumetric correlation maps for each subject, which were then normalized through the same procedure detailed above. All remaining analyses were performed on these Fisher z-transformed correlation maps.

ANALYSIS 1: CORRELATIONAL ANALYSIS WITH SPATIAL SPAN BACKWARD TOTAL SCORES

To test significant relationships between thalamic connectivity and spatial span backward total scores, we performed a voxelwise correlational analysis in the first subgroup of 67 children (**Table 1A**). Correlations between all voxels and each thalamic ROI were calculated for each participant (random effects analysis assuming unequal variance; $p \leq 0.05$), and these correlation values were then correlated (r) with the spatial span backward total score for each participant. For the voxelwise, random effects maps, we implemented a Monte Carlo simulation procedure (Forman et al., 1995). To obtain multiple comparisons corrected, $p < 0.05$ voxel clusters, a threshold of 53 contiguous voxels with a z-value >2.25 was used.

ANALYSIS 2: COMPARATIVE ANALYSIS BETWEEN CHILDREN WITH ADHD-C AND TYPICALLY DEVELOPING CHILDREN

To test significant differences in thalamic connectivity between 70 children with ADHD-C and 89 matched TDC (**Table 1B**), direct comparisons between the two groups were performed. We performed two-sample, two-tailed t-tests (random effects analysis assuming unequal variance; $p \leq 0.05$) for each thalamic ROI. For the voxelwise, random effects maps, we implemented a Monte Carlo simulation procedure (Forman et al., 1995). To obtain multiple comparisons corrected, $p < 0.05$ voxel clusters, a threshold of 53 contiguous voxels with a z-value >2.25 was used. To examine the functional connectivity maps for each group, we generated separate z-score maps across all participants in each group using a random effects analysis.

CONJUNCTION ANALYSIS

For each thalamic ROI, results of the comparative analysis were masked by results of the correlational analysis to identify areas that are both significantly different in children with ADHD as compared to TDC, and related to spatial span backward performance. This process was conducted on the Monte Carlo multiple comparisons corrected voxelwise maps generated from each of the previous analyses. This conjunction analysis produced ROIs preblurred 4 mm FWHM, with peaks within 10 mm consolidated, and only voxels with z values >2.25 or <2.25 considered. The peaks generated from the comparative analysis were masked with the results of the correlation analysis. Time courses for each ROI were extracted. Correlations between these newly produced ROIs and the five thalamic ROIs were generated to characterize the relationship between spatial span backward scores that have been adjusted for age, and the connectivity strength between the thalamic ROI and the ROIs generated from the conjunction analysis.

RESULTS

FUNCTIONAL CONNECTIVITY OF CORTICAL SUBDIVISIONS WITHIN THE THALAMUS

Five thalamic ROIs were created by subdividing the thalamus with the "winner take all" strategy in all 226 participants, displayed in **Figure 1**. These thalamic ROIs showed bilateral symmetry, and visually correspond to known human thalamic nuclear groupings (Jones, 2007). It should be noted that the subdivision of the thalamus in the current sample of children (7–11 years) most closely resembles the subdivision of the thalamus of an adolescent group (11–16 years) as opposed to the 7–9 year olds in prior work (Fair et al., 2010a). This pattern may reflect the demographic characteristics of our sample, which has a slightly greater number of older children than the prior study (mean age = 9.50 years), or might relate to increased sample size and additional movement correction procedures performed here (Smyser et al., 2010; Power et al., 2012; Shannon et al., 2011; Van Dijk et al., 2011). Nevertheless, the thalamic subdivisions generated in the current analysis resemble known nuclear groupings, supporting our use of these subdivisions as functionally defined thalamic ROIs. The prefrontal cortical subdivision showed strongest interactions with the anterior portion of the thalamus, potentially corresponding with the ventral anterior nuclei and anterior group. The temporal cortical subdivision showed strongest interactions with the medial posterior, inferior, and midline areas of the thalamus, potentially corresponding to the medial pulvinar, medial geniculate, and medial dorsal nucleus. The parietal–occipital cortical subdivision showed strongest interactions with the lateral and posterior portions of the thalamus, potentially corresponding to the lateral pulvinar and lateral geniculate. The somatosensory cortical areas strongly correlated with ventral, lateral, and posterior thalamic regions, potentially corresponding to ventral posterolateral and posteromedial nuclei. The premotor–motor cortical subdivision correlated strongly with lateral and ventral thalamic areas that presumptively correspond to ventral lateral and ventral lateral posterior nuclei. Thus, these patterns strongly suggest valid detection of actual thalamo-cortical loops by our method.

ANALYSIS 1: THALAMIC CONNECTIVITY WITH THE BASAL GANGLIA RELATES TO SPATIAL SPAN WORKING MEMORY PERFORMANCE

In our initial set of 67 children, correlational analyses revealed significant relationships between spatial span backward total scores and thalamic functional connections with the basal ganglia. Significant relationships were observed for four of our five thalamic ROIs, as illustrated in **Figure 2**. Spatial span backward total scores were negatively correlated with connectivity strength between the prefrontal thalamic ROI and bilateral putamen and bilateral globus pallidus. Similarly, spatial span backward total scores were negatively correlated with connectivity strength between the premotor–motor thalamic ROI and bilateral putamen. Lateralized relationships were observed between spatial span backward total scores and connectivity between the temporal thalamic ROI and basal ganglia, as well as the somatosensory thalamic ROI and basal ganglia. Connectivity strength between the temporal thalamic ROI and primarily the left lateral globus pallidus was negatively correlated with spatial span backward total scores, whereas connectivity

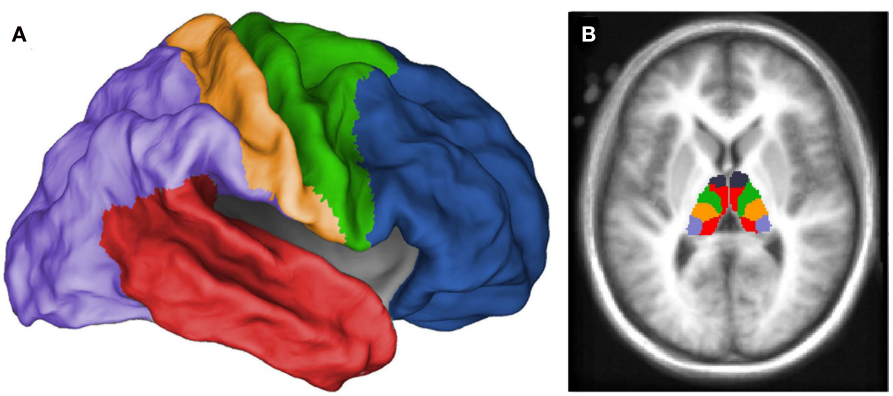

FIGURE 1 | Thalamic regions of interest generated from "winner take all" procedure (Zhang et al., 2008, 2009; Fair et al., 2010a) in all 226 children. Each voxel in the thalamus was assigned a value (designated by color in figure) corresponding to the cortical subdivision with which it was most strongly correlated. Cortical subdivisions are illustrated in **(A)**, and the thalamic subdivision is illustrated in **(B)**. Thalamic ROIs were generated from this subdivision to analyze the functional connectivity of distinct thalamic regions.

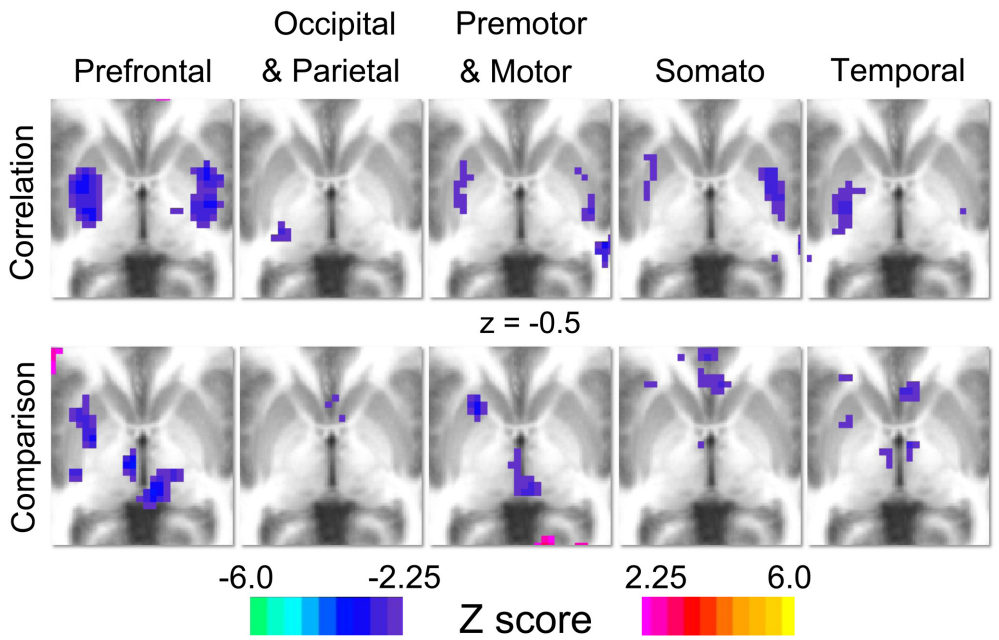

FIGURE 2 | Results for the correlation and comparison analyses. Each column represents the results for each of thalamic regions of interest (prefrontal, occipital–parietal, premotor–motor, somatosensory, and temporal). For the correlation analysis (row 1), warm colors indicate areas where connection strength positively correlates with spatial span backward total scores, and cool colors indicate areas where connection strength is negatively correlated with spatial span backward total scores. For the comparison analysis (row 2), warm colors (positive *z*-scores) indicate areas where connection strength is greater in typically developing control population, and cool colors (negative *z*-scores) indicate areas where connection strength is greater in the ADHD-C population.

strength between the somatosensory thalamic ROI and primarily the right posterior putamen was negatively correlated with spatial span backward total scores.

ANALYSIS 2: THALAMIC CONNECTIVITY WITH THE BASAL GANGLIA IS ATYPICAL IN CHILDREN WITH ADHD

Direct comparisons between 70 children diagnosed with ADHD-C and 89 TDC reveal significant differences in connectivity between the thalamus and basal ganglia portrayed in **Figure 2**. Specifically, robust differences in connectivity were found between the prefrontal thalamic ROI and the left putamen, reflecting different subcortical connectivity patterns between groups. Examination of functional connectivity patterns at the group level reveals connections between the prefrontal thalamic ROI and the putamen in the ADHD-C group that are absent altogether in the TDC group (**Figure A1** in Appendix). Children with ADHD-C also showed significantly greater connectivity strength between the occipital–parietal thalamic ROI and the left putamen and right caudate head than TDC. Connectivity differences and group level patterns between the basal ganglia and the premotor–motor thalamic ROI, somatosensory thalamic ROI, and temporal thalamic ROI were observed, although at a smaller scale. The connectivity differences observed for these three seed regions were similarly located in the putamen, with small differences observed in portions of the globus pallidus and caudate body. Children with ADHD-C showed significantly greater connectivity strength between these thalamic regions and basal ganglia than TDC.

ATYPICAL THALAMIC CONNECTIVITY WITH THE BASAL GANGLIA RELATES TO SPATIAL SPAN WORKING MEMORY PERFORMANCE AS REVEALED BY CONJUNCTION ANALYSIS

Results of the conjunction analysis reveal distinct and overlapping relationships between four of our thalamic ROIs and the basal ganglia, specifically the putamen and globus pallidus (**Figure 3**). Connections between the prefrontal thalamic ROI and the left putamen (−27, 6, 4; −25, −7, −1; −30, −22, −1) are both significantly related to spatial span backward total scores and significantly different in children with ADHD-C as compared to TDC. Similarly, connections between the premotor–motor thalamic ROI and the left putamen (−20, 13, −1), as well as connections between the temporal thalamic ROI and left putamen (−21, 2, 1), are significantly related to spatial span backward total scores and significantly different in children with ADHD-C as compared to TDC. Connections between the somatosensory thalamic RO I and the right putamen (18, −33, −14), and right lateral medial pallidus (15, −6, −5) display significant overlapping relationships in the comparative and correlational analyses (see **Table 2** for all coordinates). No connections between the occipital–parietal thalamic ROI and the basal ganglia passed the conjunction analysis. Connections to portions of the left putamen overlap across the different thalamic ROIs (**Figure 3C**). The relationship between adjusted spatial span backward total scores and connection strength between the prefrontal thalamic ROI and the left putamen (−25, −7, −1) was plotted to reveal the nature of the relationship in a *post hoc* analysis (**Figure 4**).

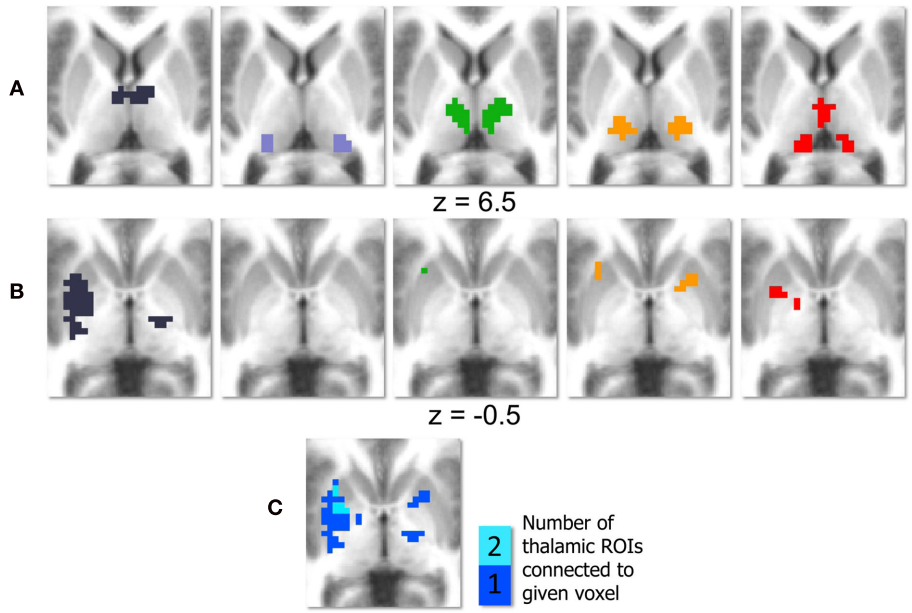

FIGURE 3 | Conjunction analysis with basal ganglia. Thalamic regions of interest (ROI) are displayed in **(A)**; deep purple corresponds to the prefrontal thalamic ROI, light purple corresponds to the occipital–parietal thalamic ROI, green corresponds to the premotor–motor thalamic ROI, orange–yellow corresponds to the somatosensory thalamic ROI, and red corresponds to the temporal thalamic ROI. Regions of the basal ganglia that survive the conjunction analysis are displayed in row **(B)**, with each column corresponding to one thalamic ROI. The colors in **(C)** indicate how many thalamic ROIs show significant connections that pass the conjunction analysis with a given area of the basal ganglia.

ATYPICAL THALAMIC CONNECTIVITY WITH CORTICAL STRUCTURES IN CHILDREN WITH ADHD RELATES TO SPATIAL SPAN WORKING MEMORY PERFORMANCE

While the focus of the current investigation was directed toward subcortical structures, connections between four of the thalamic ROIs and multiple areas of the cortex were also found to be significantly different in children with ADHD-C as compared to TDC children, and related to spatial span backward total scores (**Figure 5**). We describe the cortical results of the conjunction analysis for each thalamic ROI below. In addition, we have included details as to how these connections relate to spatial span working memory performance and differ between children with ADHD-C and TDC, illustrated in **Figures A2–A6** in Appendix.

Prefrontal thalamic ROI

Connectivity strength between the prefrontal thalamic ROI and the right superior frontal gyrus, right middle frontal gyrus, right superior frontal gyrus, was greater in children with ADHD and related to better spatial span working memory performance. Connectivity strength between the prefrontal thalamic ROI and the right precentral gyrus was greater in TDC and related to worse spatial span working memory performance. The relationship between adjusted spatial span backward total scores and connection strength between the right middle frontal gyrus (38, 41, 24) and prefrontal thalamic ROI was plotted to reveal the nature of the relationship in a *post hoc* analysis (**Figure 4**).

Premotor–motor thalamic ROI

Connectivity strength between the premotor–motor thalamic ROI and the left lingual gyrus, right lingual gyrus, left inferior occipital gyrus, and right inferior occipital gyrus was greater in TDC and related to better spatial span working memory performance. Connectivity strength between the premotor–motor thalamic ROI and the left inferior frontal gyrus and left superior temporal gyrus is greater in children with ADHD and related to worse spatial span working memory performance.

Somatosensory thalamic ROI

Connectivity strength between the somatosensory thalamic ROI and the fusiform gyrus and left lingual gyrus was greater in TDC and related to better spatial span working memory performance.

Temporal thalamic ROI

Connectivity strength between the temporal thalamic ROI and the left middle temporal gyrus and right middle temporal gyrus was greater in children with ADHD and related to worse spatial span working memory performance.

DISCUSSION

Children with ADHD show disruptions in brain circuits related to cognitive impairments associated with the disorder. ADHD is widely theorized to involve disruptions in cortico-striatal–thalamic neural circuits, but until now neuroimaging investigations have been largely restricted to examining the cortex and striatum in ADHD, leaving a crucial gap with regard to evidence of thalamic involvement. The present study reveals that thalamic connections to these regions are involved in ADHD and in its associated executive cognitive problems. Our findings suggest that on average, relative to the control population, there are

Table 2 | Peak coordinate for the conjunction analysis.

Structure	Conjunction		
	B.A.	Peak coordinates	# of voxels
PREFRONTAL THALAMIC ROI			
Left pulvinar		(−11, −24, 9)	6
Right superior frontal gyrus	9	(33, 53, 26)	11
Ventral posterior medial nucleus		(14, −20, 0)	14
Right middle frontal gyrus	9	(38, 41, 34)	22
Left putamen		(−27, 6, 4)	29
Right superior frontal gyrus	8	(29, 42, 42)	40
Left putamen		(−25, −7, −1)	70
Right precentral gyrus	6	(41, −7, 29)	14
Left putamen		(−30, −22, −1)	30
OCCIPITAL–PARIETAL THALAMIC ROI			
N/A			
PREMOTOR–MOTOR THALAMIC ROI			
Left putamen		(−20, 13, −1)	2
Left superior temporal gyrus	38	(−49, 15, −26)	4
Left lingual gyrus	18	(−16, −100, −5)	29
Right lingual gyrus	17	(21, −98, −8)	31
Left inferior occipital gyrus	18	(−30, −95, −2)	34
Right inferior occipital gyrus	18	(31, −93, −3)	37
Left inferior frontal gyrus	13	(−28, 11, −9)	6
SOMATOSENSORY THALAMIC ROI			
Right medial globus pallidus		(15, −6, −5)	2
Right culmen		(17, −33, −14)	7
Right putamen		(18, −33, −14)	9
Left lingual gyrus	18	(−16, −99, −6)	13
Left putamen		(−23, 10, −6)	13
Left fusiform gyrus	18	(−29, −94, −19)	1
Left claustrum		(−26, 18, 0)	1
TEMPORAL THALAMIC ROI			
Left thalamus		(−9, −12, 2)	2
Left putamen		(−21, 2, 1)	13
Left middle temporal gyrus	21	(−36, 5, −30)	1
Right middle temporal gyrus	21	(38, −4, −29)	9

Peak coordinates for regions in the basal ganglia and cortex that were significantly connected to each thalamic region of interest were generated through the conjunction analyses. Structure details were generated with Talairach Client (Lancaster et al., 1997, 2000). Peak coordinates are in talairach space.

altered thalamo-striatal and thalamo-cortical interactions in children with ADHD. These findings appear to relate to at least one behavioral component of ADHD – the ability to manipulate information in mind, which is atypical in ADHD (although probably only in a portion of the population (Nigg, 2005) as we discuss below).

ACCOUNTING FOR HETEROGENEITY WITHIN ADHD

The heterogeneity of cognitive and behavioral impairments present in ADHD presents a challenge for neuroimaging studies attempting to characterize atypical brain pathways associated with the disorder. By examining a dimensional neuropsychological aspect of the disorder in conjunction with a comparison analysis in a large sample of participants with and without ADHD, we are able to identify atypical cortico-striatal–thalamic pathways related to spatial working memory. However, it is important to consider that these probably are present or clinically meaningful in only a subset of children with the disorder. Future work differentiating individual variability in behavioral components of ADHD and how they are associated with underlying disruptions in brain circuitry might facilitate improved empirical and biologically based subtyping within the disorder. In this sense, while our focus here was on working memory deficits, future efforts would be needed to identify atypical brain circuits involved in other aspects of behavioral regulation thought to be disrupted in ADHD (e.g., reward processing, thought to involve pathways between the ventral striatum and prefrontal cortex; Nigg and Casey, 2005; Sonuga-Barke, 2005). Multiple ADHD related features identified in this way could then be used to sub-classify individuals based on their own unique brain–behavior relationships.

ATYPICAL CONNECTIONS BETWEEN THE BASAL GANGLIA AND ANTERIOR THALAMUS IN ADHD ARE RELATED TO SPATIAL WORKING MEMORY

Using functionally defined thalamic ROIs, we were able to examine functional connections between distinct areas of the thalamus and the basal ganglia. Given the distinct anatomical connectivity patterns of individual thalamic nuclei (Jones, 2007), this approach provided some specificity to our findings. Connectivity between the putamen and our prefrontal thalamic ROI, which encompasses the anterior portion of the thalamus, relate to spatial span working memory in TDC and in children with ADHD. Stronger thalamic–putamen connectivity correlated with lower spatial span backward total scores. In a separate comparative analysis, we found that these same connections between the prefrontal thalamic ROI and putamen were atypical in children with ADHD-C. Children with ADHD-C displayed *stronger* connectivity between our prefrontal thalamic ROI and putamen than in a matched control group (**Figure A1** in Appendix), suggesting that these connections may be of unique importance in the cortico-striatal–thalamic circuitry underlying working memory and the ADHD clinical phenotype. This work fits nicely with previous models of ADHD (see below) and also with findings highlighting the role of the anterior thalamic nuclei in spatial working memory (Aggleton et al., 1996; Jones, 2007). In addition, the specificity of our findings coincides with known anatomical striatal-thalamo links (Parent and Hazrati, 1995; Jones, 2007).

Other thalamic ROIs generated in this study, specifically the premotor–motor thalamic ROI, somatosensory thalamic ROI, and temporal thalamic ROI, similarly show greater connectivity strength with areas of the basal ganglia in children with ADHD-C relative to TDC, but to a lesser extent. The strength of these same thalamo-striatal connections are related to lower spatial span backward total scores. While the connections between these three thalamic ROIs and the basal ganglia are not as a robust as with the prefrontal thalamic ROI, they appear in similar areas of the putamen. Portions of the left putamen show atypical connections with multiple thalamic ROIs (**Figure 3C**), suggesting that functional associations between the thalamus and putamen may underlie some of the behavioral impairments in children with ADHD.

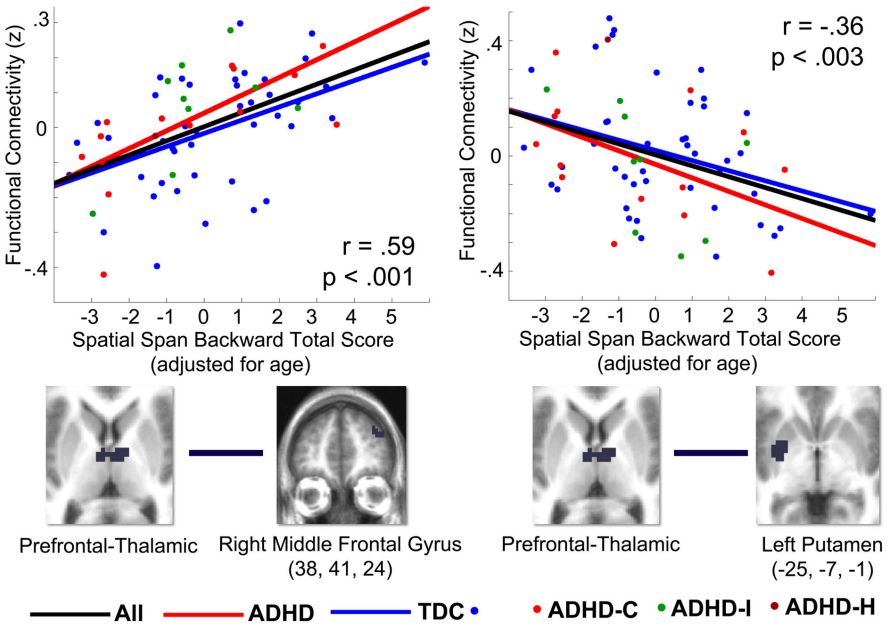

FIGURE 4 | Correlations (*r*) between select thalamo-striatal and thalamo-cortical connections and spatial span working memory performance in 67 children in the OHSU cohort, from *post hoc* analysis. Graphs plot *z*-transformed functional connectivity values on the *y*-axis with adjusted spatial span backward total scores on the *x*-axis. Spatial span backward total scores were covaried for age. The Pearson correlation coefficient (*r*) and significance are displayed for each graph. The ROIs used to generate the correlation are visualized below each graph. The left graph plots connectivity between the prefrontal thalamic ROI and the right middle frontal gyrus (38, 41, 24) with spatial span working memory performance. The right graph plots connectivity between the prefrontal thalamic ROI and the left putamen (−25, −7, −1) with spatial span working memory performance. The black line is the fitted line for all children, the blue line is the fitted line for all TDC children, and the red line is the fitted line for all children with ADHD. The dots indicate the diagnostic category for each participant: blue for TDC, red for ADHD-combined subtype, green for ADHD-inattentive subtype, and dark red for ADHD-hyperactive subtype. The choices for connections plotted in this graph were generated from the conjunction analysis, and therefore these graphs are only to illustrate the relationship between thalamo-striatal and thalamo-cortical functional connections and the adjusted spatial span behavioral measure.

THESE FINDINGS SUPPORT CORTICO-STRIATAL–THALAMIC PATHWAY MODELS OF ADHD

Cortico-thalamic circuits, in particular fronto-striatal and fronto-cerebellar circuits mediated by the thalamus, have been suggested as being impaired in children with ADHD (Castellanos, 1997; Giedd et al., 2001; Nigg and Casey, 2005; Casey et al., 2007). Traditional fMRI studies have repeatedly shown frontal and striatal areas as having atypical brain activity in children with ADHD; however, functional connections between these structures have received less attention (Dickstein et al., 2006; Liston et al., 2011).

The present study highlights the role of thalamic functional connections with the putamen, and, to a lesser extent, the caudate and globus pallidus. While structural brain imaging studies have reported inconsistent findings on putamen volume in individuals with ADHD (Casey et al., 1997; Castellanos et al., 2002; Ellison-Wright et al., 2008; Qiu et al., 2009), functional neuroimaging studies have found differences in putamen blood volume (Teicher et al., 2000), activation (Konrad et al., 2006) and functional connectivity in youth with ADHD (Cao et al., 2009). The caudate nucleus and lateral globus pallidus have held a substantial role in brain investigations of ADHD showing altered structure, function, and connectivity in individuals with the disorder (Castellanos et al., 1994, 2002; Durston et al., 2003; Booth et al., 2005; Silk et al., 2009). Our results suggest that interactions between these regions are similarly atypical in the present sample.

It is likely that a balanced relationship between these structures facilitates effective behavioral modulation to environmental contexts. Indeed, the maturation of cognitive control and voluntary planning of behavior that is seen across child and adolescent development has been proposed to reflect the underlying maturation of fronto-striatal–thalamic loops (Nigg and Casey, 2005). The thalamus plays an important role as a mediating structure in cortico-striatal circuits, as well as a potential integration site for networks that support the ability to modulate behavior (Haber and Calzavara, 2009). Alterations in functional connectivity between the thalamus and basal ganglia may reflect irregular signaling between these structures that may, in turn, alter afferent signaling from the thalamus to the cortex. The results of this study support models of ADHD in which atypical cortico-striatal–thalamic pathways underlie the breakdowns in cognitive control and behavioral adjustment observed in children with ADHD (Nigg and Casey, 2005).

ATYPICAL CONNECTIONS BETWEEN THE THALAMUS AND CORTICAL REGIONS IN ADHD ARE RELATED TO SPATIAL WORKING MEMORY

It is important to note that the results of this study were not limited to thalamo-striatal connections. Four of our five thalamic ROIs

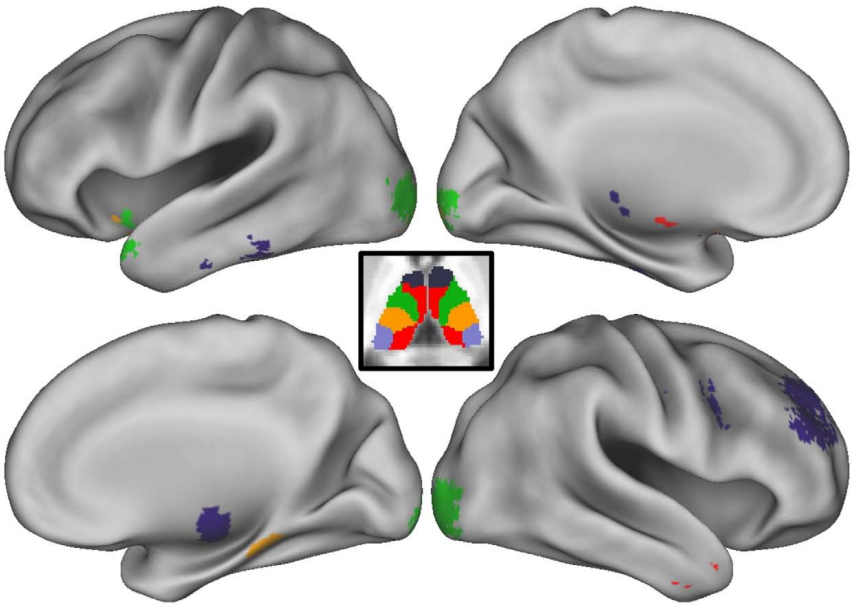

FIGURE 5 | Conjunction analysis with cortex. Thalamo-cortical connections that survive the conjunction analysis are projected onto the medial and lateral surfaces of each hemisphere. Colors correspond to which thalamic regions of interest (ROI) the cortical area is connected. The thalamic parcellation is displayed in the center of the figure as a reference. Deep purple corresponds to the prefrontal thalamic ROI, light purple corresponds to the occipital–parietal thalamic ROI, green corresponds to the premotor–motor thalamic ROI, orange–yellow corresponds to the somatosensory thalamic ROI, and red corresponds to the temporal thalamic ROI.

displayed connectivity differences between groups across areas of the cortex that also related to spatial span working memory. Connections between our prefrontal thalamic ROI, which encompasses the anterior dorsal midline areas of the thalamus, and the superior frontal and middle frontal gyri, were significantly different between groups and related to spatial span working memory. Given the role of the dorsolateral prefrontal cortex in adaptive online task control (Dosenbach et al., 2006, 2007), disruptions in subcortical connections to this region of the cortex may contribute to performance deficits in task-level control. Such a finding would suggest that this particular atypical behavior related to this circuit would expand beyond working memory, and relate to many tasks. Further exploration of connectivity differences between the striatum and cortical networks involved in task control may prove illuminative of connections that are atypical in these cortico-striatal–thalamic circuits.

CONCLUSION

As brain imaging research continues to uncover objective biological markers of psychiatric disorders, such as ADHD, the hope is for these techniques to assist in the diagnosis, subclassification, and therapy development for affected individuals. The large, multi-site dataset leveraged for our secondary analysis (http://fcon_1000.projects.nitrc.org/indi/adhd200/) in this study demonstrates the utility of rs-fcMRI in detecting atypical brain patterns in children diagnosed with ADHD. Moreover, we were able to relate these atypical brain patterns to a specific neuropsychological dimension of the disorder. It would be of further interest to investigate the effects of different treatment modalities (e.g., cognitive training, stimulant medication) on connectivity strength between regions identified in this study. Together with structural brain imaging methods, examinations of the brain's functional architecture may provide a viable clinical purpose in detecting, classifying, and treating developmental neuropsychiatric disorders.

ACKNOWLEDGMENTS

We would like to extend special thanks to the ADHD-200 Consortium (http://fcon_1000.projects.nitrc.org/indi/adhd200/) for their generosity in contributing data to this open source forum: Daniel P. Dickstein, Pediatric Mood, Imaging, and Neurodevelopment Program, Brown University; Stewart K. Mostofsky, Kennedy Krieger Institute, Johns Hopkins University; Jan K. Buitelaar, Radboud University Nijmegen Medical Centre, Nijmegen, The Netherlands; F. Xavier Castellanos and Michael P. Milham, Phyllis Green, and Randolph Cowen Institute for Pediatric Neuroscience at the Child Study Center, New York University Langone Medical Center, New York, New York, Nathan Kline Institute for Psychiatric Research, Orangeburg, NY, USA; Yu-feng Wang, Institute of Mental Health, Peking University; Yu-feng Zang, National Key Laboratory of Cognitive Neuroscience and Learning, Beijing University; Beatriz Luna, Laboratory of Neurocognitive Development, University of Pittsburgh; and Bradley L. Schlaggar and Steve Petersen, Washington University School of Medicine, St. Louis Children's Hospital. We also thank all of the families and children who participated in the study. Research was supported by the Oregon Clinical and Translational Research Institute (Fair), Medical Research Foundation (Fair), UNCF Merck (Fair), Ford Foundation (Fair), K99/R00 MH091238 (Fair), R01 MH086654 (Nigg), R01 MH59105 (Nigg), and OHSU Foundation (Nigg).

REFERENCES

Aggleton, J. P., Hunt, P. R., Nagle, S., and Neave, N. (1996). The effects of selective lesions within the anterior thalamic nuclei on spatial memory in the rat. *Behav. Brain Res.* 81, 189–198.

Baddeley, A. (1996). The fractionation of working memory. *Proc. Natl. Acad. Sci. U.S.A.* 93, 13468–13472.

Behrens, T. E., Johansen-Berg, H., Woolrich, M. W., Smith, S. M., Wheeler-Kingshott, C. A., Boulby, P. A., Barker, G. J., Sillery, E. L., Sheehan, K., Ciccarelli, O., Thompson, A. J., Brady, J. M., and Matthews, P. M. (2003). Non-invasive mapping of connections between human thalamus and cortex using diffusion imaging. *Nat. Neurosci.* 6, 750–757.

Bi, G., and Poo, M. (1999). Distributed synaptic modification in neural networks induced by patterned stimulation. *Nature* 401, 792–796.

Biswal, B., Yetkin, F. Z., Haughton, V. M., and Hyde, J. S. (1995). Functional connectivity in the motor cortex of resting human brain using echo-planar MRI. *Magn. Reson. Med.* 34, 537–541.

Booth, J. R., Burman, D. D., Meyer, J. R., Lei, Z., Trommer, B. L., Davenport, N. D., Li, W., Parrish, T. B., Gitelman, D. R., and Mesulam, M. M. (2005). Larger deficits in brain networks for response inhibition than for visual selective attention in attention deficit hyperactivity disorder (ADHD). *J. Child Psychol. Psychiatry* 46, 94–111.

Brown, A. B., Biederman, J., Valera, E., Makris, N., Doyle, A., Whitfield-Gabrieli, S., Mick, E., Spencer, T., Faraone, S., and Seidman, L. (2011). Relationship of DAT1 and adult ADHD to task-positive and task-negative working memory networks. *Psychiatry Res.* 193, 7–16.

Cao, X., Cao, Q., Long, X., Sun, L., Sui, M., Zhu, C., Zuo, X., Zang, Y., and Wang, Y. (2009). Abnormal resting-state functional connectivity patterns of the putamen in medication-naïve children with attention deficit hyperactivity disorder. *Brain Res.* 1303, 195–206.

Casey, B. J., Castellanos, F. X., Giedd, J. N., Marsh, W. L., Hamburger, S. D., Schubert, A. B., Vauss, Y. C., Vaituzis, A. C., Dickstein, D. P., Sarfatti, S. E., and Rapoport, J. L. (1997). Implication of right frontostriatal circuitry in response inhibition and attention-deficit/hyperactivity disorder. *J. Am. Acad. Child Adolesc. Psychiatry* 36, 374–383.

Casey, B. J., Nigg, J. T., and Durston, S. (2007). New potential leads in the biology and treatment of attention deficit-hyperactivity disorder. *Curr. Opin. Neurol.* 20, 119–124.

Castellanos, F. X. (1997). Toward a pathophysiology of attention-deficit/hyperactivity disorder. *Clin. Pediatr. (Phila).* 36, 381–393.

Castellanos, F. X., Giedd, J. N., Eckburg, P., Marsh, W. L., Vaituzis, A. C., Kaysen, D., Hamburger, S. D., and Rapoport, J. L. (1994). Quantitative morphology of the caudate nucleus in attention deficit hyperactivity disorder. *Am. J. Psychiatry* 151, 1791–1796.

Castellanos, F. X., Lee, P. P., Sharp, W., Jeffries, N. O., Greenstein, D. K., Clasen, L. S., Blumenthal, J. D., James, R. S., Ebens, C. L., Walter, J. M., Zijdenbos, A., Evans, A. C., Giedd, J. N., and Rapoport, J. L. (2002). Developmental trajectories of brain volume abnormalities in children and adolescents with attention-deficit/hyperactivity disorder. *JAMA* 288, 1740–1748

Castellanos, F. X., Margulies, D. S., Kelly, C., Uddin, L. Q., Ghaffari, M., Kirsch, A., Shaw, D., Shehzad, Z., Di Martino, A., Biswal, B., Sonuga-Barke, E. J., Rotrosen, J., Adler, L. A., and Milham, M. P. (2008). Cingulate-precuneus interactions: a new locus of dysfunction in adult attention-deficit/hyperactivity disorder. *Biol. Psychiatry* 63, 332–337.

Castellanos, F. X., and Tannock, R. (2002). Neuroscience of attention-deficit/hyperactivity disorder: the search for endophenotypes. *Nat. Rev. Neurosci.* 3, 617–628.

CeNeS. (1998). *Cambridge Neuropsychological Test Automated Battery* (Version 2.35). Cambridge: CeNeS Cognition.

Dickstein, S. G., Bannon, K., Castellanos, F. X., and Milham, M. P. (2006). The neural correlates of attention deficit hyperactivity disorder: an ALE meta-analysis. *J. Child Psychol. Psychiatry* 47, 1051–1062.

Dosenbach, N. U., Fair, D. A., Miezin, F. M., Cohen, A. L., Wenger, K. K., Dosenbach, R. A. T., Fox, M. D., Snyder, A. Z., Vincent, J. L., Raichle, M. E., Schlaggar, B. L., and Petersen, S. E. (2007). Distinct brain networks for adaptive and stable task control in humans. *Proc. Natl. Acad. Sci. U.S.A.* 104, 11073–11078.

Dosenbach, N. U., Visscher, K. M., Palmer, E. D., Miezin, F. M., Wenger, K. K., Kang, H. C., Burgund, E. D., Grimes, A. L., Schlaggar, B. L., and Petersen, S. E. (2006). A core system for the implementation of task sets. *Neuron* 50, 799–812.

Doyle, A. E., Faraone, S. V., Seidman, L. J., Willcutt, E. G., Nigg, J. T., Waldman, I. D., Pennington, B. F., Peart, J., and Biederman, J. (2005). Are endophenotypes based on measures of executive functions useful for molecular genetic studies of ADHD? *J. Child Psychol. Psychiatry* 46, 774–803.

Durston, S., Tottenham, N. T., Thomas, K. M., Davidson, M. C., Eigsti, I. M., Yang, Y., Ulug, A. M., and Casey, B. J. (2003). Differential patterns of striatal activation in young children with and without ADHD. *Biol. Psychiatry* 53, 871–878.

Ellison-Wright, I., Ellison-Wright, Z., and Bullmore, E. (2008). Structural brain change in attention deficit hyperactivity disorder identified by meta-analysis. *BMC Psychiatry* 8, 51. doi: 10.1186/1471-244X-8-51

Fair, D. A., Bathula, D., Mills, K. L., Dias, T. G., Blythe, M. S., Zhang, D., Snyder, A. Z., Raichle, M. E., Stevens, A. A., Nigg, J. T., and Nagel, B. J. (2010a). Maturing thalamocortical functional connectivity across development. *Front. Syst. Neurosci.* 4:10. doi: 10.3389/fnsys.2010.00010

Fair, D. A., Posner, J., Nagel, B. J., Bathula, D., Dias, T. G., Mills, K. L., Blythe, M. S., Giwa, A., Schmitt, C. F., and Nigg, J. T. (2010b). Atypical default network connectivity in youth with attention-deficit/hyperactivity disorder. *Biol. Psychiatry* 68, 1084–1091.

Fair, D. A., Cohen, A. L., Dosenbach, N. U., Church, J. A., Miezin, F. M., Barch, D. M., Raichle, M. E., Petersen, S. E., and Schlaggar, B. L. (2008). The maturing architecture of the brain's default network. *Proc. Natl. Acad. Sci. U.S.A.* 105, 4028–4032.

Fair, D. A., Cohen, A. L., Power, J. D., Dosenbach, N. U., Church, J. A., Miezin, F. M., Schlaggar, B. L., and Petersen, S. E. (2009). Functional brain networks develop from a "local to distributed" organization. *PLoS Comput. Biol.* 5, e1000381. doi: 10.1371/journal.pcbi.1000381

Fair, D. A., Dosenbach, N. U., Church, J. A., Cohen, A. L., Brahmbhatt, S., Miezin, F. M., Barch, D. M., Raichle, M. E., Petersen, S. E., and Schlaggar, B. L. (2007a). Development of distinct control networks through segregation and integration. *Proc. Natl. Acad. Sci. U.S.A.* 104, 13507–13512.

Fair, D. A., Schlaggar, B. L., Cohen, A. L., Miezin, F. M., Dosenbach, N. U., Wenger, K. K., Fox, M. D., Snyder, A. Z., Raichle, M. E., and Petersen, S. E. (2007b). A method for using blocked and event-related fMRI data to study "resting state" functional connectivity. *Neuroimage* 35, 396–405.

Finke, K., Schwarzkopf, W., Müller, U., Frodl, T., Müller, H. J., Schneider, W. X., Engel, R. R., Riedel, M., Möller, H. J., and Hennig-Fast, K. (2011). Disentangling the adult attention-deficit hyperactivity disorder endophenotype: parametric measurement of attention. *J. Abnorm. Psychol.* 120, 890–901.

Forman, S. D., Cohen, J. D., Fitzgerald, M., Eddy, W. F., Mintun, M. A., and Noll, D. C. (1995). Improved assessment of significant activation in functional magnetic resonance imaging (fMRI): use of a cluster-size threshold. *Magn. Reson. Med.* 33, 636–647.

Fox, M. D., and Raichle, M. E. (2007). Spontaneous fluctuations in brain activity observed with functional magnetic resonance imaging. *Nat. Rev. Neurosci.* 8, 700–711.

Fox, M. D., Snyder, A. Z., Vincent, J. L., Corbetta, M., Van Essen, D. C., and Raichle, M. E. (2005). The human brain is intrinsically organized into dynamic, anticorrelated functional networks. *Proc. Natl. Acad. Sci. U.S.A.* 102, 9673–9678.

Gau, S. S., and Shang, C. Y. (2010). Executive functions as endophenotypes in ADHD: evidence from the Cambridge Neuropsychological Test Battery (CANTAB). *J. Child Psychol. Psychiatry* 51, 838–849.

Giedd, J. N., Blumenthal, J., Molloy, E., and Castellanos, F. X. (2001). Brain imaging of attention deficit/hyperactivity disorder. *Ann. N. Y. Acad. Sci.* 931, 33–49.

Haber, S. N., and Calzavara, R. (2009). The cortico-basal ganglia integrative network: the role of the thalamus. *Brain Res. Bull.* 78, 69–74.

Insel, T., Cuthbert, B., Garvey, M., Heinssen, R., Pine, D. S., Quinn, K., Sanislow, C., and Wang, P. (2010). Research domain criteria (RDoC): toward a new classification framework for research on mental disorders. *Am. J. Psychiatry* 167, 748–751.

Ivanov, I., Bansal, R., Hao, X., Zhu, H., Kellendonk, C., Miller, L., Sanchez-Pena, J., Miller, A. M., Chakravarty, M. M., Klahr, K., Durkin, K, Greenhill, L. L., and Peterson, B. S. (2010). Morphological abnormalities of the thalamus in youths with attention deficit hyperactivity disorder. *Am. J. Psychiatry* 167, 397–408.

Jones, E. G. (2007). *The Thalamus.* Cambridge: University Press.

Konrad, K., Neufang, S., Hanisch, C., Fink, G. R., and Herpertz-Dahlmann, B. (2006). Dysfunctional

attentional networks in children with attention deficit/hyperactivity disorder: evidence from an event-related functional magnetic resonance imaging study. *Biol. Psychiatry* 59, 643–651.

Lancaster, J. L., Rainey, L. H., Summerlin, J. L., Freitas, C. S., Fox, P. T., Evans, A. C., Toga, A. W., and Mazziotta, J. C. (1997). Automated labeling of the human brain: a preliminary report on the development and evaluation of a forward-transform method. *Hum. Brain Mapp.* 5, 238–242.

Lancaster, J. L., Woldorff, M. G., Parsons, L. M., Liotti, M., Freitas, C. S., Rainey, L., Kochunov, P. V., Nickerson, D., Mikiten, S. A., and Fox, P. T. (2000). Automated Talairach Atlas labels for functional brain mapping. *Hum. Brain Mapp.* 10, 120–131.

Liston, C., Cohen, M. M., Teslovich, T., Levenson, D., and Casey, B. J. (2011). Atypical prefrontal connectivity in attention-deficit/hyperactivity disorder: pathway to disease or pathological end point? *Biol. Psychiatry* 69, 1168–1177.

Miezin, F. M., Maccotta, L., Ollinger, J. M., Petersen, S. E., and Buckner, R. L. (2000). Characterizing the hemodynamic response: effects of presentation rate, sampling procedure, and the possibility of ordering brain activity based on relative timing. *Neuroimage* 11, 735–759.

Milner, B. (1971). Interhemispheric differences in the localization of psychological processes in man. *Br. Med. Bull.* 27, 272–277.

Nigg, J. T. (2005). Neuropsychologic theory and findings in attention-deficit/hyperactivity disorder: the state of the field and salient challenges for the coming decade. *Biol. Psychiatry* 57, 1424–1435.

Nigg, J. T., and Casey, B. J. (2005). An integrative theory of attention-deficit/hyperactivity disorder based on the cognitive and affective neurosciences. *Dev. Psychopathol.* 17, 785–806.

Parent, A., and Hazrati, L. N. (1995). Functional anatomy of the basal ganglia I. The cortico-basal ganglia-thalamo-cortical loop. *Brain Res. Brain Res. Rev.* 20, 91–127.

Power, J. D., Barnes, K. A., Snyder, A. Z., Schlaggar, B. L., and Petersen, S. E. (2012). Spurious but systematic correlations in functional connectivity MRI networks arise from subject motion. *Neuroimage* 59, 2142–2154.

Rhodes, S. M., Park, J., Seth, S., and Coghill, D. R. (2012). A comprehensive investigation of memory impairment in attention deficit hyperactivity disorder and oppositional defiant disorder. *J. Child Psychol. Psychiatry* 53, 128–137.

Shannon, B. J., Raichle, M. E., Snyder, A. Z., Fair, D. A., Mills, K. L., Zhang, D., Bache, K., Calhoun, V. D., Nigg, J. T., Nagel, B. J., Stevens, A. A., and Kiehl, K. A. (2011). Premotor functional connectivity predicts impulsivity in juvenile offenders. *Proc. Natl. Acad. Sci. U.S.A.* 108, 11241–11245.

Silk, T. J., Vance, A., Rinehart, N., Bradshaw, J. L., and Cunnington, R. (2009). Structural development of the basal ganglia in attention deficit hyperactivity disorder: a diffusion tensor imaging study. *Psychiatry Res.* 172, 220–225.

Smyser, C. D., Inder, T. E., Shimony, J. S., Hill, J. E., Degnan, A. J., Snyder, A. Z., and Neil, J. J. (2010). Longitudinal analysis of neural network development in preterm infants. *Cereb. Cortex* 20, 2852–2862.

Sonuga-Barke, E. J. (2005). Causal models of attention-deficit/hyperactivity disorder: from common simple deficits to multiple developmental pathways. *Biol. Psychiatry* 57, 1231–1238.

Talairach, J., and Tournoux, P. (1988). *Co-Planar Stereotaxic Atlas of the Human Brain.* New York: Thieme Medical Publishers, Inc.

Teicher, M. H., Anderson, C. M., Polcari, A., Glod, C. A., Maas, L. C., and Renshaw, P. F. (2000). Functional deficits in basal ganglia of children with attention-deficit/hyperactivity disorder shown with functional magnetic resonance imaging relaxometry. *Nat. Med.* 6, 470–473.

Tillman, C., Eninger, L., Forssman, L., and Bohlin, G. (2011). The relation between working memory components and ADHD symptoms from a developmental perspective. *Dev. Neuropsychol.* 36, 181–198.

Uddin, L. Q., Kelly, A. M., Biswal, B. B., Margulies, D. S., Shehzad, Z., Shaw, D., Ghaffari, M., Rotrosen, J., Adler, L. A., Castellanos, F. X., and Milham, M. P. (2008). Network homogeneity reveals decreased integrity of default-mode network in ADHD. *J. Neurosci. Methods* 169, 249–254.

Van Dijk, K. R., Sabuncu, M. R., and Buckner, R. L. (2011). The influence of head motion on intrinsic functional connectivity MRI. *Neuroimage* 59, 431–438.

Van Essen, D. C. (2005). A population-average, landmark- and surface-based (PALS) atlas of human cerebral cortex. *Neuroimage* 28, 635–662.

Van Essen, D. C., Dickson, J., Harwell, J., Hanlon, D., Anderson, C. H., and Drury, H. A. (2001). An integrated software suite for surface-based analyses of cerebral cortex. *J. Am. Med. Inform. Assoc.* 41, 1359–1378.

Van Essen, D. C., and Drury, H. A. (1997). Structural and functional analyses of human cerebral cortex using a surface-based atlas. *J. Neurosci.* 17, 7079–7102.

Wang, L., Zhu, C., He, Y., Zang, Y., Cao, Q., Zhang, H., Zhong, Q., and Wang, Y. (2009). Altered small-world brain functional networks in children with attention-deficit/hyperactivity disorder. *Hum. Brain Mapp.* 30, 638–649.

Westerberg, H., Hirvikoski, T., Forssberg, H., and Klingberg, T. (2004). Visuo-spatial working memory span: a sensitive measure of cognitive deficits in children with ADHD. *Child Neuropsychol.* 10, 155–161.

Willcutt, E. G., Doyle, A. E., Nigg, J. T., Faraone, S. V., and Pennington, B. F. (2005). Validity of the executive function theory of attention-deficit/hyperactivity disorder: a meta-analytic review. *Biol. Psychiatry* 57, 1336–1346.

Zang, Y. F., He, Y., Zhu, C. Z., Cao, Q. J., Sui, M. Q., Liang, M., Tian, L. X., Jiang, T. Z., and Wang, Y. F. (2007). Altered baseline brain activity in children with ADHD revealed by resting-state functional MRI. *Brain Dev.* 29, 83–91.

Zhang, D., Snyder, A. Z., Fox, M. D., Sansbury, M. W., Shimony, J. S., and Raichle, M. E. (2008). Intrinsic functional relations between human cerebral cortex and thalamus. *J. Neurophysiol.* 100, 1740–1748.

Zhang, D., Snyder, A. Z., Shimony, J. S., Fox, M. D., and Raichle, M. E. (2009). Noninvasive functional and structural connectivity mapping of the human thalamocortical system. *Cereb. Cortex* 20, 1187–1194.

Conflict of Interest Statement: The authors declare that the research was conducted in the absence of any commercial or financial relationships that could be construed as a potential conflict of interest.

Received: 27 October 2011; accepted: 08 January 2012; published online: 25 January 2012.

*Citation: Mills KL, Bathula D, Dias TGC, Iyer SP, Fenesy MC, Musser ED, Stevens CA, Thurlow BL, Carpenter SD, Nagel BJ, Nigg JT and Fair DA (2012) Altered cortico-striatal–thalamic connectivity in relation to spatial working memory capacity in children with ADHD. Front. Psychiatry **3**:2. doi: 10.3389/fpsyt.2012.00002*

This article was submitted to Frontiers in Neuropsychiatric Imaging and Stimulation, a specialty of Frontiers in Psychiatry.

APPENDIX

PARTICIPANTS AND MEASURES

Data from Oregon Health and Science University, Brown University, Beijing Normal University, Kennedy Krieger Institute, and NYU Child Study Center were collected for children aged 7–11 years. Together, the total dataset comprised of 132 typically developing children (TDC) and 94 participants with ADHD. This larger dataset was then separated into two subsets for two different analyses. The first dataset included 67 children with and without ADHD diagnoses (all subtypes included), all aged 7–11 years, and from Oregon Health and Science University. Children in the first dataset were not matched on age or gender, as this group was involved in a correlational analysis that included all participants. The sample consisted of 43 TDC, 14 ADHD-C, 9 ADHD-inattentive subtype, and 1 ADHD-hyperactive only subtype children. Although this group was not matched for age, there were no significant differences in ages between children with ADHD and TDC (ADHD mean age: 8.70 years, SD: 0.82; TDC mean age: 8.50 years, SD: 0.67; $p = 0.23$). IQ was significantly different between children with ADHD and TDC (ADHD mean IQ: 106.66, SD: 13.54; TDC mean IQ: 118.35, SD: 13.82; $p < 0.01$). Movement was low across all participants (ADHD mean movement:0.44, SD:0.32; TDC mean movement:0.43, SD:0.35; $p = 0.85$). The average pairwise functional volume displacement after removing frames was also low and not significant (ADHD mean volume displacement:0.30, SD:0.19; TDC mean volume displacement:0.27, SD:0.22; $p = 0.55$).

The second dataset included 70 children diagnosed with ADHD-combined type (ADHD-C), and 89 TDC children, all aged 7–11 years, and drawn from Brown University, Beijing Normal University, Kennedy Krieger Institute, and NYU Child Study Center. Children in the second dataset were matched on age, gender, and pairwise functional volume displacement for a comparative analysis (ADHD-C mean age: 9.85 years, SD: 1.28, 20% female; TDC mean age: 9.94 years, SD: 1.23, 26.97% female; $p = 0.65$), and showed significant differences in IQ (ADHD-C mean IQ: 110.54, SD: 14.03; TDC mean IQ: 115.97, SD: 14.03; $p < 0.02$). Movement was low across both groups (ADHD-C mean movement:0.47, SD:0.25; TDC mean movement:0.45, SD:0.21; $p = 0.64$). The average pairwise functional volume displacement after removing frames was also low and not significant (ADHD-C mean volume displacement:0.17, SD:0.06; TDC mean volume displacement:0.46, SD:0.21; $p = 0.61$).

Informed written consent or assent was obtained for all participants, and procedures complied with the Human Investigation Review Board at respective universities. As data were aggregated from a larger collaborative effort (ADHD-200 dataset, see: http://fcon_1000.projects.nitrc.org/indi/adhd200), assessment protocols varied across institutions. The procedures used for each institution are detailed below.

DATA PREPROCESSING

All functional images were preprocessed in the same manner to reduce artifacts (Miezin et al., 2000). These steps included: (i) removal of a central spike caused by MR signal offset, (ii) correction of odd vs. even slice intensity differences attributable to interleaved acquisition without gaps, (iii) correction for head movement within and across runs, and (iv) within-run intensity normalization to a whole brain mode value of 1,000. Atlas transformation of the functional data was computed for each individual via the MPRAGE scan. The fMRI data then were resampled to 3 mm cubic voxels in Talairach atlas space (Talairach and Tournoux, 1988) as defined by the spatial normalization procedure (Lancaster et al., 1995). This resampling combined movement correction and atlas transformation in one interpolation. All subsequent operations were performed on the atlas-transformed volumetric time series. Participant head motion was measured and corrected using rigid body translation and rotation. Summary statistics were calculated as root mean square (RMS) values for translation and rotation about the *x*, *y*, and z-axes. Motion was corrected and quantified using an analysis of head position based on rigid body translation and rotation.

OREGON HEALTH AND SCIENCE UNIVERSITY

Psychiatric diagnoses were based on evaluations with the kiddie schedule for affective disorders and schizophrenia (KSADS-I; Puig-Antich and Ryan, 1986) administered to a parent; parent and teacher Conners' Rating Scale-3rd Edition (Conners, 2008); and a clinical review by a child psychiatrist and neuropsychologist who had to agree on the diagnosis. Intelligence was evaluated with a three-subtest short form (block design, vocabulary, and information) of the Wechsler Intelligence Scale for Children, 4th Edition (Wechsler, 2003). Children were excluded if they did not meet criteria for ADHD or non-ADHD groups. Children were also excluded if a history of neurological illness, chronic medical problems, sensorimotor handicap, autistic disorder, mental retardation, or significant head trauma (with loss of consciousness) was identified by parent report, or if they had evidence of psychotic disorder or bipolar disorder on the structured parent psychiatric interview. Children prescribed short-acting stimulant medications were scanned after a minimum washout of five half-lives (i.e., 24–48 h depending on the preparation). Typically developing children were excluded for presence of conduct disorder, major depressive disorder, or history of psychotic disorder, as well as for presence of ADHD.

Participants were scanned using a 3.0 Tesla Siemens Magnetom Tim Trio scanner with a 12-channel head coil at the OHSU Advanced Imaging Research Center. One high resolution T1-weighted MPRAGE sequence lasting 9 min and 14 s (TR = 2300 ms, TE = 3.58 ms, orientation = sagittal, 256 × 256 matrix, resolution = 13 mm) was collected. Blood–oxygen level dependent (BOLD)-weighted functional imaging data were collected in an oblique plane (parallel to the ACPC) using T2*-weighted echo-planar imaging (TR = 2500 ms, TE = 30 ms, flip angle = 90°, FOV = 240 mm, 36 slices covering the whole brain, slice thickness = 3.8 mm, in-plane resolution = 3.8 mm × 3.8 mm). Steady state magnetization was assumed after five frames (∼10 s). Three runs of 3.5 min each were obtained. During rest periods, participants were instructed to stay still, and fixate on a standard fixation-cross in the center of the display.

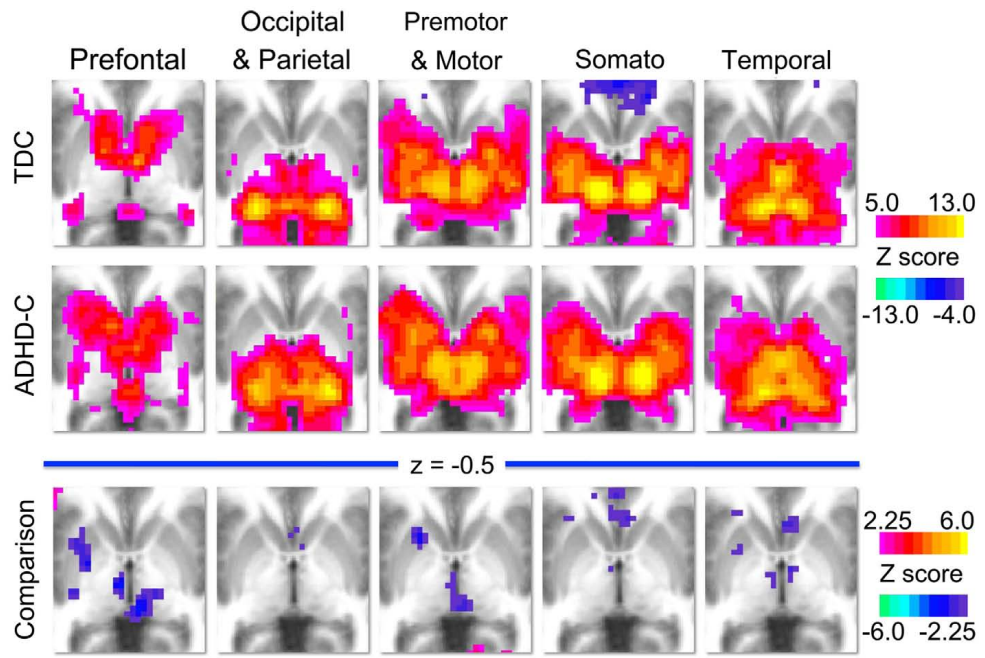

FIGURE A1 | Group level voxelwise maps. This figure displays the voxelwise connectivity maps of each thalamic ROI (prefrontal, occipital–parietal, premotor–motor, somatosensory, and temporal) for the groups analyzed in the comparative analysis. The first row illustrates the group maps for 89 typically developing children (TDC) and the second row illustrates the group maps for 70 children with ADHD-combined subtype (ADHD-C). The third row illustrates the voxelwise maps for the comparison analysis, where warm colors (positive *z*-scores) indicate areas where connection strength is greater in TDC, and cool colors (negative *z*-scores) indicate areas where connection strength is greater in the ADHD-C population.

ADHD-CONSORTIUM DATA

Kennedy Krieger Institute

Psychiatric diagnoses were based on evaluations with the Diagnostic Interview for Children and Adolescents, 4th Edition (DICA-IV; Reich et al., 1997), a structured parent interview based on DSM-IV criteria; the Conners' Parent Rating Scale-Revised, Long Form (CPRS-R; Epstein et al., 1997), and the DuPaul ADHD Rating Scale IV; DuPaul et al., 1998). Intelligence was evaluated with the Wechsler Intelligence Scale for Children-4th Edition (WISC-IV; Wechsler, 2003) and academic achievement was assessed with the Wechsler Individual Achievement Test-II.

All study participants were between 8.0 and 11.0 years, and had a Full-Scale IQ of 80 or higher. They had no history of language disorder or a Reading Disability (RD) either screened out before a visit or based on school assessment completed within 1 year of participation. RD was based on a statistically significant discrepancy between a child's FSIQ score and his/her Word Reading subtest score from the Wechsler Individual Achievement Test-IIa, or a standard score below 85 on the Word Reading subtest, regardless of IQ score. Participants with visual or hearing impairment, or history of other neurological or psychiatric disorder were excluded.

Children assigned to the ADHD group met criteria for ADHD on the DICA-IV and either had a *T*-score of 65 or greater on the CPRS-R Long Form (DSM-IV inattentive) and/or M (DSM-IV hyperactive/impulsive) or met criteria on the DuPaul ADHD Rating Scale IV (six out of nine items scored 2 or 3 from inattention items and/or six out of nine scored 2 or 3 from the hyperactivity/impulsivity items). Children with DSM-IV diagnoses other than oppositional defiant disorder or specific phobias were excluded. DSM-IV criteria and the aforementioned rating scales were also used to evaluate the three ADHD subtypes (inattentive: ADHD-I; hyperactive/impulsive: ADHD-HI; combined: ADHD-C). Children with ADHD were assigned to the ADHD-I group if they met criteria for inattentiveness but not hyperactivity/impulsivity on the DICA-IV, and had a *T*-score of 65 or greater on the CPRS Scale L, and a *T*-score of 60 or less on the CPRS Scale, or had a rating of 2 or 3 on six out of nine inattention items on the ADHD Rating Scale IV and a rating of 2 or 3 on four or fewer items on the hyperactivity/impulsivity scale. Children were assigned to the ADHD-HI if they met criteria for hyperactivity/impulsivity but not inattention on the DICA-IV, and a *T*-score of 65 or greater on the CPRS Scale M and a *T*-score of 60 or less on the CPRS Scale L, or had a rating of 2 or 3 on six out of nine hyperactivity/impulsivity items on the ADHD Rating Scale IV and a rating of 2 or 3 on four or fewer items on the inattention scale. All other children who met criteria for ADHD were assigned to the ADHD-C (combined subtype) group. Children with ADHD taking psychoactive medications other than stimulants were excluded. Children who were taking stimulant medication were removed from these medications the day before and the day of testing. TDC were required to have *T*-scores of 60 or below on the DSM-IV inattention (L) and DSM-IV hyperactivity (M) subscales of CPRS-R and no history of behavioral, emotional, or serious medical problems. Additionally, TDC were not included if there was a history of school-based intervention services as established by parent interview, or if they met

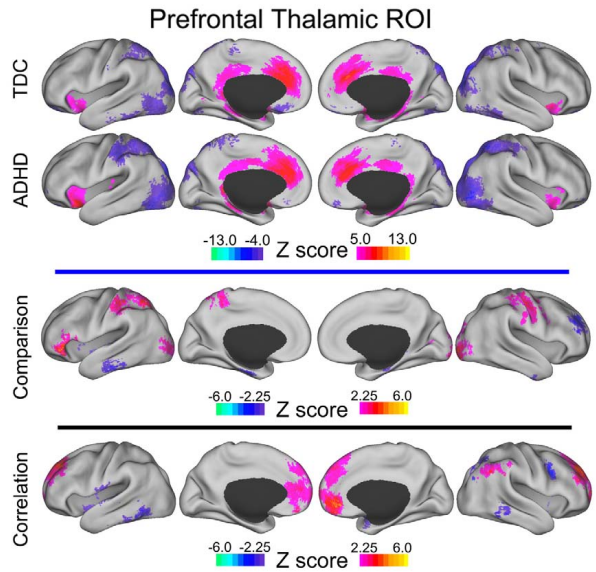

FIGURE A2 | Prefrontal thalamic voxelwise maps projected onto cortical surfaces. Each row displays the cortical surface for each voxelwise map generated from the prefrontal thalamic ROI: group maps for TDC, group maps for ADHD-C, maps from the comparative analysis (TDC vs. ADHD-C), and maps from the correlation analysis. Cortical surface projection was performed with the (PALS)-B12 atlas (Van Essen, 2005) and the software Caret (Van Essen et al., 2001).

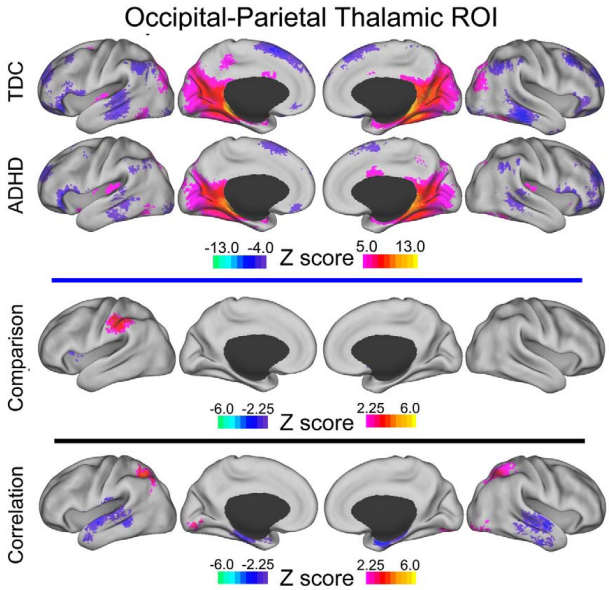

FIGURE A3 | Occipital–parietal thalamic voxelwise maps projected onto cortical surfaces. Each row displays the cortical surface for each voxelwise map generated from the occipital–parietal thalamic ROI: group maps for TDC, group maps for ADHD-C, maps from the comparative analysis (TDC vs. ADHD-C), and maps from the correlation analysis. Cortical surface projection was performed with the (PALS)-B12 atlas (Van Essen, 2005) and the software Caret (Van Essen et al., 2001).

DSM-IV psychiatric disorder except specific phobia as reported on the DICA-IV.

Participants were scanned using a 3.0 Tesla Philips scanner with an eight-channel head coil. One high resolution T1-weighted MPRAGE sequence (TR = 7.99 ms, TE = 3.76 ms, flip angle = 8°) was collected. Blood–oxygen level dependent (BOLD)-weighted functional imaging data were collected using T2*-weighted echo-planar imaging (TR = 2500 ms, TE = 30 ms, flip angle = 75°, 2D-SENSE EPI). The run lasted either 5 min 20 s or 6 min 30 s. During rest participants were instructed to relax, stay as still as possible, keep eyes open, and fixate on a center cross.

New York University

Psychiatric diagnoses were based on evaluations with the Schedule of Affective Disorders and Schizophrenia for Children – Present and Lifetime Version (KSADS-PL) administered to parents and children and the Conners' Parent Rating Scale-Revised, Long version (CPRS-LV; Epstein et al., 1997). Intelligence was evaluated with the Wechsler Abbreviated Scale of Intelligence (WASI; Wechsler, 1999). Inclusion in the ADHD group required a diagnosis of ADHD based on parent and child responses to the KSADS-PL as well as on a *T*-score greater than or equal to 60 on at least one ADHD related index of the CPRS-R: LV. Psychostimulant drugs were withheld at least 24 h before scanning. Inclusion criteria for TDC required absence of any Axis-I psychiatric diagnoses per parent and child KSADS-PL interview, as well as *T*-scores below 60 for all the CPRS-R: LV ADHD summary scales. Estimates of FSIQ above 80, right-handedness and absence of other chronic medical conditions were required for all children.

Participants were scanned using a Siemens Allegra 3.0 Tesla scanner at the NYU Center for Brain Imaging. For each participant a T1-weighted MPRAGE sequence was acquired using a magnetization prepared gradient echo sequence (TR = 2530 ms; TE = 3.25 ms; TI = 1100 ms; flip angle = 7°; 128 slices; FOV = 256 mm; acquisition voxel size = 1.31 mm × 1.3 mm). A 6-min resting scan comprising 180 contiguous whole brain functional volumes was also acquired for each participant using a multi-echo echo-planar imaging sequence (TR = 2000 ms; flip angle = 90°; 33 slices; voxel size = 3 mm × 3 mm × 4 mm; effective TE = 30 ms, FOV = 240 mm × 192 mm). During rest periods participants were instructed to lie still and relax with their eyes open, while a standard fixation-cross was presented in the center of the display.

Beijing Normal University

Study participants with the diagnosis of ADHD were initially identified using the Computerized Diagnostic Interview Schedule IV (C-DIS-IV). Upon referral for participation to the study participation, all participants (ADHD and TDC) were evaluated with the Schedule of Affective Disorders and Schizophrenia for Children – Present and Lifetime Version (KSADS-PL) with one parent for the establishment of the diagnosis for study inclusion. Additional inclusion included: (i) right-handedness, (ii) no history of neurological disease and no diagnosis of either schizophrenia, affective disorder, or pervasive development disorder and (iii) full-scale Wechsler Intelligence Scale for Chinese Children-Revised (WISCC-R) score of greater than 80.

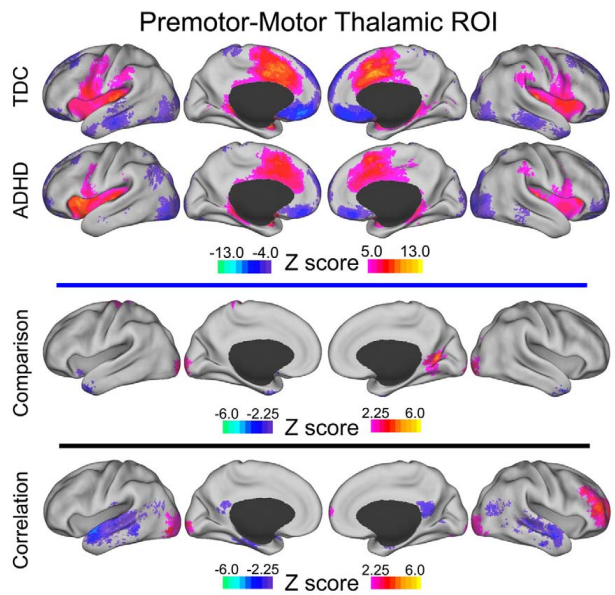

FIGURE A4 | Premotor–motor thalamic voxelwise maps projected onto cortical surfaces. Each row displays the cortical surface for each voxelwise map generated from the premotor–motor thalamic ROI: group maps for TDC, group maps for ADHD-C, maps from the comparative analysis (TDC vs. ADHD-C), and maps from the correlation analysis. Cortical surface projection was performed with the (PALS)-B12 atlas (Van Essen, 2005) and the software Caret (Van Essen et al., 2001).

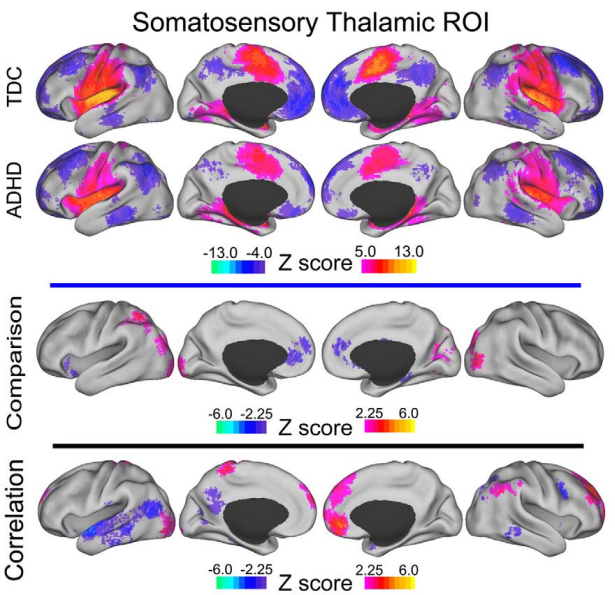

FIGURE A5 | Somatosensory thalamic voxelwise maps projected onto cortical surfaces. Each row displays the cortical surface for each voxelwise map generated from the somatosensory thalamic ROI: group maps for TDC, group maps for ADHD-C, maps from the comparative analysis (TDC vs. ADHD-C), and maps from the correlation analysis. Cortical surface projection was performed with the (PALS)-B12 atlas (Van Essen, 2005) and the software Caret (Van Essen et al., 2001).

Psychostimulant medications were withheld at least 48 h prior to scanning. All research was approved by the Research Ethics Review Board of Institute of Mental Health, Peking University. Informed consent was also obtained from the parent of each subject and all of the children agreed to participate in the study.

Dataset #1

Images were acquired using a Siemens Trio 3.0 Tesla scanner (Siemens, Erlangen, Germany) in National Key Laboratory of Cognitive Neuroscience and Learning, Beijing Normal University. For each participant, a high resolution T1-weighted anatomical image was acquired (128 sagittal slices, slice thickness/gap = 1.33/0 mm, in-plane resolution = 256 × 192, TR = 2530 ms, TE = 3.39 ms, inversion time (TI) = 1100 ms, flip angle = 7°, FOV = 256 mm × 256 mm). A resting-state scan was obtained for each participant (33 axial slices, TR = 2000 ms, TE = 30 ms, flip angle = 90°, thickness/gap = 3.5/0.7 mm, FOV = 200 mm × 200 mm, matrix = 64 × 64, 240 volumes), as well as diffusion tensor imaging.

Dataset #2

Images were acquired using a Siemens Trio 3.0 Tesla scanner (Siemens, Erlangen, Germany) in National Key Laboratory of Cognitive Neuroscience and Learning, Beijing Normal University. All of the resting-state functional data were acquired using an echo-planar imaging (EPI) sequence with the following parameters: 33 axial slices, TR = 2000 ms, TE = 30 ms, flip angle = 90°, slice thickness/skip = 3.0/0.6 mm, FOV = 200 mm × 20 mm, in-plane resolution = 64 × 64, 240 volumes. For each patient, T1-weighted structural images were acquired using a spoiled gradient-recalled sequence covering the whole brain and used for the purpose of image registration (see Data Preprocessing). Here are the parameters of T1-weighted structural images: 176 sagittal slices, TR = 2530 ms, TE = 3.45 ms, flip angle = 7°, slice thickness/skip = 1.0/0 mm, FOV = 256 mm × 256 mm, in-plane resolution = 256 × 256.

Children with ADHD were scanned twice, in a double-blinded, randomized, counterbalanced way. The two scans were at least 2 days apart, and each scan was taken 1 h after either 10 mg MPH administration or placebo (Vitamin B6, 10 mg). All the patients had not received stimulant treatment for at least 2 days before the first scan, and were asked not to take any stimulant between two scans. The control boys were scanned once without MPH or placebo taken for ethical reasons. Only placebo scans were used for the present study.

Dataset #3

Images were acquired using a Siemens Trio 3.0 Tesla scanner (Siemens, Erlangen, Germany) in the Institute of Biophysics, Chinese Academy of Sciences. Rest scans were acquired using an echo-planar imaging (EPI) sequence with the following parameters: 30 axial slices, TR = 2000 ms, TE = 30 ms, flip angle = 90°, thickness/skip = 4.5/0 mm, FOV = 220 mm × 220 mm, matrix = 64 × 64, 240 volumes. Participants were asked simply to remain still, close their eyes, think of nothing systematically and not fall asleep.

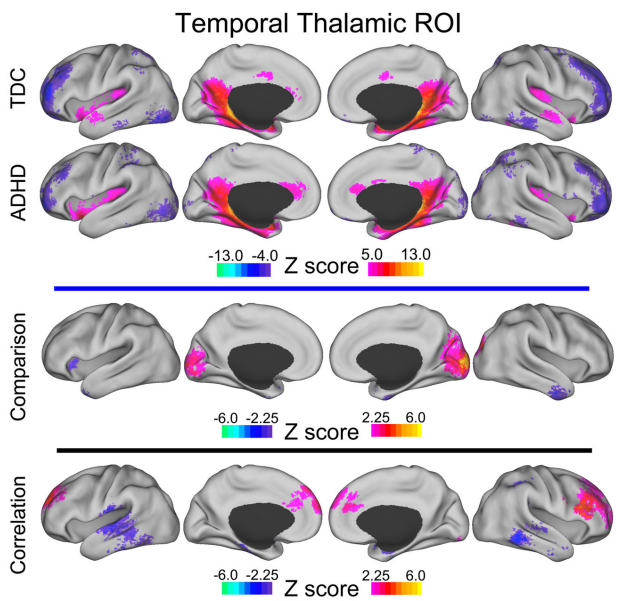

FIGURE A6 | Temporal thalamic voxelwise maps projected onto cortical surfaces. Each row displays the cortical surface for each voxelwise map generated from the temporal thalamic ROI: group maps for TDC, group maps for ADHD-C, maps from the comparative analysis (TDC vs. ADHD-C), and maps from the correlation analysis. Cortical surface projection was performed with the (PALS)-B12 atlas (Van Essen, 2005) and the software Caret (Van Essen et al., 2001).

Additionally, for each participant, a high resolution T1-weighted anatomical image using a spoiled gradient-recalled sequence covering the whole brain was acquired. The data were collected in a period of about 2 years and some modifications were made in the sequence of the structural images. Most of the participants were scanned with one of the following two kinds of parameters: (1) 192 slices, TR = 2000 ms, TE = 3.67 ms, inversion time = 1100 ms, flip angle = 12°, FOV = 240 mm × 240 mm, matrix = 256 × 256, used in 8 patients and 12 controls; (2) 176 slices, TR = 1770 ms, TE = 3.92 ms, inversion time = 1100 ms, flip angle = 12°, FOV = 256 mm × 256 mm, matrix = 512 × 512, used in 9 patients and 11 controls. Other scanning sessions, which have no relation to the present study, are not described here.

Brown University and Bradley Hospital

Psychiatric diagnoses were based on evaluation by the same board-certified child/adolescent psychiatrist (DPD) for all participants, using the Child Schedule for Affective Disorders Present and Lifetime version (KSADS-PL) administered to parents and children separately (Puig-Antich and Ryan, 1986). All participants completed the Wechsler Abbreviated Scale of Intelligence (WASI) as an overall measure of cognitive ability (Wechsler, 1999). Children in the ADHD group had to meet Diagnostic and Statistical Manual 4th Edition Text Revision (DSM-IV-TR) criteria for ADHD, as determined by parent and child answers to the KSADS-PL and were required to have ongoing psychiatric treatment. Exclusion criteria were comorbid mood or anxiety disorders, autistic or Asperger's disorder, medical illness that was unstable or could cause psychiatric symptoms, or substance abuse within <2 months of participation. All ADHD participants taking psychostimulant medications (i.e., derivatives of methylphenidate or dextroamphetamine) were scanned when medication-free for five drug half-lives. TDC inclusion criteria were a negative history of psychiatric illness in the participant and their first-degree relatives. Exclusion criteria were pregnancy, ongoing medical, or neurological illness or past/present psychiatric or substance disorder. All participants had an IQ greater than 70.

Scans were acquired on a Siemens Tim Trio 3.0 Tesla scanner with a 12-channel head coil. A high resolution T1-weighted MPRAGE anatomical image was acquired for normalization and localization (TR = 2250 ms, TE = 2.98 ms, T1 = 900 ms, flip angle = 9°, slices = 160, FOV = 256 mm, voxels = 1 mm × 1 mm × 1 mm). This scan lasted 7 min and 36 s. The resting-state functional connectivity scan contained 256 continuous blood–oxygen level dependent (BOLD) volumes (TR = 2000 ms, TE = 25 ms, flip angle = 90°, slices = 35, FOV = 192 mm, voxels = 3 mm × 3 mm × 3 mm). The scan lasted for 8 min and 36 s. During the scan, participants were instructed to rest with their eyes open while the word "relax" was back-projected via LCD projector.

REFERENCES

Conners, C. K. (2008). *Conners Manual*, 3rd Edn. Toronto: Multi-Health Systems Inc.

DuPaul, G., Power, T., Anastopoulos, A., and Reid, R. (1998). *ADHD Rating Scales-IV: Checklists, Norms and Clinical Interpretation*. New York: Guilford Press.

Epstein, J. N., Conners, C. K., Erhardt, D., March, J. S., and Swanson, J. M. (1997). Asymmetrical hemispheric control of visual-spatial attention in adults with attention deficit hyperactivity disorder. *Neuropsychology* 11, 467–473.

Lancaster, J. L., Glass, T. G., Lankipalli, B. R., Downs, H., Mayberg, H., and Fox, P. T. (1995). A modality-independent approach to spatial normalization of tomographic images of the human brain. *Hum. Brain Mapp.* 3, 209–223.

Puig-Antich, J., and Ryan, N. (1986). *The Schedule for Affective Disorders and Schizophrenia for School-Age Children*. Pittsburgh: Western Psychiatric Institute and Clinic.

Reich, W., Welner, Z., and andHerjanic, B. (1997). *Diagnostic Interview for Children and Adolescents-IV (DICA-IV)*. North Tonawanda: Multi-Health Systems, Inc.

Wechsler, D. (1999). *Wechsler Abbreviated Scale of Intelligence*, 3rd Edn. San Antonio: The Psychological Corporation.

Wechsler, D. (2003). *Wechsler Intelligence Scale for Children Technical and Interpretive Manual*, 4h Edn. San Antonio, TX: The Psychological Corporation.

frontiers in
PSYCHIATRY

ORIGINAL RESEARCH ARTICLE
published: 14 November 2011
doi: 10.3389/fpsyt.2011.00062

Altered amygdala resting-state functional connectivity in post-traumatic stress disorder

Christine A. Rabinak[1,2], Mike Angstadt[2], Robert C. Welsh[3], Amy E. Kenndy[1], Mark Lyubkin[1,2], Brian Martis[1,2] and K. Luan Phan[1,2,4]*

[1] *Mental Health Service, Veteran's Administration Ann Arbor Healthcare System, Ann Arbor, MI, USA*
[2] *Department of Psychiatry, University of Michigan, Ann Arbor, MI, USA*
[3] *Department of Radiology, University of Michigan, Ann Arbor, MI, USA*
[4] *Neuroscience Program, University of Michigan, Ann Arbor, MI, USA*

Edited by:
Ben Harrison, The University of Melbourne, Australia

Reviewed by:
Leonardo Fontenelle, Institute of Psychiatry at the Federal University of Rio de Janeiro, Brazil
Narcis Cardoner, Bellvitge University Hospital, Barcelona University, Spain

***Correspondence:**
K. Luan Phan, Department of Psychiatry, University of Michigan, Rachel Upjohn Building, Room 2751, 4250 Plymouth Road, Ann Arbor, MI 48109-2700, USA.
e-mail: luan@umich.edu

Post-traumatic stress disorder (PTSD) is often characterized by aberrant amygdala activation and functional abnormalities in corticolimbic circuitry, as elucidated by functional neuroimaging. These "activation" studies have primarily relied on tasks designed to induce region-specific, and task-dependent brain responses in limbic (e.g., amygdala) and paralimbic brain areas through the use of aversive evocative probes. It remains unknown if these corticolimbic circuit abnormalities exist at baseline or "at rest," in the absence of fear/anxiety-related provocation and outside the context of task demands. Therefore the primary aim of the present experiment was to investigate aberrant amygdala functional connectivity patterns in combat-related PTSD patients during resting-state. Seventeen Operation Enduring Freedom/Operation Iraqi Freedom (OEF/OIF) veterans with combat-related PTSD (PTSD group) and 17 combat-exposed OEF/OIF veterans without PTSD [combat-exposed control (CEC) group] underwent an 8-min resting-state functional magnetic resonance imaging scan. Using an anatomically derived amygdala "seed" region we observed stronger functional coupling between the amygdala and insula in the PTSD group compared to the CEC group, but did not find group differences in amygdala–prefrontal connectivity. These findings suggest that the aberrant amygdala and insula activation to fear-evocative probes previously characterized in PTSD may be driven by an underlying enhanced connectivity between the amygdala, a region known for perceiving threat and generating fear responses, and the insula, a region known for processing the meaning and prediction of aversive bodily states. This enhanced amygdala–insula connectivity may reflect an exaggerated, pervasive state of arousal that exists outside the presence of an overt actual threat/danger. Studying amygdala functional connectivity "at rest" extends our understanding of the pathophysiology of PTSD.

Keywords: amygdala, resting-state, functional magnetic resonance imaging, post-traumatic stress disorder

INTRODUCTION

Post-traumatic stress disorder (PTSD) is characterized by various altered emotional responses as a result of trauma exposure (e.g., combat, assault, and disasters). Patients with PTSD not only experience intense negative emotional reactions when reminded of their trauma but also report exaggerated arousal (poor sleep, restlessness, hypervigilance), anhedonia, social withdrawal, and decreased emotional expressivity, referred to as "emotional numbing." Characterizing the neural basis of these diverse, distorted emotional responses poses a major challenge to contemporary psychiatric research. Functional neuroimaging techniques have focused primarily on the study of brain function related to fear perception and response, and have consistently implicated aberrant amygdala reactivity to fear-relevant probes and other abnormalities in a broad aberrant amygdala-linked circuitry involving the medial prefrontal cortex (mPFC), insula, anterior cingulate cortex (ACC), and hippocampus (Rauch and Shin, 1997; Pitman et al., 2001; Nemeroff et al., 2006; Rauch et al., 2006; Etkin and Wager, 2007; Liberzon and Sripada, 2008; Shin, 2009; Shin and Liberzon, 2010). Together these interconnected regions form a disrupted functional network thought to be responsible for impaired regulation of fear responses, enhanced attention to threat-related stimuli, and biased memory for adverse events (Shin, 2009). Anxiety disorders, such as PTSD, are believed to manifest from dysfunction in a complex integrated functional network, largely, between cortical and limbic regions (Gilboa et al., 2004; Lanius et al., 2005; Simmons et al., 2008; Bluhm et al., 2009; Shaw et al., 2009; Daniels et al., 2010). Some studies have begun to examine these brain circuits and region-to-region interactions, by measuring the extent to which activity in one region is correlated with activity in another during a particular task. Although these dysfunctional networks have been implicated in mediating several characteristics of PTSD, such as, hyperarousal, abnormal reactivity to emotional stimuli, and avoidance of emotionally distressing memories (Nemeroff et al., 2006; Shin and Liberzon, 2010), little is known about how these regions may interact dynamically within individual subjects.

Some clues exist from anatomical and functional studies that these brain regions may indeed form a network responsible for emotion processing. Tracer studies in non-human primates (Amaral and Price, 1984; Saunders et al., 1988; Barbas and De Olmos, 1990; Stefanacci et al., 1996; Ghashghaei and Barbas, 2002; Ghashghaei et al., 2007; Freese and Amaral, 2009) and, more recently, diffusion tensor imaging studies in humans (Croxson et al., 2005; Johansen-Berg et al., 2008; Bracht et al., 2009) have identified robust bidirectional projections between the amygdala and the mPFC, rostral ACC (rACC), insula, and hippocampus. Consistent with known anatomical connections, several studies that have examined functional connectivity of the amygdala have found significant co-activation and/or functionally correlated activation of the amygdala and the mPFC, insula, hippocampus, and rACC (Phan et al., 2002; Wager et al., 2003, 2008; Stein et al., 2007a; Kober et al., 2008; Etkin et al., 2009; Roy et al., 2009). It is well established that negatively valenced emotional stimuli activate the amygdala, which mediates subjective and attentional-vigilance aspects of threat processing (Liberzon et al., 1999; Phan et al., 2002, 2004; Liberzon and Phan, 2003; Taylor et al., 2003; Wager et al., 2003; Etkin and Wager, 2007; Kober et al., 2008; Liberzon and Sripada, 2008; Etkin, 2009; Shin and Liberzon, 2010). Similarly, insula activity also increases in response to emotionally aversive stimuli that evoke visceral or somatic sensations (Simmons et al., 2004). Increased amygdala and insula activation during fear conditioning have been shown to be reliably associated with one another (Etkin and Wager, 2007). Amygdala activity is decreased in response to suppression of negative affect via reappraisal and during inhibition of conditioned fear responses as a result of increased activation in the mPFC and rACC, which exert top-down inhibitory influences on amygdala reactivity to fear and threat (Ochsner et al., 2002; Taylor et al., 2003; Phelps et al., 2004; Etkin et al., 2006, 2011; Urry et al., 2006; Delgado et al., 2008; Quirk and Mueller, 2008). The magnitude of task-dependent functional coupling between the amygdala and mPFC/rACC has been shown to be negatively correlated with intensity of subjective reports of negative affect (Banks et al., 2007). Increased functional connectivity between the amygdala and the hippocampus has been attributed to the persistence of memories for emotionally arousing events (Hamann et al., 1999; Kilpatrick and Cahill, 2003; Phelps, 2004; Ritchey et al., 2008; Murty et al., 2011). Specifically, the hippocampus forms episodic representations of the emotional significance and interpretation of events, and influences amygdala activity when emotional stimuli are encountered (Phelps, 2004). These lines of convergent evidence suggests that how the amygdala interacts with other regions may mediate the control, or lack thereof, of fear perception and emotional arousal in humans.

Dysfunctions within discrete areas that form an amygdala–paralimbic/frontal network have been implicated in mediating several characteristics of PTSD, such as, hyperarousal, abnormal reactivity to emotional stimuli, and avoidance of emotionally distressing memories (Nemeroff et al., 2006; Shin and Liberzon, 2010). In particular, many studies have shown amygdala hyperactivity in PTSD in response to trauma-related imagery (Shin et al., 1997, 2004a), combat-related sounds or smells (Liberzon et al., 1999; Pissiota et al., 2002; Vermetten et al., 2007), trauma-related photographs or words (Hendler et al., 2003; Driessen et al., 2004; Protopopescu et al., 2005; Morey et al., 2009), and fearful facial expressions (Rauch et al., 2000; Shin et al., 2005; Williams et al., 2006; Bryant et al., 2008). Exaggerated amygdala reactivity observed in PTSD has been posited to be a result of insufficient top-down regulation from the mPFC and ACC, consequently leading to hyperarousal and deficits in extinction as well as the inability to suppress enhanced fear perception or exaggerated fear responses to trauma-related stimuli (Rauch and Shin, 1997; Rauch et al., 1998; Pitman et al., 2001; Liberzon and Phan, 2003); for example, Shin et al. (2004a, 2005) have observed that exaggerated amygdala reactivity is negatively correlated with responses in the dorsal and ventral mPFC across individuals with PTSD. However, Gilboa et al. (2004) found little evidence for failure of inhibition of ACC over the amygdala in individuals with PTSD related to civilian trauma during symptom provocation and in fact found that amygdala activity significantly influenced ACC activity. Insula hyperactivity has been observed in PTSD patients and given its role in the experience (e.g., somatic sensation) of negative emotions and structural connectivity to amygdala (Augustine, 1996; Aggleton and Saunders, 2000; Freese and Amaral, 2009), the insula may be working in concert with aberrant amygdala responses (Bremner et al., 2003, 2005; Lanius et al., 2007; Vermetten et al., 2007; Lindauer et al., 2008; Simmons et al., 2008; Werner et al., 2009; Whalley et al., 2009). Although less commonly implicated, abnormal hippocampal function, and diminished hippocampal volumes in PTSD patients have been associated with deficits in contextual processing, as well as memory impairments, and neuroendocrine dysregulation (Bremner et al., 1999, 2003; Bonne et al., 2001; Shin et al., 2004a,b, 2006; Werner et al., 2009).

Recently these functional connectivity techniques have been applied to the study of corticolimbic circuitry abnormalities at baseline or "at rest" (resting-state functional connectivity). Studies of functional interconnectivity of brain regions derived from "resting-state" scans provides insight into the relationship of spontaneous brain activity between brain regions without being confounded by task influences on activation and has even been shown to reflect structural connectivity between brain regions (Greicius et al., 2009; van den Heuvel et al., 2009). In healthy humans resting-state functional connectivity of the amygdala has revealed patterns of connectivity consistent with task-based connectivity patterns (Stein et al., 2007a; Roy et al., 2009). Moreover, resting-state functional connectivity has been a useful tool for identifying abnormalities in the functional organization of brain systems in several anxiety and mood disorders (Greicius, 2008). However, little is known about what abnormalities, if any, in amygdala connectivity exist at rest in PTSD. Therefore the primary aim of the present experiment was to investigate aberrant amygdala functional connectivity patterns in returning Operation Enduring Freedom/Operation Iraqi Freedom (OEF/OIF) veterans with combat-related PTSD (PTSD group) and combat-exposed OEF/OIF veterans without PTSD [combat-exposed control (CEC) group] during resting-state. We hypothesized that amygdala connectivity to the ACC, mPFC, insula, and hippocampus would differentiate the PTSD group from the CEC group. If observed, such findings would extend our understanding of the pathophysiology of PTSD by identifying a disturbed network that exists

outside of the presence of an overt threat/danger or in the absence of stimulus or task-induced negative emotional processing.

MATERIALS AND METHODS

PARTICIPANTS

Thirty-four, right-handed, male veterans returning from OEF/OIF with documented exposure to combat-related trauma participated in this study. Based on the DSM-IV (APA, 1994), 17 participants met criteria for current PTSD (PTSD group; age: 30.12 ± 7.70 years; Caucasian = 16; Hispanic or Latino = 1) and the other 17 participants were combat-exposed matched controls without PTSD (CEC group; age: 33.71 ± 9.12; Caucasian = 16; Asian = 1). Psychiatric diagnoses were established via the Structured Clinical Interview for DSM-IV (First et al., 1996). Additional standardized clinical instruments including the Clinician Administered PTSD Scale (CAPS; Blake et al., 1995), the PTSD Checklist: Military (PCL-M; Blanchard et al., 1996), the Combat Exposure Scale (CES; Keane et al., 1989), the Hamilton Depression Inventory (HAM-D; Williams, 1988), and the Beck Depression Inventory (BDI-II; Beck et al., 1996) were administered to quantitatively characterize PTSD symptoms, severity of trauma exposure, and depression.

Table 1 shows the participant's demographic and clinical characteristics. Relative to the CEC group, the PTSD group had significantly higher scores on the CAPS, PCL-M, and HAM-D and BDI-II. Of note, the groups did not differ in severity of trauma exposure. Some of the PTSD patients had current psychiatric co-morbidity ($n = 2$ with current major depressive disorder; $n = 2$ with current alcohol abuse) or had a past co-morbidity more than 6 months ago ($n = 1$ had major depressive disorder; $n = 4$ had alcohol abuse, one of whom also had past opioid abuse; $n = 1$ had alcohol dependence in full sustained remission) at the time of scanning. In addition, some PTSD patients had a history of psychotropic medication usage ($n = 8$ had taken an selective serotonin reuptake inhibitor, one of whom had also taken a norepinephrine–dopamine reuptake inhibitor; $n = 1$ had taken a tri-cyclic antidepressant; $n = 2$ had taken a serotonin antagonist-reuptake inhibitor), but none of the PTSD patients were currently taking any psychotropic medications at the time of scanning. All participants were free of any clinically significant medical or neurologic condition that would affect brain blood flow/metabolism or function and/or task performance. None of the subjects had a positive urine toxicology screen at the time of scanning. All participants gave written informed consent after explanation of the experimental protocol, as approved by the VA Ann Arbor Healthcare System and University of Michigan Institutional Review Boards.

Table 1 | Group demographic and clinical characteristics.

	Group mean (±SD)		*t* Value	*p* Value
	PTSD	CEC		
Age	30.12 (7.70)	33.71 (9.12)	−1.24	0.22
CAPS	67.35 (12.41)	5.24 (5.75)	18.72	<0.001
PCL-M	54.59 (9.78)	25.06 (7.34)	9.96	<0.001
BDI-II	22.76 (7.46)	5.53 (6.25)	7.30	<0.001
HAM-D	10.18 (3.75)	2.18 (2.38)	7.44	<0.001
CES	23.88 (5.98)	21.47 (5.50)	1.22	0.23

PTSD, post-traumatic stress disorder; CEC, combat-exposed controls; CAPS, Clinician Administered PTSD Scale; PCL-M, PTSD Checklist: Military; BDI-II, Beck Depression Inventory; HAM-D, Hamilton Depression Inventory; CES, Combat Exposure Scale.

FUNCTIONAL IMAGING ACQUISITION

All participants underwent an 8-min resting-state fMRI scan in which they were instructed to fixate on a white crosshair that was centrally projected against a black background and let their mind wander without falling asleep. fMRI scanning was performed on a 3T GE Signa System (General Electric; Milwaukee, WI, USA) using a standard radiofrequency coil at the University of Michigan Functional MRI Laboratory. Whole-brain functional images (i.e., blood oxygenated level-dependent, BOLD) were collected from 43 axial, 3-mm-thick slices using a T_2^* -sensitive gradient echo reverse spiral acquisition sequence (repetition time, 2000 ms; echo time, 30 ms; 64 × 64 matrix; 220 mm field of view; flip angle, 90°), optimized to minimize susceptibility artifacts (signal loss) at the medial temporal lobe (including the amygdala; Stenger et al., 2000). Cardiac and respiratory cycles were recorded with MRI vendor supplied pulse-oximeter and respiratory belt for physiological corrections on resting-state data. A T_1-weighted anatomical image was collected in the same planes as the functional data, but with higher in-plane resolution (1 mm^2, T_1-overlay) to aid in later co-registration. A high resolution, T_1-weighted volumetric anatomical scan (T_1-SPGR; three-dimensional spoiled gradient echo) was also acquired for precise anatomical localization and normalization.

FUNCTIONAL IMAGING ANALYSIS

Data from 32 participants (CEC = 17; PTSD = 15) met criteria for high quality and scan stability with minimum motion correction and were subsequently included in fMRI analyses (<3 mm displacement in any one direction; two PTSD patients were excluded for poor data quality due to excessive head movement). The first four volumes were discarded to allow for T_1 equilibration effects. Functional data were processed and analyzed using Statistical Parametric Mapping software (SPM8; Wellcome Trust Centre for Neuroimaging, London[1]) using similar methods previously published from our lab (Jelsone-Swain et al., 2010). Images were corrected for physiological signal fluctuations using a custom code written in MATLAB (MathWorks, Natick, MA, USA; Noll et al., 1991). Slice timing and movement correction was done to the time-series data using SPM8. Each participant's T_1-overlay was co-registered to the time-series data and the T_1-SPGR was then co-registered to the co-registered T_1-overlay image. The co-registered T_1-SPGR was then segmented into gray matter, white matter, and cerebrospinal fluid (CSF) and normalized to Montreal Neurological Institute (MNI) space using VBM8 toolbox of SPM8 and the resulting normalization matrix was applied to the time-series data. These normalized time-series data were subsequently re-sampled

[1] www.fil.ion.ucl.ac.uk/spm

to 2 mm^3 voxels and smoothed with an 8-mm Gaussian kernel to minimize noise and effects due to residual differences in functional and gyral anatomy during inter-subject averaging. Then the resulting white matter and CSF segments were further defined using a custom algorithm previously described (Welsh et al., 2007). Each voxel's time-series was detrended to correct for linear drift over time. Nine nuisance covariates (time-series predictors for global signal, white matter, CSF, and the six movement parameters, including the first derivative, obtained during realignment to account for motion-related effects in BOLD) were sequentially regressed from the time-series. The resulting time-series were then band-passed filtered between the frequencies of 0.01 and 0.10-Hz to limit the analysis to resting-state frequencies of interest.

To determine amygdala connectivity during resting-state, seed regions in the left and right amygdala were defined by an anatomically based amygdala mask in each hemisphere (from MAsk of region of interest analysis software, MARINA; Tzourio-Mazoyer et al., 2002; Walter et al., 2003). We then extracted the averaged time course from these seed regions in each participant's data and calculated correlation coefficients between these average time courses and all other voxels of the brain resulting in an *r*-image for amygdala connectivity. The resulting correlation coefficients were then transformed into *Z*-scores using a Fisher *r*-to-*Z* transformation and the resulting *Z* images were analyzed at the second level in a random-effects statistical model. Two-tailed independent samples *t* tests were used to identify areas of the brain that exhibited activity that covaried with the amygdala differentially during resting-state between the two groups (PTSD > CEC; CEC > PTSD). Significant activations were identified with a whole-brain voxel-wise threshold of $p < 0.005$ with a minimum cluster extent of >387 contiguous voxels (3096 mm^3), to correct for multiple comparisons at a corrected $p < 0.05$ calculated using Monte-Carlo simulations (AFNI 3dClustSim[2]). Previous studies interested in differences in brain connectivity between patients with PTSD and trauma-exposed controls without PTSD have used similar significance thresholding approaches to balance Type I and II error rates (Yin et al., 2011a,b). To clarify the signal direction, variance, and specificity of differences in strength of connectivity between the CEC and PTSD groups during resting-state, we extracted individual subject's *Z*-score values from activated voxels that fell within an anatomically based mask for each *a priori* region from the between-group contrast (PTSD > CEC; Tzourio-Mazoyer et al., 2002; Walter et al., 2003). Of note, we did not conduct statistical tests on these measures, as they were defined from significant activations resulting from whole-brain maps of group differences in connectivity.

[2]http://afni.nimh.nih.gov/pub/dist/doc/program_help/3dClustSim.html

RESULTS

Across the entire brain, we observed a discretely localized difference in amygdala connectivity pattern between groups. From the right amygdala anatomical "seed" region, we observed that PTSD patients exhibited stronger connectivity with the insula than CEC subjects (MNI peak: [38, −18, −2], *Z*-score = 4.29, volume = 440 voxels; **Figure 1**); this pattern was not detected from the left amygdala seed. Follow-up ROI analyses on the extracted *Z*-scores of the strength of connectivity from the insula revealed that both groups exhibited positive amygdala–insula coupling, however, the extent of connectivity between the amygdala and insula was greater in the PTSD group than the CEC group (**Figure 1**). To explore the clinical relevance of the observed amygdala–insula connectivity abnormalities, we performed correlational analyses between the extracted values of the strength of connectivity and PTSD symptom severity measures (CAPS, BDI-II, PCL-M, and HAM-D) but did not observe any significant correlations (all *p*s >0.05, corrected for multiple comparisons). Of note, we did not observe group differences in any other *a priori* areas that we predicted, such as the ACC, mPFC, and hippocampus in relation to amygdala connectivity at rest.

DISCUSSION

This is the first study to our knowledge that examines intrinsic amygdala functional connectivity patterns during rest in returning OEF/OIF veterans with combat-related PTSD compared to a

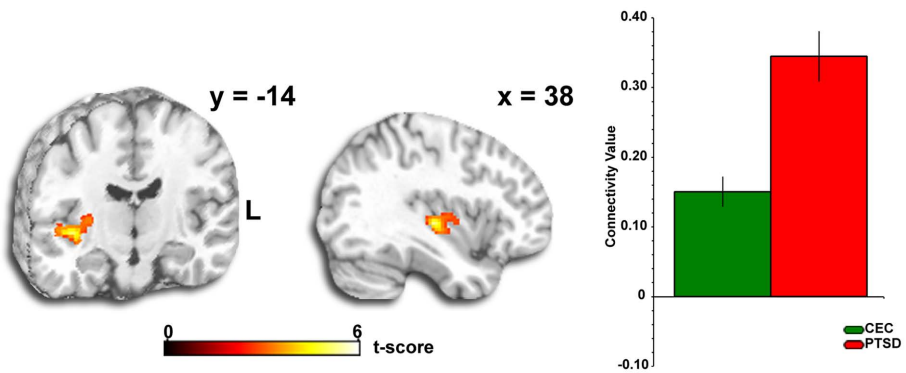

FIGURE 1 | Between-group whole-brain voxel-wise statistical *t* map overlaid on a canonical brain rendering (left, MNI coronal, *y*-plane = −14; right, MNI sagittal, *x*-plane = 38 [right]) showing stronger amygdala connectivity to the insula during rest in the PTSD group (PTSD > CEC). Connectivity "target" is displayed at whole-brain voxel-wise $p < 0.005$, uncorrected; color bar represents statistical *t*-scores; Bar graph shows mean extracted *Z*-scores (±SEM) within each group from activated voxels that fell within an anatomically based insula mask, showing stronger connectivity in PTSD patients (>CEC). PTSD, post-traumatic stress disorder; CEC, combat-exposed control; L, left.

group of OEF/OIF veterans with combat exposure, but without PTSD. We found stronger amygdala–insula resting-state functional connectivity in the PTSD group compared to the CEC group. Of note, this connectivity pattern was from the right amygdala "seed" and was not shown from the left amygdala. Although we did not make an *a priori* prediction about lateralization of amygdala resting-state connectivity several findings of amygdala hyperactivity in PTSD and correlations between PTSD symptom severity and amygdala activity have been right-sided (Rauch et al., 1996, 2000; Pissiota et al., 2002; Fredrikson and Furmark, 2003; Driessen et al., 2004; Shin et al., 2004a). Contrary to our original hypothesis we did not observe any significant differences in amygdala connectivity to any other *a priori* regions (mPFC, ACC, hippocampus) in the PTSD group compared to the CEC group at rest. This is a notable negative finding and requires replication; however, we acknowledge that the absence of differences in amygdala–frontal or amygdala–hippocampal connectivity between groups could have resulted from: (1) Our stringent, whole-brain correction for multiple comparisons to detect significance coupled with a small sample size may have led to false negatives and/or more subtle connectivity abnormalities; and/or (2) The resting-state task may be insensitive to detecting amygdala–prefrontal and amygdala–hippocampal connectivity abnormalities, which may require engagement by an overt task.

Both the amygdala and insula have been separately implicated in the pathophysiology of anxiety and PTSD (Rauch et al., 2000; Osuch et al., 2001; Pissiota et al., 2002; Shin et al., 2004a; Protopopescu et al., 2005; Nemeroff et al., 2006; Hopper et al., 2007; Carrion et al., 2008; Shin and Liberzon, 2010). The amygdala plays an important role in the subjective and attentional-vigilance aspects of threat processing, and thus abnormalities in amygdala activity may be associated with hyperarousal and hypervigilance to threat in PTSD (Etkin, 2009). Moreover, several studies have shown that the amygdala is hyperresponsive to both trauma-related (Rauch et al., 1996; Shin et al., 1997, 2004a; Liberzon et al., 1999; Pissiota et al., 2002; Hendler et al., 2003; Driessen et al., 2004; Protopopescu et al., 2005; Vermetten et al., 2007) and unrelated stimuli in PTSD (Rauch et al., 2000; Armony et al., 2005; Shin et al., 2005; Williams et al., 2006), amygdala activation is positively correlated with PTSD symptom severity (Rauch et al., 1996; Shin et al., 2004a; Armony et al., 2005; Protopopescu et al., 2005) and self-reported anxiety (Pissiota et al., 2002; Fredrikson and Furmark, 2003), and symptom reduction after treatment is associated with decreased amygdala activation (Felmingham et al., 2007). Likewise, PTSD patients display exaggerated insula activation during script-driven imagery (Lanius et al., 2007; Lindauer et al., 2008), fear conditioning and extinction (Bremner et al., 2005), the anticipation of negative images (Simmons et al., 2006), the retrieval of emotional or neutral stimuli (Bremner et al., 2003; Werner et al., 2009; Whalley et al., 2009), and aversive smells and painful stimuli (Vermetten et al., 2007) and is also positively correlated with PTSD symptom severity (Osuch et al., 2001; Hopper et al., 2007; Carrion et al., 2008). The insula controls evaluative, experiential, and expressive aspects of internal emotional states via visceral and somatic changes (e.g., autonomic "flight-or-fight" responses) evoked during presentations of aversive stimuli (Phan et al., 2002; Anderson et al., 2003; Dupont et al., 2003; Critchley et al., 2004; Simmons et al., 2004; Paulus and Stein, 2006) and it has been posited that the insula relays interoceptive information to the amygdala to help guide behavioral responses (Augustine, 1996; Craig, 2002; Simmons et al., 2004; Paulus and Stein, 2006). In fact, the insula provides some of the strongest cortical connections to the major output division of the amygdala responsible for generating fear responses to symptom-provoking stimuli (Augustine, 1996; Aggleton and Saunders, 2000; Freese and Amaral, 2009) and abnormalities in these structures has been suggested to underlie exaggerated fear responses and the persistence of traumatic memories (Shin and Liberzon, 2010), as well as anxiety proneness (Paulus and Stein, 2006; Simmons et al., 2006; Stein et al., 2007b). Furthermore, evidence from a recent study suggests that a functional network between the amygdala and insula mediates anxious anticipation of negative events and anxious individuals display exaggerated activity within this network during anticipation of aversive stimuli (Carlson et al., 2010). Individuals with PTSD display excess anticipation of negative events and because of this are preoccupied with studying their environment for possible threats (i.e., hypervigilance) and increased amygdala–insula functional coupling may be a mechanism supporting hypervigilance in patients with PTSD.

Besides the present study, others have investigated baseline connectivity patterns in patients with PTSD and observed abnormalities in functional connectivity within the default-mode network when compared to healthy controls (although sometimes inconsistent; Bluhm et al., 2009; Daniels et al., 2010; Lanius et al., 2010), not directly related to amygdala connectivity. Our study extends these findings to resting-state amygdala coupling within a corticolimbic network known to be dysfunctional during trauma-related anxiety provocation, emotionally based tasks, and evocative stimuli in PTSD patients. However, our study has some important limitations. First, our study only included males and therefore cannot be generalized to females. Second, the resting-state analysis of changes in amygdala–insula connectivity do not allow for inferences about directionality or causality, which await task-based path or dynamic causal analyses. In addition, we have interpreted our resting-state findings based on previous functional and structural imaging studies, however, research with converging methods (i.e., task-dependent and -independent fMRI, diffusion tensor imaging) are much needed to link connectivity at rest with brain structure and function. Lastly, the cross-sectional nature of our measurement does not allow us to ascertain whether enhanced amygdala–insula resting-state connectivity was present before the traumatic experience and if so, makes it a potential vulnerability maker for PTSD.

Despite these limitations, our findings demonstrate that alterations in these connectivity patterns in a network involved in emotional processing and regulation may be relevant to a brain model of PTSD that involves baseline abnormalities in amygdala–insula functional connectivity that exist even without task induction. These findings suggest that the aberrant amygdala and insula activation to fear-evocative probes previously characterized in PTSD may be driven by an underlying enhanced connectivity between amygdala, a region known for perceiving threat and generating fear responses, and the insula, a region known for processing the meaning and prediction of aversive bodily states. This enhanced

amygdala–insula connectivity may reflect an exaggerated, pervasive state of arousal that exists outside the presence of an overt, actual threat/danger. Studying amygdala functional connectivity "at rest" extends our understanding of the pathophysiology of PTSD, and the current findings prompt further investigation in this emerging area of neuroimaging research.

ACKNOWLEDGMENTS

This research was supported by the Veterans Affairs Merit Review Program Award (K. Luan Phan). The authors would like to acknowledge the OEF/OIF veterans for their participation in this research study and more importantly for their dedication and service to the United States of America.

REFERENCES

Aggleton, J. P., and Saunders, R. C. (2000). "The amygdala – what's happened in the last decade?" in *The Amygdala: A Functional Analysis*, 2nd Edn, ed. J. P. Aggleton (New York: Oxford Press), 1–30.

Amaral, D. G., and Price, J. L. (1984). Amygdalo-cortical projections in the monkey (*Macaca fascicularis*). *J. Comp. Neurol.* 230, 465–496.

Anderson, A. K., Christoff, K., Panitz, D., De Rosa, E., and Gabrieli, J. D. (2003). Neural correlates of the automatic processing of threat facial signals. *J. Neurosci.* 23, 5627–5633.

APA. (1994). *Diagnostic and Statistical Manual of Psychiatry*, 4th Edn. Washington, DC: American Psychiatric Publishing, Inc.

Armony, J. L., Corbo, V., Clement, M. H., and Brunet, A. (2005). Amygdala response in patients with acute PTSD to masked and unmasked emotional facial expressions. *Am. J. Psychiatry* 162, 1961–1963.

Augustine, J. R. (1996). Circuitry and functional aspects of the insular lobe in primates including humans. *Brain Res. Brain Res. Rev.* 22, 229–244.

Banks, S. J., Eddy, K. T., Angstadt, M., Nathan, P. J., and Phan, K. L. (2007). Amygdala-frontal connectivity during emotion regulation. *Soc. Cogn. Affect. Neurosci.* 2, 303–312.

Barbas, H., and De Olmos, J. (1990). Projections from the amygdala to basoventral and mediodorsal prefrontal regions in the rhesus monkey. *J. Comp. Neurol.* 300, 549–571.

Beck, A. T., Steer, R. A., Ball, R., and Ranieri, W. (1996). Comparison of Beck Depression Inventories-IA and -II in psychiatric outpatients. *J. Pers. Assess.* 67, 588–597.

Blake, D. D., Weathers, F. W., Nagy, L. M., Kaloupek, D. G., Gusman, F. D., Charney, D. S., and Keane, T. M. (1995). The development of a Clinician-Administered PTSD Scale. *J. Trauma Stress* 8, 75–90.

Blanchard, E. B., Jones-Alexander, J., Buckley, T. C., and Forneris, C. A. (1996). Psychometric properties of the PTSD Checklist (PCL). *Behav. Res. Ther.* 34, 669–673.

Bluhm, R. L., Williamson, P. C., Osuch, E. A., Frewen, P. A., Stevens, T. K., Boksman, K., Neufeld, R. W., Theberge, J., and Lanius, R. A. (2009). Alterations in default network connectivity in posttraumatic stress disorder related to early-life trauma. *J. Psychiatry Neurosci.* 34, 187–194.

Bonne, O., Brandes, D., Gilboa, A., Gomori, J. M., Shenton, M. E., Pitman, R. K., and Shalev, A. Y. (2001). Longitudinal MRI study of hippocampal volume in trauma survivors with PTSD. *Am. J. Psychiatry* 158, 1248–1251.

Bracht, T., Tuscher, O., Schnell, S., Kreher, B., Rusch, N., Glauche, V., Lieb, K., Ebert, D., Il'yasov, K. A., Hennig, J., Weiller, C., Van Elst, L. T., and Saur, D. (2009). Extraction of prefronto-amygdalar pathways by combining probability maps. *Psychiatry Res.* 174, 217–222.

Bremner, J. D., Narayan, M., Staib, L. H., Southwick, S. M., Mcglashan, T., and Charney, D. S. (1999). Neural correlates of memories of childhood sexual abuse in women with and without posttraumatic stress disorder. *Am. J. Psychiatry* 156, 1787–1795.

Bremner, J. D., Vermetten, E., Schmahl, C., Vaccarino, V., Vythilingam, M., Afzal, N., Grillon, C., and Charney, D. S. (2005). Positron emission tomographic imaging of neural correlates of a fear acquisition and extinction paradigm in women with childhood sexual-abuse-related post-traumatic stress disorder. *Psychol. Med.* 35, 791–806.

Bremner, J. D., Vythilingam, M., Vermetten, E., Southwick, S. M., Mcglashan, T., Staib, L. H., Soufer, R., and Charney, D. S. (2003). Neural correlates of declarative memory for emotionally valenced words in women with posttraumatic stress disorder related to early childhood sexual abuse. *Biol. Psychiatry* 53, 879–889.

Bryant, R. A., Kemp, A. H., Felmingham, K. L., Liddell, B., Olivieri, G., Peduto, A., Gordon, E., and Williams, L. M. (2008). Enhanced amygdala and medial prefrontal activation during nonconscious processing of fear in posttraumatic stress disorder: an fMRI study. *Hum. Brain Mapp.* 29, 517–523.

Carlson, J. M., Greenberg, T., Rubin, D., and Mujica-Parodi, L. R. (2010). Feeling anxious: anticipatory amygdalo-insular response predicts the feeling of anxious anticipation. *Soc. Cogn. Affect. Neurosci.* 6, 74–81.

Carrion, V. G., Garrett, A., Menon, V., Weems, C. F., and Reiss, A. L. (2008). Posttraumatic stress symptoms and brain function during a response-inhibition task: an fMRI study in youth. *Depress. Anxiety* 25, 514–526.

Craig, A. D. (2002). How do you feel? Interoception: the sense of the physiological condition of the body. *Nat. Rev. Neurosci.* 3, 655–666.

Critchley, H. D., Wiens, S., Rotshtein, P., Ohman, A., and Dolan, R. J. (2004). Neural systems supporting interoceptive awareness. *Nat. Neurosci.* 7, 189–195.

Croxson, P. L., Johansen-Berg, H., Behrens, T. E., Robson, M. D., Pinsk, M. A., Gross, C. G., Richter, W., Richter, M. C., Kastner, S., and Rushworth, M. F. (2005). Quantitative investigation of connections of the prefrontal cortex in the human and macaque using probabilistic diffusion tractography. *J. Neurosci.* 25, 8854–8866.

Daniels, J. K., Mcfarlane, A. C., Bluhm, R. L., Moores, K. A., Clark, C. R., Shaw, M. E., Williamson, P. C., Densmore, M., and Lanius, R. A. (2010). Switching between executive and default mode networks in posttraumatic stress disorder: alterations in functional connectivity. *J. Psychiatry Neurosci.* 35, 258–266.

Delgado, M. R., Nearing, K. I., Ledoux, J. E., and Phelps, E. A. (2008). Neural circuitry underlying the regulation of conditioned fear and its relation to extinction. *Neuron* 59, 829–838.

Driessen, M., Beblo, T., Mertens, M., Piefke, M., Rullkoetter, N., Silva-Saavedra, A., Reddemann, L., Rau, H., Markowitsch, H. J., Wulff, H., Lange, W., and Woermann, F. G. (2004). Posttraumatic stress disorder and fMRI activation patterns of traumatic memory in patients with borderline personality disorder. *Biol. Psychiatry* 55, 603–611.

Dupont, S., Bouilleret, V., Hasboun, D., Semah, F., and Baulac, M. (2003). Functional anatomy of the insula: new insights from imaging. *Surg. Radiol. Anat.* 25, 113–119.

Etkin, A. (2009). Functional neuroanatomy of anxiety: a neural circuit perspective. *Curr. Top. Behav. Neurosci.* 2, 251–277.

Etkin, A., Egner, T., and Kalisch, R. (2011). Emotional processing in anterior cingulate and medial prefrontal cortex. *Trends Cogn. Sci. (Regul. Ed.)* 15, 85–93.

Etkin, A., Egner, T., Peraza, D. M., Kandel, E. R., and Hirsch, J. (2006). Resolving emotional conflict: a role for the rostral anterior cingulate cortex in modulating activity in the amygdala. *Neuron* 51, 871–882.

Etkin, A., Prater, K. E., Schatzberg, A. F., Menon, V., and Greicius, M. D. (2009). Disrupted amygdalar subregion functional connectivity and evidence of a compensatory network in generalized anxiety disorder. *Arch. Gen. Psychiatry* 66, 1361–1372.

Etkin, A., and Wager, T. D. (2007). Functional neuroimaging of anxiety: a meta-analysis of emotional processing in PTSD, social anxiety disorder, and specific phobia. *Am. J. Psychiatry* 164, 1476–1488.

Felmingham, K., Kemp, A., Williams, L., Das, P., Hughes, G., Peduto, A., and Bryant, R. (2007). Changes in anterior cingulate and amygdala after cognitive behavior therapy of posttraumatic stress disorder. *Psychol. Sci.* 18, 127–129.

First, M. B., Spitzer, R. L., Gibbon, M., and Williams, J. B. (1996). *Structured Clinical Interview for the DSM-IV Axis I Disorders (SCID I/P, Version 2.0)*. New York: Biometrics Research Department, New York State Psychiatric Institute.

Fredrikson, M., and Furmark, T. (2003). Amygdaloid regional cerebral blood flow and subjective fear during symptom provocation in anxiety disorders. *Ann. N. Y. Acad. Sci.* 985, 341–347.

Freese, J. L., and Amaral, D. G. (2009). "Neuroanatomy of the primate amygdala," in *The Human Amygdala*, eds P. J. Whalen and E. A. Phelps (New York: The Guilford Press), 3–42.

Ghashghaei, H. T., and Barbas, H. (2002). Pathways for emotion: interactions of prefrontal and anterior temporal pathways in the amygdala of the rhesus monkey. *Neuroscience* 115, 1261–1279.

Ghashghaei, H. T., Hilgetag, C. C., and Barbas, H. (2007). Sequence of information processing for emotions based on the anatomic dialogue between prefrontal cortex and amygdala. *Neuroimage* 34, 905–923.

Gilboa, A., Shalev, A. Y., Laor, L., Lester, H., Louzoun, Y., Chisin, R., and Bonne, O. (2004). Functional connectivity of the prefrontal cortex and the amygdala in posttraumatic stress disorder. *Biol. Psychiatry* 55, 263–272.

Greicius, M. (2008). Resting-state functional connectivity in neuropsychiatric disorders. *Curr. Opin. Neurol.* 21, 424–430.

Greicius, M. D., Supekar, K., Menon, V., and Dougherty, R. F. (2009). Resting-state functional connectivity reflects structural connectivity in the default mode network. *Cereb. Cortex* 19, 72–78.

Hamann, S. B., Ely, T. D., Grafton, S. T., and Kilts, C. D. (1999). Amygdala activity related to enhanced memory for pleasant and aversive stimuli. *Nat. Neurosci.* 2, 289–293.

Hendler, T., Rotshtein, P., Yeshurun, Y., Weizmann, T., Kahn, I., Ben-Bashat, D., Malach, R., and Bleich, A. (2003). Sensing the invisible: differential sensitivity of visual cortex and amygdala to traumatic context. *Neuroimage* 19, 587–600.

Hopper, J. W., Frewen, P. A., Van Der Kolk, B. A., and Lanius, R. A. (2007). Neural correlates of reexperiencing, avoidance, and dissociation in PTSD: symptom dimensions and emotion dysregulation in responses to script-driven trauma imagery. *J. Trauma Stress* 20, 713–725.

Jelsone-Swain, L. M., Fling, B. W., Seidler, R. D., Hovatter, R., Gruis, K., and Welsh, R. C. (2010). Reduced interhemispheric functional connectivity in the motor cortex during rest in limb-onset amyotrophic lateral sclerosis. *Front. Syst. Neurosci.* 4:158. doi:10.3389/fnsys.2010.00158

Johansen-Berg, H., Gutman, D. A., Behrens, T. E., Matthews, P. M., Rushworth, M. F., Katz, E., Lozano, A. M., and Mayberg, H. S. (2008). Anatomical connectivity of the subgenual cingulate region targeted with deep brain stimulation for treatment-resistant depression. *Cereb. Cortex* 18, 1374–1383.

Keane, T., Fairbank, J., Caddell, J., Zimering, R., Taylor, K., and Mora, C. (1989). Clinical evaluation of a measure to assess combat exposure. *Psychol. Assess.* 1, 53–55.

Kilpatrick, L., and Cahill, L. (2003). Amygdala modulation of parahippocampal and frontal regions during emotionally influenced memory storage. *Neuroimage* 20, 2091–2099.

Kober, H., Barrett, L. F., Joseph, J., Bliss-Moreau, E., Lindquist, K., and Wager, T. D. (2008). Functional grouping and cortical-subcortical interactions in emotion: a meta-analysis of neuroimaging studies. *Neuroimage* 42, 998–1031.

Lanius, R. A., Bluhm, R. L., Coupland, N. J., Hegadoren, K. M., Rowe, B., Theberge, J., Neufeld, R. W., Williamson, P. C., and Brimson, M. (2010). Default mode network connectivity as a predictor of posttraumatic stress disorder symptom severity in acutely traumatized subjects. *Acta Psychiatr. Scand.* 121, 33–40.

Lanius, R. A., Frewen, P. A., Girotti, M., Neufeld, R. W., Stevens, T. K., and Densmore, M. (2007). Neural correlates of trauma script-imagery in posttraumatic stress disorder with and without comorbid major depression: a functional MRI investigation. *Psychiatry Res* 155, 45–56.

Lanius, R. A., Williamson, P. C., Bluhm, R. L., Densmore, M., Boksman, K., Neufeld, R. W., Gati, J. S., and Menon, R. S. (2005). Functional connectivity of dissociative responses in posttraumatic stress disorder: a functional magnetic resonance imaging investigation. *Biol. Psychiatry* 57, 873–884.

Liberzon, I., and Phan, K. L. (2003). Brain-imaging studies of posttraumatic stress disorder. *CNS Spectr.* 8, 641–650.

Liberzon, I., and Sripada, C. S. (2008). The functional neuroanatomy of PTSD: a critical review. *Prog. Brain Res.* 167, 151–169.

Liberzon, I., Taylor, S. F., Amdur, R., Jung, T. D., Chamberlain, K. R., Minoshima, S., Koeppe, R. A., and Fig, L. M. (1999). Brain activation in PTSD in response to trauma-related stimuli. *Biol. Psychiatry* 45, 817–826.

Lindauer, R. J., Booij, J., Habraken, J. B., Van Meijel, E. P., Uylings, H. B., Olff, M., Carlier, I. V., Den Heeten, G. J., Van Eck-Smit, B. L., and Gersons, B. P. (2008). Effects of psychotherapy on regional cerebral blood flow during trauma imagery in patients with post-traumatic stress disorder: a randomized clinical trial. *Psychol. Med.* 38, 543–554.

Morey, R. A., Dolcos, F., Petty, C. M., Cooper, D. A., Hayes, J. P., Labar, K. S., and Mccarthy, G. (2009). The role of trauma-related distractors on neural systems for working memory and emotion processing in posttraumatic stress disorder. *J. Psychiatr. Res.* 43, 809–817.

Murty, V. P., Ritchey, M., Adcock, R. A., and Labar, K. S. (2011). Reprint of: fMRI studies of successful emotional memory encoding: a quantitative meta-analysis. *Neuropsychologia* 49, 695–705.

Nemeroff, C. B., Bremner, J. D., Foa, E. B., Mayberg, H. S., North, C. S., and Stein, M. B. (2006). Posttraumatic stress disorder: a state-of-the-science review. *J. Psychiatr. Res.* 40, 1–21.

Noll, D. C., Meyer, C. H., Pauly, J. M., Nishimura, D. G., and Macovski, A. (1991). A homogeneity correction method for magnetic resonance imaging with time-varying gradients. *IEEE Trans. Med. Imaging* 10, 629–637.

Ochsner, K. N., Bunge, S. A., Gross, J. J., and Gabrieli, J. D. (2002). Rethinking feelings: an fMRI study of the cognitive regulation of emotion. *J. Cogn. Neurosci.* 14, 1215–1229.

Osuch, E. A., Benson, B., Geraci, M., Podell, D., Herscovitch, P., Mccann, U. D., and Post, R. M. (2001). Regional cerebral blood flow correlated with flashback intensity in patients with posttraumatic stress disorder. *Biol. Psychiatry* 50, 246–253.

Paulus, M. P., and Stein, M. B. (2006). An insular view of anxiety. *Biol. Psychiatry* 60, 383–387.

Phan, K. L., Wager, T., Taylor, S. F., and Liberzon, I. (2002). Functional neuroanatomy of emotion: a meta-analysis of emotion activation studies in PET and fMRI. *Neuroimage* 16, 331–348.

Phan, K. L., Wager, T. D., Taylor, S. F., and Liberzon, I. (2004). Functional neuroimaging studies of human emotions. *CNS Spectr.* 9, 258–266.

Phelps, E. A. (2004). Human emotion and memory: interactions of the amygdala and hippocampal complex. *Curr. Opin. Neurobiol.* 14, 198–202.

Phelps, E. A., Delgado, M. R., Nearing, K. I., and Ledoux, J. E. (2004). Extinction learning in humans: role of the amygdala and vmPFC. *Neuron* 43, 897–905.

Pissiota, A., Frans, O., Fernandez, M., Von Knorring, L., Fischer, H., and Fredrikson, M. (2002). Neurofunctional correlates of posttraumatic stress disorder: a PET symptom provocation study. *Eur. Arch. Psychiatry Clin. Neurosci.* 252, 68–75.

Pitman, R. K., Shin, L. M., and Rauch, S. L. (2001). Investigating the pathogenesis of posttraumatic stress disorder with neuroimaging. *J. Clin. Psychiatry* 62(Suppl. 17), 47–54.

Protopopescu, X., Pan, H., Tuescher, O., Cloitre, M., Goldstein, M., Engelien, W., Epstein, J., Yang, Y., Gorman, J., Ledoux, J., Silbersweig, D., and Stern, E. (2005). Differential time courses and specificity of amygdala activity in posttraumatic stress disorder subjects and normal control subjects. *Biol. Psychiatry* 57, 464–473.

Quirk, G. J., and Mueller, D. (2008). Neural mechanisms of extinction learning and retrieval. *Neuropsychopharmacology* 33, 56–72.

Rauch, S. L., and Shin, L. M. (1997). Functional neuroimaging studies in posttraumatic stress disorder. *Ann. N. Y. Acad. Sci.* 821, 83–98.

Rauch, S. L., Shin, L. M., and Phelps, E. A. (2006). Neurocircuitry models of posttraumatic stress disorder and extinction: human neuroimaging research – past, present, and future. *Biol. Psychiatry* 60, 376–382.

Rauch, S. L., Shin, L. M., Whalen, P. J., and Pitman, R. K. (1998). Neuroimaging and the neuroanatomy of PTSD. *CNS Spectr.* 3, 30–41.

Rauch, S. L., Van Der Kolk, B. A., Fisler, R. E., Alpert, N. M., Orr, S. P., Savage, C. R., Fischman, A. J., Jenike, M. A., and Pitman, R. K. (1996). A symptom provocation study of posttraumatic stress disorder using positron emission tomography and script-driven imagery. *Arch. Gen. Psychiatry* 53, 380–387.

Rauch, S. L., Whalen, P. J., Shin, L. M., Mcinerney, S. C., Macklin, M. L., Lasko, N. B., Orr, S. P., and Pitman, R. K. (2000). Exaggerated amygdala response to masked facial stimuli in posttraumatic stress disorder: a functional MRI study. *Biol. Psychiatry* 47, 769–776.

Ritchey, M., Dolcos, F., and Cabeza, R. (2008). Role of amygdala connectivity in the persistence of emotional memories over time: an event-related fMRI investigation. *Cereb. Cortex* 18, 2494–2504.

Roy, A. K., Shehzad, Z., Margulies, D. S., Kelly, A. M., Uddin, L. Q., Gotimer, K., Biswal, B. B., Castellanos, F. X., and Milham, M. P. (2009). Functional connectivity of the human amygdala using resting state fMRI. *Neuroimage* 45, 614–626.

Saunders, R. C., Rosene, D. L., and Van Hoesen, G. W. (1988). Comparison of the efferents of the amygdala and the hippocampal formation in the rhesus monkey: II. Reciprocal and non-reciprocal connections. *J. Comp. Neurol.* 271, 185–207.

Shaw, M. E., Moores, K. A., Clark, R. C., Mcfarlane, A. C., Strother, S. C., Bryant, R. A., Brown, G. C., and Taylor, J. D. (2009). Functional connectivity reveals inefficient working memory systems in post-traumatic stress disorder. *Psychiatry Res* 172, 235–241.

Shin, L. M. (2009). "The amygdala in post-traumatic stress disorder," in *Post-Traumatic Stress Disorder: Basic Science and Clinical Practice*, eds P. J. Shiromani, T. M. Keane, and J. E. Le Doux (New York: Humana Press), 319–334.

Shin, L. M., Kosslyn, S. M., Mcnally, R. J., Alpert, N. M., Thompson, W. L., Rauch, S. L., Macklin, M. L., and Pitman, R. K. (1997). Visual imagery and perception in posttraumatic stress disorder. A positron emission tomographic investigation. *Arch. Gen. Psychiatry* 54, 233–241.

Shin, L. M., and Liberzon, I. (2010). The neurocircuitry of fear, stress, and anxiety disorders. *Neuropsychopharmacology* 35, 169–191.

Shin, L. M., Orr, S. P., Carson, M. A., Rauch, S. L., Macklin, M. L., Lasko, N. B., Peters, P. M., Metzger, L. J., Dougherty, D. D., Cannistraro, P. A., Alpert, N. M., Fischman, A. J., and Pitman, R. K. (2004a). Regional cerebral blood flow in the amygdala and medial prefrontal cortex during traumatic imagery in male and female Vietnam veterans with PTSD. *Arch. Gen. Psychiatry* 61, 168–176.

Shin, L. M., Shin, P. S., Heckers, S., Krangel, T. S., Macklin, M. L., Orr, S. P., Lasko, N., Segal, E., Makris, N., Richert, K., Levering, J., Schacter, D. L., Alpert, N. M., Fischman, A. J., Pitman, R. K., and Rauch, S. L. (2004b). Hippocampal function in posttraumatic stress disorder. *Hippocampus* 14, 292–300.

Shin, L. M., Rauch, S. L., and Pitman, R. K. (2006). Amygdala, medial prefrontal cortex, and hippocampal function in PTSD. *Ann. N. Y. Acad. Sci.* 1071, 67–79.

Shin, L. M., Wright, C. I., Cannistraro, P. A., Wedig, M. M., Mcmullin, K., Martis, B., Macklin, M. L., Lasko, N. B., Cavanagh, S. R., Krangel, T. S., Orr, S. P., Pitman, R. K., Whalen, P. J., and Rauch, S. L. (2005). A functional magnetic resonance imaging study of amygdala and medial prefrontal cortex responses to overtly presented fearful faces in posttraumatic stress disorder. *Arch. Gen. Psychiatry* 62, 273–281.

Simmons, A., Matthews, S. C., Stein, M. B., and Paulus, M. P. (2004). Anticipation of emotionally aversive visual stimuli activates right insula. *Neuroreport* 15, 2261–2265.

Simmons, A., Strigo, I., Matthews, S. C., Paulus, M. P., and Stein, M. B. (2006). Anticipation of aversive visual stimuli is associated with increased insula activation in anxiety-prone subjects. *Biol. Psychiatry* 60, 402–409.

Simmons, A. N., Paulus, M. P., Thorp, S. R., Matthews, S. C., Norman, S. B., and Stein, M. B. (2008). Functional activation and neural networks in women with posttraumatic stress disorder related to intimate partner violence. *Biol. Psychiatry* 64, 681–690.

Stefanacci, L., Suzuki, W. A., and Amaral, D. G. (1996). Organization of connections between the amygdaloid complex and the perirhinal and parahippocampal cortices in macaque monkeys. *J. Comp. Neurol.* 375, 552–582.

Stein, J. L., Wiedholz, L. M., Bassett, D. S., Weinberger, D. R., Zink, C. F., Mattay, V. S., and Meyer-Lindenberg, A. (2007a). A validated network of effective amygdala connectivity. *Neuroimage* 36, 736–745.

Stein, M. B., Simmons, A. N., Feinstein, J. S., and Paulus, M. P. (2007b). Increased amygdala and insula activation during emotion processing in anxiety-prone subjects. *Am. J. Psychiatry* 164, 318–327.

Stenger, V. A., Boada, F. E., and Noll, D. C. (2000). Three-dimensional tailored RF pulses for the reduction of susceptibility artifacts in T(*)(2)-weighted functional MRI. *Magn. Reson. Med.* 44, 525–531.

Taylor, S. F., Phan, K. L., Decker, L. R., and Liberzon, I. (2003). Subjective rating of emotionally salient stimuli modulates neural activity. *Neuroimage* 18, 650–659.

Tzourio-Mazoyer, N., Landeau, B., Papathanassiou, D., Crivello, F., Etard, O., Delcroix, N., Mazoyer, B., and Joliot, M. (2002). Automated anatomical labeling of activations in SPM using a macroscopic anatomical parcellation of the MNI MRI single-subject brain. *Neuroimage* 15, 273–289.

Urry, H. L., Van Reekum, C. M., Johnstone, T., Kalin, N. H., Thurow, M. E., Schaefer, H. S., Jackson, C. A., Frye, C. J., Greischar, L. L., Alexander, A. L., and Davidson, R. J. (2006). Amygdala and ventromedial prefrontal cortex are inversely coupled during regulation of negative affect and predict the diurnal pattern of cortisol secretion among older adults. *J. Neurosci.* 26, 4415–4425.

van den Heuvel, M. P., Mandl, R. C., Kahn, R. S., and Hulshoff Pol, H. E. (2009). Functionally linked resting-state networks reflect the underlying structural connectivity architecture of the human brain. *Hum. Brain Mapp.* 30, 3127–3141.

Vermetten, E., Schmahl, C., Southwick, S. M., and Bremner, J. D. (2007). Positron tomographic emission study of olfactory induced emotional recall in veterans with and without combat-related posttraumatic stress disorder. *Psychopharmacol. Bull.* 40, 8–30.

Wager, T. D., Davidson, M. L., Hughes, B. L., Lindquist, M. A., and Ochsner, K. N. (2008). Prefrontal-subcortical pathways mediating successful emotion regulation. *Neuron* 59, 1037–1050.

Wager, T. D., Phan, K. L., Liberzon, I., and Taylor, S. F. (2003). Valence, gender, and lateralization of functional brain anatomy in emotion: a meta-analysis of findings from neuroimaging. *Neuroimage* 19, 513–531.

Walter, B., Blecker, C., Kirsch, P., Sammer, G., Schienle, A., Stark, R., and Vaitl, D. (2003). "MARINA: an easy tool for the creation for MAsks for Region of INterest Analyses," in *9th International Conference on Functional Mapping of the Human Brain: NeuroImage.*

Welsh, R. C., Rahbar, H., Foerster, B., Thurnher, M., and Sundgren, P. C. (2007). Brain diffusivity in patients with neuropsychiatric systemic lupus erythematosus with new acute neurological symptoms. *J. Magn. Reson. Imaging* 26, 541–551.

Werner, N. S., Meindl, T., Engel, R. R., Rosner, R., Riedel, M., Reiser, M., and Fast, K. (2009). Hippocampal function during associative learning in patients with posttraumatic stress disorder. *J. Psychiatr. Res.* 43, 309–318.

Whalley, M. G., Rugg, M. D., Smith, A. P., Dolan, R. J., and Brewin, C. R. (2009). Incidental retrieval of emotional contexts in post-traumatic stress disorder and depression: an fMRI study. *Brain Cogn.* 69, 98–107.

Williams, J. B. (1988). A structured interview guide for the Hamilton Depression Rating Scale. *Arch. Gen. Psychiatry* 45, 742–747.

Williams, L. M., Kemp, A. H., Felmingham, K., Barton, M., Olivieri, G., Peduto, A., Gordon, E., and Bryant, R. A. (2006). Trauma modulates amygdala and medial prefrontal responses to consciously attended fear. *Neuroimage* 29, 347–357.

Yin, Y., Jin, C., Hu, X., Duan, L., Li, Z., Song, M., Chen, H., Feng, B., Jiang, T., Jin, H., Wong, C., Gong, Q., and Li, L. (2011a). Altered resting-state functional connectivity of thalamus in earthquake-induced posttraumatic stress disorder: a functional magnetic resonance imaging study. *Brain Res.* 1411, 98–107.

Yin, Y., Li, L., Jin, C., Hu, X., Duan, L., Eyler, L. T., Gong, Q., Song, M., Jiang, T., Liao, M., Zhang, Y., and Li, W. (2011b). Abnormal baseline brain activity in posttraumatic stress disorder: a resting-state functional magnetic resonance imaging study. *Neurosci. Lett.* 498, 185–189.

Conflict of Interest Statement: The authors declare that the research was conducted in the absence of any commercial or financial relationships that could be construed as a potential conflict of interest.

Received: 30 September 2011; accepted: 28 October 2011; published online: 14 November 2011.

Citation: Rabinak CA, Angstadt M, Welsh RC, Kenndy AE, Lyubkin M, Martis B and Phan KL (2011) Altered amygdala resting-state functional connectivity in post-traumatic stress disorder. Front. Psychiatry ***2****:62. doi: 10.3389/fpsyt.2011.00062*

This article was submitted to Frontiers in Neuropsychiatric Imaging and Stimulation, a specialty of Frontiers in Psychiatry.